



THESIS APPROVAL

GRADUATE SCHOOL, KASETSART UNIVERSITY

Doctor of Engineering (Water Resources Engineering)

DEGREE

Water Resources Engineering

FIELD

Water Resources Engineering

DEPARTMENT

TITLE: Watershed Runoff Prediction, Streamflow Analysis and River Modeling in
The Chao Phraya River Basin

NAME: Mr. Chaiyapong Thepprasit

THIS THESIS HAS BEEN ACCEPTED BY

THESIS ADVISOR

(Associate Professor Kobkiat Pongput, Ph.D.)

COMMITTEE MEMBER

(Associate Professor Nutchanart Sriwongsitanon, Ph.D.)

COMMITTEE MEMBER

(Associate Professor Varawoot Vudhivanich, Ph.D.)

DEPARTMENT HEAD

(Assistant Professor Napaporn Piamsa-nga, Ph.D.)

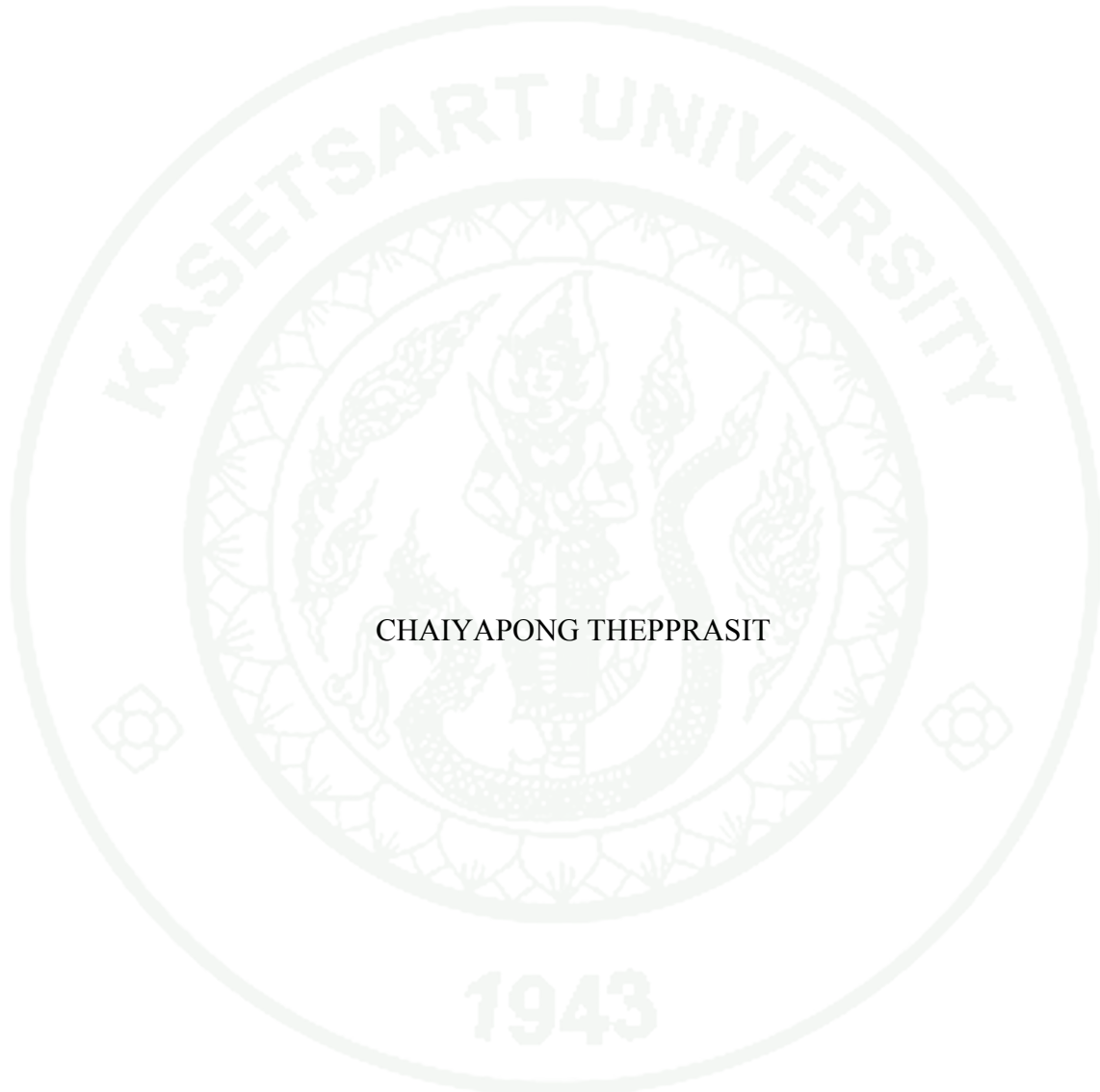
APPROVED BY THE GRADUATE SCHOOL ON

DEAN

(Associate Professor Gunjana Theeragool, D.Agr.)

THESIS

WATERSHED RUNOFF PREDICTION,
STREAMFLOW ANALYSIS AND RIVER MODELING
IN THE CHAO PHRAYA RIVER BASIN



A Thesis Submitted in Partial Fulfillment of
the Requirements for the Degree of
Doctor of Engineering (Water Resources Engineering)
Graduate School, Kasetsart University
2012

Chaiyapong Thepprasit 2012: Watershed Runoff Prediction, Streamflow Analysis and River Modeling in The Chao Phraya River Basin. Doctor of Engineering (Water Resources Engineering), Major Field: Water Resources Engineering, Department of Water Resources Engineering. Thesis Advisor: Associate Professor Kobkiat Pongput, Ph.D. 267 pages.

The purposes of this research were to determine the trends of weather variables, reference evapotranspiration and evapotranspiration parameters. In addition, the antecedent precipitation index relationships were evaluated in order to develop a rainfall-runoff model. The rainfall-runoff model was applied to evaluate outflow hydrographs at each watershed and also at the major reach of the upper Chao Phraya River Basin thus a better river basin management could be achieved.

To achieve these purposes, the daily average of evapotranspiration and evapotranspiration parameters from 1977 to 2006 was computed for each weather station by using the FAO Penman-Monteith method. The trend analysis was determined by Mann-Kendall test. Furthermore, the daily antecedent precipitation index of 112 small watersheds in the Upper Chao Phraya river basin was evaluated using the relationship of Kohler & Linsley. The watershed runoff was predicted from the best fit performance of the original antecedent precipitation index model; The antecedent precipitation index model was adjusted by evapotranspiration and critical antecedent precipitation index range models. In addition, Hydrologic Engineering Center-Hydrologic Modeling System was used to route hydrographs through the major reach of the Upper Chao Phraya River Basin.

The results revealed the weather variables to have both increasing and decreasing trends in evaporation, sunshine, and rainfall, decreasing trends in wind speed, and increasing trends in temperature and relative humidity. The evapotranspiration parameters have increasing trends in the soil heat flux and actual vapor pressure, and decreasing trends in vapor pressure deficit, net radiation, as well as evapotranspiration. In the analysis, watershed areas vary from 22.36 to 5,583.44 square kilometers. As for the study results of the soil water recession coefficient vary from 0.791 to 0.883 and the antecedent precipitation index vary from 2.55 to 5,583.44 mm/day. The finding indicates that a 60 percentage range of the critical antecedent precipitation index range which is a nonlinear multiple cubic regression, will be more appropriate for the estimated watershed runoff than the original antecedent precipitation index model, the adjusted antecedent precipitation index model and the other percentage range of the critical antecedent precipitation index range model. The accuracy of hydrograph calculated for each watershed and each major reach by using the Nash-Sutcliffe Efficiency and the correlation coefficient indicates the reliability of the model used for prediction.

Student's signature

Thesis Advisor's signature

/ /

ACKNOWLEDGEMENTS

I would like to grateful thank and deeply indebted to Assoc. Prof. Dr. Kobkiat Pongput my thesis advisor for advice, encouragement and valuable suggestion for completely writing of thesis. I would sincerely like to thank Assoc. Prof. Dr. Nutchanart Sriwongsitanon, and Assoc. Prof. Dr. Varawoot Vudhivanich, my committees, and also Prof. Dr. Gary P. Merlkey from Utah State University (USU) and Dr. Thana Boonyasirikul from Ratchaburi Electricity Generating Holding PCL for their valuable comments and suggestion.

I would like to sincerely thank Prof. Dr. G.V.Skogerboe who initiates the cooperation between Kasetsart University and Utah State University (USU.), and I gratefully thank Prof. Dr. David G. Tarboton during research work at Department of Civil and Environmental Engineering, Utah State University (USU).

I gratefully acknowledge the Thailand Research Fund through the Royal Golden Jubilee Ph.D. Program (RGJ) and Office of the Higher Education Commission for financially supporting this research. Also, I would like sincerely like to acknowledge the efforts of many people who contributed to the research and to this thesis in particular. Without them, the work would never have been undertaken.

Finally, my appreciation devote to my parents who always give me hearty support.

Chaiyapong Thepprasit

June 2012

TABLE OF CONTENTS

	Page
TABLE OF CONTENTS	i
LIST OF TABLES	ii
LIST OF FIGURES	v
INTRODUCTION	1
OBJECTIVES	2
LITERATURE REVIEW	3
MATERIALS AND METHODS	49
Materials	49
Methods	50
RESULTS AND DISCUSSION	80
CONCLUSION AND RECOMMENDATION	186
LITERATURE CITED	193
APPENDICES	204
Appendix A Data collection results	205
Appendix B Double mass curve of ET_o versus 0.7 <i>Epan</i>	226
Appendix C Compare performances of critical API range model	245
CURRICULUM VITAE	267

LIST OF TABLES

Table	Page
1 Physical characteristics of the Chao Phraya river basin	5
2 Hydrology of Chao Phraya river basin	7
3 Characteristics of major reservoirs	7
4 Groundwater storage and renewable water resource of the sub-basins	10
5 The large irrigation projects in the Chao Phraya river basin	11
6 Parameters used in the reference evapotranspiration equations	16
7 List of rainfall-runoff models with authors, and number of parameters.	25
8 Summary of small watersheds in the upper Chao Phraya river basin	51
9 Site descriptions and locations of weather stations.	54
10 Summary critical <i>API</i> range model for runoff estimation	71
11 Summary average of monthly ET_o parameters	81
12 Summary of average monthly reference evapotranspiration (ET_o)	84
13 P-value of weather variables trend	87
14 P-value of reference evapotranspiration (ET_o) trend and parameters for stations	100
15 Summary of maximum soil moisture available for evaporation (W_m) of surface soil (0-10 cm)	111
16 Daily average of soil water recession coefficient (K) for <i>API</i> analysis	115
17 Daily antecedent precipitation index (<i>API</i>)	118
18 Daily average of soil water recession coefficient adjust by ET (K_{adj})	122
19 Daily adjusted <i>API</i> by evapotranspiration (API_{adj})	125
20 Summary of critical antecedent precipitation index ($API_{critical}$)	129
21 Statistical measures of the similarity between simulated and observed hydrographs using original <i>API</i> model 1 to 6	133
22 Statistical measures of the similarity between simulated and observed hydrographs using adjusted <i>API</i> model 1 to 6	139
23 Compare performances of original <i>API</i> model and adjusted <i>API</i> model by evapotranspiration (ET)	146

LIST OF TABLES (Continued)

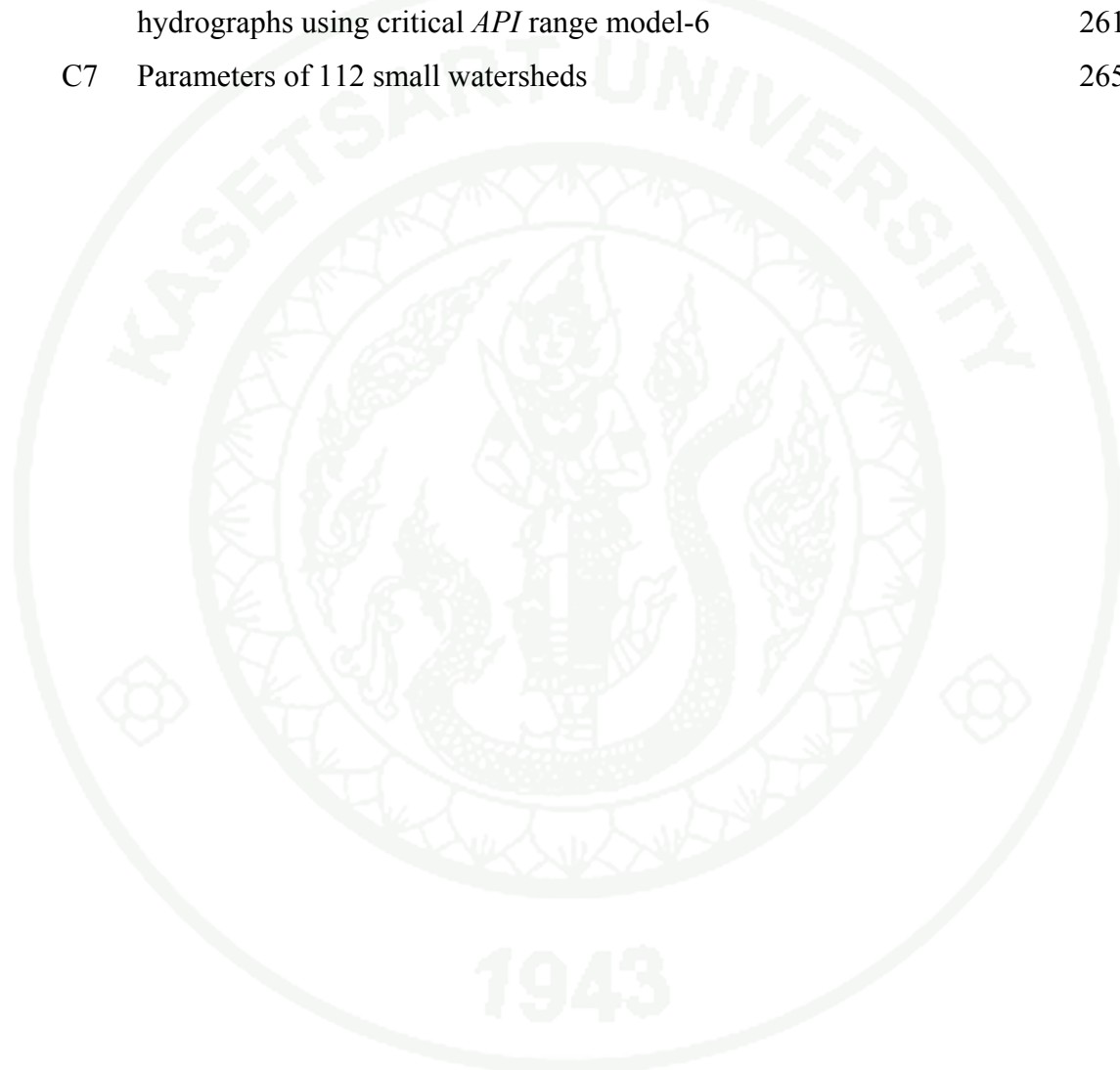
Table		Page
24	Compare performances of various range of critical <i>API</i> range model	152
25	Guideline for parameters of critical <i>API</i> range model-3 range of 60%	161
26	Model parameters of representative stream gauging stations	165
27	Sensitivity results on critical <i>API</i> range model parameters at P.14 station	166
28	Sensitivity results on critical <i>API</i> range model parameters at W.17 station	168
29	Sensitivity results on critical <i>API</i> range model parameters at Y.20 station	170
30	Sensitivity results on critical <i>API</i> range model parameters at N.24 station	172
31	Summary parameters of HEC-HMS model	184

Appendix Table

A1	List of rainfall stations used in this study	206
A2	List of stream gauging stations used in this study	210
A3	Soil test data	212
A4	Major land use of small watersheds	220
A5	Agriculture land use of small watersheds	223
C1	Statistical measures of the similarity between simulated and observed hydrographs using critical <i>API</i> range model-1	246
C2	Statistical measures of the similarity between simulated and observed hydrographs using critical <i>API</i> range model-2	249
C3	Statistical measures of the similarity between simulated and observed hydrographs using critical <i>API</i> range model-3	252
C4	Statistical measures of the similarity between simulated and observed hydrographs using critical <i>API</i> range model-4	255
C5	Statistical measures of the similarity between simulated and observed hydrographs using critical <i>API</i> range model-5	258

LIST OF TABLES (Continued)

Appendix Table	Page
C6 Statistical measures of the similarity between simulated and observed hydrographs using critical <i>API</i> range model-6	261
C7 Parameters of 112 small watersheds	265



LIST OF FIGURES

Figure	Page
1 The Chao Phraya river basin	3
2 Sub-basins of the Chao Phraya river basin	5
3 The upper and lower Chao Phraya river basin	9
4 Irrigation area in the Chao Phraya river basin	12
5 The evapotranspiration processes	13
6 Reference (ET_o), crop evapotranspiration under standard (ET_c) and non-standard conditions (ET_c adj)	17
7 A flow diagram of the Linsley and Crawford model	22
8 Classification of models based on process description	26
9 Classification of models based on space and time scale	26
10 Classification of models based on solution technique	27
11 The non-linear perturbation model with API -dependent gain factor	30
12 Schematic representation of the soil in the API -type model	32
13 Q/P as Function of P and $NAPI$ ($a = 0.5$, $b = -0.3$, $c = -0.4$)	34
14 Flow chart of model by Witthawatchutikul, (2005)	38
15 Prism storage and Wedge storage	45
16 Components of HEC-HMS	48
17 Conceptual Framework	52
18 Small watersheds of the upper Chao Phraya river basin	53
19 The location of weather stations rainfall stations and stream gauging stations in the upper Chao Phraya river basin	55
20 Schematic diagram of analytic reference evapotranspiration (ET_o)	58
21 Schematic diagram of analytic trend	60
22 Schematic diagram of analytic antecedent precipitation index (API)	61
23 Crop calendar of the upper Chao Phraya river basin	63
24 Simplified flow chart of the watershed runoff prediction	65
25 Location of stream gauging stations used for the analysis of testing the rainfall-runoff model performance	68

LIST OF FIGURES (Continued)

Figure		Page
26 Schematic diagram of the upper Ping river network		75
27 Schematic diagram of the upper Nan river network		76
28 Schematic diagram of the upper Chao Phraya (downstream of Bhumibol dam and Sirikit dam)		77
29 Schematic of calibration procedure		79
30 Mean annual reference evapotranspiration (ET_o) and their linear trends in weather stations		85
31 Summary of maximum air temperature trends		91
32 Summary of minimum air temperature trends		92
33 Summary of relative humidity trends		94
34 Summary of pan evaporation trends		95
35 Summary of sunshine duration trends		96
36 Summary of daily wind speed trends		98
37 Summary of daily rainfall trends		99
38 Summary of actual vapor pressure trends		104
39 Summary of vapor pressure deficit trends		105
40 Summary of net radiation trends		106
41 Summary of soil heat flux trends		108
42 Summary of reference evapotranspiration trends		109
43 Areal distributions of maximum soil moisture available for evaporation		113
44 Daily average of soil water recession coefficient (K) for API analysis		117
45 Daily average of antecedent precipitation index (API)		120
46 Daily average of soil water recession coefficient adjust by ET (K_{adj})		124
47 Daily average of adjusted API by evapotranspiration (ET)		127
48 Comparison of API and adjusted API by evapotranspiration (API_{adj})		128
49 Areal distribution analysis of critical antecedent precipitation index		131
50 Statistical measures of the similarity between simulated and observed hydrographs using original API model 1 to 6		135

LIST OF FIGURES (Continued)

Figure		Page
51 Statistical measures of the similarity between simulated and observed hydrographs using adjusted <i>API</i> model 1 to 6		141
52 Compare performances of original <i>API</i> model and adjusted <i>API</i> model by evapotranspiration (<i>ET</i>)		147
53 Compare performances of critical <i>API</i> range model and original <i>API</i> model		154
54 The model calibration results for the runoff station		159
55 The model performance for ungauged basin		163
56 Examples of watershed runoff estimation in year 2001		176
57 The upper Ping river network model of HEC-HMS model		178
58 The upper Nan river network model of HEC-HMS model		178
59 The upper Chao Phraya river network model of HEC-HMS model (downstream of Bhumibol dam and Sirikit dam)		178
60 Comparison of the calculate and observed outflow hydrographs at major reach of the upper Chao Phraya river network		179

Appendix Figure

B1 Double mass curve of ET_o and 0.7 <i>Epan</i> at Chiang Mai station during the 1977-2006	227
B2 Double mass curve of ET_o and 0.7 <i>Epan</i> at Bhumibol Dam station during the 1977-2006	229
B3 Double mass curve of ET_o and 0.7 <i>Epan</i> at Tak station during the 1977-2006	231
B4 Double mass curve of ET_o and 0.7 <i>Epan</i> at Lampang station during the 1977-2006	233
B5 Double mass curve of ET_o and 0.7 <i>Epan</i> at Phrae station during the 1977-2006	235

LIST OF FIGURES (Continued)

Appendix Figure	Page
B6 Double mass curve of ET_o and 0.7 <i>Epan</i> at Nan station during the 1977-2006	237
B7 Double mass curve of ET_o and 0.7 <i>Epan</i> at Uttaradit station during the 1977-2006	239
B8 Double mass curve of ET_o and 0.7 <i>Epan</i> at Phitsanulok station during the 1977-2006	241
B9 Double mass curve of ET_o and 0.7 <i>Epan</i> at Nakhon Sawan station during the 1977-2006	243

WATERSHED RUNOFF PREDICTION, STREAMFLOW ANALYSIS AND RIVER MODELING IN THE CHAO PHRAYA RIVER BASIN

INTRODUCTION

Within the Chao Phraya river basin, there is a high risk of flooding during the monsoon season while the dry season experiences significant water shortages. The amount of water is dependent on the rainfall surplus. Thus, the areal distribution of rainfall in each watershed needs to be properly evaluated in order to improve hydrological model predictions.

This doctoral research use long-term period of weather data, daily rainfall data and soil moisture data to evaluate reference evapotranspiration (ET_o) and antecedent precipitation index (API) relationship throughout the upper Chao Phraya river basin. In addition, land use data and crop coefficient (K_c) were used to adjust the recession coefficient (K) of antecedent precipitation index (API) in order to use the adjusted recession coefficient (K) to evaluate the adjusted antecedent precipitation index (API).

The results of reference evapotranspiration (ET_o), antecedent precipitation index (API) and adjusted antecedent precipitation index (API) need to be combined with existing rainfall and streamflow records in order to develop predictive relationships for streamflow runoff from the various watersheds in the Chao Phraya river basin. To be useful for river basin management, these predicted hydrographs must be incorporated into the development of river models suitable for operational management.

OBJECTIVES

The objectives for this research are:

1. Using long-term period of weather data to evaluate reference evapotranspiration (ET_o) and using Mann-Kendall statistical test, determine the trends of weather variables, reference evapotranspiration parameters and reference evapotranspiration in the upper Chao Phraya river basin.
2. Using daily rainfall data and soil moisture data with reference evapotranspiration information to evaluate antecedent precipitation index (API) relationship for the upper Chao Phraya river basin.
3. Using land use data and crop coefficient (K_c) to adjust the recession coefficient (K) of antecedent precipitation index (API) and using adjusted K to evaluate antecedent precipitation index (API) relationship.
4. Using antecedent precipitation index (API) to develop a rainfall-runoff model and to compare the result from the original recession coefficient (K) and adjusted K (K_{adj}).
5. To predict (forecast) outflow hydrographs for each of the watershed and each major reach of the upper Chao Phraya river channel network.

LITERATURE REVIEW

1. Description of the study area

1.1 Location and physical characteristics

The Chao Phraya river basin covers area of 157,926 sq.km, which is about 30 percent of Thailand area. The basin drains into the gulf of Thailand, part of the South China Sea and the Pacific Ocean. Bangkok, a city of more than 8 million people, is located near the mouth of the Chao Phraya river. Bangkok is not only Thailand's official capital city, but also the capital city for trade, government and South-East Asia air transportation, as well as being the gateway to Indochina and south China. Location map is shown in Figure 1.



Figure 1 The Chao Phraya river basin.

Source: AFDEC (2002)

The Chao Phraya river basin is Thailand's largest and most important geographical unit in terms of land and water resources development. It is located in the north and central regions of the country. Irrigation projects in the Chao Phraya

river basin consist of 26 large projects, 14 medium projects, and 119 small projects, located in 15 provinces, namely Chai Nat, Sing Buri, Ang Thong, Ayutthaya, Lop Buri, Saraburi, Nonthaburi, Pathum Thani, Nakorn Sawan, Suphan Buri, Nakorn Pathom, Samutsakorn, Samutpakan, Chachoengsao, and Bangkok. Total project area is 8.855 million rai or 70.4 percent of the Chao Phraya river basin. At the beginning stage of the rainy season, it rains locally and within short periods. Non-rain days sometimes continue for quite a long period. The runoff ratio is difficult to estimate. However, it is estimated of around between 15 and 30% (Atthaporn, 1999). Tidal effects sometimes come to Ang Thong. This area often suffers from water shortage and flooding. Therefore, water operation is essential for the prosperity of the area.

Sub-basins of the Chao Phraya river basin include the eight sub-basins of, Wang, Yom, Nan, Sakae Krang, Pasak, Tha Chin and Main Chao Phraya, and Chao Phraya sub-basins as shown in Figure 2.

The headwaters of the Chao Phraya river originate in the mountainous terrain of the northern part of the country and consist of four large tributaries: the Ping, Wang, Yom and Nan rivers. The main river system passes through or close to many of the major population centres of the country including Bangkok, which is situated at its downstream end. The four upstream tributaries flow southward to meet at Nakhon Sawan and form the Chao Phraya river. The river flows southward through a large alluvial plain, called the delta area, splitting into four channels: the Tha Chin (also called the Suphan and Nakhon Chai Si further downstream), the Noi, the Lop Buri and the Chao Phraya rivers, And Physical characteristics of the Chao Phraya river basin as shown in Table1.

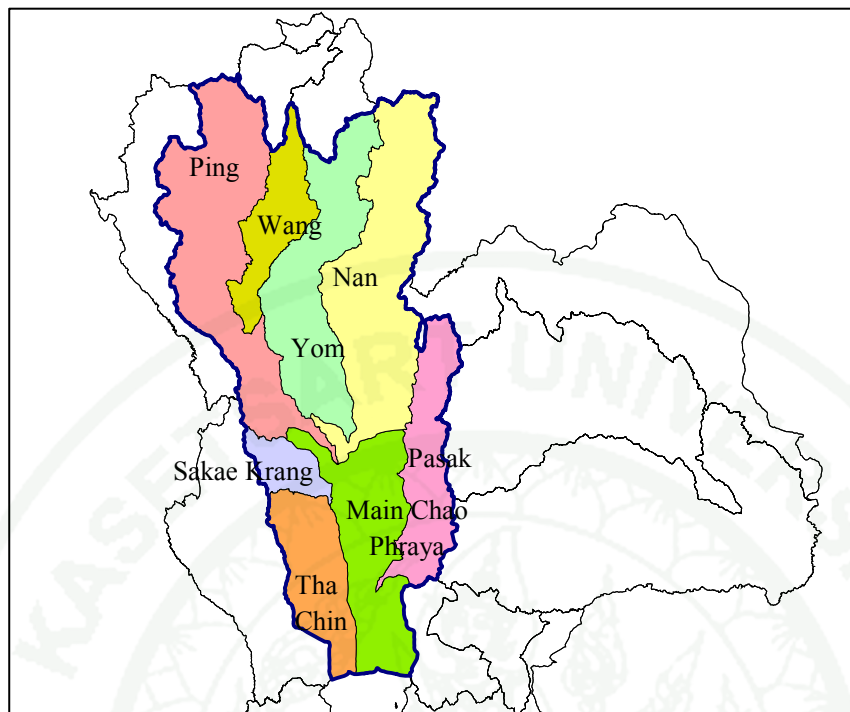


Figure 2 Sub-basins of the Chao Phraya river basin.

Table 1 Physical characteristics of the Chao Phraya river basin.

Sub-basins	Catchment Area (sq.km)	Lengths of Main Channel (km)	Major Structural in Main Channel	
			Large Reservoir	Weir and Regulator
Ping	33,898	789.70	3	3
Wang	10,791	481.99	1	0
Yom	23,616	802.52	-	1
Nan	34,330	754.72	2	0
Sakae Krang	5,192	394.22	1	0
Pasak	16,292	578.89	1	0
Tha Chin	13,682	296.28	1	5
Main Chao Phraya	20,125	369.45	1	15
Summary	157,926	4,467.77	10	24

1.2 Hydrology of Chao Phraya river basin

The Chao Phraya river basin is influenced by the southwest monsoon, northeast monsoon and depression storms to form three seasons: the rainy season between May to October; winter from November to February; and summer between the middle of February to May. Average climatology in the Chao Phraya river basin consists of average temperature of 27.1 degrees celsius, relative humidity is 72.6 percent, wind speed is 2.22 knots, cloudiness is 5.73 units, and evaporation is 1,700 mm. The Chao Phraya river basin has a total of 706 rainfall stations (Ping river basin 116 stations, Wang river basin 27 stations, Yom river basin 49 stations, Nan river basin 70 stations, Sakae Krang river basin 16 stations, Pasak river basin 64 stations, Tha Chin river basin 129 stations and Main Chao Phraya river basin 235 stations). The annual rainfall in the basin varies from 1,100 mm in the western area to 1,300 mm in the northeastern area, and the average yearly rainfall is about 1,163 mm. There are a total of 273 stream gauging stations (Ping river basin 98 stations, Wang river basin 25 stations, Yom river basin 27 stations, Nan river basin 65 stations, Sakae Krang river basin 10 stations, Pasak river basin 28 stations, Tha Chin river basin 5 stations and Main Chao Phraya river basin 15 stations). The average yearly surface runoff total about 36,833 million cubic meters (MCM), and the major runoff comes from the Ping and Nan sub-basins with 24% and 32% of the total basin runoff as shown in Table 2.

The river basin can be characterized geographically into upper and lower basins. The upper basin is mountainous. Water resources in the basin are stored at the Bhumibol reservoir dam with a storage capacity of 13,500 MCM and the Sirikit reservoir dam with a storage capacity of 9,500 MCM. The Pasak reservoir dam has a storage capacity of 960 MCM. The Chao Phraya diversion dam in the Chao Phraya river at Chainat enables the allocation of water for the delta area. The Chao Phraya river basin has 9 major reservoirs as shown in Table 3, and the two largest dams of the Chao Phraya river basin are Bumiphol and Sirikit; together, they control the runoff from 22 percent of the entire basin.

Table 2 Hydrology of Chao Phraya river basin

Sub-basins	Average annual	Average annual	Percentage of total
	Rainfall (mm)	Runoff (mcm)	annual runoff
Ping	1,152	8,800	23.9
Wang	1,102	1,624	4.4
Yom	1,167	3,648	10.0
Nan	1,295	11,936	32.4
Sakae Krang	1,179	1,080	2.9
Pasak	1,209	2,823	7.7
Tha Chin	1,102	2,449	6.7
Main Chao Phraya	1,099	4,435	12.0
Total	1,163	36,833	100.0

Source: RID (2000)

Table 3 Characteristics of major reservoirs

Reservoir name	Sub-basins	Maximum retention (mcm)	Normal retention (mcm)	Minimum retention (mcm)	Effective storage (mcm)
Bhumibol	Ping	13,456	13,462	3,800	9,662
Sirikit	Nan	10,640	9,510	2,850	6,660
Kiew Lom	Wang	112	112	4	108
Mae Ngat	Ping	325	265	10	255
Mae Kuang	Ping	263	263	14	249
Mae Chang	Wang	108	NA	NA	NA
Thap Salao	Sakae Krang	198	160	8	152
Kra Sieo	Tha Chin	363	240	40	201
Pasak	Pasak	960	NA	NA	785

Source: ONWRC (n.d.)

The Chao Phraya river basin can be divided into two regions: the upper basin (the catchment area of Chao Phraya diversion dam) and the lower basin (the downstream of dam to the Gulf of Thailand) as shown in Figure 3. The upper Chao Phraya river basin is a water source that important for water supply, agriculture and various water use of 23 million people of the Chao Phraya river basin in Thailand. The area of the upper Chao Phraya river basin is 89,422 km², representing 17.5 percent of the country's area and representing 56.6 percent of the Chao Phraya river basin's area. This upper Chao Phraya river basin is comprised of five sub-basins; Ping, Wang, Yom, Nan and a part of Chao Phraya between conjunction of Ping and Nan throughout stream gauging station C.2 at amphoe Mueang in Nakhon Sawan province.

1.3 Ground water of Chao Phraya river basin

Aquifer distribution: Hydrogeologically, the Chao Phraya river basin is comprised of seven groundwater sub-basins: Chiangmai-Lampoon basin, Lampang basin, Payao basin, Prae basin, Nan basin, Upper Chao Phraya basin and Lower Chao Phraya basin. Within these groundwater sub-basins, water is held in either confined or unconfined aquifers. Eight separate confined aquifers are located in the Upper Tertiary to Quaternary strata of the Bangkok area. The natural groundwater within this succession of aquifers is highly confined, creating artesian conditions in each. Ease of exploitation, as well as the high chemical quality, are the main reasons for the original development of this source. Groundwater storage and renewable resources have been estimated for each groundwater sub-basin, as shown in Table 4.

Recharge, flow and discharge: There are few existing estimates available of groundwater recharge on a regional basis. In an artesian aquifer, as that beneath Bangkok, storage depletion is seen through a decline in piezometric pressure and a reduction in the area in which artesian conditions exist. The continued decline in levels indicates that abstraction is not in balance with recharge. In unconfined aquifers, abstraction of resources in excess of natural recharge normally leads to a much lower rate of water leveldecline than that of confined aquifers.

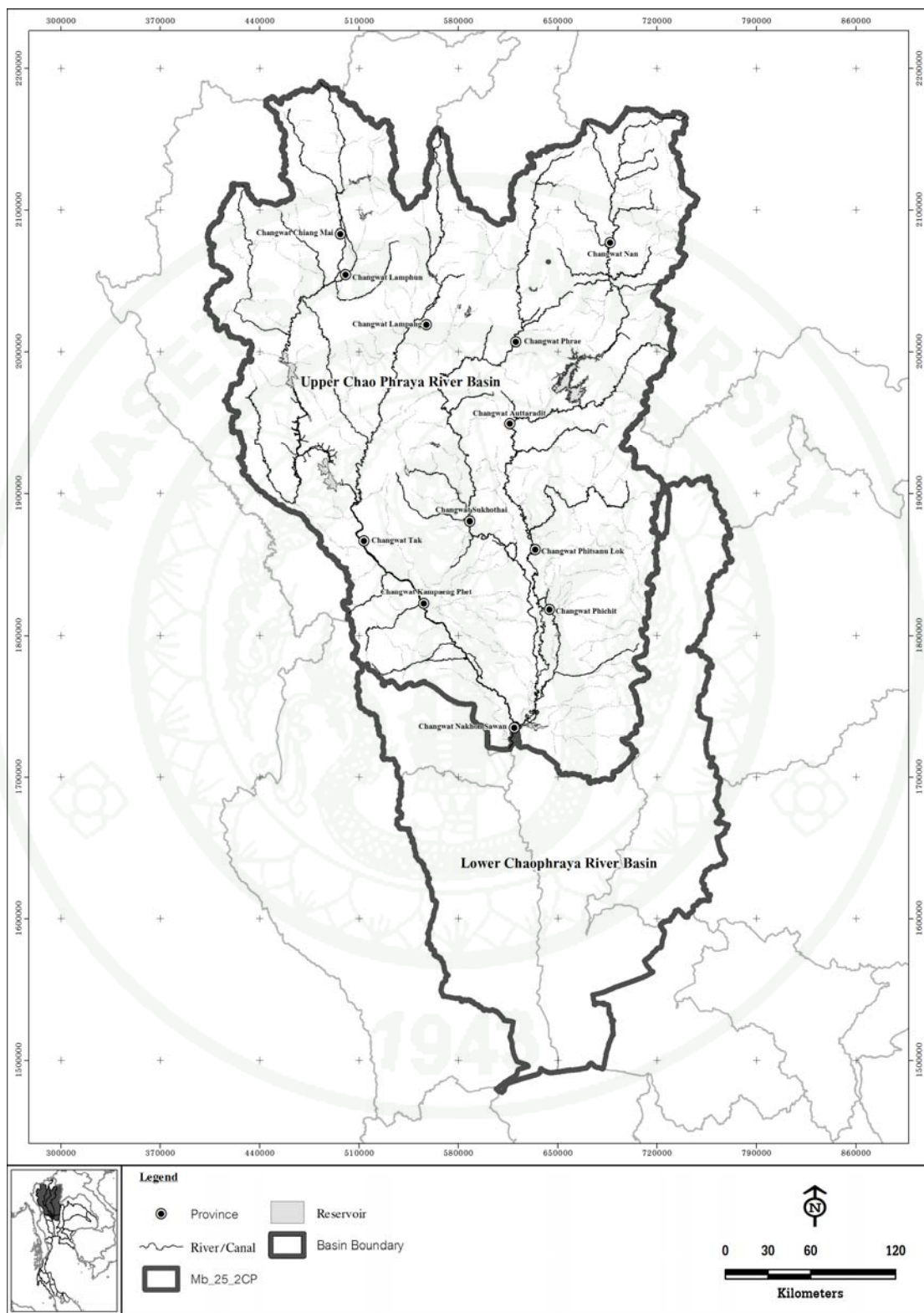


Figure 3 The upper and lower Chao Phraya river basin.

Table 4 Groundwater storage and renewable water resource of the sub-basins

Groundwater basin	Groundwater storage (mcm)	Renewable water resources (mcm)
Chiangmai-Lampoon	485	97
Lampang	295	59
Chiangrai-Payao	212	42
Prae	160	32
Nan	200	40
Upper Chao Phraya	6,400	1,280
Lower Chao Phraya	6,470	1,294
Total	14,222	2,844

Source: ONWRC (n.d.)

1.4 Water management in Chao Phraya river basin

The Chao Phraya river basin is used for agriculture and covered with forest. The major forest areas are in the northern sub-basins, those are Ping, Wang, Yom, and Nan. The Chao Phraya sub-basin also has some forest area. Agricultural areas are concentrated in the southern sub-basins and ranges from 78% in the Chao Phraya, 63% in Pasak and 55% in Tha Chin compared to 20 to 45% in the four northern sub-basins (Ping, Wang, Yom and Nan).

The large irrigation projects in the Chao Phraya river basin serve approximately 9.8 million rai, with 7.7 million rai in the Main Chao Phraya and Tha Chin, or 80% of the large irrigated area in the Chao Phraya river basin. These irrigation projects are listed by sub-basins in Table 5. (Shown in Figure 4).

Total area of the upper east bank of the Chao Phraya Delta is 1.525 million rai including 1.3625 million rai of irrigated area. The area is located in a part of Chai Nat, Nakhon Sawan, Lop Buri, Saraburi, Sing Buri, Ang Thon and Phra

Nakhon Si Ayutthaya provinces. They obtain water resources from rainfall and the Chao Phraya river. The Chainat-Pasak Canal and Chainat-Ayutthaya Canal are used to convey water from the Chao Phraya river through the Manorom Regulator and the Maharaj Regulator, respectively. The maximum flow capacity of the Chainat Pasak Canal is 210 m³/s and that of the Chinat-Ayutthaya Canal is 75 m³/s. These facilities were constructed under the Great Chao Phraya Project, along with a lateral distribution canal system and drainage system.

Table 5 The large irrigation projects in the Chao Phraya river basin.

Sub-basin	Watershed area (Million rai)	Number of large irrigation projects	Irrigation Area (rai)
Ping	21.19	9	782,900
Wang	6.74	1	130,000
Yom	14.76	1	224,000
Nan	21.46	4	667,100
Pasak	10.18	1	135,300
Sakae Krang	3.24	1	143,500
Main Chao Phraya and Tha Chin	12.58	27	7,740,443
Total	98.70	44	9,823,243

Source: RID (2000)

Water availability is a key factor for constraining future agricultural development in the Central Plain, because it is the core of multi-cropping and for crop diversification. Water management for agricultural areas must aim to achieve greater equity and efficiency in water deliveries at the basin, irrigation project, and farm level. For example the achievement of high water use efficiency through crop diversification depends on much greater local level control on water deliveries.

The Royal Irrigation Department (RID) supervises water management in Thailand. Each irrigation project is supervised by RID. Irrigation projects include large-scale, medium, small-scale and pumping projects. In the irrigation project, a zone man is responsible for the distribution of water at the farm level, where cropping patterns and water demands of farmers are recorded. A zone man looks after approximately 10,000 rai of irrigated area. The zone man will report cropping patterns of farmers in the irrigation project every week. Accordingly, the recording of accurate cropping patterns in all irrigation projects is difficult to achieve. The Chao Phraya river basin has 44 large irrigation projects. For the collection of data by RID, the zone man is the first to record and then report to the irrigation project. Thereafter, all irrigation projects report to RID.

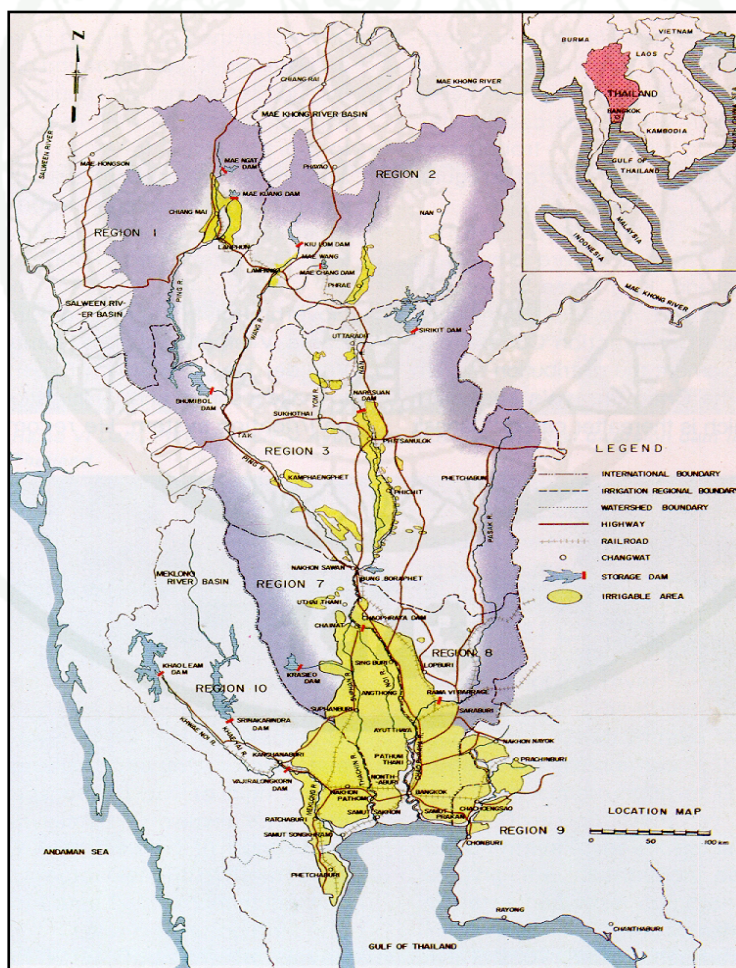


Figure 4 Irrigation area in the Chao Phraya river basin.

2. Evapotranspiration

Evapotranspiration is an important part of the hydrologic cycle and water use because it represents a considerable loss of usable water from the hydrologic supply. The process known as evapotranspiration (ET) is of great importance in many disciplines, including water demand analysis, irrigation scheduling and hydrologic and drainage studies. In a broad definition, evapotranspiration (ET) is a term used to describe the sum of evaporation and plant transpiration from the earth's land surface to atmosphere as. The evapotranspiration processes shown in Figure 5. Evaporation accounts for the movement of water to the air from sources such as the soil, canopy interception, and waterbodies. Transpiration accounts for the movement of water within a plant and the subsequent loss of water as vapor through stomata in its leaves.

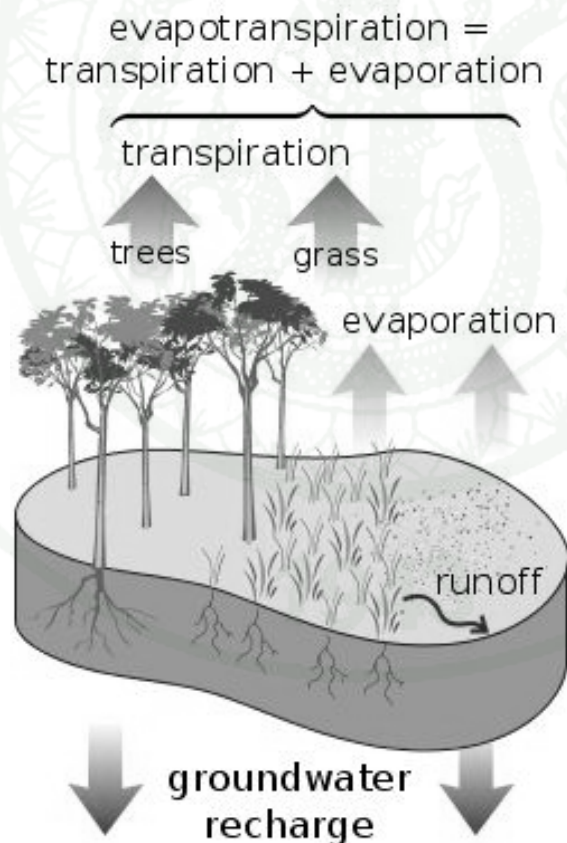


Figure 5 The evapotranspiration processes.

Source: wikipedia (2012)

2.1 Potential evapotranspiration (PET)

Potential evapotranspiration (PET) is a representation of the environmental demand for evapotranspiration and represents the evapotranspiration rate of a short green crop, completely shading the ground, of uniform height and with adequate water status in the soil profile. It is a reflection of the energy available to evaporate water, and of the wind available to transport the water vapour from the ground up into the lower atmosphere. Evapotranspiration is said to equal potential evapotranspiration when there is ample water.

The potential evapotranspiration concept was first introduced in the late 1940s and 50s by Penman and it is defined as "the amount of water transpired in a given time by a short green crop, completely shading the ground, of uniform height and with adequate water status in the soil profile". Note that in the definition of potential evapotranspiration, the evapotranspiration rate is not related to a specific crop. The main confusion with the potential evapotranspiration definition is that there are many types of horticultural and agronomic crops that fit into the description of short green crop. So, scientists may be confused as to which crop should be selected to be used as a short green crop because the evapotranspiration rates from well-watered agricultural crops may be as much as 10 to 30% greater than that occurring from short green grass (Irmak and Dorota, n.d.).

2.2 Reference crop evapotranspiration (ET_o)

Reference evapotranspiration is defined as "the rate of evapotranspiration from a hypothetical reference crop with an assumed crop height of 0.12 m (4.72 in), a fixed surface resistance of 70 sec m⁻¹ (70 sec 3.2ft⁻¹) and an albedo of 0.23, closely resembling the evapotranspiration from an extensive surface of green grass of uniform height, actively growing, well-watered, and completely shading the ground". In the reference evapotranspiration definition, the grass is specifically defined as the reference crop and this crop is assumed to be free of water stress and diseases. In the literature, the terms "reference evapotranspiration" and

"reference crop evapotranspiration" have been used interchangeably and they both represent the same evapotranspiration rate from a short, green grass surface (Irmak and Dorota, n.d.).

Reference evapotranspiration can be estimated by using parameters and weather variables. The various parameters used in the reference evapotranspiration equations such as latent heat of vaporization, slope of vapour pressure curve, psychrometric constant, atmospheric pressure, atmospheric density, saturation vapour pressure, actual vapour pressure, vapour pressure deficit, extraterrestrial radiation, daylight hours, wind speed and day wind (Smith, 1990). The parameters can be calculated by equations as shown in Table 6 and the reference crop evapotranspiration (ET_o) can be calculated on a daily basis using the FAO Penman-Monteith equation (Allen et al., 1998):

$$ET_o = \frac{0.408\Delta(R_n - G) + \gamma \frac{900}{T+273} U_2(e_a - e_d)}{\Delta + \gamma(1 + 0.34U_2)} \quad (1)$$

where ET_o is the reference crop evapotranspiration (mm d^{-1}), R_n is net radiation at crop surface ($\text{MJ m}^{-2} \text{d}^{-1}$), G is soil heat flux ($\text{MJ m}^{-2} \text{d}^{-1}$), T is average temperature ($^{\circ}\text{C}$), U_2 is windspeed measured at 2 m height (m s^{-1}), $(e_a - e_d)$ is vapour pressure deficit (kPa), Δ is slope vapour pressure curve ($\text{kPa } ^{\circ}\text{C}^{-1}$), γ is psychrometric constant ($\text{kPa } ^{\circ}\text{C}^{-1}$) and 900 is conversion factor. For this equation, reference evapotranspiration is estimated for a hypothetical short grass with a height of 0.12 m, a surface resistance of 70 s m^{-1} , and albedo of 0.23 (Allen et al., 1998).

Distinctions are made (Figure 6) between reference crop evapotranspiration (ET_o), crop evapotranspiration under standard conditions (ET_c) and crop evapotranspiration under nonstandard conditions ($ET_c \text{ adj}$). ET_o is a climatic parameter expressing the evaporation power of the atmosphere. ET_c refers to the evapotranspiration from excellently managed, large, wellwatered fields that achieve full production under the given climatic conditions. Due to suboptimal crop

management and environmental constraints that affect crop growth and limit evapotranspiration, ET_c under non-standard conditions generally requires a correction (Allen et al., 1998).

Table 6 Parameters used in the reference evapotranspiration equations

No.	Parameter	Definition
1. Latent Heat of Vaporization (λ)	$\lambda = 2.501 - (2.361 \times 10^{-3})T$	λ = latent heat of vaporization [MJ kg ⁻¹] T = air temperature [°C]
2. Slope Vapour Pressure Curve (Δ)	$\Delta = \frac{4098 e_a}{(T + 237.3)^2}$	Δ = slope vapour pressure curve [kPa °C ⁻¹] T = air temperature [°C] e_a = saturation vapour pressure at temperature T [kPa]
3. Psychrometric Constant (γ)	$\gamma = \frac{c_p P}{\varepsilon \lambda} \times 10^{-3} = 0.00163 \frac{P}{\lambda}$	γ = psychrometric constant [kPa °C ⁻¹] c_p = specific heat of moist air = 1.013 [kJ kg ⁻¹ °C ⁻¹] P = atmospheric pressure [kPa] ε = ratio molecul. weight water vapour/dry air = 0.622 λ = latent heat [MJ kg ⁻¹]
4. Atmospheric Pressure (P)	$P = P_o \left(\frac{T_{ko} - \alpha(z - z_o)}{T_{ko}} \right)^{\frac{g}{\alpha R}}$	P = atmospheric pressure at elevation z [kPa] P_o = atmospheric pressure at sea level [kPa] z = elevation [m] z_o = elevation at reference level [m] g = gravitational acceleration = 9.8 [m s ⁻²] R = specific gas constant = 287 [J kg ⁻¹ K ⁻¹] T_{ko} = reference temperature [K] at elev. z_o = 273 + T [°C] α = Constant lapse rate saturated air = 0.0065 [K m ⁻¹]
5. Atmospheric density (ρ)	$\rho = \frac{1000 P}{T_{kv} R} = 3.486 \frac{P}{T_{kv}}$	ρ = atmospheric density [kg m ⁻³] P = atmospheric pressure at elevation z [kPa] R = specific gas constant = 287 [J kg ⁻¹ K ⁻¹] T_{kv} = virtual temperature [K]
6. Saturation vapour pressure (e_a)	$e_a = 0.611 \exp \left(\frac{17.27 T}{T + 237.3} \right)$	e_a = saturation vapour pressure [kPa] T = temperature [°C]
7. Actual Vapour Pressure (e_d)	$e_d = RH_{mean} / \left(\frac{50}{e_{a(T_{min})}} + \frac{50}{e_{a(T_{max})}} \right)$	e_d = average daily vapour pressure RH_{mean} = mean daily relative humidity $e_{a(T_{min})}$ = saturation vapour pressure at T_{min} [kPa] $e_{a(T_{max})}$ = saturation vapour pressure at T_{max} [kPa]
8. Vapour Pressure Deficit (VPD)	$VPD = e_a - e_d = \frac{e_{a(T_{max})} + e_{a(T_{min})}}{2} - e_d$	VPD = vapour pressure deficit [kPa] $e_{a(T_{max})}$ = saturation vapour pressure at T_{max} [kPa] $e_{a(T_{min})}$ = saturation vapour pressure at T_{min} [kPa] e_d = actual vapour pressure [kPa]

Table 6 (Continued)

No.	Parameter	Definition
9. Extraterrestrial Radiation (R_a)	$R_a = \text{extraterrestrial radiation } [\text{MJ m}^{-2} \text{ d}^{-1}]$ $d_r = \text{relative distance Earth - Sun}$ $\delta = \text{solar declination } [\text{rad}]$ $\varphi = \text{latitude } [\text{rad}]$ $\omega_s = \text{sunrise hour angle } [\text{rad}]$ $R_a = 37.6 d_r (\omega_s \sin \varphi \sin \delta + \cos \varphi \cos \delta \sin \omega_s)$	
10. Daylight Hours (N)	$N = \text{maximum day light hours } [\text{h}]$ $N = \frac{24}{\pi} \omega_s = 7.64 \omega_s$	
11. Wind speed (U_2)	$U_z = \text{windspeed measurement at height } z [\text{ms}^{-1}]$ $U_2 = \text{windspeed measurement at 2 m height } [\text{m s}^{-1}]$ $z = \text{height windspeed measurements [m]}$ $z_2 = \text{standard height windspeed measurements [m]} = 2 \text{ [m]}$ $d = \text{zero plane displacement of wind profile [m]} = 0.08$ $z_o = \text{roughness parameter for momentum [m]} = 0.015$ $\frac{U_2}{U_z} = 4.87 / \ln(67.8 z - 5.42)$	
12. Day Wind	$U_d = \text{windspeed during day time (07.00 - 19.00 hrs)} [\text{m s}^{-1}]$ $U_n = \text{windspeed during night time (19.00 - 07.00)} [\text{m s}^{-1}]$ $U = \text{average windspeed over 24 hours} [\text{m s}^{-1}]$ $U_d = \frac{2U(U_d/U_n)}{(1+U_d/U_n)}$	

Source: Allen et al. (1998)

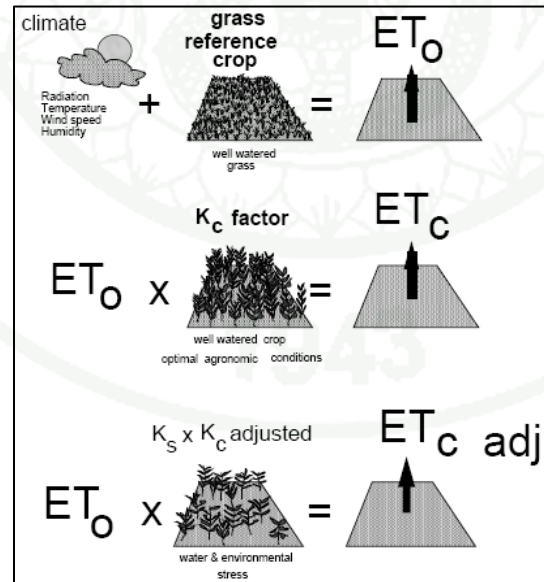


Figure 6 Reference (ET_o), crop evapotranspiration under standard (ET_c) and non-standard conditions (ET_c adj)

Source: Allen et al., 1998.

3. Antecedent precipitation index

Antecedent precipitation index (*API*) is an indicator of soil moisture content based on daily rainfall or *API* is a weighted summation of daily precipitation amounts, used as an index of soil moisture. The weight given each day's precipitation is usually assumed to be an exponential or reciprocal function of time with the most recent precipitation receiving the greatest weight. The antecedent precipitation index method is commonly used to initialize some rainfall models.

Kohler & Linsley (1951) developed a soil moisture depletion model:

$$API_i = K_i \cdot (API_{i-1}) \quad (2)$$

where API_i is the antecedent precipitation index on a given day i , K is a recession coefficient which is a function of time, soil depth, and the inverse of mean daily temperature which usually will has value 0.85 to 0.98. Furthermore, if there is rainfall event on day i , P_i . Equation (2) will change into the form of:

$$API_i = (K_i \cdot API_{i-1}) + P_i \quad (3)$$

In 1983 Choudhury and Blanchard has found the recession coefficient (K) can use soil texture information and climatological data to obtain potential evapotranspiration, it will be possible to calculate a good first approximation for the recession coefficient (K) and to simulate moisture conditions in large areas. The method of the recession coefficient given by Choudhury and Blanchard (1983):

$$K_i = \exp\left(\frac{-PET_i}{W_m}\right) \quad (4)$$

where K_i is a recession coefficient, PET_i is a potential evapotranspiration on a given day i and W_m is a maximum soil moisture available for evaporation in millimeter which;

$$W_m = (WHC / 100) * (B.D. * 100) \quad (5)$$

where WHC is a water holding capacity (%) and $B.D.$ is a bulk density (g/cm^2)

In Thailand, Witthawatchutikul (1985) has found that the value of streamflow recession is close to the value of K and can be applied as API value in estimation of flow. This is similar to the slow flow component used in the IHACRES rainfall-runoff model. The recession coefficient (K) can calculate from the ratio of flow of a given day, Q_i to flow of the previous day Q_{i-1}

$$K_i = \left(\frac{Q_i}{Q_{i-1}} \right) \quad (6)$$

Several research have used API as inputs into hydrological models, such as water infiltration and low stream flows (Papadakis & Pruel, 1973; Alikhan et al., 1972). Blanchard et al.(1981) related API to surface soil moisture content (Rosenthal et al., 1982).

In Thailand, antecedent precipitation index (API) most frequently use to warning flash flood and landslide by Thai Meteorological Department, National Park, Wildlife and Plant Conservation Department, Department of Water Resources and the research for warning flash flood and landslide from daily rainfall by using API (Pongput et al., 2008).

4. Watershed runoff analysis

4.1 Rational method

Probably the first serious attempts to estimate flood flow volumes can be traced back to a group of Irish engineers, who were given the task to design drainage channels in 1842 (Biswas, 1970). Ten years later, in 1851, Thomas Mulvaney (1822 – 1892) presented a paper which can be considered as the origin of

the so-called rational method for flood peak estimation (Dodge, 1957). The method can be written as

$$q_{max} = f_r P_{max} A \quad (7)$$

where q_{max} is the maximum rate of runoff, f_r is the runoff coefficient, P_{max} is the maximum rate of rainfall, and A is the area of the catchment. The rational method has stood the test of time well as a simple tool to estimate peak flows. The latest edition of the Handbook of Hydrology presents the rational method in the flood runoff chapter (Pilgrim and Cordery, 1992), and Pilgrim (1986) names it as the most widely used method for drainage design in urban areas.

4.2 Unit hydrograph

It took 80 years before significant progress over the rational method was achieved in representing rainfall-runoff relationships mathematically. It came with the method proposed by Sherman (1932), which allowed calculation of continuous hydrographs as opposed to merely delivering a peak flow estimate of the maximum flood event. Sherman called his method a unit-graph method, but it is presently better known as the unit hydrograph method. In essence, the unit hydrograph is equivalent to the systems analysis concept of the impulse response function, which depicts the response, $x(t)$, of a system to an infinitesimally short unit input. The output of a linear system, resulting from a continuous input, $i(t)$, is given by the following convolution integral

$$x(t) = \int i(\tau) r(t-\tau) d\tau \quad (8)$$

where $r(t)$ is the impulse response function.

In the case of rainfall-runoff computations, the input in equation (8) is rainfall multiplied by the (surface) runoff coefficient. This is because, mainly due to evapotransporative losses, not all of the rainfall is converted into streamflow.

Furthermore, Sherman thought the output of equation (8) to represent only the quick, surface runoff component. The so-called base flow, which is the part of a hydrograph preceding a storm and continuing after recession of a flow peak, he attributed to discharge of groundwater.

Since its proposal the unit hydrograph has established itself as a widely used engineering tool for assessing real floods, and for creating design floods from hypothetical storms. Pilgrim and Cordery (1992) describe the HEC-1 model as the most widely used model in the United States, and it includes the unit hydrograph as one of the two available computation methods for runoff generation. Recent publications reporting application of the unit hydrograph include Cheng and Wang (2002) and Littlewood (2001). In Finnish conditions, Mustonen (1963) derived unit hydrographs separately for storm events of short and long duration using data from a small, cultivated catchment (0.12 sq.km).

The linearity assumption behind the unit hydrograph methods was later subject to criticism and it was suggested that the unit hydrograph itself, not only the share of rainfall becoming effective rainfall, might vary with the storm intensity (e.g. Minshall, 1960). Consequently, some papers have put forward unit hydrographs that depend on the intensity of the effective rainfall (Cheng and Singh, 1986; Ding, 1974).

4.3 Conceptual of rainfall-runoff relationships

Usually analysts have some kind of a perception in their mind about the behaviour of the hydrological system under study. The rationale for incorporating such concepts into the structure of a hydrological model can be an attempt to reproduce streamflow more accurately at the point of interest, or the need to include representations of various hydrological fluxes and runoff pathways into the model.

In 1934 Zoch (1934) developed equations relating rainfall to the rate of runoff, based on the assumption that the rate of runoff is proportional to the rainfall remaining with the soil. This is probably among the first published studies, where a

linear store is applied to represent the delay between rainfall and streamflow. Later Nash (1957) showed how the response of a cascade of such linear stores could be characterized as a mathematical function involving two parameters. Nash's primary motivation was to introduce a computationally convenient form for an instantaneous unit hydrograph in order to relate its parameters to catchment characteristics. But he also made the concept of linear stores as a delay mechanism in runoff computations popular. This paved the way for the development of conceptual rainfall-runoff models, usually comprising interrelated stores recharged and depleted by appropriate component processes of the hydrological system.

One of the first conceptual, hydrological models for continuous streamflow simulation was that of Linsley and Crawford (1960), which was developed to assess increase of the capacity of one of the water supply reservoirs of the Stanford University. The structure of the model (Figure 7) is typical of many conceptual streamflow models, comprising storages representing upper level soil moisture, lower level soil moisture, groundwater, and water in the channel. The same group published later the well-known Stanford Watershed Model (Crawford and Linsley, 1966).

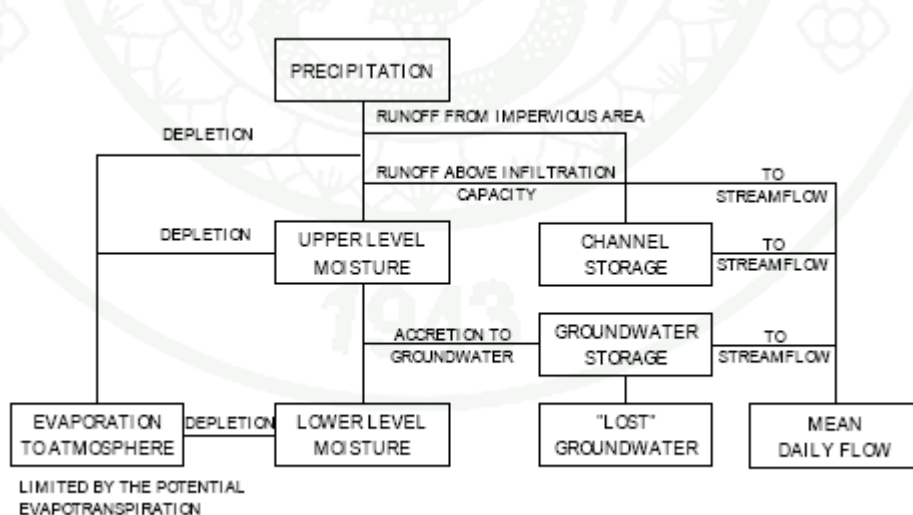


Figure 7 A flow diagram of the Linsley and Crawford model.

Source: Linsley and Crawford (1960)

Increased computing power advanced development of conceptual models, and since the early efforts in the 1960's a plethora of alternative structures for conceptual hydrological models have been suggested worldwide. Such models include the HBV model (Bergstrom and Forsman, 1973) in Sweden, the Sacramento model in the United States (Burnash et al., 1973), the TANK model (see e.g. Franchini and Pacciani, 1991) in Japan, the MODHYDROLOG model (Chiew and McMahon, 1994) in Australia, the XIANJIANG model (Zhao et al., 1980) in China, the ARNO model in Italy (Todini, 1996), and the SATT-I model in Finland (Vakkilainen and Karvonen, 1982).

Conceptual rainfall-runoff models have found wide application in practical problems. As an example, the operational flood forecasting system in the United States is based on the Sacramento model (Thiemann et al., 2001), and in Finland on the HBV model (Vehvilainen, 1992).

4.4 Classification of rainfall-runoff models

Models can be classified in different ways. According to Viraphol (n.d.) models can be classified into:

- Rainfall-runoff models or Watershed models (e.g. STANFORD model, SCS model, NAM model, SACRAMENTO model, SSARR model, TANK model)
- Multiple regression models or Time series models (e.g. SOLVE model, HEC-4 model)

Classifications by Ambroise (1998) models can be classified into:

- Deterministic or Stochastic,
- Empirical, Conceptual or Physically-based relationships,
- Lumped, Semi-Distributed or Distributed
- Kinematic or Dynamic.

Survey of modeling approaches suitable for AIMWATER (1999) models can be classified into:

- Black box models
- Conceptual models
- Physically-based distributed models

Black box models: These models are based only on a mathematical link between input and output variables of the catchment (e.g. rainfall and streamflow time-series). They do not account for the catchment behaviour. They consider the catchment as a lumped unit, without taking into account the spatial characteristics of the basin. The use of ‘blackbox’ models are quite simple, not demanding in terms of data due to their lumped nature. Examples of this type of model include ARMAX models, initially developed by Box and Jenkins, simple equations such as the Tsykin equation or the methodology developed by Pinault using signal-processing theory.

Conceptual models: The conceptual or “soil moisture accounting” models have, generally speaking, a structure of interconnected storages. Compared with black box models, these models are less simple even though they may have no straightforward physical interpretation. These models do not simulate other hydrological variables (infiltration, groundwater level, etc.) and most of them produce a single output (streamflow). Examples of this type of models include the Stanford Watershed Model, the SSARR model, the TANK model, the XINANJIANG model, the HBV model, the MODHYDROLOG model, the TOPMODEL or the SACRAMENTO model, the CEQUEAU model, Catpro model, IHACRES and the empirical GR3J models. List of models with authors, and number of parameters as shown in Table 7.

Physically-based distributed models: Physically-based models represent a further step towards complexity. Physically-based models require a much better understanding of the physical processes. They use ‘theoretical’ equations for each process, e.g. Richards equation for the movement of water in the unsaturated zone or Saint-Venant equation for the simulation of flow in streams. Examples of this

type of models include distributed models such as SHE, IHDM, SWATC model and IHC model. These models use spatially-distributed parameters/variables in order to take into account the spatial heterogeneity of the catchments. They are able to simulate other components of the hydrological cycle (canopy interception, evaporation, water uptake, water table levels, groundwater recharge, etc.).

Table 7 List of rainfall-runoff models with authors, and number of parameters.

Models (Authors)	Param.	Models (Authors)	Param.
1. Abcd (Thomas, 1981)	6	19. Blackie and Eeles (1985)	9
2. Arno (Todini, 1996)	9	20. Martine (Mazenc et al. , 1984)	7
3. Boorman and Bonvoisin B (1992)	6	21. Mhr (Leviandier et al., 1994)	4
4. Boorman and Bonvoisin C (1992)	5	22. Modalp (Arikan, 1988)	7
5. SFB (Boughton, 1984)	8	23. Modglo (Girard; Servat, 1986)	8
6. Bucket (Thornthwaite and Mather, 1957)	6	24. Modhydrolog (Porter and McMahon, 1971)	9
7. Catpro (Raper and Kuczera, 1991)	8	25. Nam (Nielsen and Hansen, 1973)	9
8. Cequeau (Girard et al., 1972)	9	26. Dawdy and O'Donnell (1965)	9
9. Crec (Cormary and Guilbot, 1973)	6	27. Pdm (Moore and Clarke, 1981)	6
10. Gardenia (Thiery, 1982)	6	28. Sacramento (Burnash et al., 1973)	9
11. Georgakakos and Baumer (1996)	9	29. Sdi (Langford and O'Shaughnessy, 1977)	9
12. Gr4 (Edijatno et al., 1999)	4	30. Sixpar (Gupta and Sorooshian, 1983)	8
13. Gr5j (Ma et al ., 1990)	6	31. Smar (O'Connal et al., 1970)	8
14. Grhum (Loumagne et al., 1996)	9	32. Tank (Sugawara, 1995)	7
15. Haan (1972)	8	33. Tmwam (Bobba and Lam, 1989)	8
16. Hbv (Bergström, 1995)	9	34. Topmodel (Beven and Kirkby, 1979)	7
17. Hms (Morel-Seytoux, 1998)	9	35. Wageningen (Warmerdam, 1994)	8
18. Ihacres (Jakeman et al. , 1990)	7	36. Xinanjiang (Zhao et al., 1980)	8

Source: AIMWATER (1999)

Singh (1995) classified rainfall-runoff models; the models are of different types and were developed for different purposes. Nevertheless, many of the models share structural similarities, because their underlying assumptions are the same, and some of the models are distinctly different. The rainfall-runoff models can be classified, as shown in Figure 8 to 10, according to different criteria that may encompass as Process description, Scale (space and time) and Technique of solution.

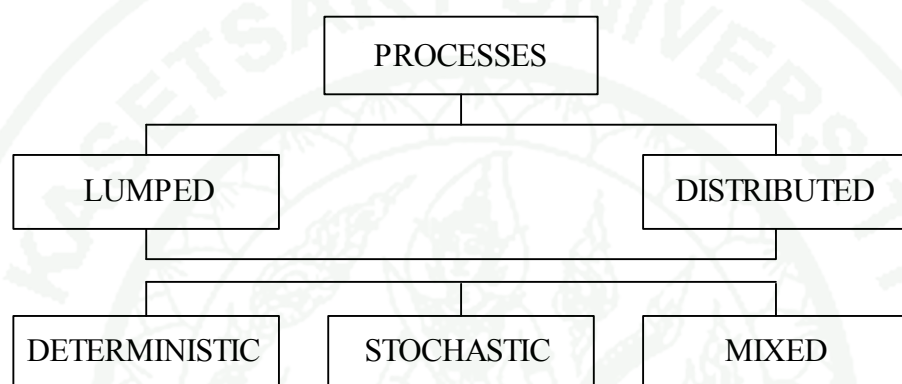


Figure 8 Classification of models based on process description.

Source: Singh (1995)

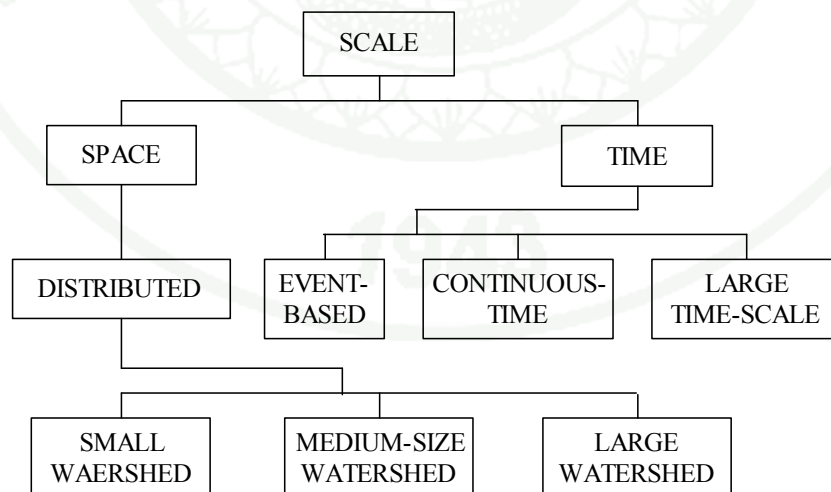


Figure 9 Classification of models based on space and time scale.

Source: Singh (1995)

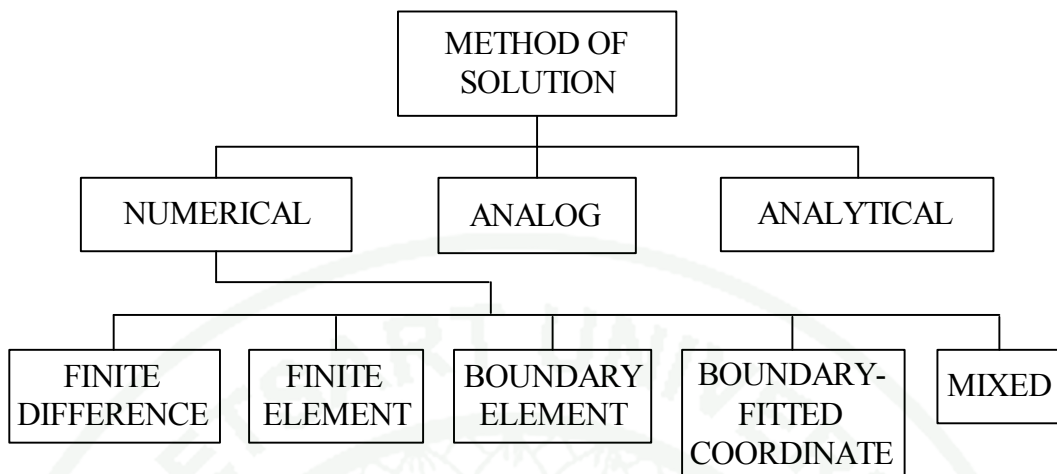


Figure 10 Classification of models based on solution technique.

Source: Singh (1995)

Malek (2002) classified rainfall-runoff models, Hydrological simulation models can be classified according to a wide range of characteristics. For watershed analysis, the major categories include lumped, distributed, event, continuous, stochastic and deterministic parameter models.

Lumped parameter model: The concept used in lumped parameter models is that all watershed processes occur at one spatial point. It transforms a series of actual rainfall input to produce runoff output. As a result, the parameters used in this type of modeling may or may not have a direct physical definition in the system.

Distributed parameter model: The distributed parameter models attempt to describe physical processes and mechanisms in space. This type of modeling is theoretically more satisfying, but often problem arises due to lack of data to calibrate and to verify the simulation results.

Event model: Event models simulate single storm responses for a given rainfall data input. Unit hydrograph or kinematic wave methods are used to generate storm hydrographs. Example of such models are HEC-1 Flood Hydrograph Package,

(Hydrologic Engineering Centre, 1981), SWMM (EPA Storm Water Management Model, 1981) and SCS TR20 (Soil Conservation Service, 1975).

Continuous model: Continuous models are based on long-term water balance equations where it is related with the effects of preliminary conditions.

Stochastic model: Stochastic models tend to reproduce the statistical behavior of hydrological time series without concerning the actual event. These models represent input rainfall used to generate time series of stream flow. The time series are evaluated using flood frequency analysis. As a result, the hydrologic synthesis produced, allow hydrologists to extend short historical records or longer sequences based on statistical methods. In short, stochastic models make predictions.

Deterministic model: A deterministic model does not consider randomness. A given input always produces the same output. In other words, deterministic models make forecasts.

4.5 The case on model details

Bell and Moore (1998) implement a grid-based rainfall-runoff model, which is a clear example of matching the process description of a conceptual model to rainfall distribution data provided by weather radar or raingauges. The model has the following components:

- The topography of the catchment system, for which rainfall is to be transformed to runoff, is used for subdivision of the catchment into isochrone bands (delineating areas of equal time of travel to the basin outlet) for flow routing, using a Digital Terrain Model (DTM).
- The catchment is further sub-divided into grid squares coincident with those used by the weather radar to utilise distributed rainfall.

- Each grid square functions as a storage with a water budget comprising rainfall as input which is transformed into:

- (a) direct runoff when storage is full
- (b) infiltration into storage if the present storage is below its capacity
- (c) slow drainage from the storage if any storage is available, and
- (d) evaporation.

- The direct runoff and drainage are summed along isochrone bands contributing separately to fast and slow routing pathways respectively.

- These flows are then routed successively from one isochrone band to the next lower one using a discrete kinematic wave routing scheme.

- At the catchment outlet the routed flows from the fast and slow pathways are summed to give the modelled catchment flow. A number of alternative mathematical formulations are considered for the runoff production and routing units of the overall Grid Model.

The insight gained by Khatibi et al., (2002) study has a bearing on parsimonious modelling, as follows:

- When errors dominate in the distributed rainfall estimates from radar, a simpler (lumped) model can provide a more robust forecasting scheme.

- When the distributed rainfall estimates can be relied on, provided the catchment response is spatially variable and/or rainfall is non-uniform in space, the distributed Grid Model can provide improved performance.

Improvement in performance is influenced if process description and the quality of the distributed data are commensurate. Thus, process description alone does not compensate for shortfalls in the data and vice versa.

4.6 Runoff estimation using an *API* concept

NLPM-API model

Xia et al., (1997) using a non-linear perturbation model (NLPM-API) for river flow forecasting is developed, based on consideration of catchment wetness using an antecedent precipitation index (*API*). There were found that the NLPM-API model was significantly more efficient than the original linear perturbation model (the LPM). The NLPM-API has concept as Figure 11.

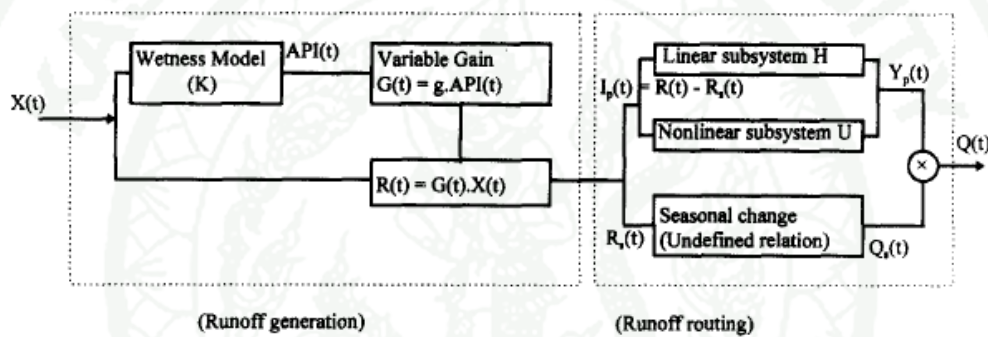


Figure 11 The non-linear perturbation model with *API*-dependent gain factor.

Source: Xia et al. (1997)

The process of catchment runoff generation of NLPM-API model is very complex as it involves many factors, such as precipitation intensity, actual rate of evaporation and catchment wetness, and their interactions. The relationship between the effective rainfall, $R(t)$, and the total precipitation, $X(t)$, over a catchment or a sub-catchment may be simply expressed in terms of a runoff coefficient $G(t)$, as

$$R(t) = G(t).X(t) \quad (9)$$

A simplified representation of non-linear runoff generation, which does not require evaporation, can be developed in terms of the time-varying runoff coefficient $G(t)$ of equation (9), as

$$G(t) = g \cdot API(t) \quad (10)$$

where the *API* is the antecedent precipitation index function, *g* is considered as a constant of the water balance, expressed in terms of the volume constraint equation.

$$g = \frac{\int Q(t)dt}{\int API(t) \cdot X(t)d(t)} \quad (11)$$

NAZASM model

Descroix et al., (2002) using a lumped deterministic API-type model, named NAZASM. The NAZASM model has been developed and used to evaluate runoff by Girard in year 1975 for sahelian regions. It relies in the following assumptions:

- The rainfall-runoff relation is assumed to hold for any rainy event, *n*:

$$\sqrt{Rd_n} = K_n (P_n - P_{0n}) \quad \text{with } P_n > P_{0n} \quad (12)$$

where Rd_n and P_n are the runoff depth and the rainfall amount, respectively, both expressed in mm. P_{0n} (mm) is the rainfall below which there is no runoff. K_n (in $\text{mm}^{-1/2}$) is a parameter depending on the soil surface hydraulic conductivity, on the catchment area and on the proportion of the catchment contributing to runoff and K_n can be expressed as:

$$K_n = K_{\min} + [(K_{\max} - K_{\min}) / (P_{0n}^{\max} - P_{0n}^{\min})] \times (P_{0n}^{\max} - P_{0n}) \quad (13)$$

where K_{\max} , K_{\min} , P_{0n}^{\max} and P_{0n}^{\min} correspond to the maximum and minimum values, respectively, of K and P_{0n} for either the plots or the catchments.

- By assimilating the soil to a reservoir, P_{0n} can be expressed as:

$$P_{0n} = C (H_{max} - API_n) \quad \text{with } API_n \leq H_{max} \quad (14)$$

where C is the parameter taking into account most likely rainfall intensity and indirectly the catchment heterogeneity, the water storage of the soil surface (including vegetation and litter) and the mechanical effect of raindrops on the soil. H_{max} is the maximum water storage of the reservoir (mm) and API_n (mm) is its actual level at a given time (Figure 12).

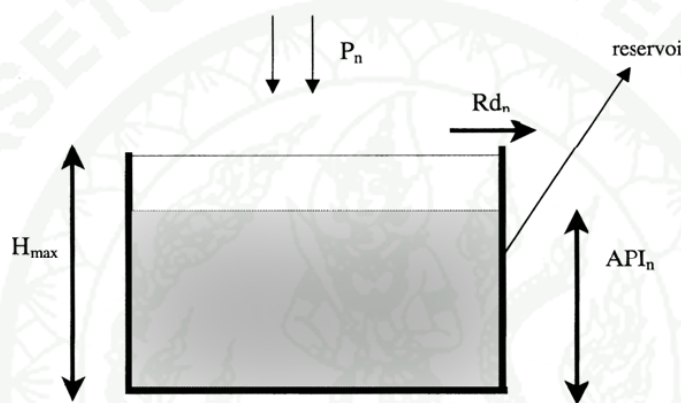


Figure 12 Schematic representation of the soil in the *API*-type model

Source: Descroix et al. (2002)

- Following the definition of the *API* (Descroix et al., 2002), API_n is calculated as:

$$API_n = (API_{n-1} + P_{n-1}) \exp (-\alpha \Delta t) \quad (15)$$

where $\Delta t = t_n - t_{n-1}$ is the time (day and/or fraction of day) elapsed between the end of the previous rain event P_{n-1} and the beginning of the current one (P_n). The parameter α (day^{-1}) is the inverse of the characteristic time of soil moisture depletion.

Introducing Eq.(15) into Eq.(14) and then into Eq.(12), gives :

$$\sqrt{Rd_n} = K_n \{P_n - C[H_{\max} - (API_{n-1} + P_{n-1}) \times \exp - \alpha(t_n - t_{n-1})]\} \quad (16)$$

The model (Eq. 16) has seven parameters (C , H_{\max} , α , K_{\max} , K_{\min} , P_{0n}^{\max} , P_{0n}^{\min}) to be determined. This was achieved by splitting the time series of observed (P_n , Rd_n) values in to parts (one event out of two): one half being used for the calibration of the parameters by best fitting between calculated and measured values of runoff depths; and the other one for the validation, the values of the parameters being kept unchanged.

The model is initialised at the beginning of the rainy season, where API_0 is assumed to be zero.

Peakflow estimation

Beschta, (1990) using an antecedent precipitation index (API) model in tropical environments for estimating peakflows on a 865 ha watershed in Hawaii, USA, and simulating stream levels of the Wainganga river in India. The result show the potential usefulness of API as a flood-stage forecasting methodology is illustrated with stage data for the Wainganga river in India.

Runoff estimation by NAPI

Richard, (2001) define the normalized antecedent precipitation index (NAPI) as follows:

$$\text{NAPI} = \frac{\sum_{t=0}^{-i} P_t k^{-t}}{\bar{P} \sum_{t=-1}^{-i} k^{-t}} \quad (17)$$

where P_0 on the day of, but before, the storm. The denominator is a normalizing operator having two components: average daily precipitation P and the Σ series. If precipitation has been P on each of the preceding i days and P_0 is zero (if it has not rained earlier in the day), NAPI is 1.0.

From Eq. (17) utilizes NAPI is an exponential estimate of runoff as follows:

$$\frac{Q}{P} = 1 - e^{a+bP+cNAPI} \quad (18)$$

where Q is runoff from event rainfall depth P . Coefficients a , b , and c are specific to a watershed. Eq. (18) extends Rallison (1980), in which a and c were 0.0. Figure 13 show an arbitrary a , b , and c set and different values of NAPI, reveals several theoretical behaviors.

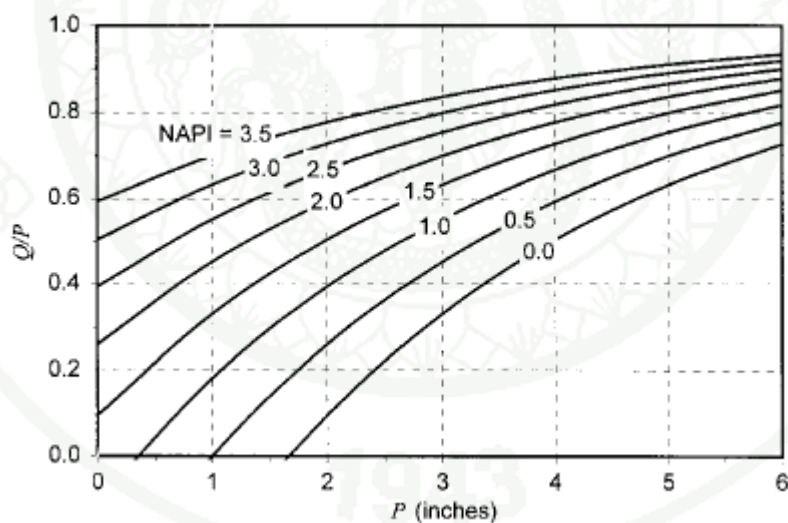


Figure 13 Q/P as Function of P and NAPI ($a = 0.5$, $b = -0.3$, $c = -0.4$)

Source: Richard (2001)

GAPI rainfall-runoff model

Jian, (2004) using a *GAPI* rainfall-runoff model to simulate runoff of Three Gorges Area in the upper Yangtze river during 1998 flood season. The *GAPI* rainfall-runoff model is a forecasting system developed by the Water Resources Research Center of Hungary. *API* represents the Antecedent Precipitation Index, which is utilized to describe the state of moisture in the catchment area, and the probability of the *API* is assumed to be Gamma distribution. Thus *GAPI* is named after the acronym of Gamma Antecedent Precipitation Index.

The *GAPI* model consists of two modules.

- *Module 1* estimates the rainfall losses and separates surface, subsurface and base runoffs;

$$\text{surface flow} \quad u_{1,t} = u_t A_{f,t} \alpha_t \quad (19)$$

$$\text{subsurface flow} \quad u_{2,t} = u_t (1-A_{f,t}) \alpha_t (1-\alpha_b) \quad (20)$$

$$\text{base flow} \quad u_{3,t} = u_t (1-A_{f,t}) \alpha_t \alpha_b \quad (21)$$

where u_t is the total volume of runoff, α_t it is volumetric runoff coefficient, and α_b is the ratio of baseflow to infiltration. For a given period, part of rainfall, forming surface and subsurface runoffs, can be expressed through a volumetric runoff coefficient

$$\alpha = \frac{\sum_{i=t+1}^{T+t} Q_i - TQ_o}{\sum_{i=1}^T P_i} \quad (22)$$

where α is a volumetric runoff coefficient, Q_o is the minimum value of runoff, t is the time lag of runoff to rainfall in unit day, T is the period of

rainfall and runoff integration, Q is the discharge at the downstream river station and P is the rate of precipitation in unit cms

$A_{f,t}$ is the ration of surface runoff can be estimated if the probability of API is know

$$A_{f,t} = \int [P(API_i)] \quad (23)$$

$$\text{and the interflow ratio} \quad A_{a,t} = 1 - A_{f,t} \quad (24)$$

- *Module 2* performs the routing of surface, subsurface and base flow, while taking into account the effect of surface and underground storage capacity. A flood routing model based on discrete linear cascade model (DLCM) combined with rainfall-runoff models (GAPI) is taken as tool for daily forecasting.

Runoff estimation using an API concept in Thailand

Withhawatchutikul, (2005) using the rainfall-runoff concept from IHACRES rainfall-runoff model and Viessman et al. (1989) to determine the runoff in sub-watershed of Mae Kuang watershed (a tributary of Ping river), which explained that runoff (Q , mm) was the result of rainfall (R , mm) and the antecedent moisture content or antecedent precipitation index (API) and has a general model for flow estimation as follows:

$$Q = a + b.R + c.API \quad (25)$$

where a , b and c are coefficients. To account for effect of large watersheds to Eq.(25). Withhawatchutikul, (2005) apply a Topographic Index (TI) in flow estimation similar to the TOPMODEL index. The index can be defined as:

$$TI = \ln(a / \tan \beta) \quad (26)$$

where a is the ratio of watershed area (A) above a given point in stream to contour length distance (cld), and $\tan \beta$ is the average slope of watershed.

The TI corresponding to each zone of watersheds will be used to weight the estimated flow from each zone using:

$$Q_w = d [\Sigma(TI_{ij} Q_{ij}) / \Sigma TI_{ij}]^e \quad (27)$$

where the i subscript refers to the day, the j subscript to the zone, and d and e are coefficients.

The model developed here works in two routes at the same time. The first route, the model will go to each zone of the watershed of physical homogeneous characteristics such as topography, soil type and moisture contents by assigning the value to each factor called topographic index (TI). In each zone, the values for different factors concerning outflow of the area consisting of topography (CN_t), infiltration (CN_s), vegetative cover (CN_v) and surface storage or (CN_{ss}), will be assigned. The CN value of the 4 factors will be added to be representative of all the factors having roles on the releasing of runoff of the watershed or runoff curve number (CN).

In the second route, the model will search for daily rainfall data and compile it. The data will be used in evaluating soil antecedent moisture content (AMC), which is needed for adjusting CN value to be an initial value of API of each zone (API_{ij}). In addition to API_{ij} value, daily rainfall (R_{tj}) will also be applied in estimating flow of each zone(Q_{ij}) by using equation (25). The model will calculate flow for every zone in the watershed.

The flow values obtained will be subtracted from rainfall as part of the rainfall infiltrated into the soil. The remaining rainfall from subtraction information will be (1) sent to the CROP MODEL and (2) used in calculation of total outflow that drains

from the watershed (Q_w) on the given day by using equation (27), which is a result of introduction of topographic index (TI_{ij}) into each zone.

In calculating flow for the next day, the model will first find a recession constant (K) for API_{ij} and then adjust it to be API_{ij} of the next day. In adjusting the API_{ij} , equation will be used instead in case of rain on the next day. The adjusted API_{ij} will be applied in calculation of flow for each zone first and then the total flow of the watershed. The detail of how the model works is shown in Figure 14.

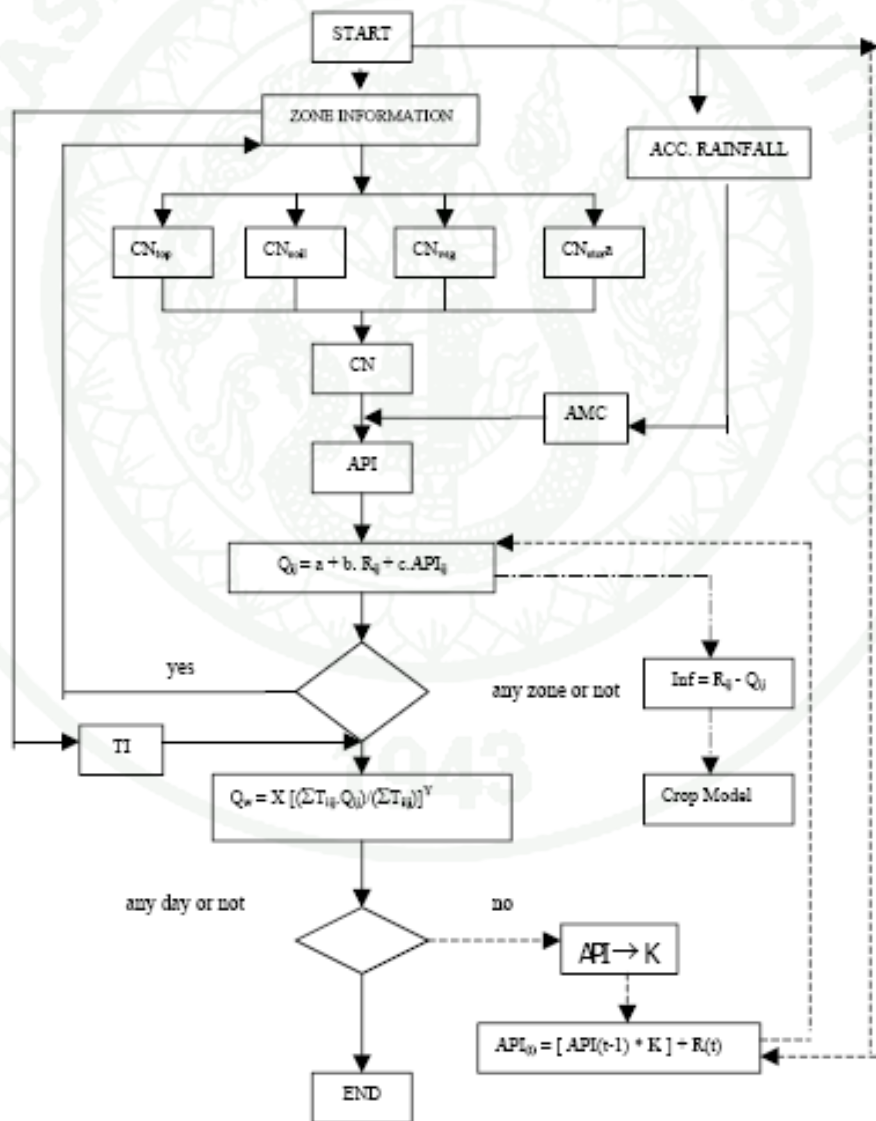


Figure 14 Flow chart of model by Witthawatchutikul, (2005)

5. Trend analysis

The basic concepts in statistical testing in for trend is description by Francis and Siriwardena, (2005) as follows:

5.1 Basic concepts

Hypothesis: the starting point of a statistical test is to define a null hypothesis and an alternative hypothesis. For example, to test for trend in a time series, null hypothesis would be that there is no trend in the data, and an alternative hypothesis would be that there is an increasing or decreasing trend.

Test static: The test statistic is a means of comparing null hypothesis and an alternative hypothesis. It is a numerical value calculated from the data series that is being tested.

Significance level: The significance level is a means of measuring whether the test statistic is very different from the (critical) values that would typically occur under null hypothesis.

Power and errors: There are two possible types of errors. Type I error is when null hypothesis is incorrectly rejected. Type II error is when null hypothesis is accepted when an alternative hypothesis is true. A test with low Type II error is said to be powerful.

5.2 Significance level

The significance level (α) is a means of measuring whether the test statistic is very different from values that would typically occur under null hypothesis (Kundzewicz, 2000).

Specifically, the significance level is the probability of a test statistic value as extreme as, or more extreme than the observed value assuming no trend/change (null hypothesis). For example, for $\alpha = 0.05$, the critical test statistic value is the value that would be exceeded by 5% of test statistic values obtained from randomly generated data. If the test statistic value is greater than the critical test statistic value, null hypothesis is rejected.

The significance level is therefore the probability that a test detects a trend/change (reject null hypothesis) when none is present (Type I error) and a possible interpretation of the significance level might be:

$\alpha > 0.1$	little evidence against null hypothesis.
$0.05 < \alpha < 0.1$	possible evidence against null hypothesis.
$0.01 < \alpha < 0.05$	strong evidence against null hypothesis.
$\alpha < 0.01$	very strong evidence against null hypothesis.

For most traditional statistical methods, critical test statistic values for various significance levels can be looked up in statistical tables or calculated from simple formulas, provided that the test assumptions are satisfied. Where test assumptions are violated, resampling methods can be used to estimate the significance level of a test statistic.

For detecting trend/change of any direction, the critical test statistic value at $\alpha/2$ is used (two-sided tail). For detecting trend/change in a pre-specified direction (e.g., an increasing trend), the critical test statistic value at α is used (one-sided tail).

5.3 Parametric and non-parametric tests

Parametric tests assume that the time series data and the errors (deviations from the trend) follow a particular distribution (usually normal distribution). Parametric tests are useful as they also quantify the change in the data

(e.g., magnitude of change in the mean or gradient of the trend). Parametric tests are generally more powerful than non-parametric tests. Where the assumption of normally distributed data is violated, resampling analysis can be used to estimate the significance level or critical test statistic values for various significance levels.

Non-parametric tests are generally distribution-free. They detect trend/change, but do not quantify the size of the trend/change. They are very useful because most hydrologic time series data are not normally distributed.

5.4 Statistical tests for trend detection

The statistical tests that can be used to test for trend, change and randomness in hydrological and other time series data:

- Mann-Kendall (non-parametric test for trend)
- Spearman's Rho (non-parametric test for trend)
- Linear Regression (parametric test for trend)
- Distribution-Free CUSUM (non-parametric test for step jump in mean)
- Cumulative Deviation (parametric test for step jump in mean)
- Worsley Likelihood Ratio (parametric test for step jump in mean)
- Rank-Sum (non-parametric test for difference in median from two data periods)
- Student's t (parametric test for difference in mean from two data periods)
- Median Crossing (non-parametric test for randomness)
- Turning Points (non-parametric test for randomness)
- Rank Difference (non-parametric test for randomness)
- Autocorrelation (parametric test for randomness).

5.5 Mann-Kendall test

The method of Mann-Kendall test defined by Mann in year 1945 and modified by Kendall in year 1975, (Mann, 1945; Kendall, 1975) for trend analysis. The non-parametric Mann-Kendall statistical test has been popularly used to assess the significance of trend in hydrological time series (Yue et al., 2004). The Mann-Kendall trend test, being a function of the ranks of the observations rather than their actual values, is not affected by the actual distribution of the data and is less sensitive to outliers. On the other hand, parametric trend tests, although more powerful, require the data to be normally distributed and are more sensitive to outliers. The Mann-Kendall test, as well as other non-parametric trend tests, is therefore more suitable for detecting trends in hydrological time series, which are usually skewed and may be contaminated with outliers (Hamed, 2008).

For a time series $X = \{x_1, x_2, \dots, x_n\}$, the null hypothesis (H_0) states that a sample of n is an independent and identically distributed random variables (Yu et al., 1993). The alternative hypothesis H_1 of a two-sided test is that the distribution of x_k and x_j are not identical for all $k, j \leq n$ with $k \neq j$. The test statistic S is calculated with (Kahya et al., 2004);

$$S = \sum_{k=1}^{n-1} \sum_{j=k+1}^n sign(x_j - x_k) \quad (28)$$

where

$$sign(x_j - x_k) = \begin{cases} +1 & \text{if } (x_j - x_k) > 0 \\ 0 & \text{if } (x_j - x_k) = 0 \\ -1 & \text{if } (x_j - x_k) < 0 \end{cases} \quad (29)$$

The mean and variance of the S statistic is (Hamed, 2008);

$$E(S) = 0 \quad (30)$$

$$V_0(S) = [n(n-1)(2n+5) - \sum_{j=1}^m t_j(t_j-1)(2t_j+5)]/18 \quad (31)$$

Kendall (1975) also shows that the distribution of S tends to normality as the number of observations becomes large. The significance of trends can be tested by comparing the standardized variable z in equation (32) with the standard normal variate at the desired significance level p , where the subtraction or addition of unity in equation (32) is a continuity correction.

$$z = \begin{cases} \frac{S-1}{\sqrt{Var(S)}} & \text{if } S > 0 \\ 0 & \text{if } S = 0 \\ \frac{S+1}{\sqrt{Var(S)}} & \text{if } S < 0 \end{cases} \quad (32)$$

6. Hydrological routing

The hydrological routing is a technique which is used to determine the flow hydrograph characteristics like shape and movement along a water course, and how these are affected by various factors like system storage and system dynamics on the shape and movement of flow hydrographs along a watercourse.

6.1 Basic principles of routing

The hydrologic routing methods use a common continuity equation as their common base. According to this equation, the difference between inflow and outflow rates is equal to the rate of change of storage. Mathematically the equation can be written as below (Gosh, 1997):

$$dS = (Idt - Odt) \quad (33)$$

where I is a rate of inflow, and at any time the corresponding outflow is O . dS is the storage that is accumulated during a very small duration of time dt . Equation (33) considers the losses due to seepage, evaporation and direct accretion to storage, as small enough to be ignored. The equation can be written in integral form as below (Watson, 1983):

$$S = \int (I - O) dt \quad (34)$$

6.2 Types of hydrological routing

In all the hydrologic analysis applications mentioned above, two categories of routing can be clearly recognized:

Reservoir routing: In this type of routing, the effect of a flood wave entering a reservoir is studied. This is done by determining the volume – elevation characteristic of a reservoir in addition to the outflow – elevation characteristic of the spillway and also other outlet structures present in the reservoirs (Chadwick and Morfett, 1986).

Channel routing: In this type of routing, a study is made of the change in shape of a hydrograph as it travels down a channel. This is done by considering a channel reach that is the specific length of the stream channel, and an input hydrograph at the upstream end of the stream.

6.3 Hydrologic channel routing

In case of reservoir routing, the storage is a function of output discharge, whereas in case of channel routing, the storage is a function of both inflow and outflow discharges. This is the main reason why entirely different routing methods are needed for Channel routing.

When a river is in flood, the flow can be characterized as gradually varied unsteady flow. In a particular channel reach the water surface as expected is not parallel to the channel both. Additionally it also varies with time. At the time of flood, the total volume in storage can be divided into two categories:

Prism storage: This is defined as the volume that would exist in case there is uniform flow at the downstream depth, that is Prism storage = $f(Qt)$

Wedge storage: This term represents the wedge-like volume which is formed between the actual water surface profile and the prism storage surface, that is Wedge storage = $f(It, Qt)$

In the downstream section of a river reach, the prism storage is observed to be constant, when the depth is fixed. However, the wedge storage changes from positive to negative depending on the type of flood. The wedge storage is positive at the time of advancing flood, while it is negative in case of a receding flood (Subramanya, 2002). The Prism storage and Wedge storage is shown in Figure 15.

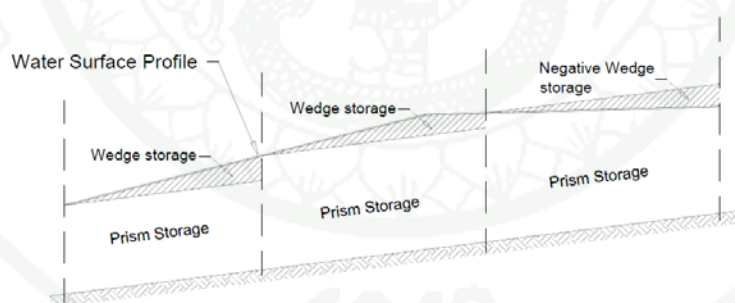


Figure 15 Prism storage and Wedge storage

Source: Linsley et al. (1982)

6.4 Muskingum methods

The Muskingum model was first developed by McCarthy in year 1938, for flood control studies in the Muskingum river basin in Ohio, USA. This method is

still one of most popular methods used for flood routing in several catchment models. The Muskingum method is a spatially lumped form of continuity equation and linear-storage and discharge relationship for a specified river reach. The first equation is common to all conceptual models. It is a physical continuity equation that is law of conservation of mass, which is later integrated over the entire river reach.

$$\frac{dS}{dt} = I - O \quad (35)$$

Muskingum method differs from other conceptual models with the second equations, which relates storage in the river reach, inflow and outflow.

$$S = K [XI + (I - X)O] \quad (36)$$

where K is a travel time of the flood wave through routing reach and X is a dimensionless weight ($0 \leq X \leq 0.5$). The total storage volume at any time instant, t , can be calculating the above two storages.

$$S_t = KO + XK(I_t - O_t) \quad (37)$$

The Muskingum equation based on equation (36) and the water balance equation can be written as:

$$O_{(t+1)} = C_1 I_{(t+1)} + C_2 I_t + C_3 O_t \quad (38)$$

where

$$O_{(t+1)} = \left(\frac{\Delta t - 2KX}{2K(1-X) + \Delta t} \right) I_{(t+1)} + \left(\frac{\Delta t + 2KX}{2K(1-X) + \Delta t} \right) I_t + \left(\frac{2K(1-X) - \Delta t}{2K(1-X) + \Delta t} \right) O_t \quad (39)$$

Therefore

$$C_1 + C_2 + C_3 = 0 \quad (40)$$

Calibrating the model using observed flows: If observed inflow and outflow hydrographs are available, the Muskingum model parameter K can be estimated as the interval between similar points on the inflow and outflow hydrographs.

Estimating the parameters for ungaged watersheds: If gaged flows required for calibration are not available, K and X can be estimated from channel characteristics as follows:

Estimate the flood wave velocity, V_w , using Seddon's law, as:

$$V_w = \frac{1}{B} \frac{dQ}{dy} \quad (41)$$

where B is a top width of the water surface, and dQ/dy is a slope of the discharge rating curve at a representative channel cross section. The flood wave velocity suggests estimating as 1.33-1.67 times the average velocity, which may be estimated with Manning's equation and representative cross section geometric information.

Estimate K as:

$$K = \frac{L}{V_w} \quad (42)$$

Experience has shown that for channels with mild slopes and overbank flow, the parameter X will approach 0.0. For steeper streams, with well-defined channels that do not have flows going out of bank, X will be closer to 0.5. Most natural channels lie somewhere in between these two limits, leaving room for engineering judgement.

Cunge (1969) estimated X as:

$$X = \frac{1}{2} \left(1 - \frac{Q_o}{BS_o c \Delta x} \right) \quad (43)$$

where Q_o is a reference flow from the inflow hydrograph, B is a top width of flow area, S_o is a friction slope or bed slope, c is a flood wave speed (celerity), and Δx is the length of reach. The reference flow is an average value for the hydrograph, midway between the base flow and the peak flow (Ponce, 1983).

Ponce (1983) suggested, C_1 should have a non-negative value. The negative values of C_1 are avoided when equation (44) is satisfied and the negative values of C_2 do not affect the routed hydrographs.

$$\frac{\Delta t}{K} > 2X \quad (44)$$

6.5 HEC-HMS model

HEC-HMS is Hydrologic Engineering Center-Hydrologic Modeling System. HEC-HMS was developed by U.S. Army Corps of Engineers (USACE) Hydrologic Engineering Center (HEC). The program simulates precipitation-runoff processes, both natural and controlled. The program is the successor to and replacement for the Flood Hydrograph Package HEC-1 and for various specialized versions of HEC-1 (USACE, 2000). HEC-HMS has components as shown in Figure 16.

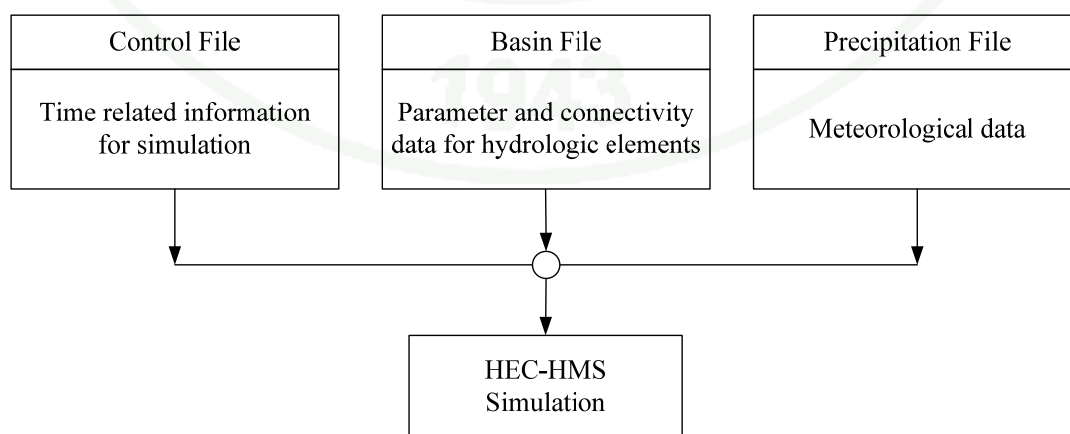


Figure 16 Components of HEC-HMS.

MATERIALS AND METHODS

Materials

The materials for this research include the following:

1. Computer laptop and laser printer
2. Topographic map of upper Chao Phraya river basin at a scale of 1:250,000 and 1:50,000
3. Arc View GIS (Version 3.2) and Arc Map (Version 9.3) software for GIS analysis
4. Microsoft Office 2007 software for trend analysis, watershed runoff analysis, editing this thesis and analyzing the results
5. Hydrologic Engineering Center Data Storage System Visual Utility Engine (HEC-DSSVue) Version 2.0 for database management
6. Hydrologic Modeling System (HEC-HMS) Version 3.5 for hydrological routing analysis

Methods

1. Conceptual framework

The methodology of this research is a combination of five main concepts regarding reference evapotranspiration (ET_o) analysis, trend analysis, antecedent precipitation index analysis, rainfall-runoff relative analysis and hydrologic routing modeling. The reference evapotranspiration is used as a tool to find antecedent precipitation index (API) while the trend of ET_o and ET_o parameters in the upper Chao Phraya river basin are determined by using non-parametric tests. The antecedent precipitation index is determined by using the difference of recession coefficient (K) which was adjusted from land use and evapotranspiration (ET). The antecedent precipitation index (API) is used as a variable in rainfall runoff relative analysis while the rainfall-runoff model is used as a tool to analyze watershed runoff.

The rainfall-runoff model is selected from the result of the comparison of performances among six models for runoff estimation. The rainfall-runoff model is improved by using adjusted API instead of original API ; and by applying the range of critical API . Outflow hydrographs for each of the watersheds are routed to each of the major reaches of the upper Chao Phraya river network by hydrologic routing model. Daily rainfall data will be taken from meteorological stations. All other parameters will be obtained from available data without working in the field. Calibration and verification must be analyzed and compared against the result of runoff from different models. The conceptual framework is shown in Figure 17.

2. Small watershed study area

This study was carried out in the upper Chao Phraya river basin. The basin has included the five sub-basins (Ping, Wang, Yom, Nan and a part of Main Chao Phraya between the conjunction of Ping and Nan throughout the stream gauging station C.2 located at amphoe Mueang in Nakhon Sawan province).

This study divided sub-basins into seventy small watersheds, thirty two of which were from Ping river basin, twenty one from Wang river basin, thirty one from Yom river basin, twenty six from Nan river basin and two from Main Chao Phraya river basin.

One hundred and twelve small watersheds located throughout the upper Chao Phraya river basin were separated as predictive watershed runoff as shown in Figure 18. The catchment areas of these small watersheds vary from 22 to 5,585 square kilometers as shown in summary of small watersheds in Table 8.

Table 8 Summary of small watersheds in the upper Chao Phraya river basin.

Sub-basin	Sub-basin Catchment Area (sq.km)	Number of Small Watersheds	Range of Small Watersheds Catchment Area (sq.km)
Ping	33,898	32	53 - 3,195
Wang	10,791	21	22 - 1,759
Yom	23,616	31	150 - 2,313
Nan	34,330	26	159 - 5,585
Main Chao Phraya	4,949	2	1,546 - 3,402
Summary	107,584	112	22 - 5,585

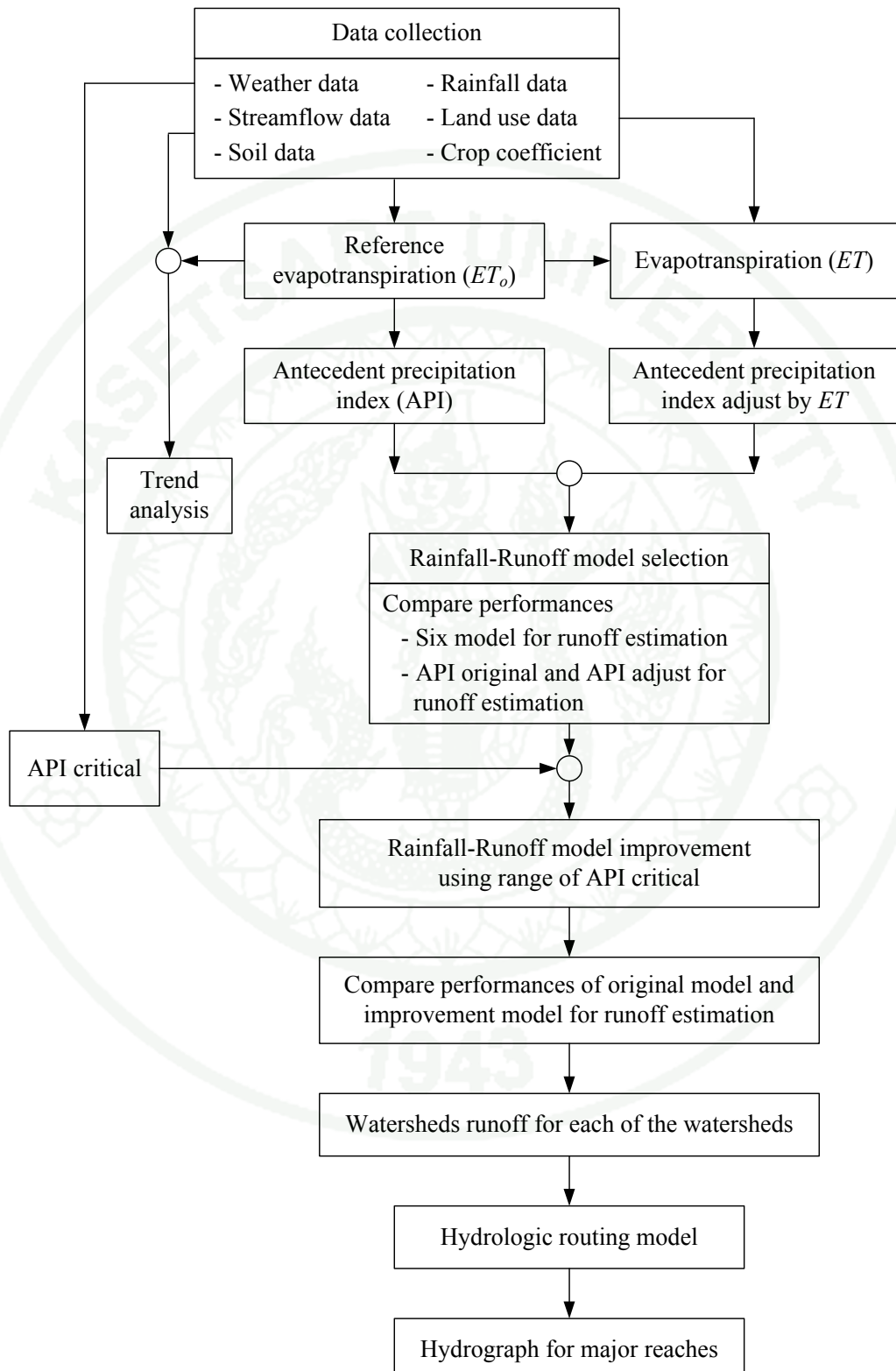


Figure 17 Conceptual framework.

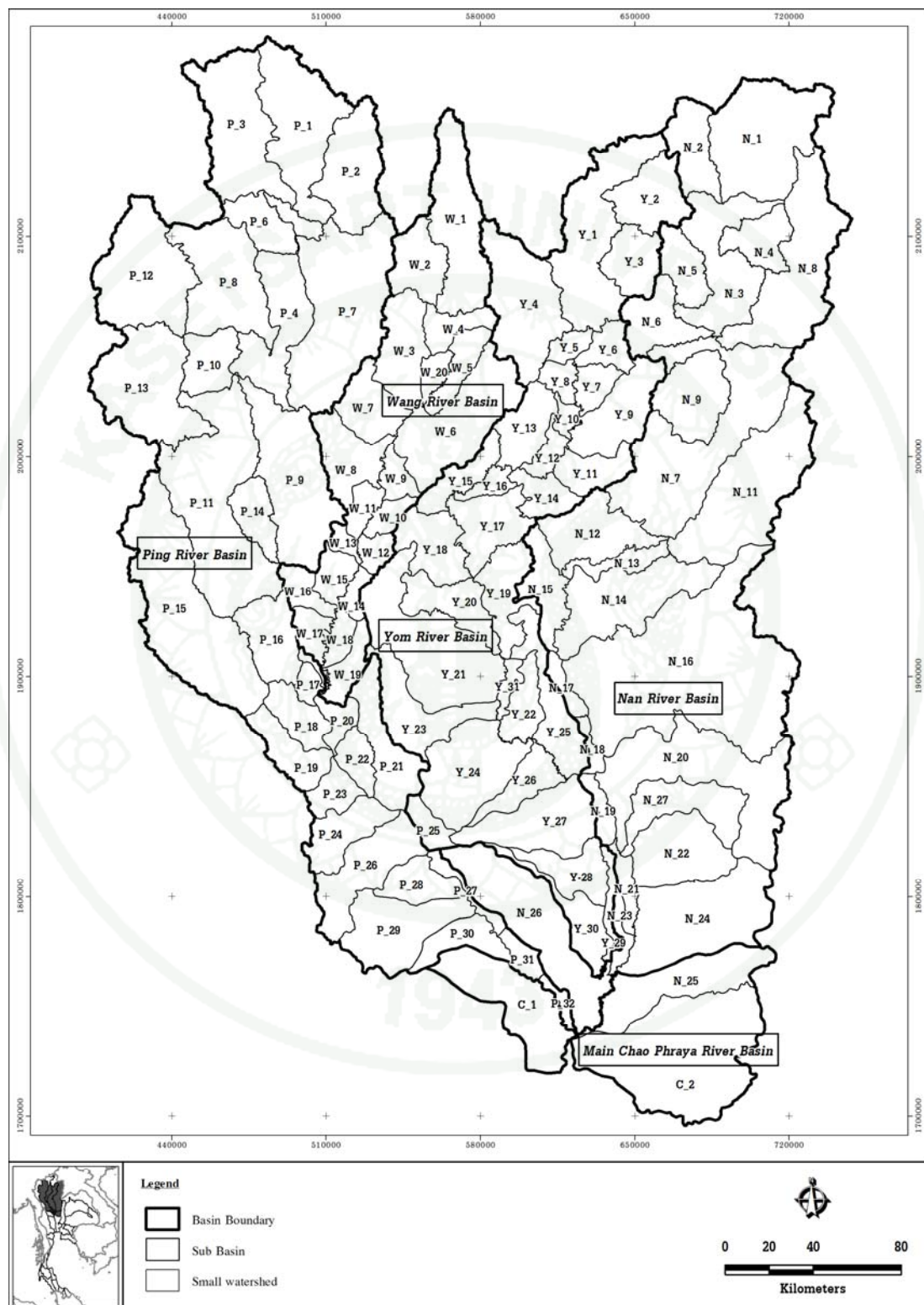


Figure 18 Small watersheds of the upper Chao Phraya river basin.

3. Data collection

3.1 Weather data

Weather data was collected from 9 weather stations operated by Thai Meteorological Department (TMD) for a 30-year period (1977-2006) in the upper Chao Phraya river basin. The weather data was used to compute reference evapotranspiration (ET_o) and antecedent precipitation index (API). The locations of weather stations are shown in Figure 19 and listed in Table 9.

Table 9 Site descriptions and locations of weather stations.

No.	Station	Latitude (°N)	Longitude (°E)	Elevation of Station above MSL. (m)	Height of wind vane above ground (m)
1.	Chiang Mai	18° 47'	98° 59'	312.0	8.9
2.	Bhumibol Dam	17° 15'	99° 01'	142.0	16.0
3.	Tak	16° 53'	99° 09'	121.0	12.5
4.	Lampang	18° 17'	99° 31'	241.0	11.8
5.	Phrae	18° 10'	100° 10'	161.0	15.0
6.	Nan	18° 46'	100° 46'	200.0	18.8
7.	Uttaradit	17° 37'	100° 06'	63.0	13.8
8.	Phitsanulok	16° 47'	100° 16'	44.0	12.5
9.	Nakhon Sawan	15° 48'	100° 10'	34.0	14.0

3.2 Rainfall data

Daily rainfall data was collected from 116 rainfall stations operated by Thai Meteorological Department (TMD) for a 30-year period (1974-2003) in the upper Chao Phraya river basin. The daily rainfall data was used to compute antecedent precipitation index (API) and to derive predictive outflow hydrographs for each of the watersheds. The locations of rainfall stations are shown in Figure 19 and listed in Appendix Table A1.



Figure 19 The location of weather stations rainfall stations and stream gauging stations in the upper Chao Phraya river basin.

3.3 Streamflow data

Daily streamflow data was collected from 54 stream gauging stations operated by Royal Irrigation Department (RID) for a 30-year period (1974-2003) in the upper Chao Phraya river basin. The daily streamflow data was used to calibrate and to verify the simulation results and the comparison of the result of runoff from different models. The locations of stream gauging stations are shown in Figure 19 and listed in Appendix Table A2.

3.4 Soil data

Soil data for the year 2003 was collected from 197 soil testing results for physical properties from Department of Water Resources (DWR) in the upper Chao Phraya river basin. The testing results were composed of bulk density ($B.D.$), water holding capacity (WHC) and saturation percentage of soil. These testing results were used to analyze maximum soil moisture available for evaporation (W_m) and antecedent precipitation index (API). The soil test data are shown in Appendix Table A3.

3.5 Landuse data

Landuse data for the year 2000 in the upper Chao Phraya river basin was collected from Land Development Department (LDD). The landuse data was used to define crop coefficient and to analyze evapotranspiration (ET). Major land use and agriculture land use of one hundred and twelve small watersheds are shown in Appendix Table A4 and Appendix Table A5.

3.6 Crop coefficient (K_c)

Crop coefficient (K_c) calculated by Penman-Monteith equation was collected from the results from Royal Irrigation Department (RID). Crop coefficient (K_c) was used to analyze evapotranspiration (ET).

4. Reference evapotranspiration

To compute reference evapotranspiration (ET_o) for each weather station, the FAO Penman-Monteith method was used. The weather data was collected from nine weather stations of Thai Meteorological Department in the upper Chao Phraya river basin for a 30-year period (1977-2006). The locations of weather stations are shown in Figure 19 and listed in Table 9.

The reference evapotranspiration (ET_o) can be estimated by using weather variables and parameters as shown in Table 6. Some of the weather variables used to calculate the parameters of ET_o were maximum temperature, minimum temperature, relative humidity, evaporation, sunshine, rainfall, and wind speed. Moreover, various parameters were used in the ET_o equations such as actual vapor pressure, vapor pressure deficit, extraterrestrial radiation and soil heat flux. The ET_o parameters can be calculated by equations as shown in Table 6 and the ET_o can be calculated on a daily basis using the FAO Penman-Monteith equation (Allen et al., 1998) as shown in equation (1). The schematic diagram of analytic reference evapotranspiration is shown in Figure 20.

5. Trend analysis

This study adopted the method of Mann-Kendall test (Mann, 1945; Kendall, 1975) for trend analysis. The Mann-Kendall trend test is one of the widely used non-parametric tests to detect significant trends in time series. The Mann-Kendall trend test, being a function of the ranks of the observations rather than their actual values, is not affected by the actual distribution of the data and is less sensitive to outliers. On the other hand, parametric trend tests, although more powerful, require the data to be normally distributed and are more sensitive to outliers. The Mann-Kendall test, as well as other non-parametric trend tests, is therefore more suitable for detecting trends in hydrological time series, which are usually skewed and may be contaminated with outliers (Hamed, 2008).

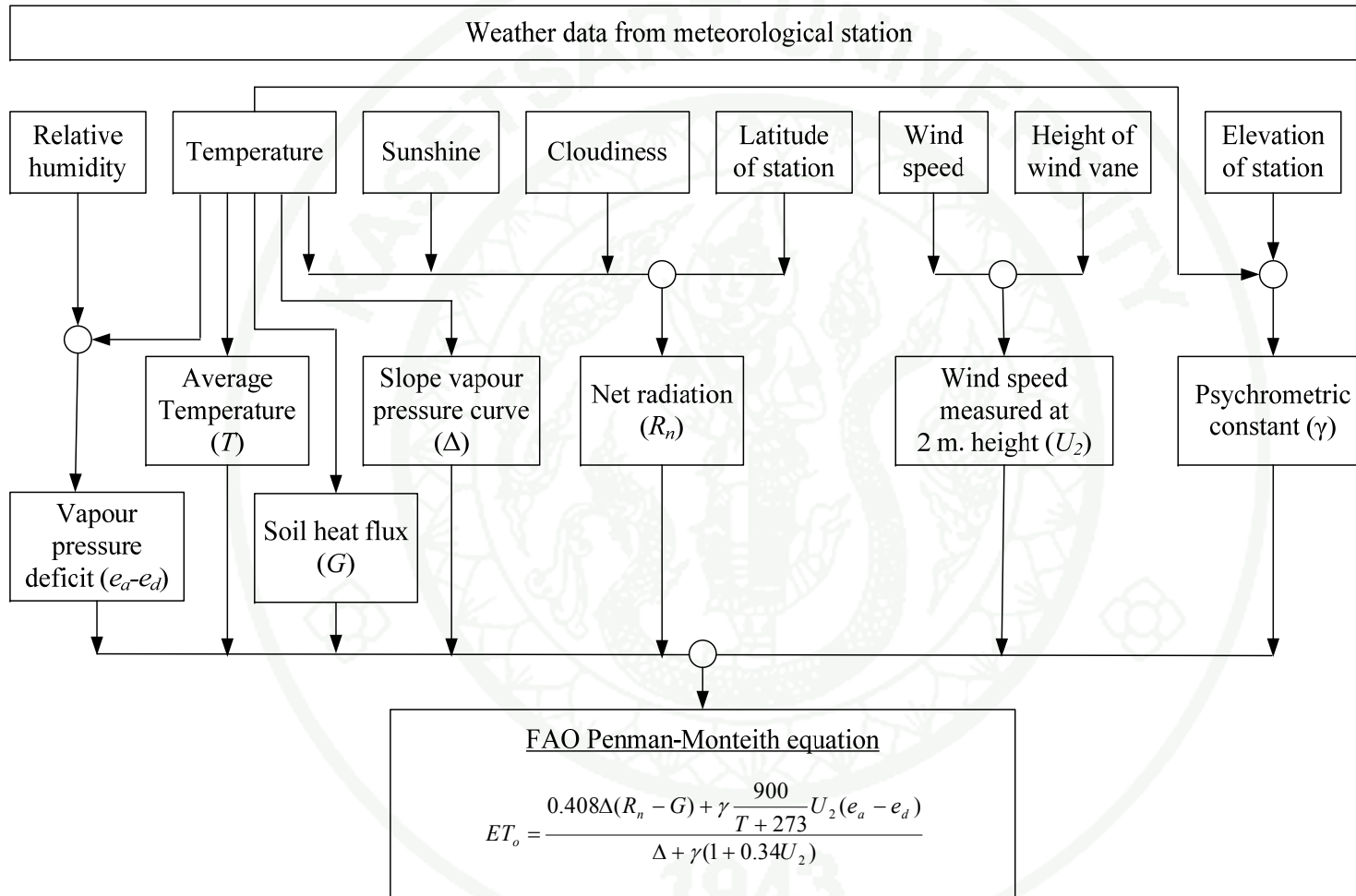


Figure 20 Schematic diagram of analytic reference evapotranspiration (ET_o)

The non-parametric Mann-Kendall statistical test has been popularly used to assess the significance of trends in hydrological time series (Yue et al., 2004).

The Mann-Kendall test was performed on all stations to detect daily trends of weather variables, ET_o parameters and reference evapotranspiration. For a time series $X = \{x_1, x_2, \dots, x_n\}$, the null hypothesis H_0 states that there is a sample of n independent and identically distributed random variables (Yu et al., 1993). The alternative hypothesis H_1 of a two-sided test is that the distribution of x_k and x_j are not identical for all $k, j \leq n$ with $k \neq j$. The test statistic S is calculated with (Kahya et al., 2004) as shown in equation (28) and (29).

The significance of trends can be tested by comparing the standardized variable z in equation (32) with the standard normal variate at the desired significance level, where the subtraction or addition of unity in equation (32) is a continuity correction (Kendall, 1975).

Positive values of z in equation (32) indicate increasing trends while negative z values indicate decreasing trends when testing either increasing or decreasing trends at a significance level (p -value). In this work, significance levels of $p < 0.10$, $p < 0.05$ and $p < 0.01$ were applied.

The Schematic diagram of analytic trend is shown in Figure 21.

6. Antecedent precipitation index (API)

The analysis of the antecedent precipitation index (API) for each small watersheds of the upper Chao Phraya river basin is shown in Figure 22. The details are shown below.

- 1) Weather data and land use data were collected.

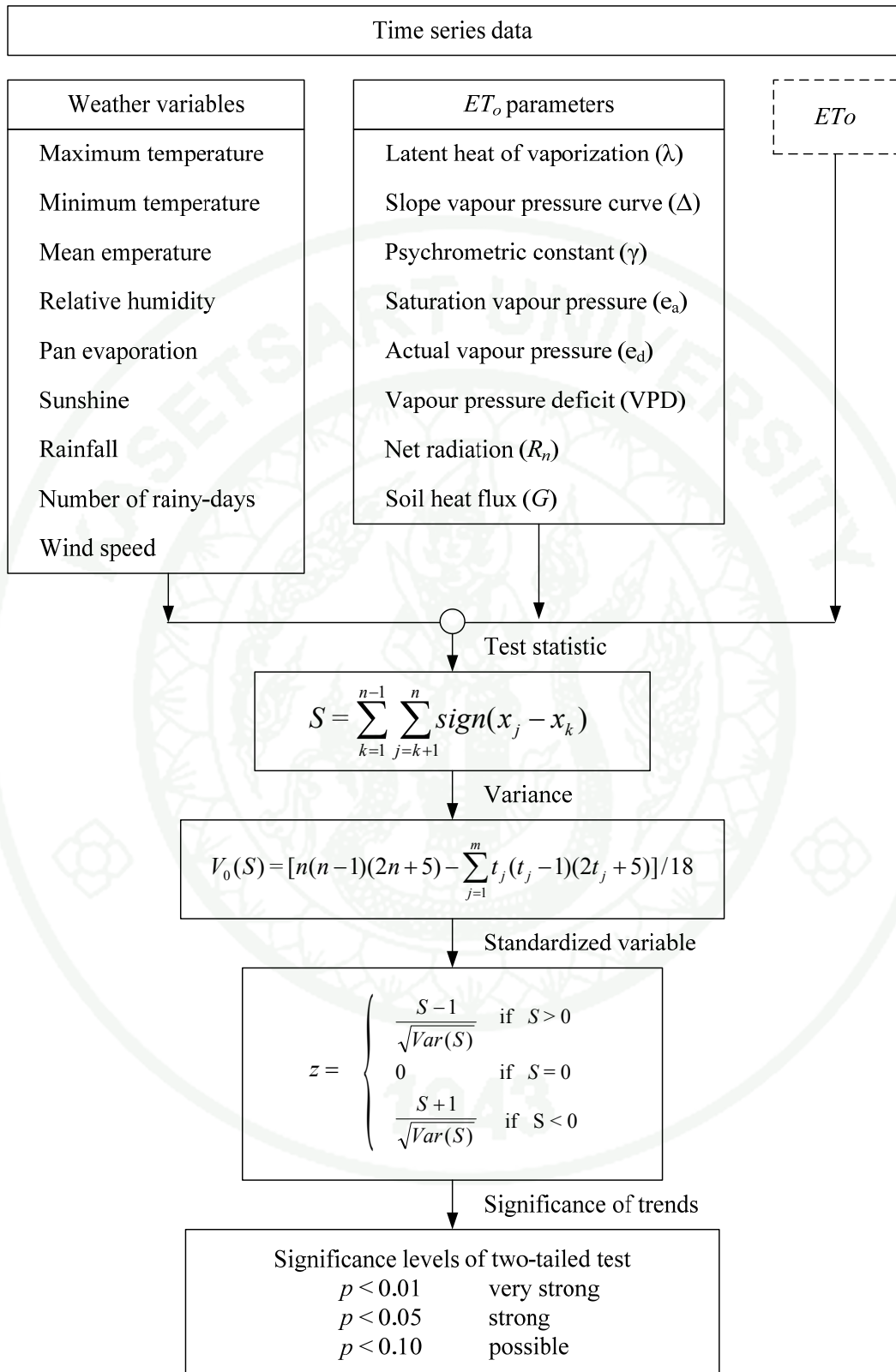


Figure 21 Schematic diagram of analytic trend.

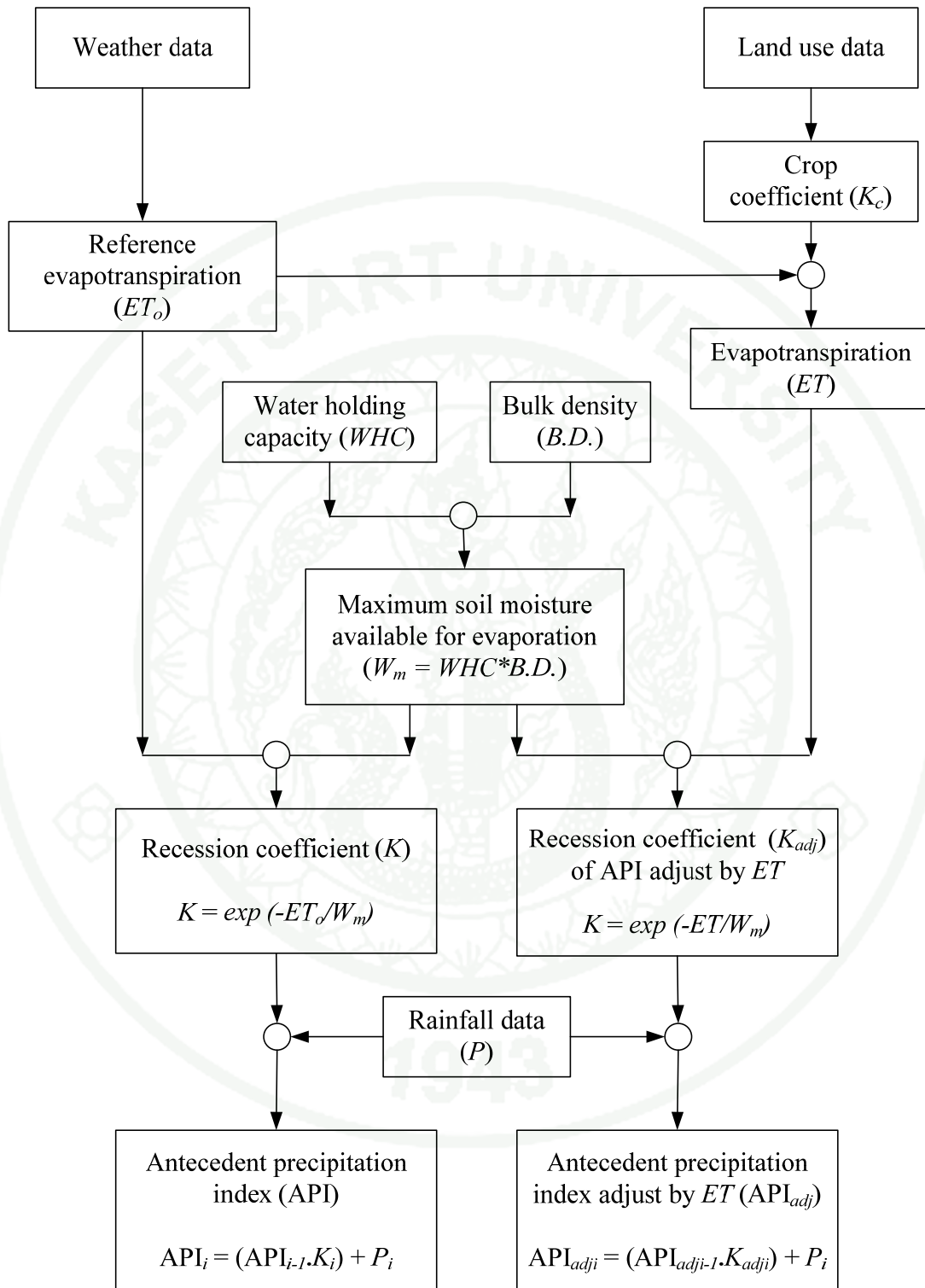


Figure 22 Schematic diagram of analytic antecedent precipitation index (API).

- 2) The weather data is used to analyze reference evapotranspiration (ET_o).
- 3) Collecting crop coefficient (K_c) from land use data and crop calendar period as shown in crop calendar in Figure 23. In addition, the research used agricultural area of off-season rice field equal to in-season rice field in irrigation area during dry season.
- 4) The result of reference evapotranspiration (ET_o), land use and crop coefficient (K_c) were used to analyze evapotranspiration (ET).
- 5) Physical soil testing was collected in order to analyze antecedent precipitation index (API).
- 6) Analysis of maximum soil moisture available for evaporation (W_m) of surface soil (0-10 cm), which is related to the bulk density of soil ($B.D.$) and the water holding capacity (WHC) as shown in equation (5).
- 7) Analysis of recession coefficient (K), which is the function of reference evapotranspiration (ET_o) and the maximum soil moisture available for evaporation (W_m) from Chodhury and Blanchard (1983) as show in equation (4)
- 8) Analysis of recession coefficient of adjusted API by evapotranspiration (K_{adj}), which evapotranspiration (ET) was used instead of the reference evapotranspiration (ET_o) is show in equation below.

$$K_{adj} = \exp\left(\frac{-ET}{W_m}\right) \quad (45)$$

- 9) The antecedent precipitation index (API) is intended to reflect the changeable infiltration capacity of the soil related to the frequency and depth of previous rainfall events. Kohler & Linsley (1951) developed the API as a soil moisture depletion model as shown in equation (3).

Subbasin	Crops	Jan	Feb	Mar	Apr	May	Jun	Jul	Aug	Sep	Oct	Nov	Dec
Ping river basin	Rainfed lowland rice												
	Irrigated rice												
	Field crops												
	Horticulture												
Wang river basin	Rainfed lowland rice												
	Irrigated rice												
	Field crops												
	Horticulture												
Yom river basin	Rainfed lowland rice												
	Irrigated rice												
	Field crops												
	Horticulture												
Nan river basin	Rainfed lowland rice												
	Irrigated rice												
	Field crops												
	Horticulture												
Main Chao Phraya river basin	Rainfed lowland rice												
	Irrigated rice												
	Field crops												
	Horticulture												

Figure 23 Crop calendar of the upper Chao Phraya river basin.

- 10) Analysis of the *API* and adjusted *API* by using recession coefficient (*K*) and recession coefficient of adjusted *API* by evapotranspiration (*K_{adj}*)

7. Critical antecedent precipitation index (*API_{critical}*)

The concept to calculate critical antecedent precipitation index (*API_{critical}*) is an efficiency of soil water capacity and soil moisture accumulated. The critical antecedent precipitation index is a maximum soil water capacity value. When water in soil has more than critical antecedent precipitation index value, the rainfall will immediately produce surface runoff. The method can be written as

$$\text{API}_{\text{critical}} = SL \quad (46)$$

where *S* is a saturation percentage of soil and *L* is a depth of soil. The research use depth of soil from 0-15 cm, 15-30 cm, 30-50 cm, 50-70 cm and 70-100 cm to calculate an *API_{critical}*.

8. Watershed runoff prediction

To predict outflow hydrographs for each small watershed of the upper Chao Phraya river basin, the relationship between antecedent precipitation index (*API*), daily rainfall and daily discharge were used in order to develop a rainfall-runoff model. This study compares rainfall-runoff models using various antecedent precipitation index (*API*) relationships. For example, the *API* model for runoff estimation of Viessman et al., (1989) which was compared to 5 different nonlinear *API* models for runoff estimation. In addition, the comparison of performances of original *API* model for runoff estimation of Viessman et al., (1989) with 6 of adjusted *API* rainfall-runoff models by evapotranspiration (*ET*) and 6 of *API* rainfall-runoff models was improved by using the ranges of critical *API* as shown in the flow chart of the watershed runoff prediction in Figure 24. The details are shown below.

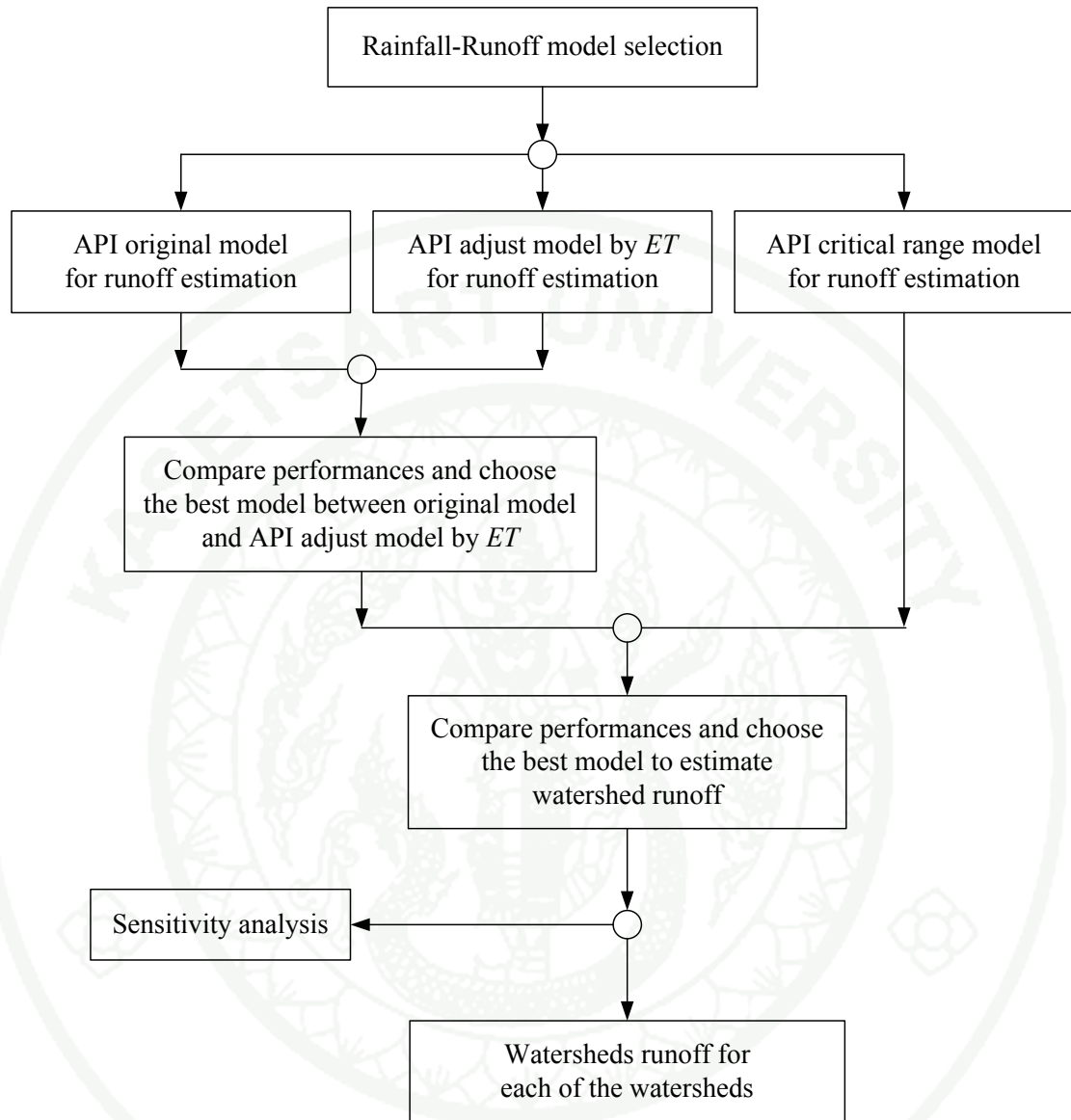


Figure 24 Simplified flow chart of the watershed runoff prediction.

1) The representative stream gauging stations were selected from every sub-basin of upper Chao Phraya river basin. By this selection, 36 stream gauging stations collected daily streamflow data during year 1977 to 2002. In order to calibrate and verify the simulation results, and to compare the results of runoff from different models, the representative stations were comprised of 10 stations from Ping river basin, 4 stations from Wang river basin, 7 stations from Yom river basin and 15 stations from Nan river basin as shown in Figure 25.

2) Areal distribution analysis of daily rainfall depth of index raingauge stations for watershed area of representative stream gauging stations during year 1977 to 2002 by Thiessen average was used.

3) Daily antecedent precipitation index (*API*) analysis of watershed area of representative stream gauging stations was used.

4) Analysis of daily watershed runoff of representative stream gauging stations by using the six models of relationship between antecedent precipitation index (*API*) and daily rainfall is show in equation below.

$$\text{Model-1: } Q = a + b.P + c.API \quad (47)$$

$$\text{Model-2: } Q = a + b.P + c.P^2 + d.API + e.API^2 \quad (48)$$

$$\text{Model-3: } Q = a + b.P + c.P^2 + d.P + e.API + f.API^2 + g.API^3 \quad (49)$$

$$\text{Model-4: } Q = a + b.P^c + d.API^e \quad (50)$$

$$\text{Model-5: } Q = a + b.exp^{c.P} + d.exp^{e.API} \quad (51)$$

$$\text{Model-6: } Q = a + b.\ln(P) + c.\ln(API) \quad (52)$$

Model-1 is a linear correlation of Viessman et al., (1989) studied, model-2 is a nonlinear multiple quadratic regression, model-3 is a nonlinear multiple cubic regression, model-4 is a nonlinear multiple power regression, model-5 is a nonlinear multiple exponential regression and model-6 is a nonlinear multiple logarithmic regression.

5) Nash-Sutcliffe efficiency (*NSE*), correlation coefficient (*r*) and root mean square error (*RMSE*) as shown in equation (53) to (55) are used for evaluates goodness of fit between the observed and calculated discharges in order to decide upon the most appropriate of parameters for each model and each stream gauging stations.

$$NSE = 1 - \frac{\sum_{i=1}^n (Q_{obs,i} - Q_{sim,i})^2}{\sum_{i=1}^n (Q_{obs,i} - Q_{avg})^2} \quad (53)$$

where NSE is Nash-Sutcliffe efficiency, $Q_{obs,i}$ is observed discharge, $Q_{sim,i}$ is modeled discharge and Q_{avg} is average of observed discharge. The Nash–Sutcliffe efficiency can range from $-\infty$ to 1, $NSE = 1$ corresponds to a perfect match of modeled discharge to the observed data, $NSE \geq 0.75$ corresponds to a good prediction, $0.36 \leq NSE \leq 0.75$ corresponds to a satisfactory prediction and $NSE = 0$ indicates that the model predictions are as accurate as the arithmetic mean of the observed data (Vudhivanich, 2010).

$$r = \frac{COV(X,Y)}{\sqrt{VAR(X).VAR(Y)}} \quad (54)$$

where r is correlation coefficient, $COV(X,Y)$ is covariance between variables X and Y , $VAR(X)$ is variance of variable X and $VAR(Y)$ is variance of variable Y . The correlation coefficient can range in value from -1 to +1, $r = 1$ corresponds to a perfect correlation, $r = -1$ indicating perfect negative correlation and $r = 0$ is absence of correlation.

$$RMSE = \sqrt{\frac{\sum_{i=1}^n (Q_{obs,i} - Q_{sim,i})^2}{n}} \quad (55)$$

where $RMSE$ is root mean square error, $Q_{obs,i}$ is observed discharge, $Q_{sim,i}$ is modeled discharge. Lower values of $RMSE$ indicate better fit of modeled discharge to the observed data.

6) Comparison of between the statistical measures of the similarity between simulated hydrographs and observed hydrographs using *API* rainfall-runoff model-1 to model-6 was conducted.

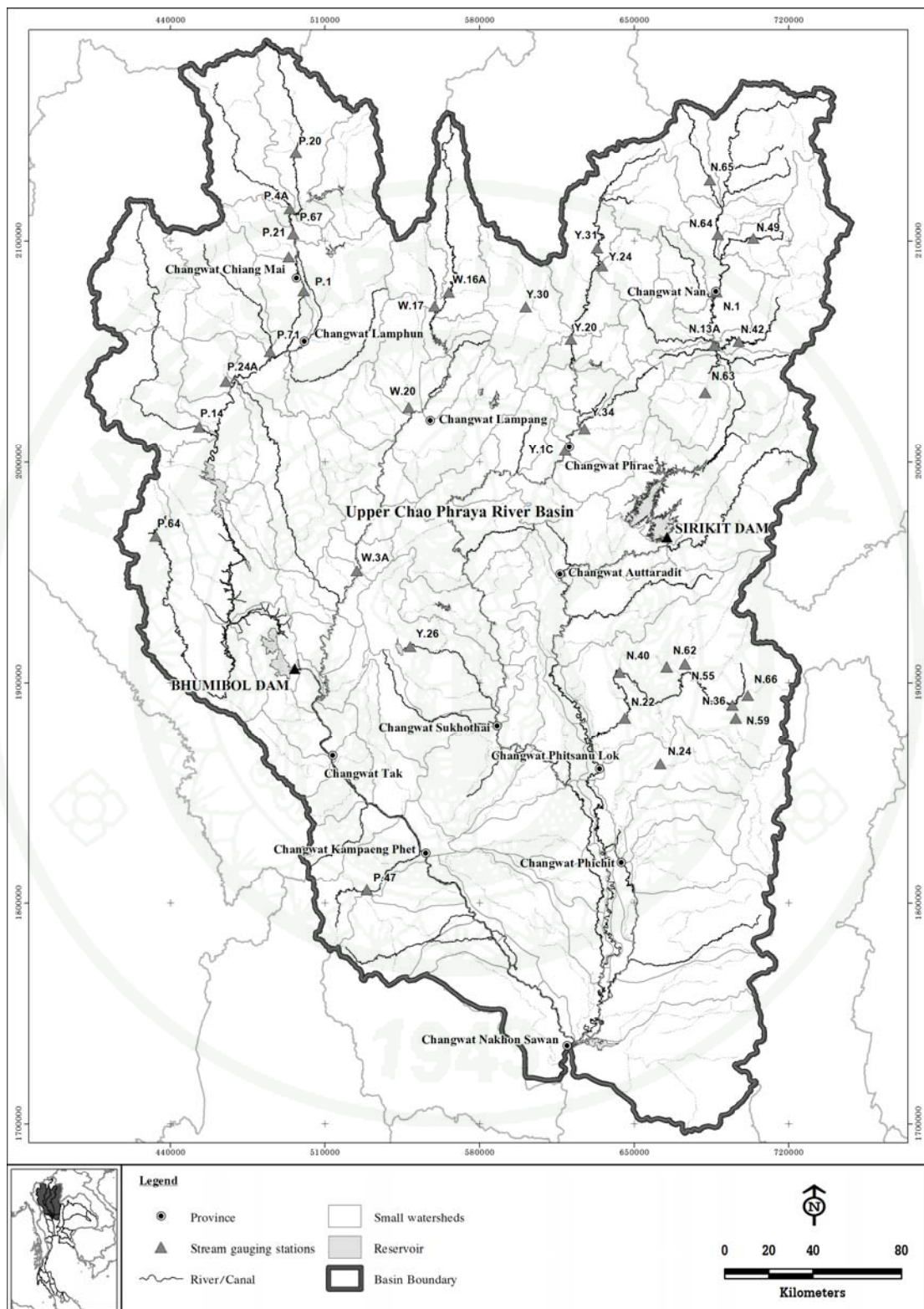


Figure 25 Location of stream gauging stations used for the analysis of testing the rainfall-runoff model performance.

7) Analysis of daily watershed runoff of representative stream gauging stations by using the 6 models of relationship between daily rainfall and antecedent precipitation index (*API*) adjusted by evapotranspiration (*ET*) using adjusted recession coefficient (K_{adj}) is show in equation below.

$$\text{Model-1: } Q = a + b.P + c.(API_{adj}) \quad (56)$$

$$\text{Model-2: } Q = a + b.P + c.P^2 + d.(API_{adj}) + e.(API_{adj})^2 \quad (57)$$

$$\begin{aligned} \text{Model-3: } Q = a + b.P + c.P^2 + d.P^3 + e.(API_{adj}) + f.(API_{adj})^2 \\ + g.(API_{adj})^3 \end{aligned} \quad (58)$$

$$\text{Model-4: } Q = a + b.P^c + d.(API_{adj})^e \quad (59)$$

$$\text{Model-5: } Q = a + b.\exp^{c.P} + d.\exp^{e(API_{adj})} \quad (60)$$

$$\text{Model-6: } Q = a + b.\ln(P) + c.\ln(API_{adj}) \quad (61)$$

Model-1 is a linear correlation which is modified from Viessman et al., (1989) studied, model-2 is a nonlinear multiple quadratic regression, model-3 is a nonlinear multiple cubic regression, model-4 is a nonlinear multiple power regression, model-5 is a nonlinear multiple exponential regression and model-6 is a nonlinear multiple logarithmic regression.

9) Comparison of the statistical measures of the similarity between simulated hydrographs and observed hydrographs using adjusted *API* by evapotranspiration (*ET*) rainfall-runoff model-1 to model-6 was conducted.

10) The performance comparison of the *API* rainfall-runoff model 1 to 6 and the *API* adjusted by evapotranspiration (*ET*) rainfall-runoff model-1 to model-6 were verified at representative stream gauging stations in the upper Chao Phraya river basin.

11) Analysis of daily watershed runoff of representative stream gauging stations by using the 6 models of relationship between daily rainfall and antecedent precipitation index (*API*) was improved by using the ranges of critical *API*. The ranges are defined by percentage of critical *API* which is divided into 10 rang (10,

20, 30, 40, 50, 60, 70, 80, 90 and 100 percentage of critical API). For each percentage range, the critical API models will have 3 sets of model parameters. Each set of parameters is derived by comparing daily API with critical API . The first set of parameters is $API < \text{percentage of } API_{\text{critical}}$; the second set is $\text{percentage of } API_{\text{critical}} < API < API_{\text{critical}}$; and the third set is $API > API_{\text{critical}}$; as shown below; and the summary of critical API range model for runoff estimation is shown in Table 10.

Parameters set 1: $API < \text{percentage of } API_{\text{critical}}$ $(a_1, b_1, c_1, d_1, e_1, f_1, g_1)$

Parameters set 2: $\text{Percentage of } API_{\text{critical}} < API < API_{\text{critical}}$ $(a_2, b_2, c_2, d_2, e_2, f_2, g_2)$

Parameters set 3: $API > API_{\text{critical}}$ $(a_3, b_3, c_3, d_3, e_3, f_3, g_3)$

12) Comparison of the statistical measures of the similarity between simulated and observed hydrographs using API rainfall-runoff was improved by using the 10 ranges of critical API (10, 20, 30, 40, 50, 60, 70, 80, 90 and 100 percentage) of model-1 to model-6.

13) Comparison of performances of original model and improvement model (adjusted API model and critical API range model) for runoff estimation was done in order to select the appropriate model for estimating the watershed runoff.

14) After the appropriate model was chosen for estimation daily watershed runoff at 36 representative stream gauging stations during year 1977 to 2002 was used for model calibration. The outcome of the calibration of each year was used to determine suitable value of each model parameter for each watershed.

15) The appropriate model and model parameters from 14) were used to estimate daily watershed runoff at 4 stream gauging stations which the station do not use to model calibration in step 14) was not applied to. The comparison of result between simulated runoff and observed runoff was used to determine model performance for ungauged basin runoff prediction.

Table 10 Summary critical API range model for runoff estimation

Percentage of $API_{critical}$	Parameters of API critical range model for runoff estimation		
	$API < \% \text{ of } API_{critical}$	$\% \text{ of } API_{critical} < API$	$API > API_{critical}$
Model-1 Linear (Plan) $Q = a_n + b_n.P + c_n.API$			
10%	a_1, b_1, c_1	a_2, b_2, c_2	a_3, b_3, c_3
20%	a_1, b_1, c_1	a_2, b_2, c_2	a_3, b_3, c_3
30%	a_1, b_1, c_1	a_2, b_2, c_2	a_3, b_3, c_3
40%	a_1, b_1, c_1	a_2, b_2, c_2	a_3, b_3, c_3
50%	a_1, b_1, c_1	a_2, b_2, c_2	a_3, b_3, c_3
60%	a_1, b_1, c_1	a_2, b_2, c_2	a_3, b_3, c_3
70%	a_1, b_1, c_1	a_2, b_2, c_2	a_3, b_3, c_3
80%	a_1, b_1, c_1	a_2, b_2, c_2	a_3, b_3, c_3
90%	a_1, b_1, c_1	a_2, b_2, c_2	a_3, b_3, c_3
100%	a_1, b_1, c_1	a_2, b_2, c_2	a_3, b_3, c_3
Model-2 Quadratic (Paraboloid) $Q = a_n + b_n.P + c_n.P^2 + d_n.API + e_n.API^2$			
10%	a_1, b_1, c_1, d_1, e_1	a_2, b_2, c_2, d_2, e_2	a_3, b_3, c_3, d_3, e_3
20%	a_1, b_1, c_1, d_1, e_1	a_2, b_2, c_2, d_2, e_2	a_3, b_3, c_3, d_3, e_3
30%	a_1, b_1, c_1, d_1, e_1	a_2, b_2, c_2, d_2, e_2	a_3, b_3, c_3, d_3, e_3
40%	a_1, b_1, c_1, d_1, e_1	a_2, b_2, c_2, d_2, e_2	a_3, b_3, c_3, d_3, e_3
50%	a_1, b_1, c_1, d_1, e_1	a_2, b_2, c_2, d_2, e_2	a_3, b_3, c_3, d_3, e_3
60%	a_1, b_1, c_1, d_1, e_1	a_2, b_2, c_2, d_2, e_2	a_3, b_3, c_3, d_3, e_3
70%	a_1, b_1, c_1, d_1, e_1	a_2, b_2, c_2, d_2, e_2	a_3, b_3, c_3, d_3, e_3
80%	a_1, b_1, c_1, d_1, e_1	a_2, b_2, c_2, d_2, e_2	a_3, b_3, c_3, d_3, e_3
90%	a_1, b_1, c_1, d_1, e_1	a_2, b_2, c_2, d_2, e_2	a_3, b_3, c_3, d_3, e_3
100%	a_1, b_1, c_1, d_1, e_1	a_2, b_2, c_2, d_2, e_2	a_3, b_3, c_3, d_3, e_3
Model-3 Cubic $Q = a_n + b_n.P + c_n.P^2 + d_n.P^3 + e_n.API + f_n.API^2 + g_n.API^3$			
10%	$a_1, b_1, c_1, d_1, e_1, f_1, g_1$	$a_2, b_2, c_2, d_2, e_2, f_2, g_2$	$a_3, b_3, c_3, d_3, e_3, f_3, g_3$
20%	$a_1, b_1, c_1, d_1, e_1, f_1, g_1$	$a_2, b_2, c_2, d_2, e_2, f_2, g_2$	$a_3, b_3, c_3, d_3, e_3, f_3, g_3$
30%	$a_1, b_1, c_1, d_1, e_1, f_1, g_1$	$a_2, b_2, c_2, d_2, e_2, f_2, g_2$	$a_3, b_3, c_3, d_3, e_3, f_3, g_3$
40%	$a_1, b_1, c_1, d_1, e_1, f_1, g_1$	$a_2, b_2, c_2, d_2, e_2, f_2, g_2$	$a_3, b_3, c_3, d_3, e_3, f_3, g_3$
50%	$a_1, b_1, c_1, d_1, e_1, f_1, g_1$	$a_2, b_2, c_2, d_2, e_2, f_2, g_2$	$a_3, b_3, c_3, d_3, e_3, f_3, g_3$
60%	$a_1, b_1, c_1, d_1, e_1, f_1, g_1$	$a_2, b_2, c_2, d_2, e_2, f_2, g_2$	$a_3, b_3, c_3, d_3, e_3, f_3, g_3$
70%	$a_1, b_1, c_1, d_1, e_1, f_1, g_1$	$a_2, b_2, c_2, d_2, e_2, f_2, g_2$	$a_3, b_3, c_3, d_3, e_3, f_3, g_3$
80%	$a_1, b_1, c_1, d_1, e_1, f_1, g_1$	$a_2, b_2, c_2, d_2, e_2, f_2, g_2$	$a_3, b_3, c_3, d_3, e_3, f_3, g_3$
90%	$a_1, b_1, c_1, d_1, e_1, f_1, g_1$	$a_2, b_2, c_2, d_2, e_2, f_2, g_2$	$a_3, b_3, c_3, d_3, e_3, f_3, g_3$
100%	$a_1, b_1, c_1, d_1, e_1, f_1, g_1$	$a_2, b_2, c_2, d_2, e_2, f_2, g_2$	$a_3, b_3, c_3, d_3, e_3, f_3, g_3$

Table 10 (Continued)

Percentage of $API_{critical}$	Parameters of API critical range model for runoff estimation		
	$API < \% \text{ of } API_{critical}$	$\% \text{ of } API_{critical} < API$	$API > API_{critical}$
	$API < API_{critical}$		
Model-4 Power $Q = a_n + b_n.P^{cn} + d_n.API^{en}$			
10%	a_1, b_1, c_1, d_1, e_1	a_2, b_2, c_2, d_2, e_2	a_3, b_3, c_3, d_3, e_3
20%	a_1, b_1, c_1, d_1, e_1	a_2, b_2, c_2, d_2, e_2	a_3, b_3, c_3, d_3, e_3
30%	a_1, b_1, c_1, d_1, e_1	a_2, b_2, c_2, d_2, e_2	a_3, b_3, c_3, d_3, e_3
40%	a_1, b_1, c_1, d_1, e_1	a_2, b_2, c_2, d_2, e_2	a_3, b_3, c_3, d_3, e_3
50%	a_1, b_1, c_1, d_1, e_1	a_2, b_2, c_2, d_2, e_2	a_3, b_3, c_3, d_3, e_3
60%	a_1, b_1, c_1, d_1, e_1	a_2, b_2, c_2, d_2, e_2	a_3, b_3, c_3, d_3, e_3
70%	a_1, b_1, c_1, d_1, e_1	a_2, b_2, c_2, d_2, e_2	a_3, b_3, c_3, d_3, e_3
80%	a_1, b_1, c_1, d_1, e_1	a_2, b_2, c_2, d_2, e_2	a_3, b_3, c_3, d_3, e_3
90%	a_1, b_1, c_1, d_1, e_1	a_2, b_2, c_2, d_2, e_2	a_3, b_3, c_3, d_3, e_3
100%	a_1, b_1, c_1, d_1, e_1	a_2, b_2, c_2, d_2, e_2	a_3, b_3, c_3, d_3, e_3
Model-5 Exponential $Q = a_n + b_n.exp^{cn.P} + d_n.exp^{en.API}$			
10%	a_1, b_1, c_1, d_1, e_1	a_2, b_2, c_2, d_2, e_2	a_3, b_3, c_3, d_3, e_3
20%	a_1, b_1, c_1, d_1, e_1	a_2, b_2, c_2, d_2, e_2	a_3, b_3, c_3, d_3, e_3
30%	a_1, b_1, c_1, d_1, e_1	a_2, b_2, c_2, d_2, e_2	a_3, b_3, c_3, d_3, e_3
40%	a_1, b_1, c_1, d_1, e_1	a_2, b_2, c_2, d_2, e_2	a_3, b_3, c_3, d_3, e_3
50%	a_1, b_1, c_1, d_1, e_1	a_2, b_2, c_2, d_2, e_2	a_3, b_3, c_3, d_3, e_3
60%	a_1, b_1, c_1, d_1, e_1	a_2, b_2, c_2, d_2, e_2	a_3, b_3, c_3, d_3, e_3
70%	a_1, b_1, c_1, d_1, e_1	a_2, b_2, c_2, d_2, e_2	a_3, b_3, c_3, d_3, e_3
80%	a_1, b_1, c_1, d_1, e_1	a_2, b_2, c_2, d_2, e_2	a_3, b_3, c_3, d_3, e_3
90%	a_1, b_1, c_1, d_1, e_1	a_2, b_2, c_2, d_2, e_2	a_3, b_3, c_3, d_3, e_3
100%	a_1, b_1, c_1, d_1, e_1	a_2, b_2, c_2, d_2, e_2	a_3, b_3, c_3, d_3, e_3
Model-6 Logarithm $Q = a_n + b_n.ln(P) + c_n.ln(API)$			
10%	a_1, b_1, c_1	a_2, b_2, c_2	a_3, b_3, c_3
20%	a_1, b_1, c_1	a_2, b_2, c_2	a_3, b_3, c_3
30%	a_1, b_1, c_1	a_2, b_2, c_2	a_3, b_3, c_3
40%	a_1, b_1, c_1	a_2, b_2, c_2	a_3, b_3, c_3
50%	a_1, b_1, c_1	a_2, b_2, c_2	a_3, b_3, c_3
60%	a_1, b_1, c_1	a_2, b_2, c_2	a_3, b_3, c_3
70%	a_1, b_1, c_1	a_2, b_2, c_2	a_3, b_3, c_3
80%	a_1, b_1, c_1	a_2, b_2, c_2	a_3, b_3, c_3
90%	a_1, b_1, c_1	a_2, b_2, c_2	a_3, b_3, c_3
100%	a_1, b_1, c_1	a_2, b_2, c_2	a_3, b_3, c_3

16) Sensitivity analysis of appropriate *API* model parameters was evaluated in order to understand the characteristics of the hydrograph outputs of model which are affected by each model parameter. The results of sensitivity analysis are applied to set up the model for other watershed area. The method of sensitivity analysis is presented below.

16.1) selected the representative stream gauging stations from every subbasin of upper Chao Phraya river basin were selected. By this selection, 4 stream gauging stations were collected daily streamflow data which comprised of P.14 from Ping river basin, W.17 from Wang river basin, Y.20 from Yom river basin and N.24 from Nan river basin.

16.2) The appropriate model was chosen for estimating daily watershed runoff. The model was applied to the analysis of trend and affect of each model parameter on the characteristics of the hydrograph which useful for predictive outflow hydrographs for each watershed.

16.3) Each parameters of the appropriate model was analysed against the sensitivity of model parameters by increasing and decreasing parameter values from -30% to 30% of parameter values (-30%, -20%, -10%, +10%, +20% and +30%). Moreover, these parameters were used to estimate watershed runoff of each range.

16.4) Comparison of the changing parameter values affected the peak discharge, time to peak and discharge volume of watershed runoff.

17) Analysis of areal daily rainfall depths of 112 small watersheds in the upper Chao Phraya river basin with Thiessen Polygon technique in period of water year 1977 to 2002 was conducted.

18) Analysis of daily antecedent precipitation Index (*API*) of 112 small watersheds in the upper Chao Phraya river basin by method is shown in Figure 22.

19) Analysis of daily watersheds runoff of 112 small watersheds by using the appropriate model was chosen from 13) in order to predict outflow hydrographs for each watershed of the upper Chao Phraya river network was conducted.

9. Hydrologic routing model

To predict outflow hydrographs for each major reach of the upper Chao Phraya river network, Muskingum routing model of HEC-HMS version 3.5 was used in this study. The details of analytic hydrologic routing model are shown below.

- 1) The schematic diagram of the upper Chao Phraya river network was set up as shown in Figure 26 to 28.
- 2) The representative stream gauging stations for calibration and verification in the upper Chao Phraya river network were selected. Moreover, daily inflow and daily outflow data were collected from Bhumibol dam and Sirikit dam in order to calibrate and to verify the simulation results; and to compare the result between runoff from observed.
- 3) Daily watershed runoff (I) of 112 small watersheds was analysed with *API* rainfall-runoff model. Thereafter, Muskingum routing model of HEC-HMS model was applied to route outflow hydrographs of each watershed during year 1994 to 2002.
- 4) Iteration time step t , estimate initial travel time of the runoff hydrograph through a stream reach (K) and dimensionless weighting factor (X) which was estimated from channel characteristics and velocity of peak flow using equations (42) and (43). The value of X must be between 0.0 and 0.5; moreover negative values of C_1 are avoided by using equations (44).

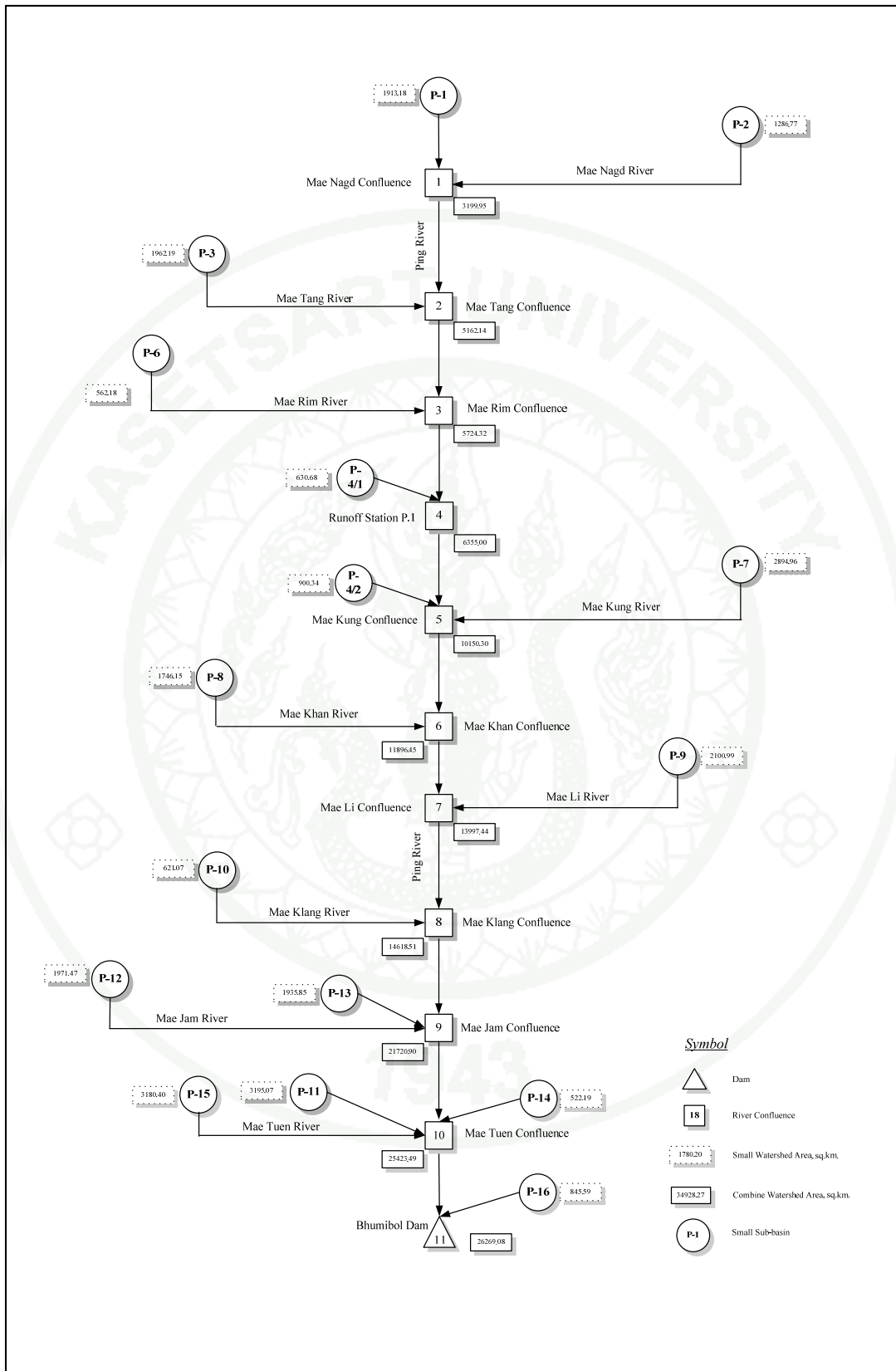


Figure 26 Schematic diagram of the upper Ping river network.

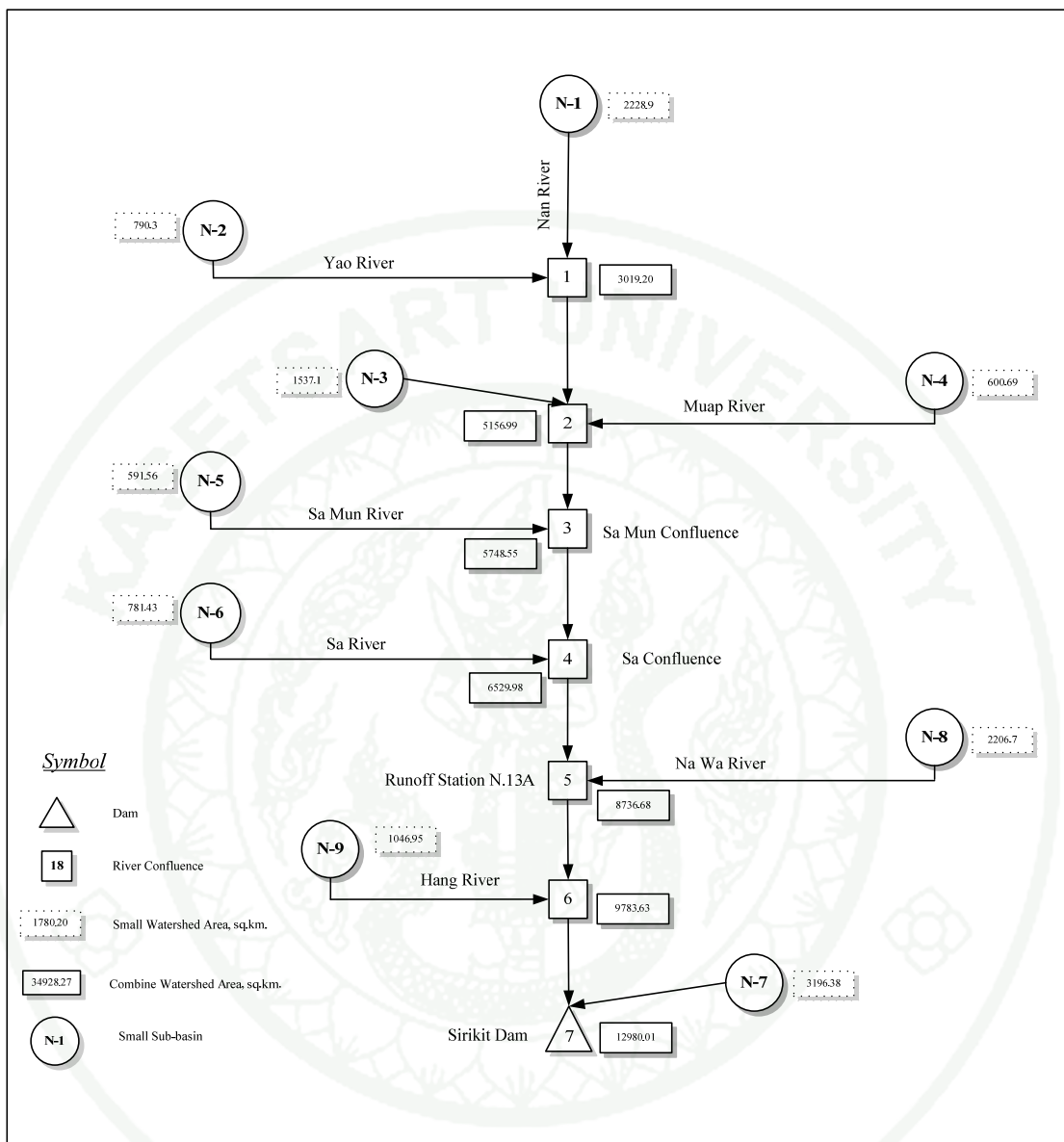


Figure 27 Schematic diagram of the upper Nan river network.

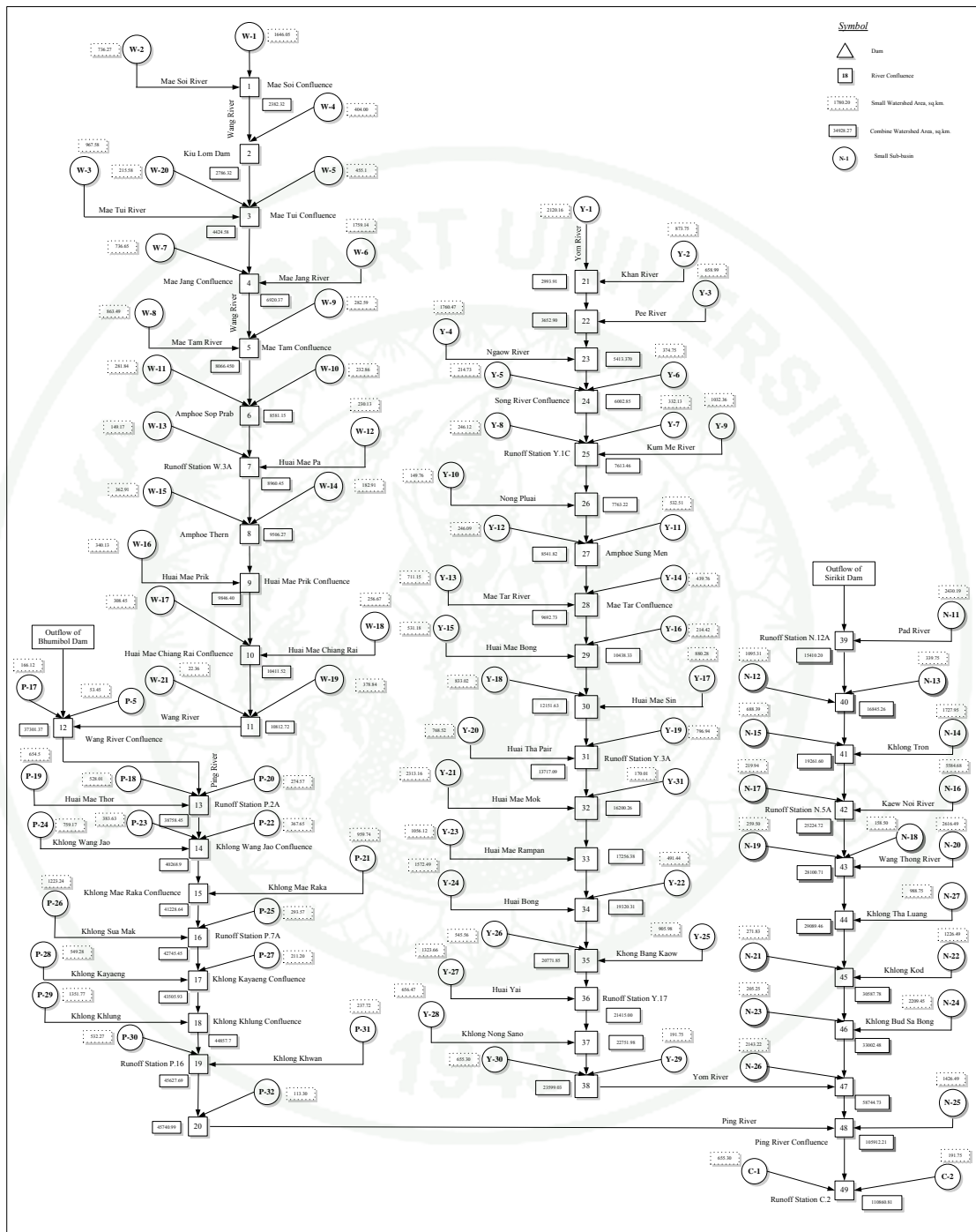


Figure 28 Schematic diagram of the upper Chao Phraya (downstream of Bhumibol dam and Sirikit dam).

- 5) Iteration time step t , estimate C_1 , C_2 and C_3 and estimate outflow hydrograph (O_{t+1}) of next time step $t + 1$ until time step n using equations (38) and (39).
- 6) Outflow hydrographs of stream reach in step 4) was combined with runoff hydrographs of various small watersheds at control point. The outcome of routing and combining is the outflow hydrographs for each major reach of the upper Chao Phraya river network.
- 7) Calibrating the model with the comparison between observed runoff and simulate runoff by running each parameter of HEC-HMS model through trial and error. The calibration techniques will test each parameter one by one while the other parameters were fixed until the parameters obtain the best model performances as shown in calibration procedure of HEC-HMS model in Figure 29. Furthermore, the range of parameter of HEC-HMS model, Muskingum K (travel time of the flood wave through routing reach) value is between 0.1 and 150 hour, Muskingum X (dimensionless weighting factor) value is between 0.0 and 0.5 hour, the number of steps value is between 1 and 100.
- 8) Comparison of the statistical measures of the similarity between outflow hydrographs was simulated in step 6) and daily observed hydrographs included with 12 stream gauging stations and daily inflow and daily outflow of Bhumibol dam and Sirikit dam. After that, trial by changing parameter of stream reach (K) and dimensionless weighting factor (X) in order to find the best fit of outflow hydrographs for each major reach of the upper Chao Phraya river network.

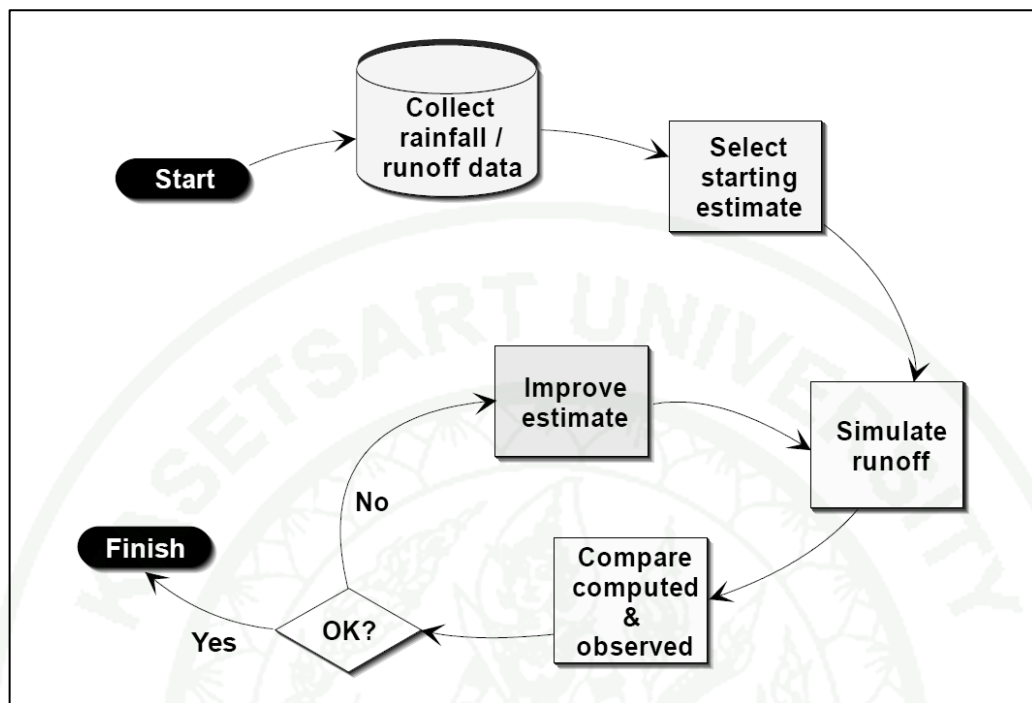


Figure 29 Schematic of calibration procedure.

Source: USACE (2000)

RESULTS AND DISCUSSION

1. Reference evapotranspiration

Reference evapotranspiration (ET_o) for each weather station in the upper Chao Phraya river basin (Table 9) was estimated by using FAO Penman-Monteith method. The weather variables used to calculate the parameters of ET_o . In addition, ET_o parameters were used to calculate reference evapotranspiration (ET_o) by equations as shown in Table 6. The ET_o parameters were used to analyze reference evapotranspiration (ET_o) as shown in Figure 20 with latent heat of vaporization (λ), slope vapour pressure curve (Δ), atmospheric pressure (P), psychrometric constant (γ), saturation vapour pressure (e_a), actual vapour pressure (e_d), vapour pressure deficit (VPD), extraterrestrial radiation (R_a), daylight hours (N), net radiation and soil heat flux.

The averages of monthly ET_o parameters from 1977 and 2006 over 9 weather stations are shown in Table 11. The summary of average monthly reference evapotranspiration (ET_o) over 9 weather stations are shown in Table 12; and time series of annual reference evapotranspiration (ET_o) from 1977 and 2006 are plotted in Figure 30. It is seen that the mean annual reference evapotranspiration (ET_o) in all the stations have decreased during a 23-year period.

Table 11 Summary average of monthly ET_o parameters

No.	Station	Time interval											
		Jan	Feb	Mar	Apr	May	Jun	Jul	Aug	Sep	Oct	Nov	Dec
1.	Latent Heat of Vaporization (λ)												
	Bhumibol Dam	2.44	2.44	2.43	2.43	2.43	2.43	2.43	2.43	2.43	2.44	2.44	2.45
	Chiang Mai	2.45	2.44	2.44	2.43	2.43	2.43	2.44	2.44	2.44	2.44	2.44	2.45
	Lampang	2.45	2.44	2.43	2.43	2.43	2.43	2.43	2.43	2.43	2.44	2.44	2.45
	Nakhon Sawan	2.44	2.43	2.43	2.43	2.43	2.43	2.43	2.43	2.43	2.43	2.44	2.44
	Nan	2.45	2.44	2.44	2.43	2.43	2.43	2.43	2.44	2.44	2.44	2.44	2.45
	Phitsanulok	2.44	2.44	2.43	2.43	2.43	2.43	2.43	2.43	2.43	2.43	2.44	2.44
	Phrae	2.45	2.44	2.43	2.43	2.43	2.43	2.43	2.43	2.43	2.44	2.44	2.45
	Tak	2.44	2.44	2.43	2.42	2.43	2.43	2.43	2.43	2.43	2.44	2.44	2.45
	Uttaradit	2.44	2.44	2.43	2.43	2.43	2.43	2.43	2.43	2.43	2.43	2.44	2.44
	Average Monthly	2.44	2.44	2.43	2.43	2.43	2.43	2.43	2.43	2.43	2.44	2.44	2.45
2.	Slope Vapour Pressure Curve (Δ)												
	Bhumibol Dam	0.20	0.23	0.26	0.28	0.25	0.24	0.23	0.23	0.23	0.22	0.20	0.18
	Chiang Mai	0.17	0.20	0.23	0.25	0.24	0.23	0.22	0.22	0.22	0.21	0.19	0.17
	Lampang	0.18	0.21	0.24	0.27	0.25	0.24	0.23	0.23	0.22	0.22	0.20	0.18
	Nakhon Sawan	0.21	0.24	0.26	0.28	0.26	0.25	0.24	0.24	0.23	0.23	0.21	0.20
	Nan	0.18	0.20	0.23	0.25	0.24	0.23	0.23	0.22	0.22	0.22	0.19	0.17
	Phitsanulok	0.20	0.22	0.25	0.27	0.26	0.24	0.24	0.23	0.23	0.23	0.21	0.19
	Phrae	0.19	0.21	0.24	0.27	0.25	0.24	0.23	0.23	0.22	0.22	0.20	0.18
	Tak	0.20	0.23	0.27	0.28	0.26	0.24	0.23	0.23	0.23	0.22	0.20	0.19
	Uttaradit	0.20	0.22	0.25	0.27	0.26	0.24	0.23	0.23	0.23	0.23	0.21	0.19
	Average Monthly	0.19	0.22	0.25	0.27	0.25	0.24	0.23	0.23	0.23	0.22	0.20	0.18
3.	Atmospheric Pressure (P)												
	Bhumibol Dam	99.60	99.60	99.60	99.60	99.60	99.60	99.60	99.60	99.60	99.60	99.60	99.60
	Chiang Mai	97.70	97.70	97.70	97.70	97.70	97.70	97.70	97.70	97.70	97.70	97.70	97.70
	Lampang	98.50	98.50	98.50	98.50	98.50	98.50	98.50	98.50	98.50	98.50	98.50	98.50
	Nakhon Sawan	100.90	100.90	100.90	100.90	100.90	100.90	100.90	100.90	100.90	100.90	100.90	100.90
	Nan	99.00	99.00	99.00	99.00	99.00	99.00	99.00	99.00	99.00	99.00	99.00	99.00
	Phitsanulok	100.80	100.80	100.80	100.80	100.80	100.80	100.80	100.80	100.80	100.80	100.80	100.80
	Phrae	99.40	99.40	99.40	99.40	99.40	99.40	99.40	99.40	99.40	99.40	99.40	99.40
	Tak	99.90	99.90	99.90	99.90	99.90	99.90	99.90	99.90	99.90	99.90	99.90	99.90
	Uttaradit	100.60	100.60	100.60	100.60	100.60	100.60	100.60	100.60	100.60	100.60	100.60	100.60
	Average Monthly	99.60	99.60	99.60	99.60	99.60	99.60	99.60	99.60	99.60	99.60	99.60	99.60
4.	Psychrometric Constant (γ)												
	Bhumibol Dam	0.07	0.07	0.07	0.07	0.07	0.07	0.07	0.07	0.07	0.07	0.07	0.07
	Chiang Mai	0.06	0.07	0.07	0.07	0.07	0.07	0.07	0.07	0.07	0.07	0.07	0.06
	Lampang	0.07	0.07	0.07	0.07	0.07	0.07	0.07	0.07	0.07	0.07	0.07	0.07
	Nakhon Sawan	0.07	0.07	0.07	0.07	0.07	0.07	0.07	0.07	0.07	0.07	0.07	0.07
	Nan	0.07	0.07	0.07	0.07	0.07	0.07	0.07	0.07	0.07	0.07	0.07	0.07
	Phitsanulok	0.07	0.07	0.07	0.07	0.07	0.07	0.07	0.07	0.07	0.07	0.07	0.07
	Phrae	0.07	0.07	0.07	0.07	0.07	0.07	0.07	0.07	0.07	0.07	0.07	0.07
	Tak	0.07	0.07	0.07	0.07	0.07	0.07	0.07	0.07	0.07	0.07	0.07	0.07
	Uttaradit	0.07	0.07	0.07	0.07	0.07	0.07	0.07	0.07	0.07	0.07	0.07	0.07
	Average Monthly	0.07	0.07	0.07	0.07	0.07	0.07	0.07	0.07	0.07	0.07	0.07	0.07

Table 11 (Continued)

No.	Station	Time interval											
		Jan	Feb	Mar	Apr	May	Jun	Jul	Aug	Sep	Oct	Nov	Dec
5.	Saturation Vapour Pressure (ea)												
	Bhumibol Dam	3.38	3.94	4.58	4.93	4.45	4.12	4.06	4.03	3.94	3.74	3.45	3.12
	Chiang Mai	2.92	3.35	3.94	4.40	4.14	3.95	3.82	3.75	3.72	3.60	3.23	2.83
	Lampang	3.14	3.62	4.28	4.76	4.39	4.16	4.04	3.97	3.89	3.72	3.36	2.98
	Nakhon Sawan	3.65	4.17	4.69	5.03	4.64	4.39	4.27	4.14	4.02	3.93	3.70	3.38
	Nan	3.00	3.42	4.06	4.46	4.25	4.07	3.90	3.84	3.86	3.72	3.31	2.88
	Phitsanulok	3.43	3.88	4.41	4.81	4.52	4.24	4.09	3.99	3.97	3.91	3.63	3.27
	Phrae	3.16	3.59	4.27	4.74	4.39	4.13	3.97	3.92	3.88	3.77	3.41	3.01
	Tak	3.41	4.00	4.73	5.12	4.53	4.12	4.02	3.96	3.92	3.72	3.44	3.13
	Uttaradit	3.43	3.84	4.40	4.85	4.55	4.24	4.09	4.02	4.04	3.98	3.66	3.30
	Average Monthly	3.28	3.76	4.37	4.79	4.43	4.16	4.03	3.96	3.92	3.79	3.47	3.10
6.	Actual Vapour Pressure (ed)												
	Bhumibol Dam	1.87	1.80	1.98	2.43	2.82	2.82	2.75	2.78	2.91	2.82	2.43	1.96
	Chiang Mai	1.63	1.54	1.69	2.14	2.66	2.83	2.83	2.86	2.83	2.61	2.18	1.75
	Lampang	1.75	1.71	1.90	2.35	2.83	2.91	2.90	2.97	3.01	2.79	2.29	1.82
	Nakhon Sawan	1.98	2.21	2.50	2.77	3.01	2.98	2.97	3.02	3.11	2.98	2.51	1.98
	Nan	1.80	1.83	2.04	2.52	2.90	2.99	3.00	3.05	3.03	2.77	2.30	1.83
	Phitsanulok	1.94	2.11	2.37	2.63	2.89	2.98	2.98	3.00	3.02	2.85	2.38	1.90
	Phrae	1.87	1.93	2.14	2.57	2.94	3.04	3.01	3.06	3.08	2.88	2.38	1.88
	Tak	1.77	1.75	1.97	2.40	2.81	2.85	2.79	2.79	2.90	2.84	2.40	1.88
	Uttaradit	1.93	2.01	2.26	2.62	2.97	3.08	3.07	3.12	3.12	2.89	2.42	1.95
	Average Monthly	1.84	1.88	2.10	2.49	2.87	2.94	2.92	2.96	3.00	2.83	2.36	1.88
7.	Vapour Pressure Deficit (VPD)												
	Bhumibol Dam	1.51	2.13	2.60	2.51	1.63	1.30	1.32	1.24	1.04	0.92	1.03	1.16
	Chiang Mai	1.29	1.80	2.25	2.25	1.48	1.12	0.98	0.89	0.89	0.99	1.05	1.07
	Lampang	1.40	1.91	2.38	2.41	1.56	1.25	1.13	1.00	0.88	0.93	1.07	1.16
	Nakhon Sawan	1.67	1.96	2.19	2.26	1.64	1.42	1.30	1.12	0.91	0.96	1.20	1.40
	Nan	1.20	1.59	2.02	1.94	1.35	1.08	0.90	0.80	0.84	0.95	1.02	1.05
	Phitsanulok	1.49	1.77	2.04	2.18	1.64	1.26	1.12	0.99	0.95	1.06	1.25	1.38
	Phrae	1.29	1.66	2.13	2.17	1.45	1.09	0.96	0.86	0.81	0.89	1.03	1.13
	Tak	1.64	2.25	2.76	2.72	1.72	1.26	1.23	1.17	1.03	0.88	1.05	1.25
	Uttaradit	1.50	1.83	2.14	2.23	1.58	1.16	1.03	0.90	0.92	1.09	1.24	1.35
	Average Monthly	1.44	1.88	2.28	2.30	1.56	1.22	1.11	1.00	0.92	0.96	1.10	1.22
8.	Extraterrestrial Radiation (Ra)												
	Bhumibol Dam	28.20	31.80	35.60	38.20	38.90	38.90	38.80	38.10	36.10	32.50	28.90	27.10
	Chiang Mai	27.40	31.10	35.20	38.10	39.20	39.30	39.00	38.20	35.80	31.90	28.10	26.30
	Lampang	27.70	31.30	35.40	38.10	39.10	39.20	39.00	38.20	35.90	32.10	28.40	26.60
	Nakhon Sawan	29.00	32.30	35.90	38.20	38.70	38.60	38.50	38.00	36.30	33.00	29.60	27.90
	Nan	27.40	31.10	35.20	38.10	39.20	39.30	39.00	38.20	35.80	31.90	28.10	26.30
	Phitsanulok	28.50	32.00	35.70	38.20	38.90	38.80	38.70	38.10	36.20	32.70	29.10	27.40
	Phrae	27.80	31.40	35.40	38.10	39.10	39.10	38.90	38.10	35.90	32.10	28.40	26.60
	Tak	28.40	31.90	35.70	38.20	38.90	38.80	38.70	38.10	36.20	32.60	29.10	27.30
	Uttaradit	28.00	31.60	35.50	38.10	39.00	39.00	38.80	38.10	36.00	32.40	28.70	26.90
	Average Monthly	28.10	31.60	35.50	38.10	39.00	39.00	38.80	38.10	36.00	32.40	28.70	26.90

Table 11 (Continued)

No.	Station	Time interval											
		Jan	Feb	Mar	Apr	May	Jun	Jul	Aug	Sep	Oct	Nov	Dec
9.	Daylight Hours (N)												
	Bhumibol Dam	11.10	11.40	11.90	12.40	12.80	13.00	12.90	12.50	12.10	11.60	11.20	11.00
	Chiang Mai	11.00	11.40	11.90	12.50	12.90	13.10	13.00	12.60	12.10	11.50	11.10	10.90
	Lampang	11.00	11.40	11.90	12.50	12.90	13.10	13.00	12.60	12.10	11.50	11.10	10.90
	Nakhon Sawan	11.20	11.50	11.90	12.40	12.80	12.90	12.80	12.50	12.10	11.60	11.20	11.10
	Nan	11.00	11.40	11.90	12.50	12.90	13.10	13.00	12.60	12.10	11.50	11.10	10.90
	Phitsanulok	11.10	11.50	11.90	12.40	12.80	13.00	12.90	12.50	12.10	11.60	11.20	11.00
	Phrae	11.00	11.40	11.90	12.50	12.90	13.10	13.00	12.60	12.10	11.50	11.10	10.90
	Tak	11.10	11.50	11.90	12.40	12.80	13.00	12.90	12.50	12.10	11.60	11.20	11.00
	Uttaradit	11.10	11.40	11.90	12.40	12.90	13.10	12.90	12.60	12.10	11.60	11.10	10.90
	Average Monthly	11.10	11.40	11.90	12.40	12.90	13.10	12.90	12.60	12.10	11.60	11.10	10.90
10.	Net Radiation												
	Bhumibol Dam	8.90	10.10	12.20	13.90	13.50	11.80	11.40	11.00	11.30	11.40	9.90	8.60
	Chiang Mai	8.60	10.30	11.50	13.20	13.00	11.30	10.40	10.30	10.70	10.20	9.00	7.90
	Lampang	8.50	10.00	12.00	14.00	14.00	12.80	12.00	11.60	11.90	11.30	9.50	8.20
	Nakhon Sawan	9.50	11.30	12.80	14.30	13.60	12.10	11.70	11.30	11.30	11.30	10.10	8.90
	Nan	8.60	10.20	12.30	14.30	14.20	13.00	12.10	11.60	12.20	11.50	9.40	8.10
	Phitsanulok	9.40	11.20	12.70	14.20	13.70	12.10	11.50	11.20	11.10	11.10	10.00	8.80
	Phrae	8.70	10.30	12.20	14.00	13.90	12.70	12.10	11.50	11.90	11.30	9.60	8.30
	Tak	8.70	10.10	12.00	13.80	13.50	12.10	11.70	10.90	11.20	11.10	9.80	8.60
	Uttaradit	8.90	10.50	12.60	14.30	13.90	12.40	11.70	11.20	11.90	11.70	9.80	8.40
	Average Monthly	8.90	10.50	12.30	14.00	13.70	12.30	11.60	11.20	11.50	11.20	9.70	8.40
11.	Soil Heat Flux												
	Bhumibol Dam	0.16	0.36	0.39	0.21	-0.21	-0.16	-0.03	-0.02	-0.06	-0.13	-0.22	-0.29
	Chiang Mai	0.04	0.29	0.41	0.32	-0.08	-0.09	-0.07	-0.04	-0.03	-0.09	-0.29	-0.36
	Lampang	0.08	0.30	0.43	0.32	-0.11	-0.10	-0.07	-0.04	-0.05	-0.12	-0.29	-0.34
	Nakhon Sawan	0.16	0.34	0.31	0.18	-0.17	-0.12	-0.07	-0.06	-0.07	-0.06	-0.18	-0.27
	Nan	0.07	0.28	0.43	0.30	-0.04	-0.07	-0.09	-0.03	0.00	-0.12	-0.32	-0.40
	Phitsanulok	0.09	0.30	0.33	0.22	-0.13	-0.14	-0.07	-0.05	-0.01	-0.05	-0.21	-0.29
	Phrae	0.08	0.29	0.45	0.31	-0.14	-0.12	-0.08	-0.03	-0.03	-0.09	-0.29	-0.36
	Tak	0.16	0.39	0.46	0.22	-0.26	-0.20	-0.05	-0.04	-0.04	-0.13	-0.23	-0.29
	Uttaradit	0.06	0.25	0.35	0.27	-0.11	-0.14	-0.08	-0.04	0.00	-0.05	-0.24	-0.28
	Average Monthly	0.10	0.31	0.39	0.26	-0.14	-0.12	-0.07	-0.04	-0.03	-0.09	-0.25	-0.32

Table 12 Summary of average monthly reference evapotranspiration (ET_o)

Station	Reference Evapotranspiration (mm/day)											
	Jan	Feb	Mar	Apr	May	Jun	Jul	Aug	Sep	Oct	Nov	Dec
Bhumibol Dam	3.07	3.85	4.86	5.44	4.97	4.28	4.14	4.01	3.80	3.67	3.23	2.86
Chiang Mai	2.98	3.88	4.76	5.57	5.01	4.17	3.76	3.62	3.70	3.58	3.21	2.86
Lampang	2.72	3.32	4.19	4.98	4.86	4.41	4.07	3.87	3.85	3.63	3.09	2.66
Nakhon Sawan	3.47	4.71	5.78	6.17	5.25	4.60	4.34	4.00	3.76	3.76	3.51	3.22
Nan	2.60	3.18	3.98	4.73	4.69	4.27	3.92	3.73	3.88	3.66	3.01	2.56
Phitsanulok	3.12	3.87	4.67	5.31	4.97	4.24	3.94	3.77	3.67	3.69	3.40	3.04
Phrae	2.80	3.46	4.43	5.21	4.88	4.38	4.08	3.79	3.85	3.68	3.19	2.76
Tak	2.91	3.79	4.90	5.72	5.11	4.38	4.25	4.00	3.73	3.60	3.16	2.80
Uttaradit	2.88	3.47	4.29	4.97	4.78	4.16	3.86	3.67	3.85	3.83	3.30	2.87
Average	2.96	3.73	4.65	5.35	4.95	4.32	4.04	3.83	3.79	3.68	3.24	2.86

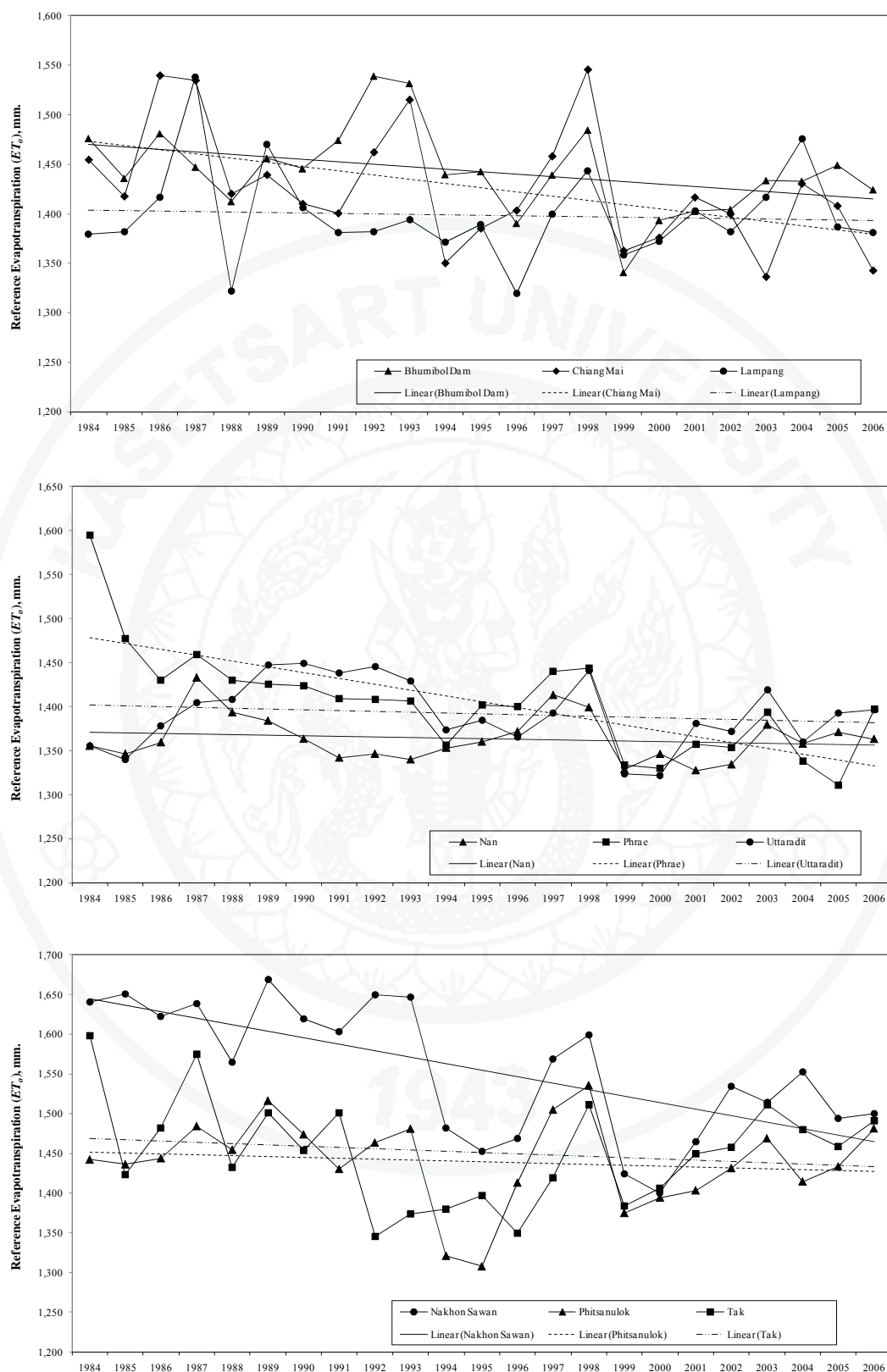


Figure 30 Mean annual reference evapotranspiration (ET_0) and their linear trends in weather stations.

2. Trend analysis

The trend of weather variables, ET_o parameters and reference evapotranspiration (ET_o) for each station was determined by using Mann-Kendall test. The purpose of trend analysis was to understand the impact of climate change on ET_o and ET_o parameters. The results are shown below.

2.1 Trend analysis of weather variables

The weather variables affecting reference evapotranspiration (ET_o) are air temperature, relative humidity, evaporation, sunshine duration, and wind speed. The reference evapotranspiration (ET_o) rate is high in hot air temperature and in long duration of sunshine while wind affects reference evapotranspiration (ET_o) by bringing heat energy into the area and removing the vaporized moisture. On the other hand, in humid weather conditions, the high humidity of the air causes the reference evapotranspiration (ET_o) rate to be lower.

The Mann-Kendall was applied to detect trends of weather variables for all selected stations. The results of trend analysis of weather variables with statistically significant trends at $p < 0.10$, $p < 0.05$ and $p < 0.01$ significance levels are shown in Table 13.

Trend of air temperature

The increase of air temperature will cause the heat to transfer energy to the crop; and will consequently influence on the rate of evapotranspiration. In hot air temperature the loss of water by evapotranspiration is greater than in cloudy and cool weather.

The results trend analysis of daily maximum and minimum air temperature for each month is shown in Table 13 and Figure 31 and Figure 32.

Most of the stations show only one or two months with statistically significant trends. An increasing trend occurs more frequently in October for maximum and in December for minimum temperature while the decreasing trend is infrequent at significant level for each particular month. In summary, the results show that the air temperature has significant increasing trend in January and from August to December.

Table 13 P-value of weather variables trend.

Stations	Wind speed trends by Mann-Kendall test											
	Jan	Feb	Mar	Apr	May	Jun	Jul	Aug	Sep	Oct	Nov	Dec
Chiang Mai	0.02	0.13	0.02	0.06	0.00	0.12	0.01	0.03	0.22	0.09	0.11	0.00
	(c)	(a)	(c)	(d)	(b)	(a)	(c)	(c)	(a)	(d)	(a)	(b)
Bhumibol Dam	0.16	0.01	0.00	0.00	0.01	0.02	0.00	0.00	0.00	0.00	0.00	0.01
	(a)	(c)	(b)	(b)	(b)	(c)	(b)	(b)	(b)	(b)	(b)	(c)
Tak	0.41	0.08	0.01	0.02	0.03	0.16	0.01	0.09	0.18	0.10	0.54	0.39
	(a)	(d)	(c)	(c)	(c)	(a)	(b)	(d)	(a)	(a)	(a)	(a)
Lampang	0.01	0.00	0.02	0.00	0.00	0.00	0.00	0.00	0.00	0.00	0.00	0.00
	(c)	(b)	(c)	(b)								
Phrae	0.00	0.00	0.00	0.00	0.00	0.00	0.00	0.00	0.00	0.00	0.00	0.00
	(b)	(b)	(b)	(b)	(b)	(b)	(b)	(b)	(b)	(b)	(b)	(b)
Nan	0.00	0.00	0.00	0.00	0.00	0.00	0.00	0.00	0.00	0.00	0.00	0.00
	(b)	(b)	(b)	(b)	(b)	(b)	(b)	(b)	(b)	(b)	(b)	(b)
Uttaradit	0.00	0.05	0.09	0.04	0.22	0.04	0.04	0.01	0.00	0.00	0.00	0.00
	(b)	(c)	(d)	(c)	(a)	(c)	(c)	(c)	(b)	(b)	(b)	(b)
Phitsanulok	0.46	0.04	0.00	0.00	0.02	0.11	0.00	0.04	0.02	0.17	0.57	0.62
	(a)	(c)	(b)	(b)	(c)	(a)	(b)	(c)	(c)	(a)	(a)	(a)
Nakhon Sawan	0.00	0.00	0.00	0.00	0.00	0.00	0.00	0.00	0.00	0.00	0.00	0.00
	(b)	(b)	(b)	(b)	(b)	(b)	(b)	(b)	(b)	(b)	(b)	(b)

(a) No significant trend

(b) Trends statistically significant at $p < 0.01$

(c) Trends statistically significant at $p < 0.05$

(d) Trends statistically significant at $p < 0.10$

Table 13 (Continued)

Stations	Maximum air temperature trends by Mann-Kendall test												Minimum air temperature trends by Mann-Kendall test											
	Jan	Feb	Mar	Apr	May	Jun	Jul	Aug	Sep	Oct	Nov	Dec	Jan	Feb	Mar	Apr	May	Jun	Jul	Aug	Sep	Oct	Nov	Dec
Chiang Mai	0.12	0.87	1.00	0.75	0.36	0.75	0.11	0.12	0.05	0.76	0.57	0.40	0.63	0.30	0.34	0.87	0.22	0.41	0.62	0.16	0.36	0.90	0.82	0.14
	(a)	(a)	(a)	(a)	(a)	(a)	(a)	(a)	(c)	(a)	(a)	(a)	(a)	(a)	(a)	(a)	(a)	(a)	(a)	(a)	(a)	(a)	(a)	(a)
Bhumibol Dam	0.05	0.52	0.82	0.58	0.45	0.21	0.91	0.28	0.16	0.00	0.05	0.11	0.14	0.63	0.49	0.96	0.51	0.40	0.60	0.38	0.09	0.09	0.16	0.13
	(d)	(a)	(b)	(c)	(a)	(a)	(a)	(a)	(a)	(a)	(a)	(a)	(d)	(d)	(a)	(a)	(a)							
Tak	0.12	0.79	0.39	0.80	0.16	0.75	0.75	0.78	0.25	0.01	0.06	0.28	0.02	0.42	0.31	0.45	0.72	0.02	0.00	0.00	0.00	0.00	0.00	0.00
	(a)	(a)	(a)	(a)	(a)	(a)	(a)	(a)	(a)	(c)	(d)	(a)	(c)	(a)	(a)	(a)	(a)	(c)	(b)	(b)	(b)	(b)	(b)	(b)
Lampang	0.00	0.00	0.39	0.68	0.83	0.09	0.05	0.18	0.01	0.00	0.00	0.00	0.05	0.12	0.01	0.01	0.61	0.82	0.42	0.14	0.03	0.17	0.29	0.03
	(b)	(b)	(a)	(a)	(a)	(d)	(d)	(a)	(b)	(b)	(b)	(b)	(c)	(a)	(b)	(b)	(a)	(a)	(a)	(a)	(c)	(a)	(a)	(c)
Phrae	0.45	0.90	0.39	0.39	0.41	0.57	0.82	0.51	0.73	0.17	0.48	0.45	0.08	0.25	0.02	0.40	0.30	0.00	0.00	0.00	0.00	0.02	0.04	0.02
	(a)	(a)	(a)	(a)	(a)	(a)	(a)	(a)	(a)	(a)	(a)	(a)	(d)	(a)	(c)	(a)	(a)	(b)	(b)	(b)	(b)	(c)	(c)	(c)
Nan	0.02	0.07	0.94	0.80	0.87	0.32	0.15	0.97	0.62	0.00	0.02	0.01	0.34	0.31	0.11	0.83	0.86	0.48	0.76	0.16	0.73	0.25	0.16	0.05
	(c)	(d)	(a)	(a)	(a)	(a)	(a)	(a)	(b)	(c)	(c)	(a)	(a)	(a)	(a)	(a)	(a)	(a)	(a)	(a)	(a)	(a)	(a)	(c)
Uttaradit	0.73	0.40	0.02	0.05	0.18	0.71	0.40	0.49	0.94	0.03	0.39	0.56	0.04	0.15	0.01	0.13	0.42	0.33	0.03	0.12	0.29	0.10	0.10	0.01
	(a)	(a)	(c)	(d)	(a)	(a)	(a)	(a)	(c)	(a)	(a)	(c)	(c)	(a)	(b)	(a)	(a)	(c)	(a)	(a)	(a)	(a)	(a)	(c)
Phitsanulok	0.48	0.18	0.07	0.69	0.58	0.50	0.42	0.25	0.97	0.02	0.18	0.46	0.43	0.39	0.07	0.16	0.12	0.67	0.69	0.84	0.40	0.96	0.30	0.08
	(a)	(a)	(d)	(a)	(a)	(a)	(a)	(a)	(c)	(a)	(a)	(a)	(a)	(a)	(d)	(a)	(d)							
Nakhon Sawan	0.51	0.53	0.24	0.82	0.45	0.63	0.30	0.05	0.08	0.01	0.10	0.34	0.24	0.71	0.68	0.50	0.84	0.97	0.36	0.00	0.05	0.05	0.07	0.09
	(a)	(a)	(a)	(a)	(a)	(a)	(c)	(d)	(b)	(a)	(a)	(a)	(a)	(a)	(a)	(a)	(a)	(a)	(a)	(b)	(d)	(d)	(d)	(d)

Table 13 (Continued)

Stations	Relative humidity trends by Mann-Kendall test												Evaporation trends by Mann-Kendall test											
	Jan	Feb	Mar	Apr	May	Jun	Jul	Aug	Sep	Oct	Nov	Dec	Jan	Feb	Mar	Apr	May	Jun	Jul	Aug	Sep	Oct	Nov	Dec
Chiang Mai	0.29	0.73	0.08	0.62	0.05	0.01	0.00	0.00	0.00	0.02	0.08		1.00	0.90	0.17	0.15	0.31	0.60	0.57	0.45	0.43	0.67	0.14	0.60
	(a)	(a)	(d)	(a)	(d)	(c)	(b)	(b)	(b)	(c)	(d)		(a)	(a)	(a)	(a)	(a)	(a)	(a)	(a)	(a)	(a)	(a)	(a)
Bhumibol Dam	0.24	0.07	0.01	0.00	0.00	0.26	0.03	0.02	0.12	0.01	0.15	0.04	0.78	0.25	0.07	0.01	0.04	0.69	0.02	0.15	0.79	0.04	0.74	0.55
	(a)	(d)	(c)	(b)	(b)	(a)	(c)	(c)	(a)	(b)	(a)	(c)		(a)	(a)	(d)	(c)	(c)	(a)	(c)	(a)	(a)	(c)	(a)
Tak	0.68	0.40	0.02	0.16	0.17	0.43	0.49	0.93	0.53	0.03	0.03	0.29	0.06	0.27	0.69	1.00	0.45	0.01	0.28	0.01	0.12	0.00	0.00	0.00
	(a)	(a)	(c)	(a)	(a)	(a)	(a)	(a)	(c)	(c)	(a)		(d)	(a)	(a)	(a)	(b)	(a)	(b)	(a)	(b)	(b)	(b)	(b)
Lampang	0.20	0.19	0.44	0.39	0.50	0.73	0.97	0.93	0.59	0.00	0.16	0.35	0.12	0.28	0.93	0.90	0.26	0.49	0.34	0.17	0.34	0.17	0.08	0.27
	(a)	(a)	(a)	(a)	(a)	(a)	(a)	(a)	(b)	(a)	(a)		(a)	(a)	(a)	(a)	(a)	(a)	(a)	(a)	(a)	(a)	(d)	(a)
Phrae	0.64	0.37	0.01	0.05	0.30	0.73	0.45	0.58	0.68	0.84	0.75	0.56	0.22	0.69	0.34	0.85	0.85	0.76	0.74	0.78	0.04	0.28	0.48	0.41
	(a)	(a)	(b)	(c)	(a)		(a)	(a)	(a)	(a)	(a)	(a)	(a)	(a)	(c)	(a)	(a)	(a)						
Nan	0.82	0.44	0.26	0.64	0.55	0.18	0.08	0.13	0.13	0.01	0.17	0.03	0.61	0.75	0.43	0.15	0.08	0.62	0.48	0.26	0.08	0.20	0.37	0.83
	(a)	(a)	(a)	(a)	(a)	(d)	(a)	(a)	(b)	(a)	(c)		(a)	(a)	(a)	(a)	(d)	(a)	(a)	(a)	(d)	(a)	(a)	(a)
Uttaradit	0.74	0.87	0.01	0.06	0.53	0.93	0.87	0.77	0.38	0.01	0.21	0.09	0.01	0.01	0.41	0.53	0.07	0.00	0.01	0.01	0.02	0.00	0.00	0.00
	(a)	(a)	(b)	(d)	(a)	(a)	(a)	(a)	(c)	(a)	(d)		(b)	(c)	(a)	(a)	(d)	(b)	(c)	(b)	(c)	(b)	(b)	(b)
Phitsanulok	0.00	0.00	0.00	0.09	0.40	0.77	0.82	0.32	0.67	0.08	0.50	0.59	0.36	0.21	0.04	0.12	0.15	0.06	0.01	0.06	0.01	0.00	0.03	0.11
	(b)	(b)	(b)	(d)	(a)	(a)	(a)	(a)	(d)	(a)	(a)		(a)	(a)	(c)	(a)	(a)	(d)	(c)	(d)	(b)	(b)	(c)	(a)
Nakhon Sawan	0.00	0.00	0.00	0.02	0.03	0.03	0.08	0.27	0.17	0.76	0.54	0.04	0.00	0.00	0.00	0.00	0.00	0.02	0.00	0.01	0.19	0.35	0.02	0.00
	(b)	(b)	(b)	(c)	(c)	(c)	(d)	(a)	(a)	(a)	(c)		(b)	(b)	(b)	(b)	(b)	(c)	(b)	(b)	(a)	(a)	(c)	(b)

Table 13 (Continued)

Stations	Sunshine trends by Mann-Kendall test												Rainfall trends by Mann-Kendall test											
	Jan	Feb	Mar	Apr	May	Jun	Jul	Aug	Sep	Oct	Nov	Dec	Jan	Feb	Mar	Apr	May	Jun	Jul	Aug	Sep	Oct	Nov	Dec
Chiang Mai	0.00	0.02	0.19	0.02	0.00	0.06	0.02	0.03	0.00	0.06	0.42	0.06	0.71	0.97	0.11	0.76	0.54	0.50	0.94	0.75	0.78	1.00	0.73	0.67
	(b)	(c)	(a)	(c)	(b)	(d)	(c)	(c)	(b)	(d)	(a)	(d)	(a)	(a)	(a)	(a)	(a)	(a)	(a)	(a)	(a)	(a)	(a)	(a)
Bhumibol Dam	0.72	0.52	0.98	0.01	0.02	0.00	0.00	0.02	0.00	0.00	0.07	0.49	0.38	0.35	0.08	0.08	0.52	0.43	0.28	0.62	0.41	0.75	0.86	0.41
	(a)	(a)	(a)	(b)	(c)	(b)	(b)	(c)	(b)	(b)	(d)	(a)	(a)	(a)	(d)	(d)	(a)							
Tak	0.54	0.07	0.03	0.04	0.09	0.03	0.02	0.06	0.00	0.00	0.04	0.37	0.81	0.59	0.36	0.04	0.64	0.91	0.57	0.51	0.45	0.39	0.32	0.56
	(a)	(d)	(c)	(c)	(d)	(c)	(c)	(d)	(b)	(b)	(c)	(a)	(a)	(a)	(a)	(c)	(a)							
Lampang	0.75	0.73	0.77	0.01	0.11	0.06	0.03	0.08	0.19	0.00	0.94	0.32	0.86	0.13	0.14	0.53	0.63	0.29	0.66	0.54	0.50	0.10	0.97	0.97
	(a)	(a)	(a)	(c)	(a)	(d)	(c)	(d)	(a)	(b)	(a)	(a)	(a)	(a)	(a)	(a)	(a)	(a)	(a)	(a)	(d)	(a)	(a)	(a)
Phrae	0.65	0.41	0.26	0.01	0.07	0.41	0.26	0.76	0.60	0.57	0.60	0.90	0.80	0.78	0.06	0.69	0.48	0.54	0.11	0.37	0.54	0.67	0.63	0.98
	(a)	(a)	(a)	(c)	(d)	(a)	(a)	(a)	(d)	(a)														
Nan	0.12	0.14	0.03	0.27	0.23	0.94	0.50	0.67	0.59	0.00	0.20	0.01	1.00	0.54	0.28	0.80	0.69	0.41	0.80	0.19	1.00	0.24	0.48	0.38
	(a)	(a)	(c)	(a)	(a)	(a)	(a)	(a)	(a)	(b)	(a)	(c)	(a)	(a)	(a)	(a)	(a)	(a)	(a)	(a)	(a)	(a)	(a)	(a)
Uttaradit	0.26	0.01	1.00	0.38	0.94	0.61	0.51	0.40	0.63	0.09	0.80	0.97	0.46	0.83	0.09	0.59	0.94	0.30	0.89	0.14	0.94	0.06	1.00	0.89
	(a)	(c)	(a)	(d)	(a)	(a)	(a)	(a)	(a)	(d)	(a)	(a)	(a)	(a)	(a)	(d)	(a)	(a)						
Phitsanulok	0.78	0.62	0.67	0.42	0.25	0.60	0.01	0.07	0.75	0.69	1.00	0.45	0.93	0.90	0.67	1.00	0.57	0.59	0.91	1.00	0.58	0.86	0.87	0.78
	(a)	(a)	(a)	(a)	(a)	(a)	(c)	(d)	(a)	(a)	(a)	(a)	(a)	(a)	(a)	(a)	(a)	(a)	(a)	(a)	(a)	(a)	(a)	(a)
Nakhon Sawan	0.05	0.04	0.28	0.83	0.07	0.48	0.05	0.34	0.35	0.64	0.71	0.23	0.69	0.56	0.21	0.80	0.97	0.01	0.49	0.52	0.75	0.64	0.53	0.95
	(d)	(c)	(a)	(a)	(d)	(a)	(c)	(a)	(a)	(a)	(a)	(a)	(a)	(a)	(a)	(a)	(a)	(a)	(c)	(a)	(a)	(a)	(a)	(a)

(a) No significant trend

(b) Trends statistically significant at $p < 0.01$ (c) Trends statistically significant at $p < 0.05$ (d) Trends statistically significant at $p < 0.10$

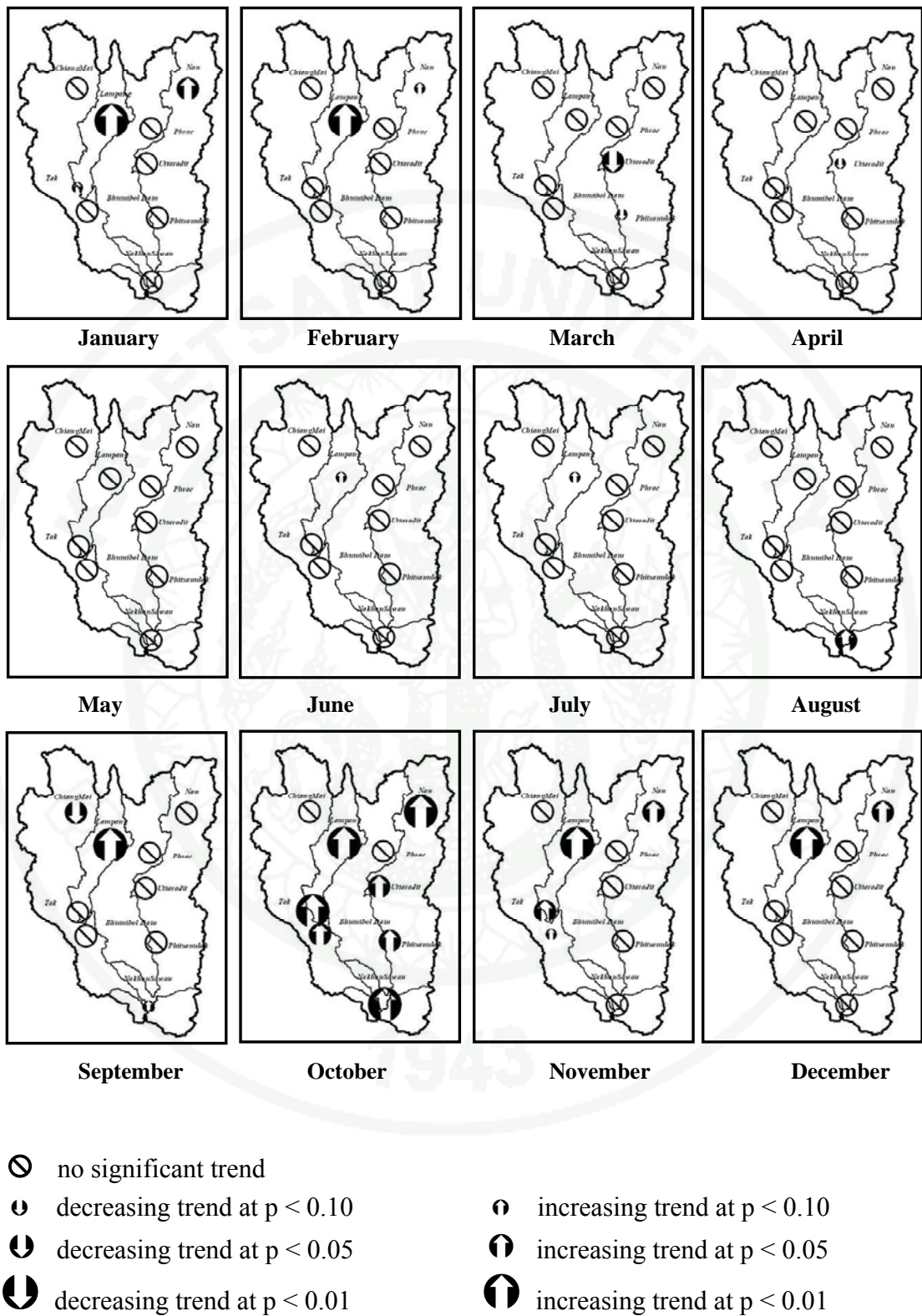


Figure 31 Summary of maximum air temperature trends.

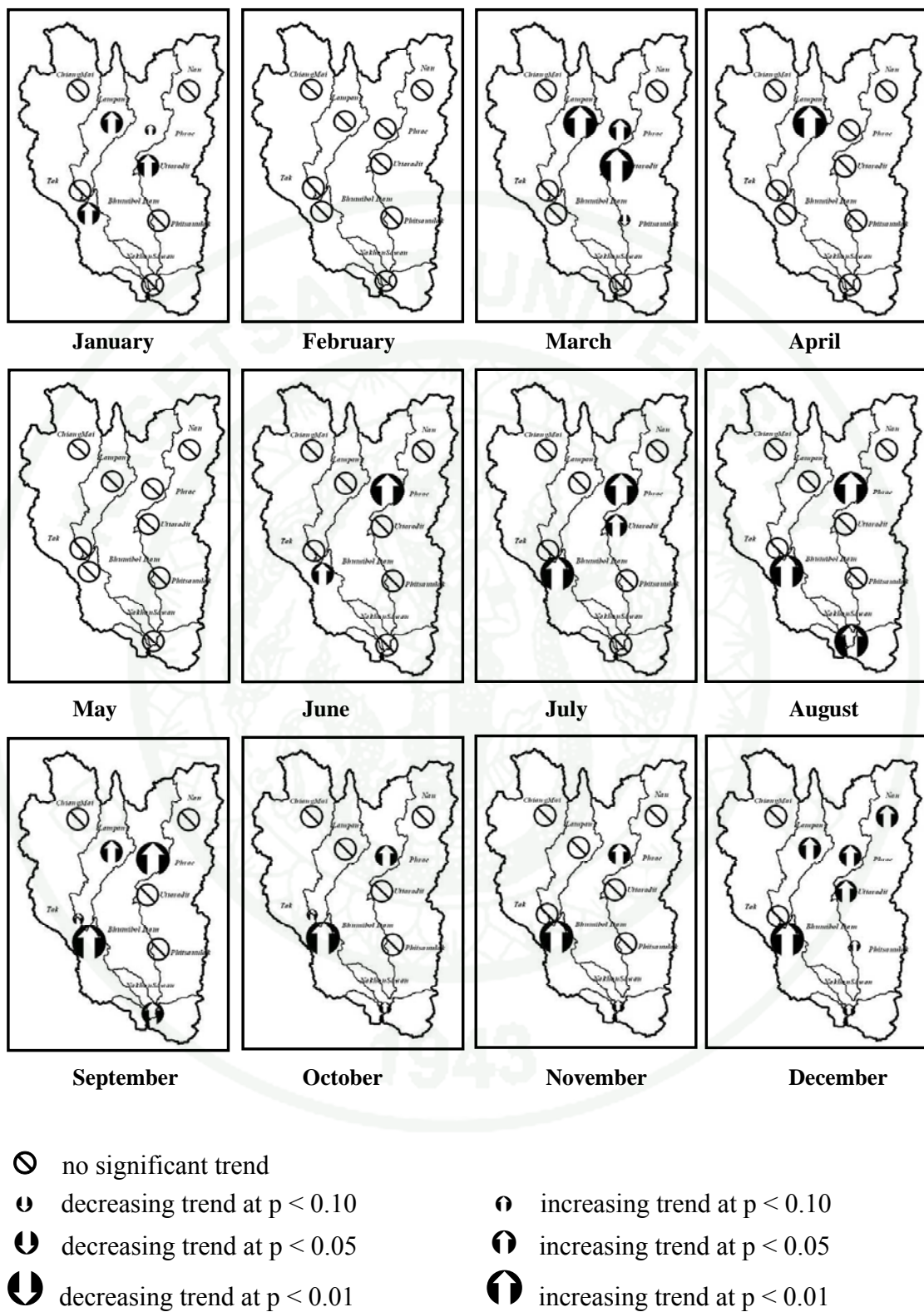


Figure 32 Summary of minimum air temperature trends.

Trend of relative humidity

Relative humidity is the ratio between the amount of water the ambient air actually holds and the amount it could hold at the same temperature. The high relative humidity means the air has high humidity; thus causes the ET_o rate to be lower. The result of trend analysis of daily relative humidity for each month is shown in Table 13 and Figure 33. The result shows both rising and declining trends depending on the station. However, most of the stations show increasing trend and which occur more frequently in March while the decreasing trend occurs more frequently in October. In summary, the results show that the relative humidity has significant increasing trend in January to September.

Trend of evaporation

The result of trend analysis of daily evaporation for each month is shown in Table 13 and Figure 34. The result shows both rising and declining trends almost every month, except from March to May which shows a decreasing trend.

Trend of sunshine

The measured sunshine duration is often used to estimate solar radiation from extraterrestrial radiation. While evapotranspiration process is determined by the amount of energy available to vaporize water, the solar radiation is the largest energy source and is able to change large quantities of liquid water into water vapour. The result of trend analysis of daily sunshine duration for each month is shown in Table 13 and Figure 35. The result shows both rising and declining trends almost every month, except in January and December, which show a decreasing trend while an increasing trend occurs in June, October and November.

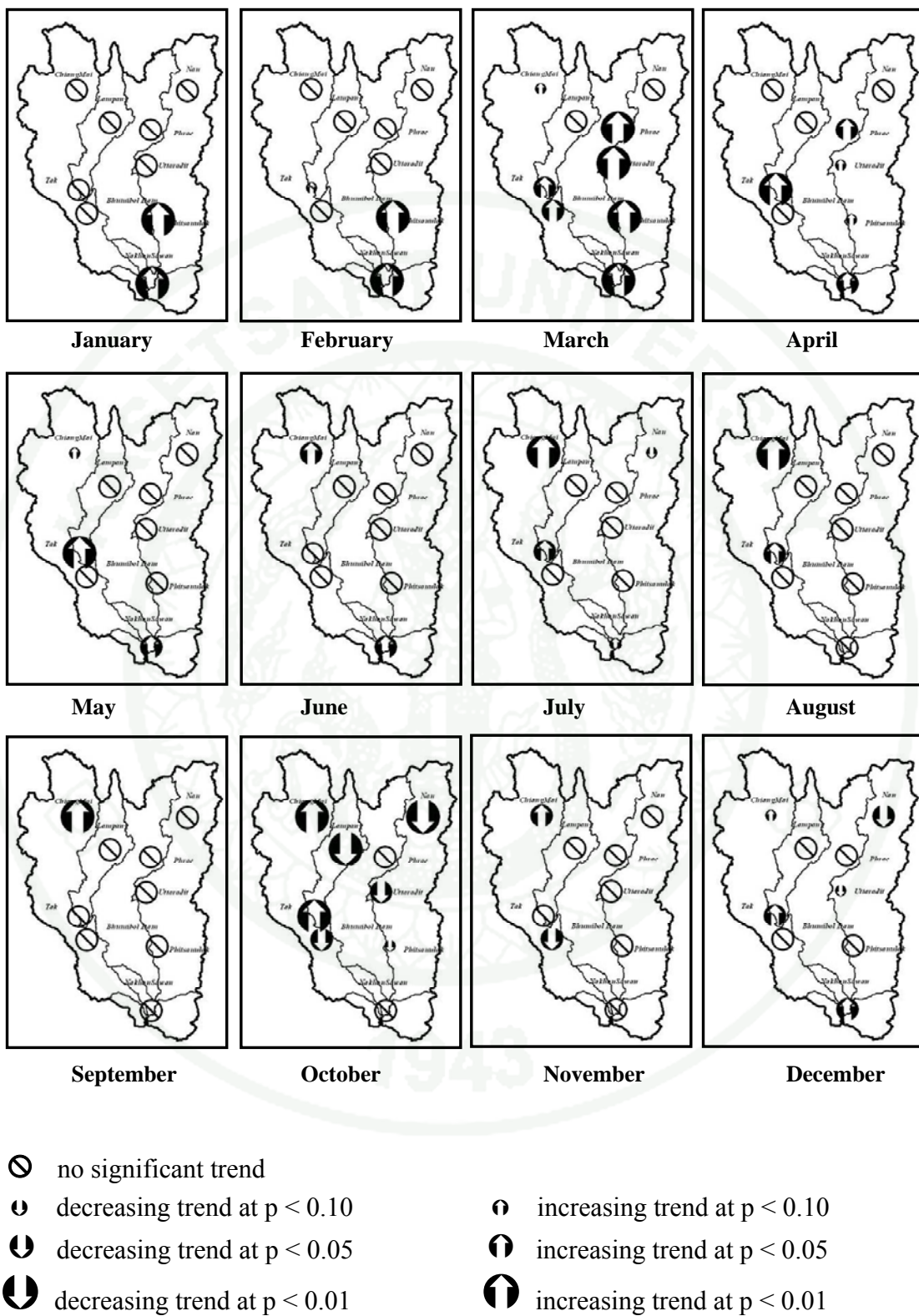


Figure 33 Summary of relative humidity trends.

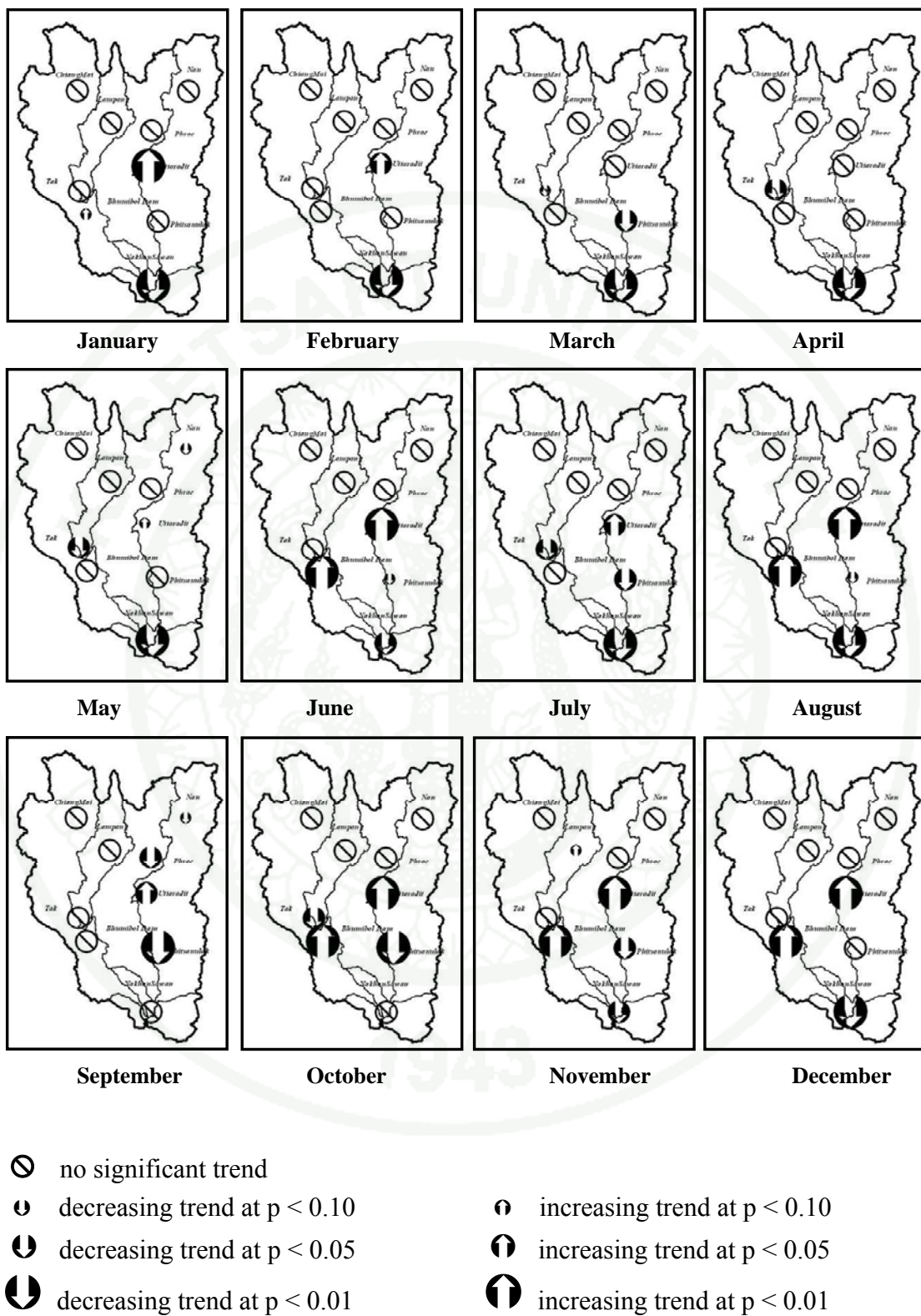


Figure 34 Summary of pan evaporation trends.

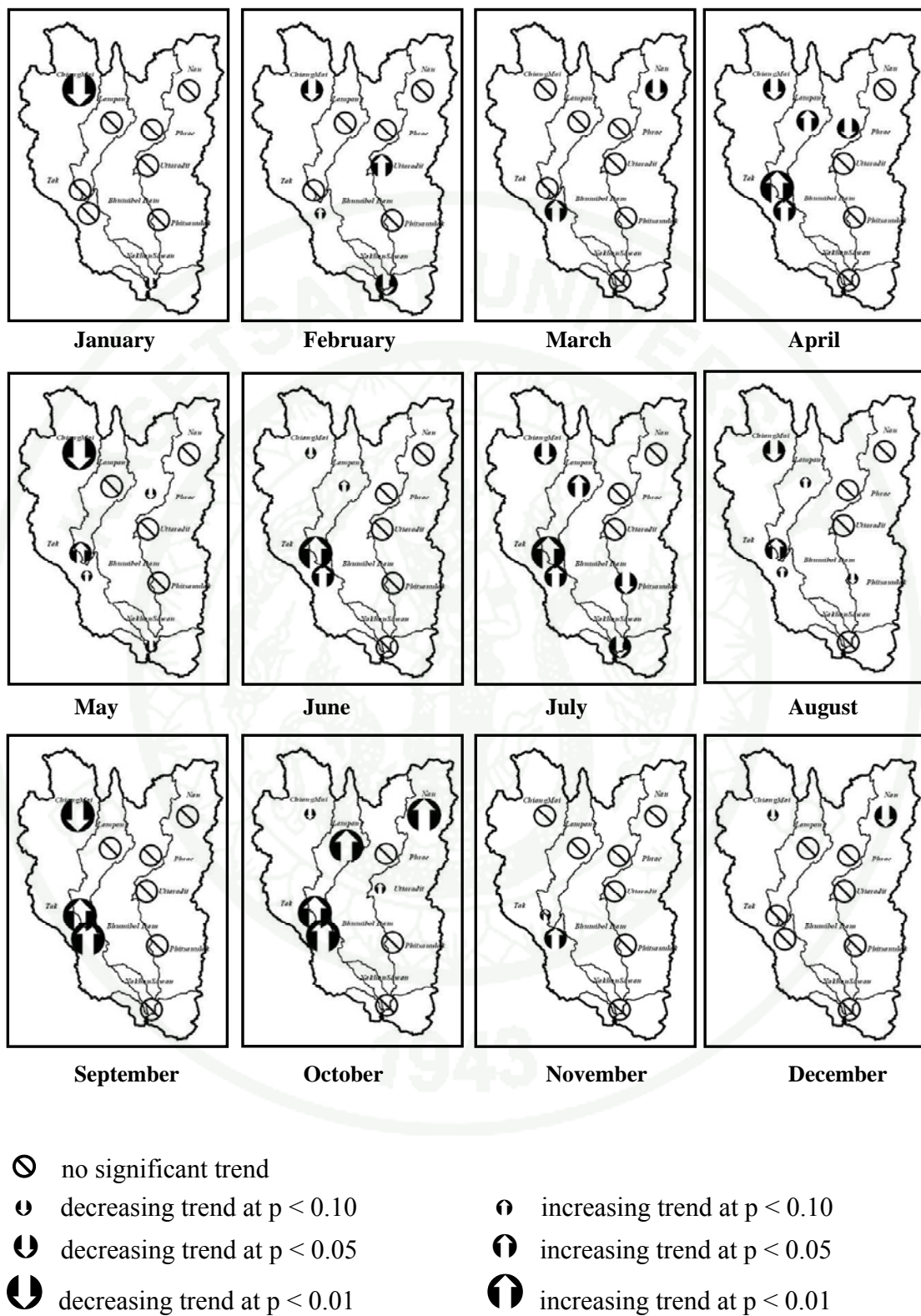


Figure 35 Summary of sunshine duration trends.

Trend of wind speed

The process of air movement and vapor removal depends on wind to the large extent. Wind is a major factor in transporting the water vapor transpired from the plant into the atmosphere. Wind can help to maintain a vapor pressure deficit around the plant surface. The result of trend analysis of daily wind speed for each month is shown in Table 13 and Figure 36. The decreasing trend occurs every month at many stations, except at the Chiang Mai station where some increasing trends occur.

Trend of rainfall

Rainfall is a water source for crop water requirement. Water shortage occurs when evapotranspiration exceeds rainfall. The result of trend analysis of daily rainfall for each month is shown in Table 13 and Figure 37. Most of the stations show no significant trend. However, some stations show an increasing trend in March, April, and June while the decreasing trend occurs in October.

2.2 Trend analysis of the ET_o parameters

The ET_o parameters used for calculating ET_o by FAO Penman-Monteith equation are actual vapor pressure, vapor pressure deficit, net radiation, and soil heat flux. The high vapor pressure deficit and net radiation cause the ET_o rate to be higher while the high actual vapor pressure and soil heat flux cause the ET_o to be lower.

The Mann-Kendall was applied to detect trends of parameters used in the ET_o equations for all selected stations. The results of trend analysis of the ET_o parameters with statistically significant trends at $p < 0.10$, $p < 0.05$ and $p < 0.01$ significance levels are shown in Table 14.

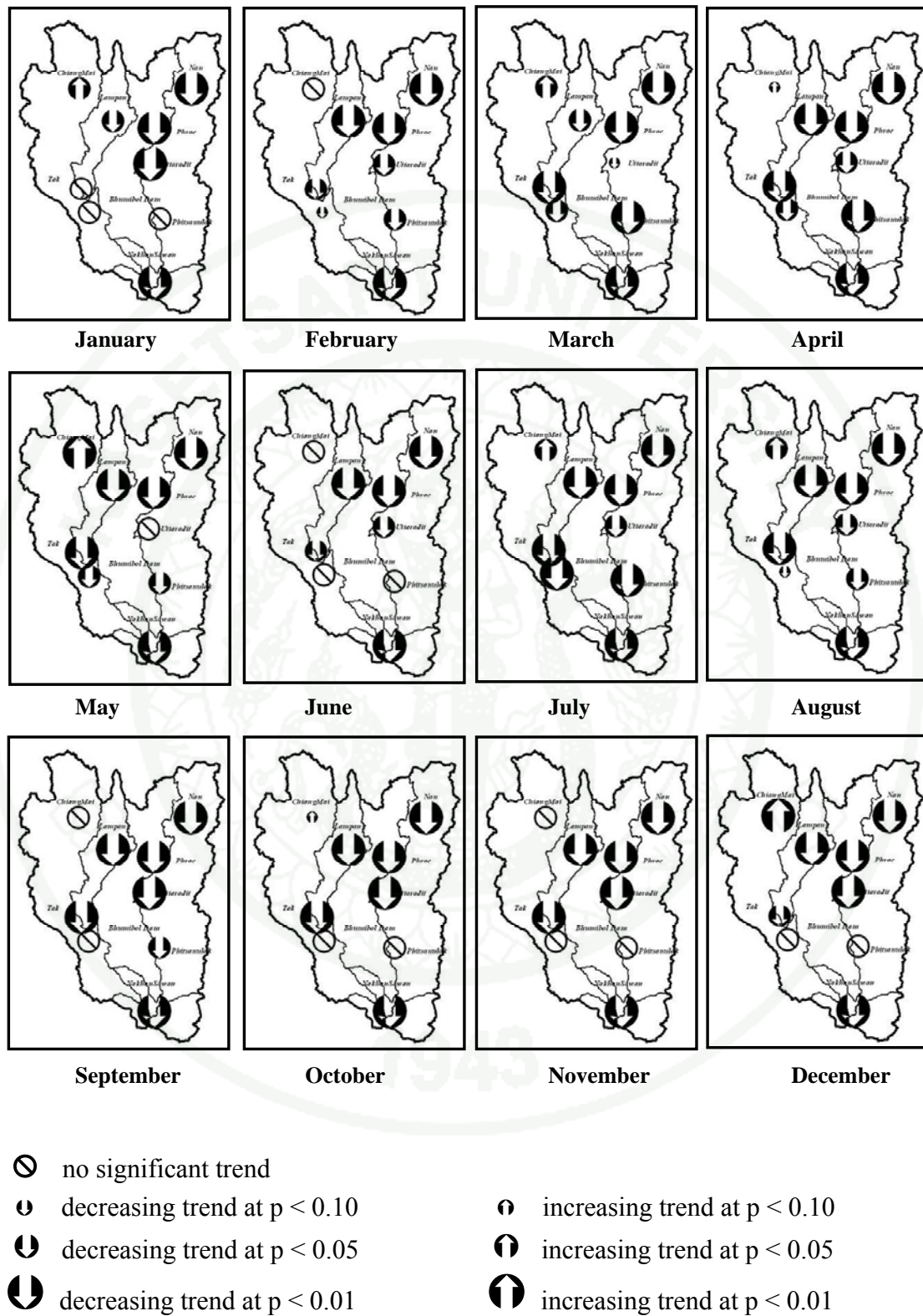


Figure 36 Summary of daily wind speed trends.

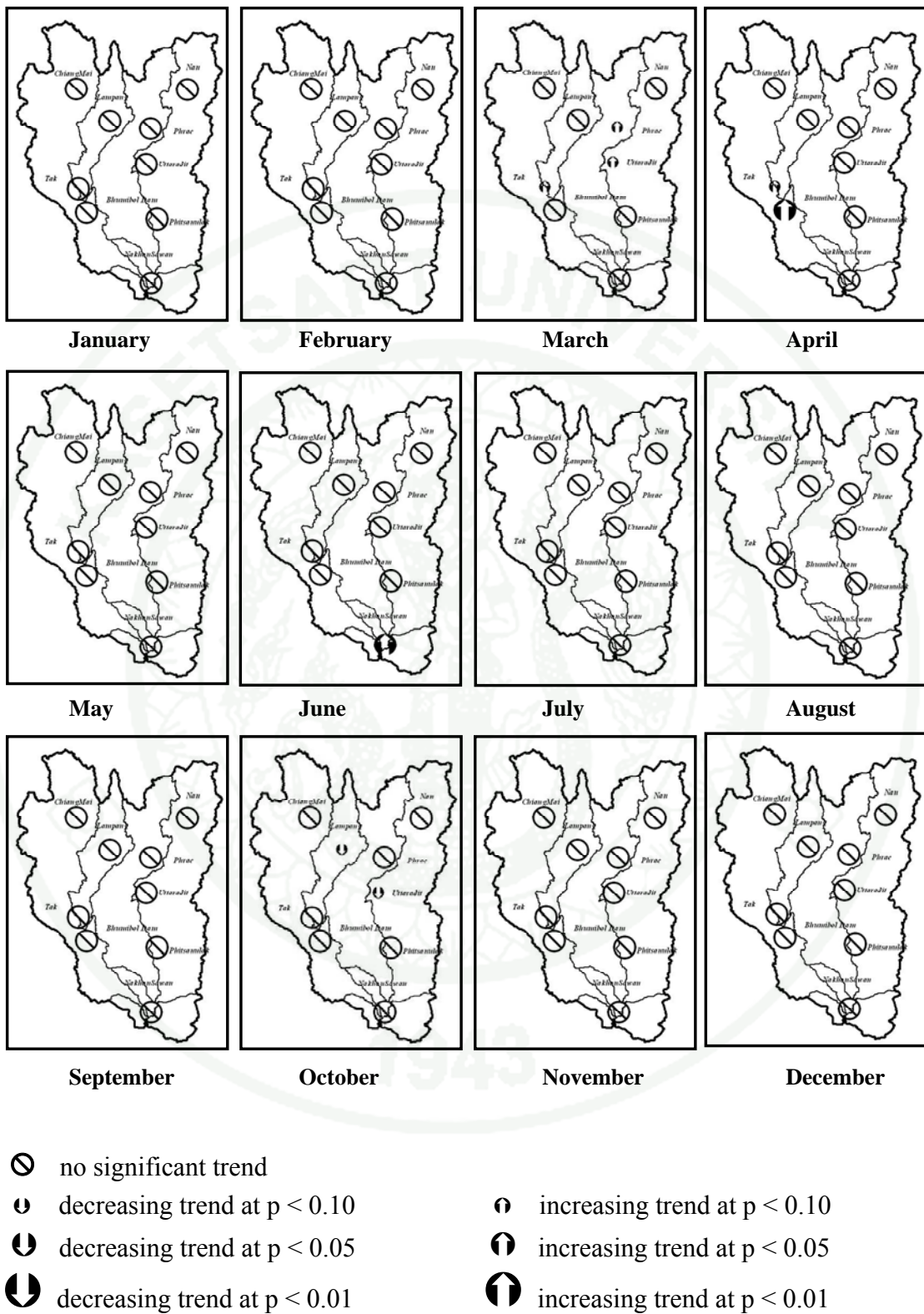


Figure 37 Summary of daily rainfall trends.

Table 14 P-value of reference evapotranspiration (ET_o) trend and parameters for stations.

Stations	Reference crop evapotranspiration trends by Mann-Kendall test											
	Jan	Feb	Mar	Apr	May	Jun	Jul	Aug	Sep	Oct	Nov	Dec
Chiang Mai	0.07 (d)	0.28 (a)	0.62 (a)	0.94 (a)	0.15 (a)	0.20 (a)	0.04 (c)	0.01 (c)	0.00 (b)	0.21 (a)	0.83 (a)	0.43 (a)
Bhumibol Dam	0.00 (b)	0.00 (b)	0.00 (b)	0.00 (b)	0.00 (b)	0.09 (d)	0.01 (b)	0.00 (b)	0.12 (a)	0.04 (c)	0.00 (b)	0.00 (b)
Tak	0.00 (b)	0.00 (b)	0.00 (b)	0.00 (b)	0.01 (b)	0.21 (a)	0.13 (a)	0.05 (d)	0.59 (a)	0.78 (a)	0.45 (a)	0.40 (a)
Lampang	0.33 (a)	0.01 (b)	0.07 (d)	0.00 (b)	0.08 (d)	0.42 (a)	0.56 (a)	0.56 (a)	0.75 (a)	0.76 (a)	0.04 (c)	0.18 (a)
Phrae	0.00 (b)	0.00 (b)	0.00 (b)	0.00 (b)	0.00 (b)	0.01 (b)	0.00 (b)	0.01 (c)	0.02 (c)	0.02 (c)	0.00 (b)	0.01 (b)
Nan	0.00 (b)	0.00 (b)	0.01 (b)	0.00 (b)	0.51 (a)	0.01 (b)	0.10 (a)	0.08 (d)	0.12 (a)	0.72 (a)	0.00 (b)	0.00 (b)
Uttaradit	0.12 (a)	1.00 (a)	0.17 (a)	0.06 (d)	0.13 (a)	0.23 (a)	0.16 (a)	0.38 (a)	0.44 (a)	0.49 (a)	0.10 (d)	0.06 (d)
Phitsanulok	0.86 (a)	0.43 (a)	0.01 (c)	0.28 (a)	0.08 (d)	0.86 (a)	0.12 (a)	0.35 (a)	0.52 (a)	0.67 (a)	0.94 (a)	0.54 (a)
Nakhon Sawan	0.00 (b)	0.00 (b)	0.00 (b)	0.00 (b)	0.00 (b)	0.00 (b)	0.00 (b)	0.00 (b)	0.07 (d)	0.50 (a)	0.30 (a)	0.01 (b)

(a) No significant trend

(b) Trends statistically significant at $p < 0.01$

(c) Trends statistically significant at $p < 0.05$

(d) Trends statistically significant at $p < 0.10$

Table 14 (Continued)

Stations	Actual vapor pressure trends by Mann-Kendall test												Vapor pressure deficit trends by Mann-Kendall test											
	Jan	Feb	Mar	Apr	May	Jun	Jul	Aug	Sep	Oct	Nov	Dec	Jan	Feb	Mar	Apr	May	Jun	Jul	Aug	Sep	Oct	Nov	Dec
Chiang Mai	0.41	0.83	0.21	0.64	0.06	0.00	0.00	0.00	0.00	0.12	0.13	0.64	0.78	0.21	0.89	0.19	0.05	0.00	0.00	0.00	0.01	0.25	0.59	
	(a)	(a)	(a)	(a)	(d)	(b)	(b)	(b)	(b)	(a)	(a)	(a)	(a)	(a)	(a)	(a)	(a)	(d)	(b)	(b)	(b)	(c)	(a)	(a)
Bhumibol Dam	0.00	0.04	0.00	0.00	0.00	0.01	0.00	0.00	0.00	0.02	0.01	0.91	0.27	0.07	0.06	0.01	0.78	0.12	0.23	0.41	0.27	0.99	0.41	
	(b)	(c)	(b)	(c)	(c)	(a)	(a)	(d)	(d)	(c)	(a)													
Tak	0.09	0.28	0.00	0.04	0.12	0.14	0.03	0.02	0.09	0.18	0.57	0.16	0.35	0.39	0.09	0.52	0.16	0.57	0.30	1.00	0.43	0.08	0.11	0.50
	(d)	(a)	(b)	(c)	(a)	(a)	(c)	(c)	(d)	(a)	(a)	(a)	(a)	(a)	(d)	(a)	(a)	(a)	(a)	(a)	(a)	(d)	(a)	(a)
Lampang	0.64	0.81	0.21	0.08	0.96	0.52	0.19	0.23	0.02	0.67	0.69	0.22	0.03	0.17	0.61	0.42	0.38	0.30	0.29	0.50	0.16	0.00	0.17	0.22
	(a)	(a)	(a)	(d)	(a)	(a)	(a)	(a)	(c)	(a)	(a)	(a)	(c)	(a)	(b)	(a)	(a)							
Phrae	0.07	0.07	0.00	0.00	0.19	0.14	0.01	0.01	0.09	0.25	0.75	0.42	0.91	0.52	0.02	0.10	0.28	0.69	0.41	0.45	0.62	0.75	0.72	0.51
	(d)	(d)	(b)	(b)	(a)	(a)	(b)	(c)	(d)	(a)	(a)	(a)	(a)	(a)	(c)	(a)								
Nan	0.20	0.21	0.12	0.34	0.37	0.41	0.62	0.04	0.48	0.78	0.30	0.15	0.09	0.32	0.48	0.91	0.89	0.18	0.05	0.27	0.13	0.00	0.11	0.02
	(a)	(a)	(a)	(a)	(a)	(a)	(c)	(a)	(a)	(a)	(a)	(d)	(a)	(a)	(a)	(a)	(c)	(a)	(a)	(b)	(a)	(c)		
Uttaradit	0.11	0.52	0.00	0.03	0.78	0.48	0.12	0.09	0.19	0.75	0.43	0.27	0.87	0.37	0.00	0.03	0.37	1.00	0.91	0.69	0.40	0.02	0.32	0.35
	(a)	(a)	(b)	(c)	(a)	(a)	(d)	(a)	(a)	(a)	(a)	(a)	(a)	(a)	(b)	(c)	(a)	(a)	(a)	(a)	(a)	(c)	(a)	(a)
Phitsanulok	0.13	0.16	0.07	0.09	0.83	0.29	0.52	0.75	0.54	0.45	0.69	0.16	0.04	0.01	0.02	0.28	0.64	0.99	1.00	0.20	0.52	0.04	0.30	0.54
	(a)	(a)	(d)	(d)	(a)	(c)	(b)	(c)	(a)	(c)	(a)	(a)												
Nakhon Sawan	0.01	0.04	0.00	0.00	0.00	0.01	0.01	0.00	0.00	0.02	0.06	0.03	0.02	0.03	0.02	0.13	0.09	0.04	0.01	0.48	0.76	0.49	0.94	0.50
	(b)	(c)	(b)	(b)	(b)	(c)	(b)	(b)	(c)	(d)	(c)	(c)	(c)	(c)	(a)	(d)	(c)	(b)	(a)	(a)	(a)	(a)	(a)	(a)

Table 14 (Continued)

Stations	Net radiation trends by Mann-Kendall test												Soil heat flux trends by Mann-Kendall test											
	Jan	Feb	Mar	Apr	May	Jun	Jul	Aug	Sep	Oct	Nov	Dec	Jan	Feb	Mar	Apr	May	Jun	Jul	Aug	Sep	Oct	Nov	Dec
Chiang Mai	0.01	0.00	0.62	0.02	0.00	0.09	0.06	0.07	0.00	0.12	0.62	0.25	0.21	0.97	0.89	0.90	0.12	0.25	0.45	0.87	0.60	0.23	0.91	0.51
	(c)	(b)	(a)	(c)	(b)	(d)	(d)	(d)	(b)	(a)	(a)	(a)	(a)	(a)	(a)	(a)	(a)	(a)	(a)	(a)	(a)	(a)	(a)	(a)
Bhumibol Dam	0.04	0.89	0.77	0.28	0.77	0.20	0.30	0.56	0.71	0.01	0.43	0.87	0.83	0.22	0.97	0.69	0.31	0.10	0.29	0.63	0.37	0.57	0.16	0.86
	(c)	(a)	(b)	(a)	(a)	(a)	(a)	(a)	(a)	(d)	(a)													
Tak	0.77	0.95	0.07	0.08	0.59	0.40	0.31	0.40	0.06	0.02	0.57	0.93	0.83	0.21	0.60	0.54	0.28	0.10	0.72	0.36	0.75	0.68	0.05	0.76
	(a)	(a)	(d)	(d)	(a)	(a)	(a)	(a)	(d)	(c)	(a)	(a)	(a)	(a)	(a)	(a)	(d)	(a)	(a)	(a)	(a)	(a)	(c)	(a)
Lampang	0.23	0.24	0.98	0.26	0.35	0.18	0.06	0.24	0.14	0.06	0.20	0.92	0.81	0.26	0.29	0.13	0.30	0.18	0.80	0.57	0.23	0.04	0.14	0.44
	(a)	(a)	(a)	(a)	(a)	(d)	(a)	(a)	(d)	(a)	(a)	(a)	(a)	(a)	(a)	(a)	(a)	(a)	(a)	(a)	(a)	(c)	(a)	(a)
Phrae	0.72	0.75	0.69	0.04	0.01	0.13	0.09	0.64	0.38	0.20	0.26	0.53	0.84	0.84	0.51	0.71	0.51	0.19	0.50	0.63	0.58	0.26	0.34	0.51
	(a)	(a)	(a)	(c)	(c)	(a)	(d)	(a)	(a)	(a)	(a)	(a)	(a)	(a)	(a)	(a)	(a)	(a)	(a)	(a)	(a)	(a)	(a)	(a)
Nan	0.01	0.20	0.27	0.59	0.87	0.09	0.78	0.12	0.28	0.07	0.03	0.00	0.93	0.76	0.51	0.30	0.56	0.34	0.68	0.22	0.58	0.03	0.41	0.75
	(c)	(a)	(a)	(a)	(a)	(d)	(a)	(a)	(d)	(c)	(b)	(a)	(a)	(a)	(a)	(a)	(a)	(a)	(a)	(a)	(a)	(c)	(a)	(a)
Uttaradit	0.56	0.17	0.07	0.36	0.40	0.87	0.56	0.54	0.76	0.64	0.69	0.90	0.67	0.45	0.49	0.43	0.48	0.06	0.76	0.87	0.87	0.16	0.45	0.69
	(a)	(a)	(d)	(a)	(a)	(a)	(a)	(d)	(a)															
Phitsanulok	0.13	0.09	0.59	0.39	0.20	0.78	0.11	0.28	0.75	0.72	0.80	1.00	0.59	0.16	0.72	0.84	0.90	0.04	0.67	0.69	0.34	0.05	0.43	0.96
	(a)	(d)	(a)	(a)	(a)	(a)	(c)	(a)	(a)	(a)	(c)	(a)	(a)	(a)										
Nakhon Sawan	0.86	0.62	0.89	0.34	0.18	0.64	0.09	0.41	0.54	0.72	0.89	0.72	0.96	0.33	0.49	0.93	0.59	0.48	0.59	0.03	0.83	0.36	0.22	0.75
	(a)	(a)	(a)	(a)	(a)	(d)	(a)	(a)	(a)	(a)	(a)	(a)	(a)	(a)	(c)	(a)	(a)	(a)						

(a) No significant trend

(b) Trends statistically significant at $p < 0.01$ (c) Trends statistically significant at $p < 0.05$ (d) Trends statistically significant at $p < 0.10$

Trend of actual vapor pressure

Actual vapor pressure (e_d) is a measurement of the amount of water vapor in a volume of air; it increases as the amount of water vapor increases. When the vapor pressure in the air is less than that in the leaf cells, the plants have transpiration. The result of trend analysis of daily actual vapor pressure (e_d) for each month is shown in Table 14 and Figure 38. The result mostly shows statistically significant rising trends in every month at many stations.

Trend of vapor pressure deficit

Vapor pressure deficit (VPD) is equal to the difference between saturated and actual vapor pressure; and is related to evapotranspiration. The result of trend analysis of daily vapor pressure deficit (VPD) for each month is shown in Table 14 and Figure 39. The result showed no significant trend in November while the other month showed decreasing trend at many stations, except in January, from October to December where some increasing trends occur. In summary, the results show that the vapor pressure deficit has significant decreasing trends in February to September.

Trend of net radiation

Net radiation (R_n) is the net radiant energy available at the surface of the earth for evaporating water, heating the surface, and heating the air. It is calculated as a balance between the incoming and outgoing radiation of both short and long wavelengths. The result of trend analysis of net radiation (R_n) for each month is shown in Table 14 and Figure 40. The result shows decreasing trend in most of the stations while a few increasing trends occur in March and October. In addition, both rising and declining trends occur in July. In summary, the results show that the net radiation has significant decreasing trends throughout the year, except in March, July and October.

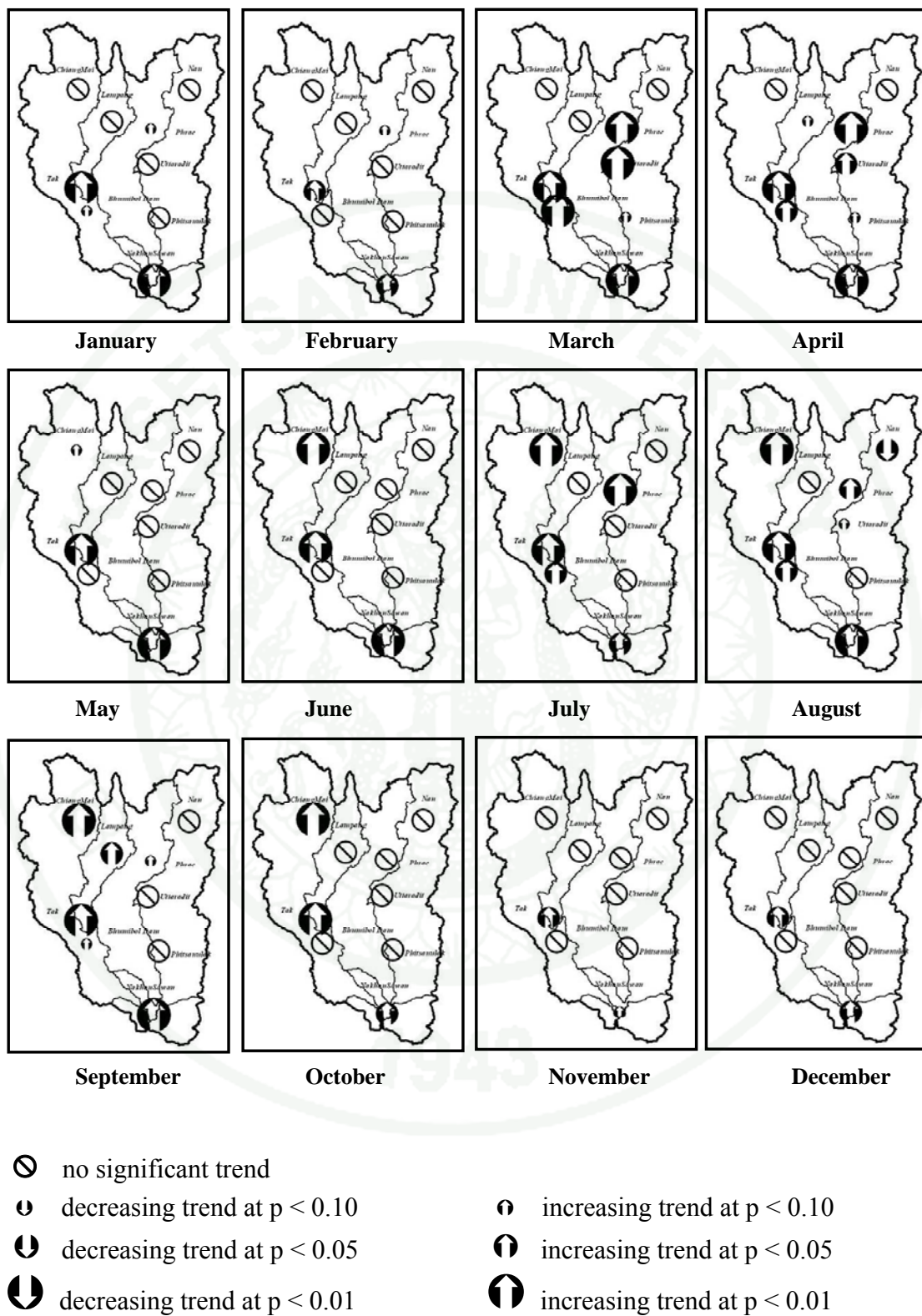


Figure 38 Summary of actual vapor pressure trends.

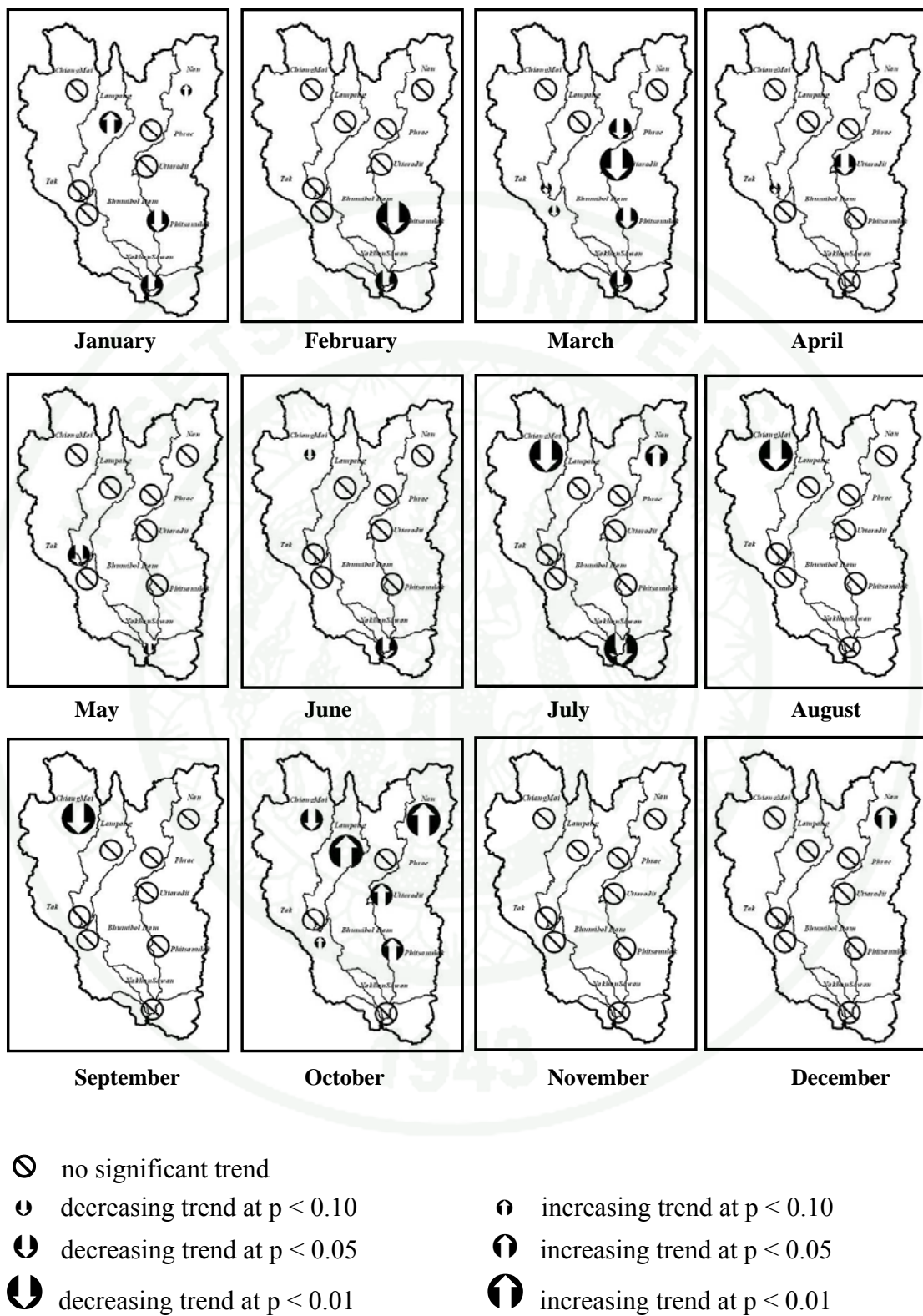
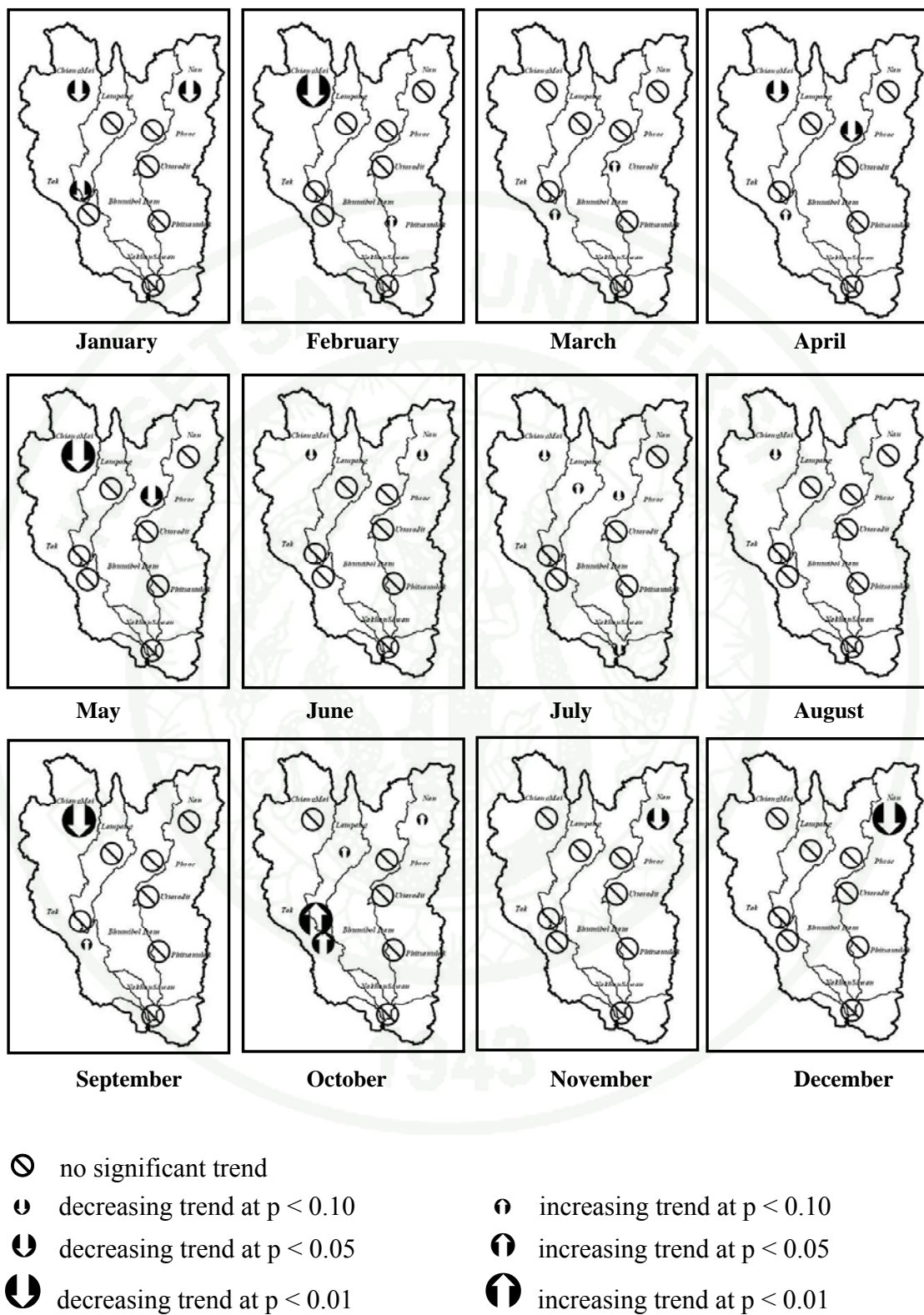


Figure 39 Summary of vapor pressure deficit trends.

**Figure 40** Summary of net radiation trends.

Trend of soil heat flux

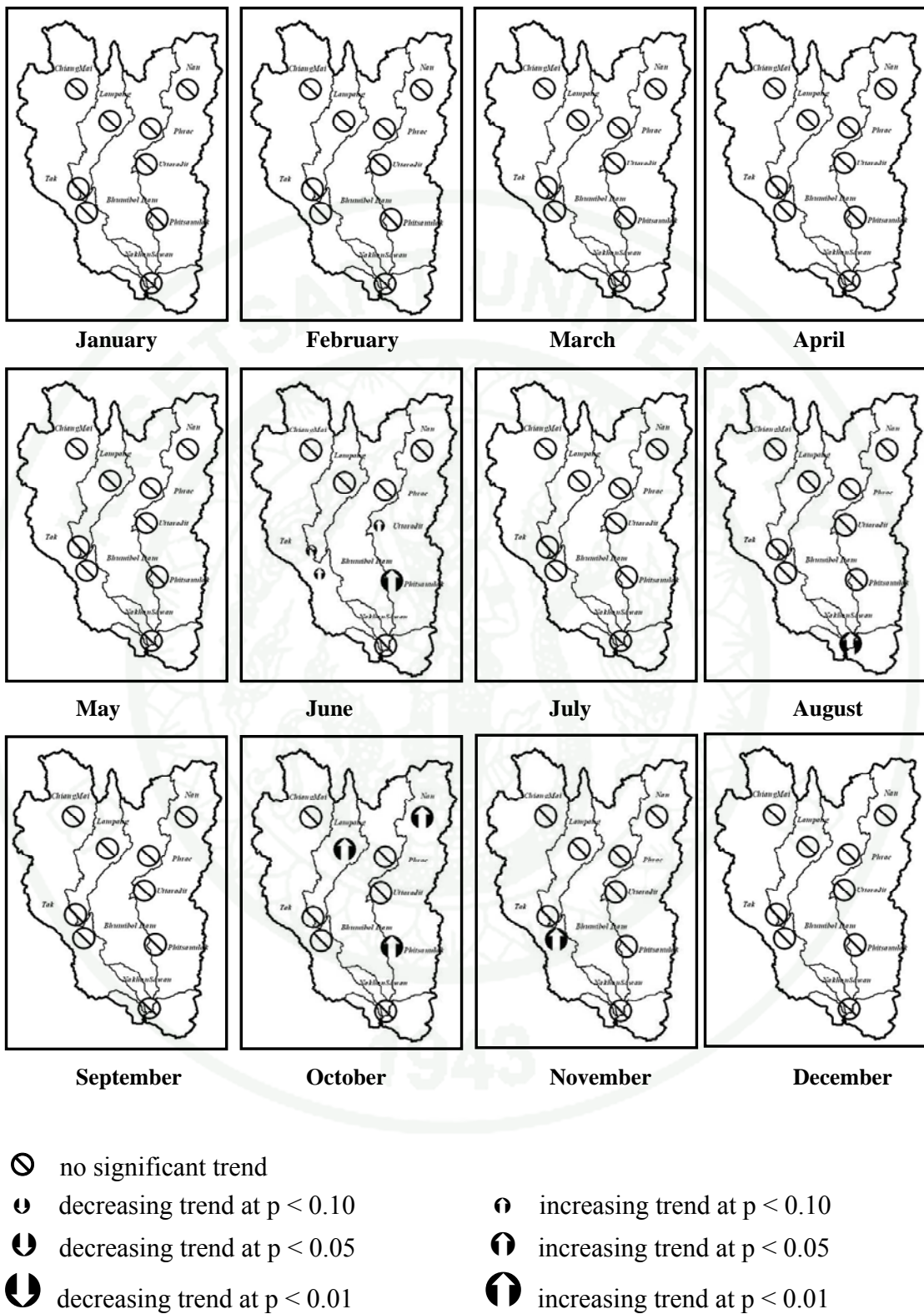
Soil heat flux (G) is the energy utilized in heating the soil. The soil heat flux is an important component to derive evapotranspiration from the theory of the surface energy budget of activities occurring at the crop surface. The result of trend analysis of soil heat flux (G) for each month is shown in Table 14 and Figure 41. The result shows significant increasing trend in June, August, October and November while the other months show insignificant trends.

2.3 Trend analysis of reference evapotranspiration

The Mann-Kendall was applied to detect trends of reference evapotranspiration (ET_o) for all selected stations. The results of trend analysis of the ET_o are shown in Table 14 and Figure 42. The results have clearly shown many stations with statistically significant trends at $p < 0.10$, $p < 0.05$ and $p < 0.01$ significance levels. Like ET_o (mm/day), most of the stations show significant decreasing trends, except at the Chiang Mai station which shows an increasing trend in January. In summary, the results show that the ET_o has significant decreasing trends throughout the year.

The double mass curve is used to check the consistency of reference evapotranspiration (ET_o) and pan evaporation. The double mass curves of ET_o and 0.7 E_{pan} at all stations during the 1977-2006 are shown in Appendix Figure C1 to Appendix Figure C9. The results show that ET_o has consistency in pan evaporation.

A comparison between trend of evaporation and the estimated ET_o shows that these two value sets are in good agreement between March and May, but inconsistent between January and February and also between June and December. This is because these two value sets are affected by different environmental factors. The evaporation values increase rapidly with increasing air temperatures but the ET_o values significantly increase with decreasing relative humidity and increasing wind speed (Bois, 2005; Liang, 2008).

**Figure 41** Summary of soil heat flux trends.

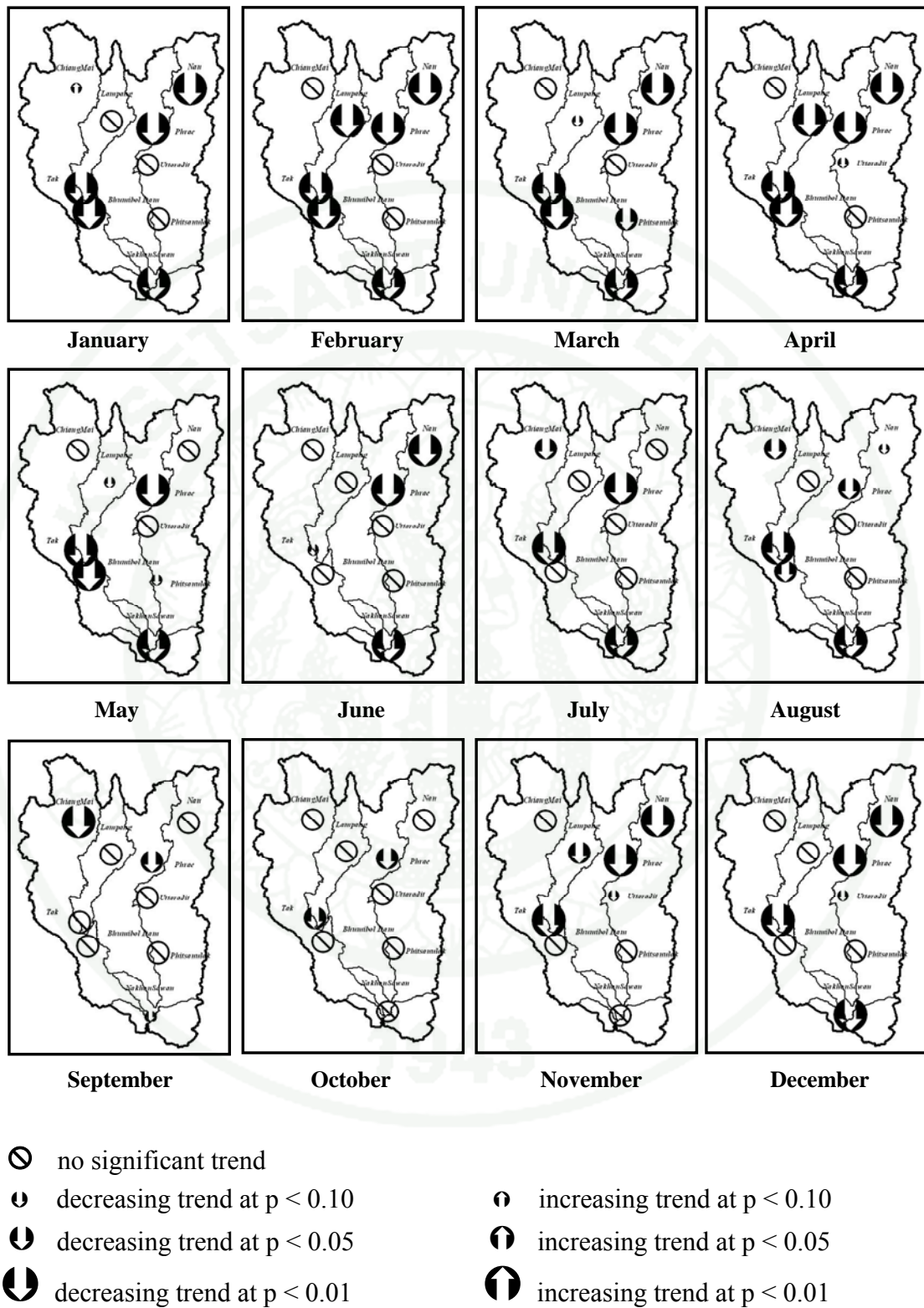


Figure 42 Summary of reference evapotranspiration trends.

3. Antecedent precipitation index

Daily antecedent precipitation Index (*API*) analysis during 1975 to 2003 (29-year period) which is composed of the results of maximum soil moisture available for evaporation (W_m), soil water recession coefficient (K), daily antecedent precipitation index (*API*), daily *API* adjusted by evapotranspiration (API_{adj}) and the results of critical antecedent precipitation index ($API_{critical}$) is shown below.

3.1 Maximum soil moisture available for evaporation

Maximum soil moisture available for evaporation (W_m) of surface soil (0-10 cm) was calculated by equation (5). The maximum soil moisture available for evaporation (W_m) is related to bulk density of soil (*B.D.*) and soil water holding capacity (*WHC*). 197 soil testing results for physical properties from Department of Water Resources (*DWR*) in the upper Chao Phraya river basin were collected. The soil test data is shown in Appendix Table A3. Moreover, the results of maximum soil moisture available for evaporation (W_m) of 112 small watersheds of the upper Chao Phraya river basin are shown in Table 15; and areal distributions of W_m is shown in Figure 43. The results show that the maximum soil moisture available for evaporation (W_m) of Ping river basin varies from 8.18 – 25.56 millimeter with the average of 22.93 millimeter, Wang river basin varies from 19.13 – 25.64 millimeter with the average of 23.46 millimeter, Yom river basin varies from 21.07 – 26.75 millimeter with the average of 23.34 millimeter, Nan river basin varies from 21.24 – 25.20 millimeter with the average of 22.59 millimeter and overall of the upper Chao Phraya river basin varies from 18.18 – 26.75 millimeter with the average of 23.05 millimeter.

Table 15 Summary of maximum soil moisture available for evaporation (W_m) of surface soil (0-10 cm).

No.	Code	Small watershed area (sq.km)	W_m (mm)	No.	Code	Small watershed area (sq.km)	W_m (mm)
1.	C_1	1,545.8	22.26	36.	P_8	1,745.8	22.07
2.	C_2	3,401.7	21.37	37.	P_9	2,100.5	24.28
3.	N_1	2,228.4	22.07	38.	P_10	620.9	22.80
4.	N_2	790.1	21.89	39.	P_11	3,194.4	24.70
5.	N_3	1,536.8	21.73	40.	P_12	1,971.0	22.04
6.	N_4	600.6	22.12	41.	P_13	1,935.4	23.64
7.	N_5	591.4	21.82	42.	P_14	522.1	24.76
8.	N_6	781.3	21.24	43.	P_15	3,179.7	24.84
9.	N_7	3,195.7	21.75	44.	P_16	845.4	25.14
10.	N_8	2,206.2	22.29	45.	P_17	166.1	25.56
11.	N_9	1,046.7	21.62	46.	P_18	527.9	25.22
12.	N_11	2,429.7	22.09	47.	P_19	654.4	23.74
13.	N_12	1,095.1	23.53	48.	P_20	274.5	25.06
14.	N_13	339.7	24.14	49.	P_21	959.5	24.58
15.	N_14	1,727.6	24.44	50.	P_22	367.6	24.54
16.	N_15	688.2	25.20	51.	P_23	383.5	22.81
17.	N_16	5,583.4	23.91	52.	P_24	759.0	22.84
18.	N_17	219.9	25.18	53.	P_25	293.5	23.04
19.	N_18	158.5	24.13	54.	P_26	1,223.0	22.94
20.	N_19	259.5	22.74	55.	P_27	211.2	23.19
21.	N_20	2,615.9	22.54	56.	P_28	549.2	22.97
22.	N_21	271.8	21.97	57.	P_29	1,351.5	23.09
23.	N_22	1,226.2	22.07	58.	P_30	532.2	23.18
24.	N_23	205.2	21.61	59.	P_31	237.7	22.17
25.	N_24	2,209.0	21.28	60.	P_32	133.3	21.34
26.	N_25	1,426.2	21.33	61.	W_1	1,645.7	19.13
27.	N_26	2,142.7	22.52	62.	W_2	736.1	19.28
28.	N_27	988.5	22.23	63.	W_3	967.4	21.44
29.	P_1	1,912.7	18.18	64.	W_4	403.9	21.52
30.	P_2	1,286.5	18.70	65.	W_5	455.1	21.80
31.	P_3	1,961.7	18.45	66.	W_6	1,758.8	22.30
32.	P_4	1,530.7	21.75	67.	W_7	736.5	21.96
33.	P_5	53.4	25.55	68.	W_8	863.3	22.58
34.	P_6	562.1	19.52	69.	W_9	282.5	24.05
35.	P_7	2,894.3	21.17	70.	W_10	232.8	25.18

Table 15 (Continued)

No.	Code	Small watershed area (sq.km)	W_m (mm)	No.	Code	Small watershed area (sq.km)	W_m (mm)
71.	W_11	281.8	24.98	92.	Y_11	532.4	22.23
72.	W_12	230.1	25.25	93.	Y_12	246.0	22.28
73.	W_13	149.1	25.18	94.	Y_13	711.0	22.27
74.	W_14	182.9	25.16	95.	Y_14	439.7	22.81
75.	W_15	362.8	24.81	96.	Y_15	531.1	23.70
76.	W_16	340.1	25.64	97.	Y_16	214.4	23.14
77.	W_17	308.4	25.40	98.	Y_17	880.1	24.99
78.	W_18	256.6	25.21	99.	Y_18	832.8	25.98
79.	W_19	378.8	25.25	100.	Y_19	796.8	26.22
80.	W_20	215.5	21.94	101.	Y_20	768.4	26.49
81.	W_21	22.4	24.58	102.	Y_21	2,312.7	25.96
82.	Y_1	2,119.7	21.21	103.	Y_22	491.3	26.53
83.	Y_2	873.6	21.66	104.	Y_23	1,055.9	25.48
84.	Y_3	658.8	21.27	105.	Y_24	1,572.1	25.31
85.	Y_4	1,760.1	21.07	106.	Y_25	905.8	25.24
86.	Y_5	214.7	21.26	107.	Y_26	545.4	23.97
87.	Y_6	374.7	21.16	108.	Y_27	1,323.4	23.61
88.	Y_7	332.1	21.16	109.	Y_28	656.3	22.59
89.	Y_8	246.1	21.34	110.	Y_29	191.7	22.07
90.	Y_9	1,032.1	22.14	111.	Y_30	655.3	22.22
91.	Y_10	149.7	21.38	112.	Y_31	170.0	26.75

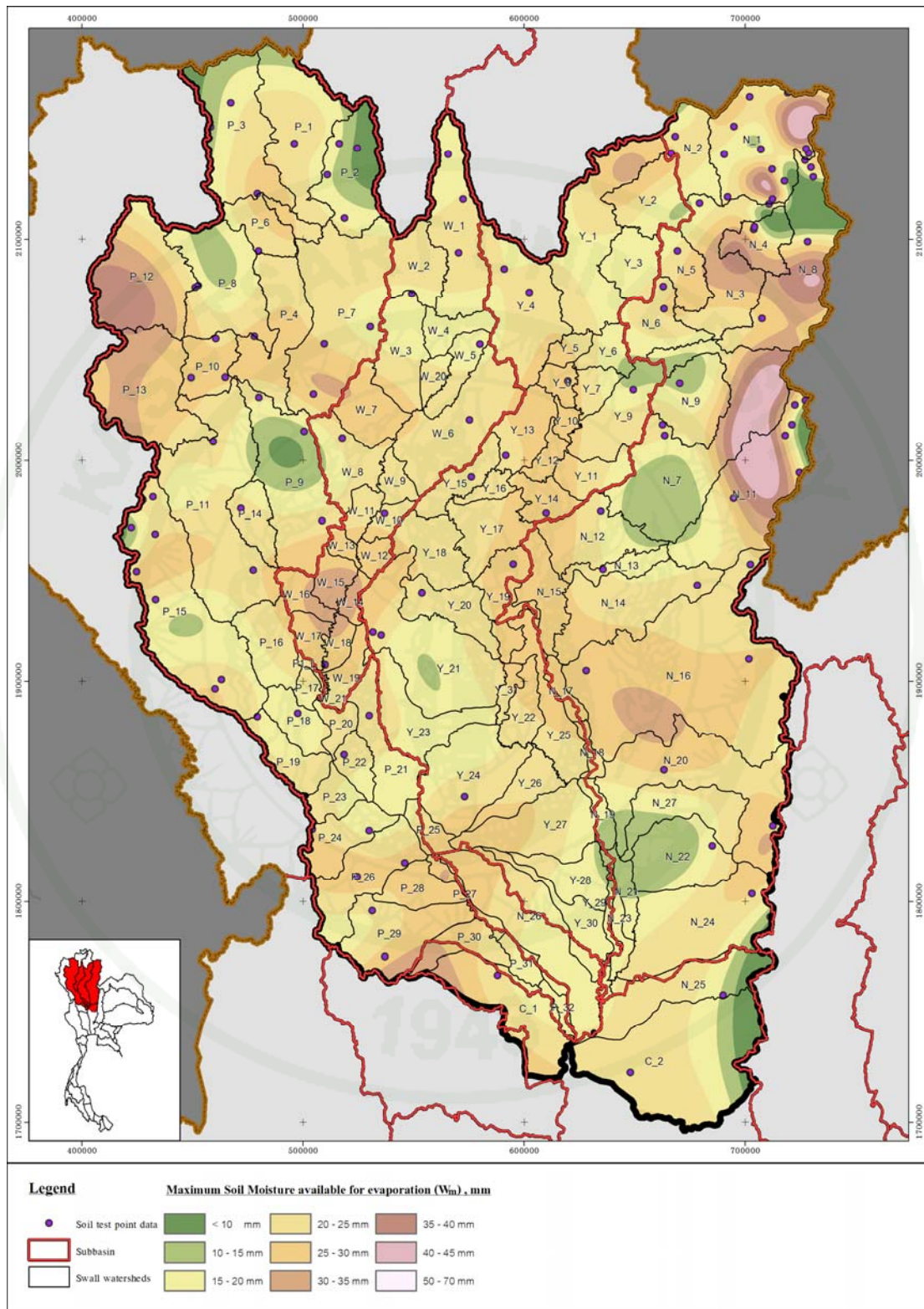


Figure 43 Areal distributions of maximum soil moisture available for evaporation.

3.2 Soil water recession coefficient (K)

After daily reference evapotranspiration (ET_o) and maximum soil moisture available for evaporation (W_m) of study area were calculated in previous section; the daily soil water recession coefficient (K) during 1975 to 2003 were analysed by equation (4). Moreover, the summary of daily average of soil water recession coefficient (K) for antecedent precipitation index (API) analysis is show in Table 16 and Figure 44. The results show that the daily average of soil water recession coefficient (K) is 0.842 which varies from 0.791 in July to 0.883 in March.

3.3 Daily antecedent precipitation index (API)

After daily soil water recession coefficient (K) and areal rainfall distribution were calculated during 1977-2003, the daily antecedent precipitation index (API) was analysed by equation (3) of Kohler & Linsley. In addition, the summary of daily antecedent precipitation index (API) in each month is shown in Table 17 and Figure 45. The results show that the daily average of antecedent precipitation index (API) of the upper Chao Phraya river basin is 17.27 mm/day which varies from 2.55 mm/day in December to 54.63 mm/day in September.

3.4 Soil water recession coefficient adjustment

The agriculture landuse data was used to decide the crop coefficient (K_c). Crop coefficient (K_c) calculated by Penman-Monteith equation was collected from the results from Royal Irrigation Department (RID). Thereafter, evapotranspiration (ET) was calculated from crop coefficient (K_c) and reference evapotranspiration (ET_o). After that evapotranspiration (ET) and maximum soil moisture available for evaporation (W_m) in Table 15 and Figure 43 were use to calculate the daily soil water recession coefficient adjusted by evapotranspiration (K_{adj}) by using evapotranspiration (ET) instead of reference evapotranspiration (ET_o) as shown in equation (45).

Table 16 Daily average of soil water recession coefficient (K) for API analysis.

No.	Code	Watershed area (sq.km)	Soil water recession coefficient (K)												
			Apr	May	Jun	Jul	Aug	Sep	Oct	Nov	Dec	Jan	Feb	Mar	
1	C_1	1,545.8	0.857	0.808	0.772	0.756	0.788	0.811	0.820	0.834	0.844	0.846	0.855	0.865	
2	C_2	3,401.7	0.851	0.801	0.764	0.748	0.781	0.804	0.814	0.828	0.838	0.840	0.850	0.860	
3	N_1	2,228.4	0.889	0.866	0.835	0.807	0.809	0.824	0.838	0.845	0.839	0.848	0.872	0.891	
4	N_2	790.1	0.888	0.865	0.834	0.805	0.808	0.823	0.837	0.843	0.837	0.846	0.871	0.890	
5	N_3	1,536.8	0.887	0.864	0.833	0.804	0.806	0.822	0.836	0.842	0.836	0.845	0.870	0.889	
6	N_4	600.6	0.889	0.866	0.835	0.807	0.809	0.824	0.838	0.845	0.839	0.848	0.872	0.891	
7	N_5	591.4	0.888	0.864	0.833	0.805	0.807	0.822	0.836	0.843	0.837	0.846	0.871	0.889	
8	N_6	781.3	0.885	0.861	0.829	0.800	0.802	0.818	0.832	0.839	0.833	0.842	0.868	0.887	
9	N_7	3,195.7	0.887	0.864	0.833	0.804	0.806	0.822	0.836	0.843	0.836	0.846	0.870	0.889	
10	N_8	2,206.2	0.890	0.867	0.836	0.808	0.811	0.826	0.839	0.846	0.840	0.849	0.873	0.892	
11	N_9	1,046.7	0.879	0.851	0.815	0.782	0.796	0.815	0.828	0.838	0.835	0.843	0.862	0.880	
12	N_11	2,429.7	0.878	0.855	0.824	0.798	0.805	0.829	0.840	0.848	0.840	0.842	0.860	0.877	
13	N_12	1,095.1	0.885	0.863	0.834	0.809	0.815	0.838	0.849	0.856	0.849	0.851	0.868	0.884	
14	N_13	339.7	0.887	0.866	0.837	0.814	0.820	0.842	0.852	0.860	0.852	0.854	0.871	0.887	
15	N_14	1,727.6	0.889	0.868	0.839	0.816	0.822	0.844	0.854	0.861	0.854	0.856	0.873	0.888	
16	N_15	688.2	0.892	0.871	0.844	0.821	0.827	0.848	0.858	0.865	0.858	0.860	0.876	0.892	
17	N_16	5,583.4	0.878	0.850	0.822	0.801	0.812	0.837	0.847	0.854	0.857	0.857	0.859	0.869	0.881
18	N_17	219.9	0.884	0.857	0.830	0.810	0.820	0.845	0.854	0.861	0.864	0.865	0.875	0.887	
19	N_18	158.5	0.879	0.851	0.823	0.802	0.813	0.838	0.848	0.855	0.859	0.860	0.870	0.882	
20	N_19	259.5	0.872	0.843	0.814	0.792	0.803	0.830	0.840	0.847	0.851	0.852	0.863	0.875	
21	N_20	2,615.9	0.871	0.841	0.812	0.790	0.802	0.828	0.839	0.846	0.849	0.851	0.862	0.874	
22	N_21	271.8	0.855	0.806	0.769	0.754	0.786	0.808	0.818	0.832	0.842	0.844	0.853	0.864	
23	N_22	1,226.2	0.869	0.838	0.809	0.786	0.798	0.825	0.835	0.843	0.846	0.848	0.859	0.872	
24	N_23	205.2	0.853	0.803	0.766	0.750	0.783	0.806	0.815	0.830	0.840	0.842	0.851	0.861	
25	N_24	2,209.0	0.851	0.800	0.763	0.747	0.780	0.803	0.813	0.827	0.837	0.840	0.849	0.860	
26	N_25	1,426.2	0.851	0.801	0.763	0.747	0.780	0.803	0.813	0.828	0.838	0.840	0.849	0.860	
27	N_26	2,142.7	0.858	0.810	0.774	0.759	0.790	0.813	0.822	0.836	0.846	0.848	0.857	0.867	
28	N_27	988.5	0.857	0.808	0.772	0.756	0.788	0.810	0.820	0.834	0.844	0.846	0.855	0.865	
29	P_1	1,912.7	0.848	0.807	0.769	0.736	0.758	0.793	0.812	0.818	0.814	0.819	0.839	0.855	
30	P_2	1,286.5	0.852	0.812	0.774	0.742	0.764	0.798	0.817	0.822	0.818	0.824	0.843	0.858	
31	P_3	1,961.7	0.850	0.809	0.772	0.739	0.761	0.796	0.814	0.820	0.816	0.822	0.841	0.857	
32	P_4	1,530.7	0.871	0.836	0.803	0.774	0.793	0.824	0.840	0.845	0.842	0.846	0.863	0.877	
33	P_5	53.4	0.889	0.858	0.829	0.804	0.821	0.848	0.862	0.866	0.864	0.868	0.883	0.894	
34	P_6	562.1	0.857	0.819	0.783	0.752	0.773	0.806	0.824	0.829	0.825	0.831	0.849	0.864	
35	P_7	2,894.3	0.868	0.832	0.798	0.769	0.788	0.819	0.836	0.841	0.838	0.843	0.860	0.874	
36	P_8	1,745.8	0.873	0.838	0.805	0.777	0.796	0.826	0.842	0.847	0.844	0.849	0.865	0.879	
37	P_9	2,100.5	0.884	0.852	0.821	0.795	0.813	0.841	0.856	0.860	0.857	0.861	0.877	0.889	
38	P_10	620.9	0.877	0.843	0.811	0.783	0.802	0.831	0.847	0.852	0.848	0.853	0.869	0.882	
39	P_11	3,194.4	0.886	0.854	0.824	0.798	0.816	0.843	0.858	0.862	0.859	0.863	0.879	0.891	
40	P_12	1,971.0	0.868	0.837	0.802	0.777	0.795	0.823	0.829	0.832	0.844	0.850	0.863	0.878	
41	P_13	1,935.4	0.881	0.848	0.817	0.790	0.808	0.837	0.852	0.856	0.853	0.858	0.874	0.886	
42	P_14	522.1	0.886	0.854	0.824	0.799	0.816	0.843	0.858	0.862	0.860	0.864	0.879	0.891	
43	P_15	3,179.7	0.882	0.854	0.822	0.799	0.816	0.841	0.846	0.849	0.860	0.866	0.878	0.891	
44	P_16	845.4	0.884	0.856	0.824	0.801	0.818	0.843	0.848	0.851	0.862	0.867	0.879	0.893	
45	P_17	166.1	0.885	0.858	0.826	0.804	0.820	0.846	0.850	0.853	0.864	0.869	0.881	0.894	

Table 16 (Continued)

No.	Code	Watershed area (sq.km)	Soil water recession coefficient (<i>K</i>)											
			Apr	May	Jun	Jul	Aug	Sep	Oct	Nov	Dec	Jan	Feb	Mar
46	P_18	527.9	0.891	0.858	0.821	0.792	0.814	0.841	0.846	0.854	0.865	0.869	0.883	0.895
47	P_19	654.4	0.884	0.850	0.811	0.781	0.804	0.832	0.838	0.845	0.857	0.862	0.876	0.889
48	P_20	274.5	0.890	0.857	0.820	0.791	0.813	0.840	0.845	0.853	0.864	0.868	0.882	0.895
49	P_21	959.5	0.888	0.855	0.817	0.787	0.810	0.837	0.843	0.850	0.862	0.866	0.880	0.893
50	P_22	367.6	0.888	0.855	0.817	0.787	0.809	0.837	0.842	0.850	0.862	0.866	0.879	0.893
51	P_23	383.5	0.880	0.845	0.804	0.773	0.797	0.826	0.832	0.840	0.852	0.856	0.871	0.885
52	P_24	759.0	0.880	0.845	0.805	0.773	0.797	0.826	0.832	0.840	0.852	0.857	0.871	0.885
53	P_25	293.5	0.881	0.846	0.806	0.775	0.799	0.827	0.833	0.841	0.853	0.858	0.872	0.886
54	P_26	1,223.0	0.881	0.845	0.805	0.774	0.798	0.826	0.832	0.841	0.853	0.857	0.872	0.885
55	P_27	211.2	0.882	0.847	0.807	0.776	0.800	0.828	0.834	0.842	0.854	0.859	0.873	0.887
56	P_28	549.2	0.881	0.846	0.806	0.774	0.798	0.827	0.833	0.841	0.853	0.857	0.872	0.886
57	P_29	1,351.5	0.881	0.846	0.807	0.775	0.799	0.827	0.833	0.841	0.854	0.858	0.872	0.886
58	P_30	532.2	0.862	0.815	0.780	0.765	0.796	0.817	0.827	0.840	0.850	0.852	0.860	0.870
59	P_31	237.7	0.856	0.808	0.771	0.756	0.788	0.810	0.820	0.833	0.843	0.845	0.855	0.865
60	P_32	133.3	0.851	0.801	0.763	0.747	0.780	0.803	0.813	0.828	0.838	0.840	0.849	0.860
61	W_1	1,645.7	0.867	0.840	0.803	0.769	0.775	0.796	0.810	0.819	0.818	0.828	0.851	0.870
62	W_2	736.1	0.868	0.841	0.804	0.771	0.776	0.797	0.812	0.820	0.819	0.829	0.852	0.871
63	W_3	967.4	0.880	0.856	0.822	0.791	0.796	0.815	0.829	0.836	0.836	0.845	0.866	0.883
64	W_4	403.9	0.881	0.856	0.823	0.792	0.797	0.816	0.830	0.837	0.836	0.846	0.866	0.883
65	W_5	455.1	0.882	0.858	0.825	0.794	0.799	0.818	0.831	0.839	0.838	0.848	0.868	0.885
66	W_6	1,758.8	0.885	0.861	0.828	0.798	0.803	0.822	0.835	0.842	0.842	0.851	0.870	0.887
67	W_7	736.5	0.883	0.859	0.826	0.795	0.801	0.819	0.833	0.840	0.839	0.849	0.868	0.885
68	W_8	863.3	0.886	0.863	0.830	0.801	0.805	0.824	0.837	0.844	0.843	0.852	0.872	0.888
69	W_9	282.5	0.893	0.870	0.840	0.812	0.816	0.834	0.846	0.853	0.852	0.861	0.879	0.895
70	W_10	232.8	0.897	0.876	0.846	0.819	0.824	0.840	0.852	0.859	0.858	0.867	0.884	0.899
71	W_11	281.8	0.896	0.875	0.845	0.818	0.822	0.839	0.851	0.858	0.857	0.866	0.883	0.899
72	W_12	230.1	0.898	0.876	0.847	0.820	0.824	0.841	0.853	0.859	0.859	0.867	0.885	0.900
73	W_13	149.1	0.897	0.876	0.846	0.819	0.824	0.840	0.852	0.859	0.858	0.867	0.884	0.899
74	W_14	182.9	0.884	0.856	0.824	0.801	0.818	0.843	0.848	0.851	0.862	0.867	0.879	0.893
75	W_15	362.8	0.882	0.854	0.822	0.799	0.815	0.841	0.846	0.849	0.860	0.866	0.878	0.891
76	W_16	340.1	0.886	0.858	0.827	0.805	0.821	0.846	0.851	0.854	0.864	0.870	0.881	0.895
77	W_17	308.4	0.885	0.857	0.825	0.803	0.819	0.845	0.849	0.852	0.863	0.868	0.880	0.894
78	W_18	256.6	0.884	0.856	0.824	0.802	0.818	0.844	0.848	0.851	0.862	0.867	0.880	0.893
79	W_19	378.8	0.884	0.856	0.824	0.802	0.818	0.844	0.849	0.852	0.862	0.868	0.880	0.893
80	W_20	215.5	0.883	0.859	0.826	0.795	0.800	0.819	0.833	0.840	0.839	0.848	0.868	0.885
81	W_21	22.4	0.895	0.873	0.843	0.815	0.820	0.837	0.849	0.856	0.855	0.864	0.882	0.897
82	Y_1	2,119.7	0.885	0.861	0.829	0.800	0.802	0.818	0.832	0.839	0.833	0.842	0.867	0.886
83	Y_2	873.6	0.887	0.863	0.832	0.803	0.806	0.821	0.835	0.842	0.836	0.845	0.870	0.889
84	Y_3	658.8	0.885	0.861	0.829	0.800	0.803	0.818	0.832	0.839	0.833	0.842	0.868	0.887
85	Y_4	1,760.1	0.876	0.848	0.810	0.778	0.791	0.811	0.824	0.834	0.832	0.839	0.859	0.877
86	Y_5	214.7	0.877	0.849	0.812	0.779	0.793	0.813	0.825	0.836	0.833	0.840	0.860	0.878
87	Y_6	374.7	0.877	0.849	0.811	0.778	0.792	0.812	0.824	0.835	0.832	0.840	0.859	0.878
88	Y_7	332.1	0.877	0.849	0.811	0.778	0.792	0.812	0.824	0.835	0.832	0.840	0.859	0.878
89	Y_8	246.1	0.878	0.850	0.812	0.780	0.793	0.813	0.826	0.836	0.833	0.841	0.860	0.879
90	Y_9	1,032.1	0.882	0.855	0.819	0.787	0.800	0.819	0.831	0.842	0.839	0.846	0.865	0.883

Table 16 (Continued)

No.	Code	Watershed area (sq.km)	Soil water recession coefficient (K)											
			Apr	May	Jun	Jul	Aug	Sep	Oct	Nov	Dec	Jan	Feb	Mar
91	Y_10	149.7	0.878	0.850	0.813	0.780	0.794	0.814	0.826	0.836	0.834	0.841	0.860	0.879
92	Y_11	532.4	0.882	0.855	0.819	0.788	0.801	0.820	0.832	0.842	0.840	0.847	0.865	0.883
93	Y_12	246.0	0.882	0.856	0.820	0.788	0.801	0.820	0.832	0.842	0.840	0.847	0.866	0.883
94	Y_13	711.0	0.882	0.855	0.819	0.788	0.801	0.820	0.832	0.842	0.840	0.847	0.866	0.883
95	Y_14	439.7	0.881	0.859	0.829	0.804	0.810	0.834	0.844	0.852	0.844	0.846	0.864	0.881
96	Y_15	531.1	0.886	0.864	0.835	0.811	0.817	0.839	0.850	0.857	0.850	0.852	0.869	0.885
97	Y_16	214.4	0.883	0.861	0.831	0.806	0.813	0.836	0.846	0.854	0.846	0.848	0.866	0.882
98	Y_17	880.1	0.891	0.870	0.842	0.819	0.825	0.847	0.857	0.864	0.857	0.859	0.876	0.891
99	Y_18	832.8	0.895	0.875	0.848	0.826	0.831	0.852	0.862	0.869	0.862	0.864	0.880	0.895
100	Y_19	796.8	0.896	0.876	0.849	0.827	0.833	0.854	0.863	0.870	0.863	0.865	0.881	0.896
101	Y_20	768.4	0.889	0.863	0.838	0.818	0.828	0.852	0.861	0.867	0.870	0.871	0.881	0.892
102	Y_21	2,312.7	0.887	0.861	0.835	0.815	0.825	0.849	0.858	0.865	0.868	0.869	0.879	0.890
103	Y_22	491.3	0.890	0.863	0.838	0.819	0.829	0.852	0.861	0.868	0.871	0.872	0.881	0.892
104	Y_23	1,055.9	0.885	0.858	0.832	0.812	0.822	0.846	0.856	0.863	0.866	0.867	0.877	0.888
105	Y_24	1,572.1	0.885	0.857	0.831	0.811	0.821	0.845	0.855	0.862	0.865	0.866	0.876	0.887
106	Y_25	905.8	0.884	0.857	0.830	0.810	0.821	0.845	0.855	0.861	0.864	0.865	0.876	0.887
107	Y_26	545.4	0.879	0.850	0.822	0.801	0.812	0.838	0.847	0.855	0.858	0.859	0.869	0.881
108	Y_27	1,323.4	0.877	0.848	0.820	0.799	0.810	0.835	0.845	0.853	0.856	0.857	0.868	0.879
109	Y_28	656.3	0.872	0.842	0.813	0.791	0.802	0.829	0.839	0.846	0.850	0.851	0.862	0.874
110	Y_29	191.7	0.869	0.838	0.809	0.786	0.798	0.825	0.835	0.843	0.846	0.848	0.859	0.872
111	Y_30	655.3	0.870	0.839	0.810	0.787	0.799	0.826	0.836	0.844	0.847	0.849	0.860	0.872
112	Y_31	170.0	0.890	0.865	0.839	0.820	0.830	0.853	0.862	0.869	0.872	0.873	0.882	0.893
Mean		887.4	0.881	0.853	0.826	0.806	0.816	0.841	0.851	0.858	0.861	0.862	0.872	0.884
Maximum		2,312.7	0.890	0.865	0.839	0.820	0.830	0.853	0.862	0.869	0.872	0.873	0.882	0.893
Minimum		170.0	0.869	0.838	0.809	0.786	0.798	0.825	0.835	0.843	0.846	0.848	0.859	0.872

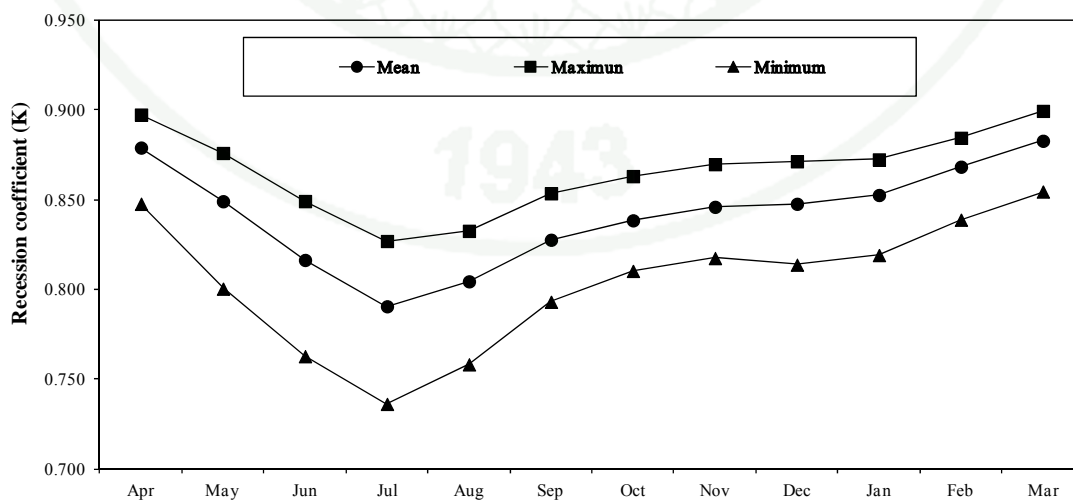
**Figure 44** Daily average of soil water recession coefficient (K) for API analysis.

Table 17 Daily antecedent precipitation index (*API*).

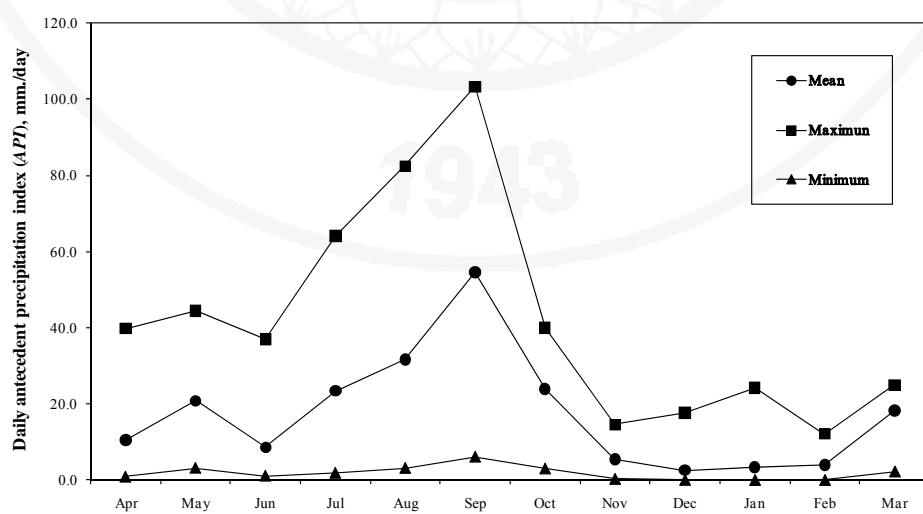
No.	Subbsin	Subbasin	Daily antecedent precipitation index (<i>API</i>), mm/day											
			Code	Area (sq.km)	Apr	May	Jun	Jul	Aug	Sep	Oct	Nov	Dec	Jan
1	C_1	1,545.8	9.2	23.5	5.6	13.7	26.4	24.3	12.7	3.4	1.5	0.8	5.6	17.7
2	C_2	3,401.7	8.2	18.7	11.4	20.2	40.5	52.0	13.5	0.4	1.3	0.5	0.4	16.3
3	N_1	2,228.4	20.5	29.1	10.2	63.6	51.4	56.7	13.5	13.5	5.6	6.6	3.6	23.9
4	N_2	790.1	21.5	34.3	11.0	64.1	56.0	56.7	16.9	12.8	6.7	7.5	2.3	23.1
5	N_3	1,536.8	18.7	31.2	7.3	43.0	46.4	49.3	22.3	8.8	7.6	6.5	6.1	21.1
6	N_4	600.6	19.7	26.4	5.2	39.9	39.2	44.6	18.2	7.3	5.3	5.7	9.0	21.6
7	N_5	591.4	17.8	38.2	7.7	49.6	50.7	56.4	23.4	9.7	8.8	8.3	5.0	21.3
8	N_6	781.3	13.0	29.8	7.1	38.8	38.1	42.9	23.6	6.8	4.8	4.7	5.3	20.0
9	N_7	3,195.7	8.1	21.0	4.7	22.9	24.9	27.5	9.1	2.0	2.2	3.7	2.4	13.8
10	N_8	2,206.2	18.3	11.4	2.2	33.5	26.5	33.4	12.7	6.5	3.2	2.3	12.1	20.8
11	N_9	1,046.7	12.0	27.0	5.8	29.9	31.6	35.2	9.3	1.9	2.7	4.6	2.3	16.4
12	N_11	2,429.7	9.3	19.2	3.9	33.2	29.5	30.1	10.4	3.6	0.4	0.8	1.4	18.6
13	N_12	1,095.1	5.7	30.7	13.1	29.2	39.9	64.4	20.3	3.1	1.2	1.6	4.9	23.2
14	N_13	339.7	7.0	35.9	12.3	33.4	41.0	62.5	19.1	2.8	0.8	1.7	4.5	23.4
15	N_14	1,727.6	2.8	8.1	3.1	9.0	13.5	16.8	4.8	1.0	0.0	0.2	0.6	6.7
16	N_15	688.2	10.2	28.7	10.6	33.7	49.7	64.3	23.8	5.0	0.1	0.8	1.2	23.2
17	N_16	5,583.4	6.9	23.8	7.9	31.7	34.9	41.6	15.5	2.8	0.0	0.9	0.7	22.0
18	N_17	219.9	7.5	16.1	17.0	30.9	46.6	83.1	17.6	1.7	0.0	0.0	4.6	23.4
19	N_18	158.5	17.1	15.2	21.9	34.5	38.1	103.3	21.8	2.2	2.1	1.5	4.1	23.5
20	N_19	259.5	7.5	15.3	9.8	28.4	41.3	71.0	19.6	0.7	0.8	0.6	1.4	2.2
21	N_20	2,615.9	3.8	5.0	3.0	7.7	9.7	18.6	7.0	0.9	0.5	0.3	1.4	6.1
22	N_21	271.8	5.1	17.5	9.8	32.6	48.6	63.1	23.6	0.9	3.7	1.8	0.3	18.2
23	N_22	1,226.2	7.9	26.0	13.7	46.9	52.9	56.6	34.8	1.2	4.9	2.9	0.1	20.1
24	N_23	205.2	5.5	12.1	15.6	16.7	41.2	51.3	11.4	0.6	4.3	1.9	0.3	16.4
25	N_24	2,209.0	3.6	9.2	12.0	18.4	43.9	61.1	11.4	0.6	4.1	2.0	0.3	17.7
26	N_25	1,426.2	5.3	7.8	12.4	15.0	31.7	42.5	10.5	1.5	4.9	2.2	1.1	15.4
27	N_26	2,142.7	7.9	21.0	5.6	14.8	23.2	43.5	14.4	3.9	1.4	0.9	4.4	18.1
28	N_27	988.5	13.0	19.9	10.0	29.2	37.2	60.2	35.9	3.7	2.2	0.9	4.9	21.1
29	P_1	1,912.7	38.1	42.7	25.0	46.8	79.2	41.4	19.7	3.7	1.6	6.7	0.5	17.8
30	P_2	1,286.5	16.9	19.6	5.5	24.0	30.1	38.2	25.7	6.3	5.0	24.2	3.3	15.9
31	P_3	1,961.7	39.8	44.4	27.1	48.7	82.4	44.1	19.5	3.3	1.0	3.8	0.2	18.1
32	P_4	1,530.7	13.1	17.0	11.5	20.1	32.1	57.2	32.4	8.9	4.7	9.0	2.9	14.6
33	P_5	53.4	14.7	19.6	4.4	10.6	20.1	50.6	30.8	5.4	3.3	2.0	4.3	18.1
34	P_6	562.1	17.5	18.8	16.2	27.7	32.2	67.6	34.2	3.4	2.4	4.7	0.5	16.7
35	P_7	2,894.3	8.8	17.5	7.2	18.2	27.6	43.7	18.7	5.0	6.1	7.9	3.9	12.1
36	P_8	1,745.8	11.1	15.2	13.9	17.0	29.4	47.6	23.2	5.7	5.1	11.2	1.5	12.8
37	P_9	2,100.5	0.9	3.2	1.1	1.9	3.2	6.1	3.0	1.2	1.0	1.0	0.1	3.6
38	P_10	620.9	14.2	17.1	21.3	14.3	35.5	77.0	24.3	9.6	17.7	14.2	9.2	15.4
39	P_11	3,194.4	2.2	3.5	1.5	2.1	4.3	11.9	5.3	2.1	2.1	1.7	1.0	3.2
40	P_12	1,971.0	10.2	17.9	30.1	19.0	28.0	52.4	22.1	3.4	7.5	11.6	1.4	15.3
41	P_13	1,935.4	13.6	27.2	37.0	24.6	30.7	68.2	26.7	4.9	9.5	14.3	3.5	16.3
42	P_14	522.1	14.7	16.2	2.8	13.8	26.0	67.2	24.5	10.6	8.3	4.7	6.7	18.0
43	P_15	3,179.7	16.1	21.2	5.8	9.7	18.6	49.4	32.4	6.4	5.1	5.0	6.1	18.3
44	P_16	845.4	14.1	15.7	2.4	9.1	18.5	45.8	24.5	5.1	3.4	2.2	4.7	17.6
45	P_17	166.1	10.9	17.3	2.2	12.1	12.5	43.7	26.8	5.7	1.6	1.1	2.6	18.0

Table 17 (Continued)

No.	Subbsin	Subbasin	Daily antecedent precipitation index (<i>API</i>), mm/day											
			Code	Area (sq.km)	Apr	May	Jun	Jul	Aug	Sep	Oct	Nov	Dec	Jan
46	P_18	527.9	6.8	20.2	1.8	17.1	11.3	48.2	30.9	9.9	0.9	0.3	0.9	18.6
47	P_19	654.4	3.5	21.0	1.5	13.3	13.3	45.2	31.4	12.6	1.6	0.4	1.5	18.5
48	P_20	274.5	4.9	20.8	1.7	17.4	11.4	47.8	31.5	11.4	0.9	0.2	0.7	18.9
49	P_21	959.5	12.1	18.7	2.2	16.5	14.8	61.7	33.8	9.5	1.1	0.5	2.9	20.1
50	P_22	367.6	2.7	22.4	1.6	11.2	15.5	46.1	33.6	14.6	2.3	0.5	2.0	19.4
51	P_23	383.5	2.4	21.2	1.4	10.2	14.9	43.2	31.4	13.6	2.1	0.5	2.0	18.2
52	P_24	759.0	4.3	17.9	4.1	13.3	19.3	51.1	30.4	12.7	1.6	0.4	5.5	22.1
53	P_25	293.5	14.2	14.2	5.8	17.3	20.2	73.2	32.2	8.8	0.5	0.2	8.0	20.6
54	P_26	1,223.0	6.3	12.4	8.5	18.7	25.6	61.9	28.0	11.1	0.7	0.3	10.8	23.4
55	P_27	211.2	8.6	23.0	8.1	16.4	21.6	63.0	23.5	7.4	0.4	0.4	7.6	20.7
56	P_28	549.2	6.3	13.9	8.4	16.9	21.4	68.9	25.7	9.8	0.5	0.2	8.7	22.5
57	P_29	1,351.5	8.4	9.6	7.4	11.9	8.3	46.7	21.1	6.4	0.1	0.0	6.6	23.5
58	P_30	532.2	10.0	21.6	7.4	14.4	19.8	37.6	17.2	3.5	0.2	0.4	7.5	20.7
59	P_31	237.7	10.0	27.5	5.1	16.0	25.8	27.6	14.6	3.8	0.7	0.6	5.3	18.1
60	P_32	133.3	6.7	25.6	4.1	12.5	25.3	15.5	9.6	3.6	2.9	1.2	3.9	16.7
61	W_1	1,645.7	14.4	37.8	6.5	39.0	32.6	33.0	34.5	13.1	7.2	10.9	3.1	16.5
62	W_2	736.1	11.2	27.4	5.9	28.5	30.2	34.3	29.1	9.9	6.7	8.7	4.4	16.1
63	W_3	967.4	13.5	20.4	5.3	26.1	30.5	47.8	32.3	4.6	4.8	7.0	3.3	16.8
64	W_4	403.9	10.5	23.1	5.3	21.9	23.9	42.3	31.8	5.5	5.1	7.9	3.3	17.8
65	W_5	455.1	16.3	25.8	5.6	26.2	41.9	70.4	37.1	7.1	3.0	7.5	4.1	17.9
66	W_6	1,758.8	14.2	26.6	6.5	24.6	40.1	78.9	34.8	7.3	1.7	6.2	6.4	17.7
67	W_7	736.5	18.3	20.6	9.2	23.0	44.8	72.8	22.5	4.1	4.3	8.9	6.5	17.5
68	W_8	863.3	15.2	23.1	9.6	19.2	40.6	75.3	25.9	4.9	4.4	7.4	5.9	18.0
69	W_9	282.5	11.1	22.9	7.8	18.6	30.3	77.6	30.3	5.9	2.5	5.2	9.2	18.2
70	W_10	232.8	9.8	21.3	6.5	19.3	22.6	73.4	30.4	5.7	2.3	4.9	11.5	17.8
71	W_11	281.8	9.9	20.9	6.6	19.1	22.1	72.3	30.0	5.6	2.3	4.8	11.1	17.9
72	W_12	230.1	11.9	15.2	12.7	16.6	29.3	76.7	34.0	8.5	1.4	3.5	2.4	20.5
73	W_13	149.1	10.1	11.2	12.6	16.9	22.1	71.5	34.6	9.2	0.3	2.2	2.0	19.8
74	W_14	182.9	11.8	11.8	8.8	20.5	33.7	43.8	28.9	7.5	0.1	3.0	3.1	19.4
75	W_15	362.8	10.1	10.9	9.5	17.6	26.4	51.8	29.1	7.4	0.1	2.5	2.4	19.4
76	W_16	340.1	15.0	14.1	5.8	23.3	43.6	33.3	16.8	4.8	1.8	4.1	4.9	19.1
77	W_17	308.4	14.1	15.2	5.2	19.1	34.7	33.0	27.8	3.6	1.1	3.2	4.3	18.5
78	W_18	256.6	12.6	14.9	5.9	21.0	35.2	33.5	30.7	4.5	1.0	3.3	4.1	19.0
79	W_19	378.8	9.5	16.2	4.3	17.8	20.9	41.1	29.2	5.9	1.3	2.0	2.9	19.0
80	W_20	215.5	15.7	21.6	4.4	28.3	30.4	48.3	40.0	5.7	4.0	5.1	1.8	17.2
81	W_21	22.4	9.5	18.8	4.7	16.8	17.6	50.0	33.1	7.5	2.3	1.9	3.2	18.6
82	Y_1	2,119.7	14.4	37.1	9.0	37.2	35.2	53.6	37.7	11.2	5.0	8.6	4.9	18.7
83	Y_2	873.6	18.2	38.7	8.6	44.4	39.9	55.2	37.0	12.9	7.0	9.4	5.3	20.3
84	Y_3	658.8	15.9	40.3	8.0	43.5	39.2	55.6	34.9	11.5	6.4	9.1	5.3	19.9
85	Y_4	1,760.1	6.1	14.6	4.4	9.1	15.1	25.5	13.5	3.3	1.5	3.7	1.5	8.0
86	Y_5	214.7	8.8	35.5	7.3	28.9	38.1	55.6	31.1	5.8	1.2	4.5	4.5	19.2
87	Y_6	374.7	7.6	33.1	7.1	35.9	37.2	51.3	23.4	4.5	1.4	3.3	3.1	19.8
88	Y_7	332.1	5.0	35.1	9.0	28.9	34.3	57.0	21.6	5.0	1.0	2.9	2.6	18.1
89	Y_8	246.1	5.3	35.4	10.2	30.2	34.3	54.4	16.5	4.3	0.8	1.1	0.9	18.0
90	Y_9	1,032.1	6.4	26.2	7.1	30.8	35.1	56.9	21.4	4.3	1.5	3.0	4.0	19.4

Table 17 (Continued)

No.	Subbasin	Subbasin Code	Area (sq.km)	Daily antecedent precipitation index (<i>API</i>), mm/day											
				Apr	May	Jun	Jul	Aug	Sep	Oct	Nov	Dec	Jan	Feb	Mar
91	Y_10	149.7	7.9	22.8	6.0	13.4	29.8	60.2	21.7	3.4	1.0	1.4	5.7	16.7	
92	Y_11	532.4	8.6	18.8	12.4	15.1	36.8	69.5	20.7	3.6	2.9	6.3	8.9	17.4	
93	Y_12	246.0	8.4	20.9	12.9	12.6	38.9	74.3	22.5	3.0	1.6	3.2	7.4	17.2	
94	Y_13	711.0	8.4	25.9	6.9	16.4	33.4	70.2	28.3	4.6	1.2	2.2	5.4	17.8	
95	Y_14	439.7	8.0	22.2	20.4	11.7	47.7	88.7	21.6	1.2	0.2	0.4	6.5	20.0	
96	Y_15	531.1	4.1	27.2	7.5	16.5	41.9	90.0	36.0	5.4	0.6	1.5	10.1	22.4	
97	Y_16	214.4	6.9	26.9	7.2	16.0	36.5	82.0	33.2	5.0	0.9	2.0	7.7	20.4	
98	Y_17	880.1	4.1	27.7	14.8	25.1	47.2	89.9	35.6	6.1	0.2	0.6	7.6	25.0	
99	Y_18	832.8	3.9	10.9	9.5	26.5	40.7	87.3	34.3	6.1	0.6	1.3	9.0	23.9	
100	Y_19	796.8	6.8	21.7	12.4	29.4	40.5	73.2	31.7	7.1	2.2	0.2	1.7	22.9	
101	Y_20	768.4	8.5	11.4	8.6	24.9	29.3	72.7	26.6	4.3	2.1	0.3	1.8	21.3	
102	Y_21	2,312.7	10.9	14.3	5.8	19.9	21.5	65.7	16.9	2.5	0.1	0.6	1.7	19.2	
103	Y_22	491.3	7.3	11.4	7.8	25.0	24.5	60.2	25.5	2.0	0.0	0.0	5.5	23.6	
104	Y_23	1,055.9	10.1	11.1	1.9	21.3	13.0	52.0	8.5	0.7	0.1	0.1	0.8	16.4	
105	Y_24	1,572.1	15.4	13.7	3.5	22.1	18.2	71.0	25.1	3.3	0.1	0.2	4.7	22.9	
106	Y_25	905.8	6.1	10.1	7.8	19.9	25.0	54.7	19.0	1.7	0.6	0.2	3.7	15.9	
107	Y_26	545.4	6.9	11.8	6.1	24.8	26.5	68.7	26.8	1.5	0.0	0.2	5.1	21.0	
108	Y_27	1,323.4	4.4	13.9	7.0	24.5	37.9	68.4	23.1	1.2	0.0	0.1	2.1	19.3	
109	Y_28	656.3	3.8	17.6	5.6	26.8	45.3	58.2	14.7	0.3	0.3	0.2	0.0	18.0	
110	Y_29	191.7	9.9	22.9	14.5	30.8	46.1	56.7	21.9	0.8	2.7	1.5	0.4	18.0	
111	Y_30	655.3	11.5	21.2	15.2	22.8	42.4	59.5	16.0	0.9	1.7	1.0	0.7	17.5	
112	Y_31	170.0	5.1	9.6	5.6	18.5	24.5	56.7	19.4	4.2	0.1	0.0	2.1	22.0	
Average		989.8	10.5	20.9	8.6	23.4	31.6	54.6	23.9	5.4	2.6	3.4	4.0	18.3	
Maximum		5,583.4	39.8	44.4	37.0	64.1	82.4	103.3	40.0	14.6	17.7	24.2	12.1	25.0	
Minimum		22.4	0.9	3.2	1.1	1.9	3.2	6.1	3.0	0.3	0.0	0.0	0.0	2.2	

**Figure 45** Daily average of antecedent precipitation index (*API*).

The results of daily soil water recession coefficient adjusted by evapotranspiration (K_{adj}) calculation show that the daily average of adjusted K of the upper Chao Phraya river basin is 0.889 which varies from 0.810 in October to 0.978 in April as shown in Table 18 and Figure 46.

3.5 API adjusted by evapotranspiration (API_{adj})

The results of daily soil water recession coefficient adjusted by evapotranspiration (K_{adj}) and daily areal rainfall data in 1977 to 2003 were used to analyse API by equation (3). Moreover, the summary of daily average antecedent precipitation index adjusted by evapotranspiration (API_{adj}) is shown in Table 19 and Figure 47. The results show that the average of API_{adj} in the upper Chao Phraya river basin is 30.90 mm/day which varies from 10.00 mm/day in December to 62.47 mm/day in May.

Comparison between the results of daily antecedent precipitation index (API) and daily API adjusted by evapotranspiration (API_{adj}) in the upper Chao Phraya river basin is shown in Figure 48. This comparison found the daily average of adjusted API to be higher than the original API of the same time from 7.82 to 481.64 percentage. Furthermore, the value of API adjusted by evapotranspiration (API_{adj}) is higher in May and September while the value of original API is higher in September.

Table 18 Daily average of soil water recession coefficient adjust by $ET (K_{adj})$.

No.	Subsin	Subbasin	Soil water recession coefficient adjust by evapotranspiration (K_{adj})											
			Code	Area (sq.km)	Apr	May	Jun	Jul	Aug	Sep	Oct	Nov	Dec	Jan
1	C_1	1,545.8	0.999	0.998	0.998	0.937	0.886	0.847	0.794	0.845	0.891	0.856	0.865	0.925
2	C_2	3,401.7	0.999	0.999	0.999	0.919	0.853	0.830	0.795	0.859	0.901	0.869	0.878	0.932
3	N_1	2,228.4	0.987	0.985	0.970	0.952	0.949	0.811	0.789	0.832	0.822	0.800	0.863	0.948
4	N_2	790.1	0.998	0.997	0.887	0.780	0.784	0.979	0.976	0.981	0.980	0.978	0.985	0.994
5	N_3	1,536.8	0.951	0.946	0.930	0.903	0.891	0.781	0.765	0.785	0.786	0.775	0.825	0.924
6	N_4	600.6	0.948	0.943	0.931	0.907	0.894	0.777	0.761	0.780	0.781	0.772	0.820	0.922
7	N_5	591.4	0.962	0.958	0.958	0.949	0.939	0.768	0.748	0.781	0.777	0.760	0.821	0.926
8	N_6	781.3	0.965	0.961	0.957	0.945	0.936	0.771	0.750	0.785	0.779	0.762	0.824	0.928
9	N_7	3,195.7	0.956	0.953	0.918	0.880	0.880	0.818	0.803	0.824	0.823	0.812	0.857	0.940
10	N_8	2,206.2	0.986	0.984	0.948	0.907	0.905	0.844	0.826	0.859	0.852	0.836	0.886	0.956
11	N_9	1,046.7	0.986	0.984	0.920	0.852	0.859	0.869	0.852	0.881	0.879	0.865	0.901	0.961
12	N_11	2,429.7	0.963	0.966	0.863	0.784	0.817	0.947	0.938	0.954	0.950	0.939	0.959	0.986
13	N_12	1,095.1	0.947	0.949	0.867	0.807	0.838	0.914	0.903	0.918	0.916	0.904	0.926	0.971
14	N_13	339.7	0.963	0.966	0.873	0.803	0.835	0.947	0.938	0.954	0.950	0.939	0.958	0.986
15	N_14	1,727.6	0.969	0.971	0.876	0.801	0.830	0.956	0.948	0.962	0.958	0.949	0.966	0.989
16	N_15	688.2	0.900	0.904	0.866	0.862	0.912	0.836	0.818	0.842	0.839	0.818	0.858	0.942
17	N_16	5,583.4	0.998	0.997	0.895	0.804	0.817	0.954	0.947	0.960	0.959	0.951	0.964	0.986
18	N_17	219.9	0.979	0.977	0.975	0.973	0.975	0.814	0.789	0.832	0.833	0.803	0.851	0.940
19	N_18	158.5	0.976	0.973	0.974	0.970	0.965	0.800	0.775	0.816	0.819	0.789	0.836	0.932
20	N_19	259.5	0.996	0.996	0.996	0.995	0.995	0.804	0.774	0.830	0.826	0.790	0.848	0.942
21	N_20	2,615.9	0.995	0.994	0.880	0.778	0.791	0.962	0.956	0.965	0.965	0.959	0.969	0.987
22	N_21	271.8	0.995	0.994	0.994	0.994	0.993	0.780	0.745	0.812	0.815	0.779	0.837	0.936
23	N_22	1,226.2	0.957	0.952	0.896	0.836	0.837	0.847	0.833	0.846	0.856	0.843	0.864	0.937
24	N_23	205.2	0.999	0.999	0.999	0.998	0.998	0.779	0.743	0.814	0.816	0.778	0.839	0.938
25	N_24	2,209.0	0.992	0.990	0.960	0.933	0.941	0.803	0.772	0.830	0.835	0.803	0.853	0.942
26	N_25	1,426.2	0.985	0.981	0.849	0.744	0.777	0.930	0.921	0.934	0.940	0.932	0.943	0.975
27	N_26	2,142.7	0.994	0.992	0.963	0.937	0.945	0.815	0.785	0.841	0.845	0.815	0.863	0.946
28	N_27	988.5	0.999	0.999	0.859	0.749	0.784	0.958	0.951	0.965	0.966	0.958	0.970	0.989
29	P_1	1,912.7	0.928	0.917	0.864	0.797	0.799	0.799	0.765	0.712	0.778	0.796	0.807	0.927
30	P_2	1,286.5	0.905	0.890	0.884	0.858	0.847	0.793	0.788	0.703	0.708	0.732	0.746	0.903
31	P_3	1,961.7	0.944	0.935	0.857	0.772	0.780	0.810	0.761	0.726	0.826	0.841	0.850	0.944
32	P_4	1,530.7	0.936	0.926	0.923	0.905	0.897	0.859	0.855	0.758	0.751	0.780	0.792	0.935
33	P_5	53.4	0.991	0.989	0.920	0.850	0.863	0.914	0.869	0.823	0.903	0.923	0.928	0.991
34	P_6	562.1	0.961	0.954	0.939	0.914	0.912	0.899	0.888	0.763	0.757	0.796	0.809	0.960
35	P_7	2,894.3	0.948	0.939	0.936	0.922	0.915	0.883	0.880	0.766	0.751	0.785	0.798	0.947
36	P_8	1,745.8	0.981	0.977	0.970	0.957	0.956	0.950	0.944	0.805	0.782	0.825	0.837	0.980
37	P_9	2,100.5	0.971	0.966	0.901	0.831	0.840	0.876	0.834	0.797	0.878	0.894	0.900	0.971
38	P_10	620.9	0.898	0.882	0.882	0.860	0.847	0.784	0.782	0.726	0.735	0.749	0.762	0.896
39	P_11	3,194.4	0.914	0.901	0.882	0.844	0.837	0.800	0.787	0.750	0.784	0.794	0.804	0.913
40	P_12	1,971.0	1.000	1.000	1.000	1.000	1.000	1.000	1.000	0.809	0.781	0.835	0.844	1.000
41	P_13	1,935.4	0.993	0.992	0.948	0.902	0.910	0.943	0.913	0.820	0.851	0.884	0.893	0.993
42	P_14	522.1	0.971	0.966	0.880	0.793	0.806	0.857	0.803	0.795	0.915	0.921	0.926	0.971
43	P_15	3,179.7	0.999	0.999	0.986	0.973	0.975	0.986	0.975	0.825	0.820	0.865	0.872	0.999
44	P_16	845.4	1.000	1.000	1.000	1.000	1.000	1.000	1.000	0.831	0.805	0.854	0.862	1.000
45	P_17	166.1	1.000	1.000	0.955	0.912	0.921	0.958	0.923	0.823	0.868	0.902	0.908	1.000

Table 18 (Continued)

No.	Subbasin	Subbasin	Soil water recession coefficient adjust by evapotranspiration (K_{adj})											
			Code	Area (sq.km)	Apr	May	Jun	Jul	Aug	Sep	Oct	Nov	Dec	Jan
46	P_18	527.9	0.999	0.999	0.942	0.884	0.898	0.944	0.900	0.820	0.884	0.913	0.919	0.999
47	P_19	654.4	0.985	0.983	0.982	0.978	0.976	0.965	0.962	0.807	0.791	0.834	0.845	0.985
48	P_20	274.5	1.000	1.000	0.958	0.915	0.925	0.960	0.927	0.824	0.863	0.897	0.904	1.000
49	P_21	959.5	0.996	0.995	0.968	0.938	0.945	0.965	0.943	0.819	0.838	0.876	0.884	0.996
50	P_22	367.6	0.990	0.988	0.988	0.985	0.984	0.976	0.974	0.818	0.800	0.843	0.853	0.990
51	P_23	383.5	0.994	0.993	0.871	0.756	0.782	0.872	0.783	0.785	0.961	0.968	0.970	0.994
52	P_24	759.0	0.995	0.993	0.872	0.756	0.782	0.872	0.784	0.786	0.962	0.969	0.971	0.995
53	P_25	293.5	0.998	0.997	0.862	0.735	0.764	0.867	0.769	0.788	0.990	0.992	0.992	0.998
54	P_26	1,223.0	0.993	0.992	0.890	0.791	0.813	0.888	0.813	0.789	0.929	0.944	0.947	0.993
55	P_27	211.2	0.986	0.983	0.920	0.854	0.867	0.908	0.859	0.791	0.870	0.895	0.901	0.985
56	P_28	549.2	0.989	0.986	0.870	0.758	0.783	0.865	0.780	0.781	0.951	0.957	0.959	0.988
57	P_29	1,351.5	0.998	0.997	0.880	0.769	0.795	0.884	0.798	0.792	0.957	0.967	0.969	0.998
58	P_30	532.2	0.984	0.980	0.861	0.764	0.794	0.862	0.783	0.780	0.932	0.940	0.941	0.984
59	P_31	237.7	1.000	0.999	0.893	0.807	0.835	0.906	0.835	0.790	0.908	0.930	0.932	1.000
60	P_32	133.3	1.000	1.000	0.913	0.841	0.864	0.924	0.865	0.788	0.874	0.904	0.906	1.000
61	W_1	1,645.7	0.993	0.992	0.992	0.991	0.890	0.738	0.733	0.826	0.776	0.755	0.846	0.925
62	W_2	736.1	0.996	0.996	0.996	0.995	0.894	0.740	0.736	0.830	0.778	0.758	0.850	0.927
63	W_3	967.4	0.981	0.980	0.979	0.975	0.896	0.756	0.747	0.828	0.792	0.767	0.848	0.946
64	W_4	403.9	0.998	0.998	0.998	0.998	0.907	0.764	0.759	0.849	0.801	0.779	0.866	0.941
65	W_5	455.1	0.984	0.982	0.982	0.978	0.901	0.761	0.750	0.834	0.798	0.769	0.852	0.955
66	W_6	1,758.8	0.999	0.999	0.999	0.998	0.899	0.769	0.775	0.847	0.797	0.796	0.871	0.901
67	W_7	736.5	1.000	1.000	1.000	1.000	0.900	0.767	0.771	0.847	0.796	0.793	0.870	0.905
68	W_8	863.3	0.993	0.993	0.993	0.991	0.894	0.768	0.774	0.840	0.794	0.796	0.866	0.896
69	W_9	282.5	1.000	1.000	1.000	1.000	0.922	0.789	0.780	0.870	0.826	0.798	0.882	0.964
70	W_10	232.8	1.000	1.000	1.000	1.000	0.904	0.791	0.802	0.861	0.813	0.823	0.886	0.891
71	W_11	281.8	1.000	1.000	1.000	1.000	0.903	0.790	0.801	0.859	0.811	0.822	0.885	0.890
72	W_12	230.1	0.969	0.966	0.966	0.959	0.887	0.777	0.777	0.822	0.797	0.796	0.851	0.909
73	W_13	149.1	0.951	0.947	0.946	0.934	0.867	0.765	0.768	0.793	0.778	0.788	0.831	0.885
74	W_14	182.9	0.998	0.998	0.998	0.998	0.903	0.795	0.794	0.853	0.819	0.820	0.879	0.894
75	W_15	362.8	0.993	0.992	0.992	0.991	0.899	0.790	0.787	0.845	0.814	0.814	0.872	0.895
76	W_16	340.1	1.000	1.000	1.000	1.000	0.903	0.798	0.800	0.855	0.820	0.827	0.883	0.885
77	W_17	308.4	0.997	0.996	0.996	0.996	0.921	0.801	0.783	0.865	0.836	0.807	0.880	0.963
78	W_18	256.6	0.991	0.989	0.989	0.988	0.907	0.794	0.784	0.849	0.823	0.809	0.872	0.927
79	W_19	378.8	0.999	0.999	0.999	0.999	0.906	0.797	0.793	0.856	0.822	0.819	0.880	0.905
80	W_20	215.5	0.999	0.999	0.999	0.999	0.910	0.769	0.764	0.854	0.806	0.783	0.870	0.945
81	W_21	22.4	1.000	1.000	1.000	1.000	0.908	0.789	0.794	0.862	0.814	0.814	0.883	0.909
82	Y_1	2,119.7	0.998	0.997	0.997	0.997	0.996	0.819	0.757	0.810	0.842	0.776	0.832	0.977
83	Y_2	873.6	1.000	1.000	1.000	1.000	1.000	0.829	0.761	0.814	0.853	0.781	0.834	0.984
84	Y_3	658.8	0.998	0.998	0.998	0.997	0.997	0.813	0.759	0.813	0.833	0.777	0.839	0.969
85	Y_4	1,760.1	0.997	0.996	0.996	0.995	0.995	0.811	0.745	0.804	0.839	0.772	0.822	0.973
86	Y_5	214.7	0.965	0.961	0.960	0.952	0.945	0.792	0.727	0.767	0.817	0.755	0.789	0.957
87	Y_6	374.7	0.971	0.967	0.966	0.959	0.953	0.799	0.728	0.771	0.825	0.757	0.791	0.965
88	Y_7	332.1	0.991	0.990	0.990	0.988	0.986	0.796	0.746	0.803	0.820	0.770	0.826	0.957
89	Y_8	246.1	0.980	0.978	0.978	0.973	0.969	0.794	0.740	0.789	0.817	0.765	0.813	0.955
90	Y_9	1,032.1	0.987	0.985	0.985	0.981	0.979	0.792	0.755	0.808	0.812	0.776	0.834	0.946

Table 18 (Continued)

No.	Subbasin	Subbasin	Soil water recession coefficient adjust by evapotranspiration (K_{adj})												
			Code	Area (sq.km)	Apr	May	Jun	Jul	Aug	Sep	Oct	Nov	Dec	Jan	Feb
91	Y_10	149.7	0.972	0.969	0.968	0.961	0.956	0.805	0.730	0.773	0.833	0.759	0.791	0.970	
92	Y_11	532.4	0.882	0.869	0.866	0.838	0.818	0.712	0.693	0.687	0.717	0.713	0.731	0.875	
93	Y_12	246.0	0.977	0.974	0.973	0.967	0.963	0.780	0.752	0.799	0.797	0.772	0.829	0.934	
94	Y_13	711.0	0.982	0.980	0.980	0.975	0.972	0.791	0.753	0.803	0.810	0.775	0.830	0.944	
95	Y_14	439.7	0.914	0.907	0.908	0.891	0.873	0.752	0.734	0.741	0.749	0.732	0.764	0.891	
96	Y_15	531.1	0.951	0.947	0.948	0.938	0.927	0.786	0.761	0.787	0.789	0.762	0.806	0.919	
97	Y_16	214.4	0.936	0.931	0.931	0.919	0.905	0.769	0.749	0.767	0.768	0.748	0.789	0.904	
98	Y_17	880.1	0.907	0.900	0.900	0.883	0.863	0.760	0.746	0.746	0.754	0.744	0.769	0.889	
99	Y_18	832.8	0.926	0.920	0.921	0.906	0.891	0.781	0.763	0.771	0.778	0.762	0.791	0.905	
100	Y_19	796.8	0.992	0.992	0.992	0.990	0.989	0.854	0.796	0.838	0.871	0.804	0.841	0.980	
101	Y_20	768.4	0.987	0.985	0.985	0.983	0.981	0.849	0.789	0.829	0.874	0.810	0.835	0.976	
102	Y_21	2,312.7	0.991	0.990	0.991	0.989	0.988	0.828	0.795	0.840	0.848	0.810	0.855	0.952	
103	Y_22	491.3	0.998	0.998	0.998	0.998	0.997	0.869	0.793	0.838	0.898	0.816	0.838	0.998	
104	Y_23	1,055.9	0.994	0.994	0.994	0.993	0.992	0.837	0.790	0.837	0.860	0.808	0.848	0.965	
105	Y_24	1,572.1	0.999	0.999	0.999	0.999	0.999	0.827	0.796	0.846	0.847	0.811	0.862	0.952	
106	Y_25	905.8	0.962	0.942	0.945	0.938	0.994	0.830	0.791	0.840	0.852	0.808	0.854	0.958	
107	Y_26	545.4	0.995	0.994	0.995	0.994	0.993	0.852	0.772	0.819	0.883	0.797	0.820	0.994	
108	Y_27	1,323.4	0.974	0.971	0.972	0.967	0.963	0.825	0.761	0.799	0.851	0.783	0.807	0.967	
109	Y_28	656.3	0.994	0.993	0.993	0.992	0.991	0.806	0.770	0.823	0.828	0.787	0.840	0.945	
110	Y_29	191.7	0.980	0.977	0.978	0.974	0.971	0.813	0.754	0.798	0.839	0.776	0.809	0.960	
111	Y_30	655.3	0.946	0.939	0.941	0.932	0.922	0.797	0.776	0.796	0.810	0.790	0.818	0.918	
112	Y_31	170.0	0.917	0.907	0.910	0.896	0.882	0.747	0.727	0.740	0.760	0.741	0.768	0.888	
Average			887.4	0.978	0.974	0.975	0.971	0.973	0.823	0.776	0.817	0.846	0.795	0.830	0.956
Maximum			2,312.7	0.999	0.999	0.999	0.999	0.999	0.869	0.796	0.846	0.898	0.816	0.862	0.998
Minimum			170.0	0.917	0.907	0.910	0.896	0.882	0.747	0.727	0.740	0.760	0.741	0.768	0.888

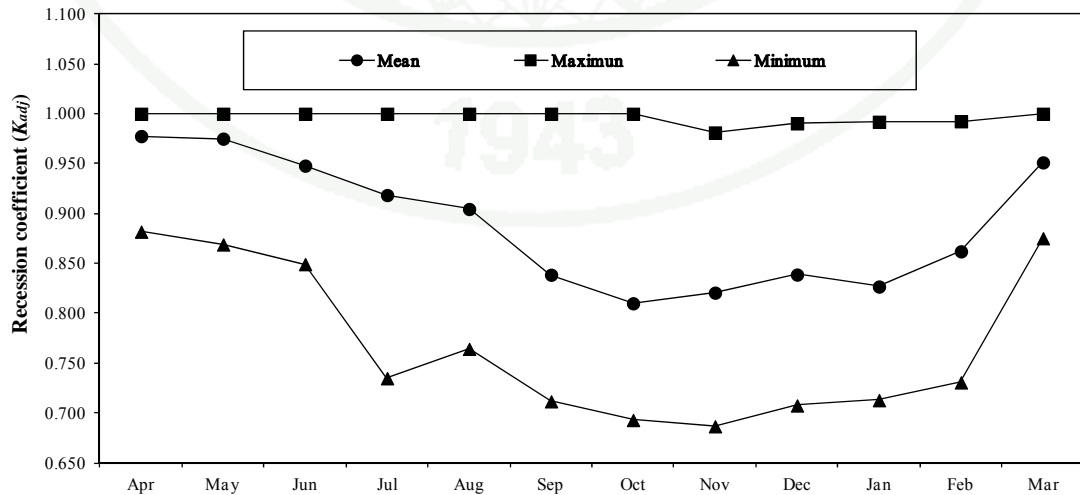
**Figure 46** Daily average of soil water recession coefficient adjust by ET (K_{adj}).

Table 19 Daily *API* adjust by evapotranspiration (API_{adj}).

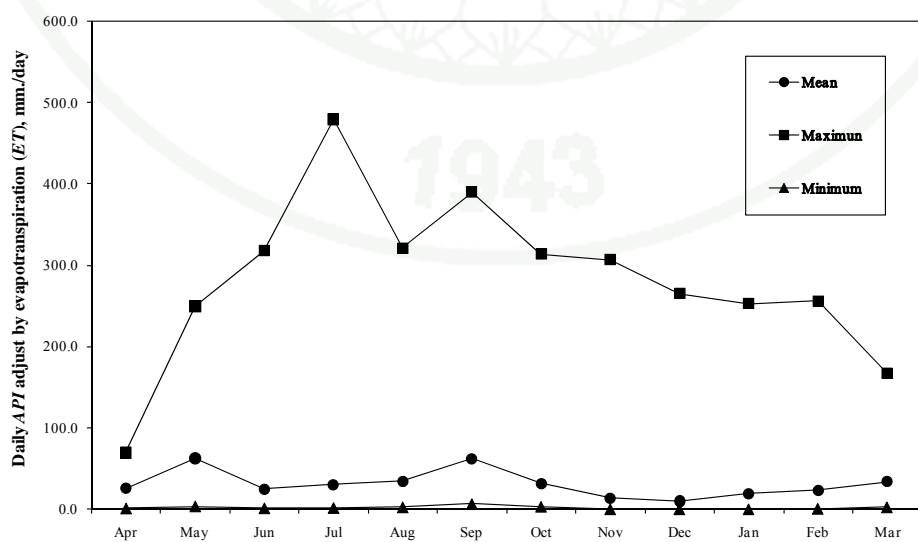
No.	Subbsin	Subbasin	Daily <i>API</i> adjust by evapotranspiration (API_{adj}), mm/day											
			Code	Area (sq.km)	Apr	May	Jun	Jul	Aug	Sep	Oct	Nov	Dec	Jan
1	C_1	1,545.8	22.5	46.0	11.2	12.2	27.0	33.7	15.2	3.3	1.7	5.7	24.2	27.8
2	C_2	3,401.7	17.7	28.9	15.3	19.0	45.8	87.5	20.8	0.7	1.5	4.6	5.1	24.8
3	N_1	2,228.4	57.2	86.5	22.6	51.0	42.8	53.6	10.2	10.6	7.7	21.6	26.0	34.1
4	N_2	790.1	19.7	29.6	32.7	192.7	321.2	390.0	295.4	211.1	175.7	186.9	183.3	167.0
5	N_3	1,536.8	32.2	53.4	9.7	33.0	32.4	37.9	15.1	5.3	8.2	15.1	11.8	20.7
6	N_4	600.6	34.9	47.1	7.1	29.7	25.9	33.3	11.7	3.8	5.6	11.4	17.2	20.5
7	N_5	591.4	42.4	102.8	16.8	35.8	34.1	41.9	14.7	5.9	9.3	22.7	13.4	25.4
8	N_6	781.3	31.0	76.8	14.3	28.6	26.8	33.1	15.9	3.3	5.6	15.3	12.8	23.9
9	N_7	3,195.7	11.8	31.2	7.4	20.0	21.7	26.1	7.4	1.4	2.5	9.7	5.8	15.0
10	N_8	2,206.2	33.5	22.6	5.0	31.5	25.8	37.1	12.2	6.0	5.0	8.7	40.8	26.5
11	N_9	1,046.7	16.7	36.4	13.0	33.6	41.1	51.1	12.6	2.8	3.4	21.9	17.8	23.9
12	N_11	2,429.7	8.9	19.0	12.0	56.1	91.7	107.8	45.2	20.7	8.0	6.4	4.6	51.0
13	N_12	1,095.1	5.5	33.3	26.0	38.3	66.8	115.0	41.9	8.3	2.7	4.8	10.2	38.5
14	N_13	339.7	6.6	36.9	34.2	55.1	108.4	171.5	83.1	23.3	9.6	9.4	13.0	59.8
15	N_14	1,727.6	2.6	8.1	9.2	17.1	36.0	58.9	28.6	10.2	4.5	3.0	2.4	20.4
16	N_15	688.2	12.9	49.4	15.7	28.6	42.6	58.1	17.8	3.2	0.1	0.8	1.4	23.9
17	N_16	5,583.4	7.1	22.9	22.3	57.5	111.0	148.8	75.7	28.8	11.6	12.5	14.8	70.2
18	N_17	219.9	17.2	70.9	25.4	23.5	39.2	71.6	10.9	0.7	0.0	0.0	5.6	30.4
19	N_18	158.5	48.6	74.3	28.2	24.0	31.2	84.7	13.3	0.8	2.7	8.0	8.8	28.5
20	N_19	259.5	24.6	87.7	27.9	20.8	38.5	65.7	12.9	0.2	1.2	5.2	6.6	15.8
21	N_20	2,615.9	3.6	4.7	8.2	21.2	31.1	68.1	42.7	17.7	8.9	9.4	10.4	24.6
22	N_21	271.8	26.3	101.1	26.8	24.1	45.3	57.9	16.3	0.3	5.7	23.7	20.2	34.5
23	N_22	1,226.2	10.1	30.6	17.4	46.4	54.0	62.2	34.1	1.1	6.3	12.7	3.1	22.4
24	N_23	205.2	24.4	86.3	30.9	12.4	38.2	48.2	7.7	0.2	6.7	29.8	29.2	33.4
25	N_24	2,209.0	9.7	24.9	16.8	15.4	44.8	64.7	9.2	0.4	6.3	24.6	18.5	25.1
26	N_25	1,426.2	5.2	7.7	29.8	32.5	68.0	112.3	43.8	9.6	9.5	25.6	17.1	37.4
27	N_26	2,142.7	18.3	64.0	14.3	12.5	23.8	45.9	12.0	3.0	2.2	9.1	17.1	25.3
28	N_27	988.5	12.7	19.4	29.8	79.3	124.7	251.6	177.4	72.5	35.0	41.7	50.7	90.8
29	P_1	1,912.7	47.0	51.1	28.0	38.9	53.7	29.1	16.9	2.9	1.8	13.3	2.7	16.6
30	P_2	1,286.5	27.7	31.2	6.8	21.3	19.1	24.7	15.5	2.5	5.3	36.7	6.4	14.1
31	P_3	1,961.7	44.1	46.9	31.1	39.7	57.4	39.1	21.6	4.2	1.2	9.0	2.4	18.1
32	P_4	1,530.7	25.7	34.2	17.0	22.0	23.1	36.2	21.1	4.6	5.3	17.7	7.0	14.9
33	P_5	53.4	17.8	24.9	12.2	11.3	15.8	64.3	49.5	17.4	13.2	15.5	21.8	29.7
34	P_6	562.1	39.7	47.8	36.6	41.1	27.5	49.5	24.3	2.5	3.1	14.1	5.5	22.3
35	P_7	2,894.3	18.6	40.5	16.6	23.1	21.9	27.5	12.6	3.0	7.6	20.3	11.0	14.4
36	P_8	1,745.8	29.8	56.4	59.5	46.6	29.9	33.8	17.5	4.9	6.6	39.5	27.5	24.6
37	P_9	2,100.5	1.0	3.5	1.6	1.7	2.4	6.4	3.9	1.8	1.5	3.5	1.6	4.3
38	P_10	620.9	20.2	22.8	17.7	10.4	21.9	43.8	12.1	3.8	17.6	17.7	11.7	11.5
39	P_11	3,194.4	2.7	4.0	1.3	1.6	2.6	7.8	3.1	1.2	2.1	2.3	1.5	2.5
40	P_12	1,971.0	46.5	143.2	317.8	479.5	100.7	36.9	17.5	3.3	12.5	77.1	87.4	84.5
41	P_13	1,935.4	23.4	50.6	92.7	60.5	30.0	64.0	29.7	8.3	15.3	67.5	68.8	26.7
42	P_14	522.1	14.4	14.8	3.6	10.9	17.7	92.8	50.8	22.2	16.3	22.3	23.3	24.2
43	P_15	3,179.7	41.8	105.8	108.0	78.8	26.9	38.3	29.3	7.3	10.8	37.0	61.0	58.1
44	P_16	845.4	50.9	145.1	196.4	219.1	57.3	32.8	20.2	5.0	8.6	19.7	34.0	100.8
45	P_17	166.1	18.7	35.7	20.9	19.8	12.9	44.2	32.5	11.0	7.3	10.9	18.7	35.6

Table 19 (Continued)

No.	Subbasin	Subbasin	Daily API adjust by evapotranspiration (API_{adj}), mm/day											
			Code	Area (sq.km)	Apr	May	Jun	Jul	Aug	Sep	Oct	Nov	Dec	Jan
46	P_18	527.9	9.9	33.8	11.9	23.2	11.1	53.4	41.7	20.6	6.1	7.1	9.5	35.4
47	P_19	654.4	8.7	79.2	49.4	38.6	18.4	31.6	24.0	10.6	3.1	3.4	5.6	44.0
48	P_20	274.5	8.4	44.1	20.4	30.1	13.4	46.5	35.9	18.2	4.4	5.3	7.3	38.4
49	P_21	959.5	24.3	56.0	33.1	34.8	18.0	53.0	32.4	11.8	3.5	4.9	9.9	41.6
50	P_22	367.6	7.0	85.5	68.8	49.5	22.8	32.3	26.3	12.8	4.7	5.5	9.1	54.7
51	P_23	383.5	2.2	18.7	2.1	8.6	11.4	92.5	121.1	99.0	60.5	52.3	48.1	62.9
52	P_24	759.0	4.0	16.4	6.3	11.0	15.2	110.8	128.8	102.7	61.8	54.0	59.0	76.5
53	P_25	293.5	12.1	12.6	8.5	13.1	16.1	206.4	313.7	306.6	265.1	252.6	256.0	149.3
54	P_26	1,223.0	7.0	14.1	15.5	17.1	20.8	101.0	72.9	46.4	16.9	15.2	39.4	48.9
55	P_27	211.2	11.9	32.1	19.4	19.4	17.5	66.9	30.1	13.1	1.8	2.7	14.7	29.2
56	P_28	549.2	6.0	13.7	12.0	13.5	16.7	136.6	102.4	62.7	26.4	19.0	32.2	52.4
57	P_29	1,351.5	8.3	9.5	11.3	10.2	6.7	90.2	97.0	68.8	37.6	34.7	41.7	79.3
58	P_30	532.2	9.9	20.3	10.7	11.9	15.0	60.4	48.1	20.7	4.4	4.4	13.3	38.3
59	P_31	237.7	12.0	32.6	13.2	17.5	21.2	38.8	30.2	18.0	4.5	9.4	17.5	35.2
60	P_32	133.3	9.9	37.6	13.9	16.7	21.8	17.9	13.9	9.7	5.4	20.8	43.6	28.9
61	W_1	1,645.7	55.7	128.9	6.9	29.2	31.7	29.6	25.4	9.5	9.1	42.6	44.6	26.5
62	W_2	736.1	41.8	102.2	6.2	21.9	29.5	31.1	21.1	7.0	8.5	36.8	44.6	26.5
63	W_3	967.4	42.5	93.9	6.0	20.1	30.5	44.5	21.9	2.7	6.1	29.2	36.0	27.6
64	W_4	403.9	28.9	67.0	5.5	16.5	20.9	36.1	20.3	2.9	6.6	26.5	22.0	23.0
65	W_5	455.1	50.9	88.6	6.5	18.9	39.8	61.8	23.9	3.6	3.6	24.2	23.9	22.9
66	W_6	1,758.8	54.3	106.5	6.6	18.7	39.9	65.4	24.0	5.7	1.8	20.0	34.7	26.1
67	W_7	736.5	54.6	110.3	8.6	18.0	45.2	62.0	16.0	2.8	4.5	30.5	45.4	27.9
68	W_8	863.3	45.1	87.2	8.5	14.9	39.0	60.1	17.7	3.4	4.3	22.3	33.0	25.3
69	W_9	282.5	43.9	88.8	9.5	13.6	32.2	74.8	19.9	3.4	2.9	20.8	43.7	32.2
70	W_10	232.8	46.1	73.2	6.0	15.0	21.6	58.3	21.0	4.6	2.2	14.7	42.2	28.7
71	W_11	281.8	46.8	72.9	6.1	14.9	21.1	57.3	20.7	4.6	2.2	14.6	41.3	28.5
72	W_12	230.1	30.2	34.1	9.9	11.9	23.5	55.3	20.9	4.8	1.3	7.1	7.5	21.0
73	W_13	149.1	22.8	18.3	9.0	11.7	15.3	46.3	20.4	4.8	0.0	3.6	4.0	17.2
74	W_14	182.9	49.5	74.0	7.6	16.3	32.7	35.0	20.7	6.7	0.1	10.3	17.4	28.8
75	W_15	362.8	43.6	53.9	7.9	13.7	24.6	40.7	20.2	6.1	0.1	7.9	12.5	26.6
76	W_16	340.1	53.8	97.7	5.5	19.0	42.9	26.0	11.9	4.5	1.7	14.1	26.7	28.9
77	W_17	308.4	47.8	90.1	6.1	14.9	35.3	31.8	19.0	1.9	2.6	11.7	20.8	28.5
78	W_18	256.6	40.2	70.1	5.6	16.5	32.9	27.9	21.4	2.6	1.4	10.5	16.7	25.2
79	W_19	378.8	32.8	70.1	4.1	14.6	20.1	33.7	20.8	4.6	1.5	7.3	14.9	27.7
80	W_20	215.5	50.1	105.5	5.7	21.5	30.4	45.2	27.3	3.2	5.1	22.7	26.0	28.7
81	W_21	22.4	28.4	65.8	4.7	14.1	16.6	41.3	23.4	5.9	2.6	6.1	14.1	27.9
82	Y_1	2,119.7	53.0	206.1	65.5	27.0	28.3	58.4	28.5	5.4	6.9	44.2	52.6	45.8
83	Y_2	873.6	69.2	249.5	81.7	32.5	31.2	63.8	28.6	6.6	11.3	53.4	65.6	55.3
84	Y_3	658.8	58.3	229.6	66.6	32.2	31.4	57.7	26.0	6.3	9.2	48.2	57.1	49.6
85	Y_4	1,760.1	24.9	89.6	26.3	6.7	12.8	27.5	10.0	1.6	1.9	18.8	20.4	17.8
86	Y_5	214.7	24.3	96.5	22.0	20.1	27.1	50.8	21.0	2.0	1.4	12.3	12.4	24.8
87	Y_6	374.7	23.2	97.7	23.9	24.8	26.8	49.9	16.2	1.6	1.8	10.7	9.8	26.9
88	Y_7	332.1	19.8	139.1	41.1	21.1	29.2	56.1	15.6	2.3	1.2	12.9	15.2	35.0
89	Y_8	246.1	22.8	109.7	32.7	21.3	28.6	51.0	11.4	1.9	1.1	4.1	4.9	27.6
90	Y_9	1,032.1	22.3	108.4	25.5	22.8	28.1	51.3	15.0	1.8	1.8	13.3	15.9	33.1

Table 19 (Continued)

No.	Subbasin	Subbasin	Daily API adjust by evapotranspiration (API_{adj}), mm/day											
			Code	Area (sq.km)	Apr	May	Jun	Jul	Aug	Sep	Oct	Nov	Dec	Jan
91	Y_10	149.7	26.3	73.5	18.4	10.1	21.8	62.2	15.6	1.1	1.2	5.4	13.5	25.1
92	Y_11	532.4	10.9	20.6	8.2	10.0	19.8	37.4	10.6	0.8	2.8	6.2	9.6	11.6
93	Y_12	246.0	27.2	72.8	21.7	9.9	31.8	60.7	14.7	1.2	1.9	10.2	23.9	24.8
94	Y_13	711.0	32.6	93.5	23.2	12.6	26.8	61.9	18.9	2.4	1.3	8.8	19.1	27.9
95	Y_14	439.7	13.0	31.1	15.8	8.5	30.9	52.3	11.1	0.3	0.2	0.6	9.0	15.8
96	Y_15	531.1	10.0	51.8	12.1	12.2	30.3	64.6	20.7	2.4	0.5	3.2	18.3	22.2
97	Y_16	214.4	14.5	44.8	9.2	11.7	24.0	55.1	18.2	2.3	0.9	3.7	12.8	18.3
98	Y_17	880.1	5.8	33.6	11.0	17.2	27.2	50.8	17.7	1.9	0.1	0.7	9.1	17.6
99	Y_18	832.8	6.5	15.6	7.8	18.0	25.0	53.6	17.7	2.1	0.5	1.8	12.0	18.4
100	Y_19	796.8	22.0	83.1	40.0	22.8	31.3	79.6	23.4	3.5	4.8	3.6	6.0	37.2
101	Y_20	768.4	28.2	51.6	22.3	18.9	21.3	76.5	18.8	2.0	4.7	3.4	5.8	31.9
102	Y_21	2,312.7	39.6	77.8	22.4	15.2	17.5	60.4	10.6	1.3	0.1	1.9	4.8	31.6
103	Y_22	491.3	33.0	76.0	33.2	19.2	18.0	75.8	21.1	0.7	0.0	0.0	7.0	46.2
104	Y_23	1,055.9	31.9	74.0	19.6	16.0	9.7	52.2	5.5	0.3	0.1	0.3	1.5	28.2
105	Y_24	1,572.1	42.8	129.0	31.0	17.1	15.1	66.5	16.3	1.9	0.1	0.7	7.4	43.9
106	Y_25	905.8	13.5	42.6	18.2	15.2	21.6	53.2	12.7	0.8	0.9	1.1	4.6	21.4
107	Y_26	545.4	23.5	67.9	28.0	18.1	20.8	82.9	21.2	0.5	0.0	0.6	7.5	40.4
108	Y_27	1,323.4	10.2	42.3	15.9	16.8	29.7	67.7	15.3	0.5	0.0	0.3	2.8	25.1
109	Y_28	656.3	7.5	73.5	22.4	19.7	41.4	54.5	9.8	0.0	0.5	1.8	1.4	31.1
110	Y_29	191.7	16.7	37.6	12.5	19.7	29.7	34.9	12.3	0.1	3.0	3.2	0.6	14.4
111	Y_30	655.3	32.0	92.9	31.3	16.1	34.3	58.9	11.0	0.3	2.3	6.9	4.4	25.1
112	Y_31	170.0	9.9	18.2	6.3	13.4	15.9	39.6	10.2	1.8	0.0	0.1	2.4	19.2
Average		989.8	25.5	62.5	24.6	30.3	34.1	62.1	31.6	13.7	10.0	19.0	23.2	34.0
Maximum		5,583.4	69.2	249.5	317.8	479.5	321.2	390.0	313.7	306.6	265.1	252.6	256.0	167.0
Minimum		22.4	1.0	3.5	1.3	1.6	2.4	6.4	3.1	0.0	0.0	0.0	0.6	2.5

**Figure 47** Daily average of API adjust by evapotranspiration (ET).

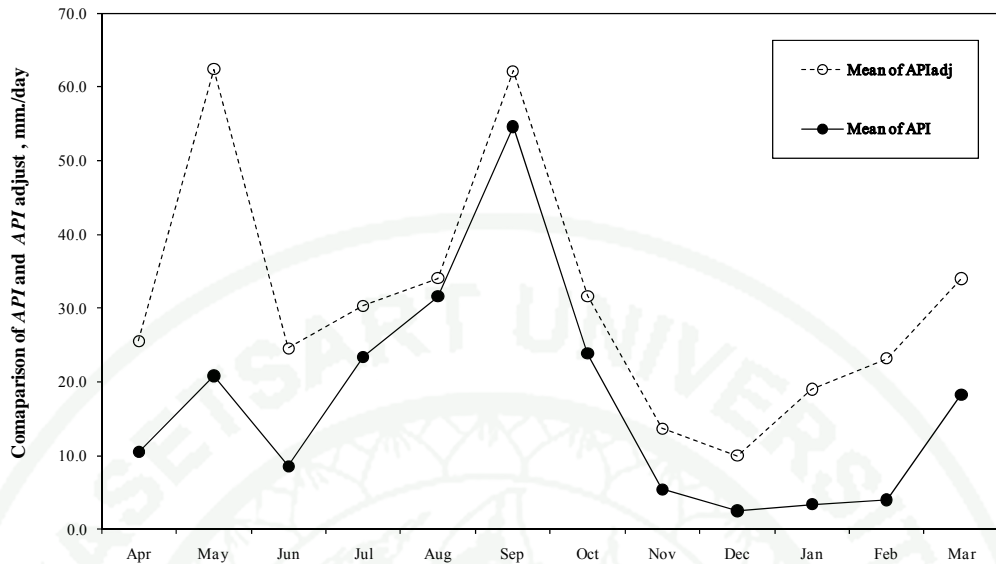


Figure 48 Comparison of *API* and *API* adjust by evapotranspiration (API_{adj}).

3.6 Critical antecedent precipitation index ($API_{critical}$)

The critical antecedent precipitation index ($API_{critical}$) is a maximum soil water capacity value. The critical antecedent precipitation index ($API_{critical}$) will consider the depth of soil from 0-15, 15-30, 30-50, 50-70 and 70-100 cm depending on the depth of soil at testing site data. The antecedent precipitation index (API) at each range of soil depth was calculated by equation (46), then critical API was evaluated by cumulating API of all ranges of soil depth as shown in Table 20; and show areal distribution analysis of critical API is shown in Figure 49.

The results show that the critical antecedent precipitation index ($API_{critical}$) of Ping river basin varies from 212.11 – 235.24 mm with the average of 222.85 mm, Wang river basin varies from 223.22 – 263.10 mm with the average of 239.42 mm, Yom river basin varies from 214.64 – 293.23 mm with the average of 252.76 mm, Nan river basin varies from 199.41 – 262.54 mm with the average of 238.07 mm and overall of the upper Chao Phraya river basin varies from 199.41 – 293.23 mm with the average of 237.90 mm.

Table 20 Summary of critical antecedent precipitation index ($API_{critical}$).

No.	Code	Small watershed area (sq.km)	$API_{critical}$ (mm)	No.	Code	Small watershed area (sq.km)	$API_{critical}$ (mm)
1.	C_1	1,545.8	229.91	36.	P_8	1,745.8	224.33
2.	C_2	3,401.7	230.55	37.	P_9	2,100.5	226.76
3.	N_1	2,228.4	200.69	38.	P_10	620.9	226.28
4.	N_2	790.1	199.41	39.	P_11	3,194.4	218.03
5.	N_3	1,536.8	226.96	40.	P_12	1,971.0	222.40
6.	N_4	600.6	218.26	41.	P_13	1,935.4	219.97
7.	N_5	591.4	230.85	42.	P_14	522.1	220.19
8.	N_6	781.3	252.52	43.	P_15	3,179.7	217.57
9.	N_7	3,195.7	255.87	44.	P_16	845.4	220.36
10.	N_8	2,206.2	223.92	45.	P_17	166.1	220.46
11.	N_9	1,046.7	257.26	46.	P_18	527.9	221.46
12.	N_11	2,429.7	251.38	47.	P_19	654.4	222.15
13.	N_12	1,095.1	262.54	48.	P_20	274.5	219.86
14.	N_13	339.7	258.16	49.	P_21	959.5	218.98
15.	N_14	1,727.6	256.64	50.	P_22	367.6	220.70
16.	N_15	688.2	258.49	51.	P_23	383.5	225.61
17.	N_16	5,583.4	255.17	52.	P_24	759.0	217.91
18.	N_17	219.9	241.64	53.	P_25	293.5	212.11
19.	N_18	158.5	233.93	54.	P_26	1,223.0	213.11
20.	N_19	259.5	235.85	55.	P_27	211.2	220.64
21.	N_20	2,615.9	239.10	56.	P_28	549.2	217.78
22.	N_21	271.8	236.55	57.	P_29	1,351.5	214.85
23.	N_22	1,226.2	233.78	58.	P_30	532.2	223.99
24.	N_23	205.2	230.59	59.	P_31	237.7	231.68
25.	N_24	2,209.0	234.02	60.	P_32	133.3	231.80
26.	N_25	1,426.2	232.56	61.	W_1	1,645.7	237.74
27.	N_26	2,142.7	228.36	62.	W_2	736.1	235.23
28.	N_27	988.5	235.22	63.	W_3	967.4	252.62
29.	P_1	1,912.7	233.41	64.	W_4	403.9	258.01
30.	P_2	1,286.5	232.32	65.	W_5	455.1	261.71
31.	P_3	1,961.7	230.52	66.	W_6	1,758.8	259.00
32.	P_4	1,530.7	225.13	67.	W_7	736.5	242.44
33.	P_5	53.4	222.30	68.	W_8	863.3	238.65
34.	P_6	562.1	223.36	69.	W_9	282.5	243.66
35.	P_7	2,894.3	235.24	70.	W_10	232.8	243.99

Table 20 (Continued)

No.	Code	Small watershed	$API_{critical}$	No.	Code	Small watershed	$API_{critical}$
		area (sq.km)	(mm)			area (sq.km)	(mm)
71.	W_11	281.8	234.06	92.	Y_11	532.4	276.40
72.	W_12	230.1	247.61	93.	Y_12	246.0	278.61
73.	W_13	149.1	227.60	94.	Y_13	711.0	280.45
74.	W_14	182.9	232.11	95.	Y_14	439.7	265.83
75.	W_15	362.8	229.49	96.	Y_15	531.1	254.26
76.	W_16	340.1	225.36	97.	Y_16	214.4	265.28
77.	W_17	308.4	223.49	98.	Y_17	880.1	257.71
78.	W_18	256.6	224.57	99.	Y_18	832.8	252.02
79.	W_19	378.8	223.22	100.	Y_19	796.8	250.96
80.	W_20	215.5	263.10	101.	Y_20	768.4	250.28
81.	W_21	22.4	224.20	102.	Y_21	2,312.7	233.75
82.	Y_1	2,119.7	244.51	103.	Y_22	491.3	230.70
83.	Y_2	873.6	218.40	104.	Y_23	1,055.9	220.29
84.	Y_3	658.8	233.59	105.	Y_24	1,572.1	214.64
85.	Y_4	1,760.1	270.21	106.	Y_25	905.8	235.70
86.	Y_5	214.7	293.23	107.	Y_26	545.4	217.52
87.	Y_6	374.7	288.00	108.	Y_27	1,323.4	229.54
88.	Y_7	332.1	289.12	109.	Y_28	656.3	233.71
89.	Y_8	246.1	292.71	110.	Y_29	191.7	233.62
90.	Y_9	1,032.1	274.67	111.	Y_30	655.3	230.97
91.	Y_10	149.7	285.05	112.	Y_31	170.0	233.70

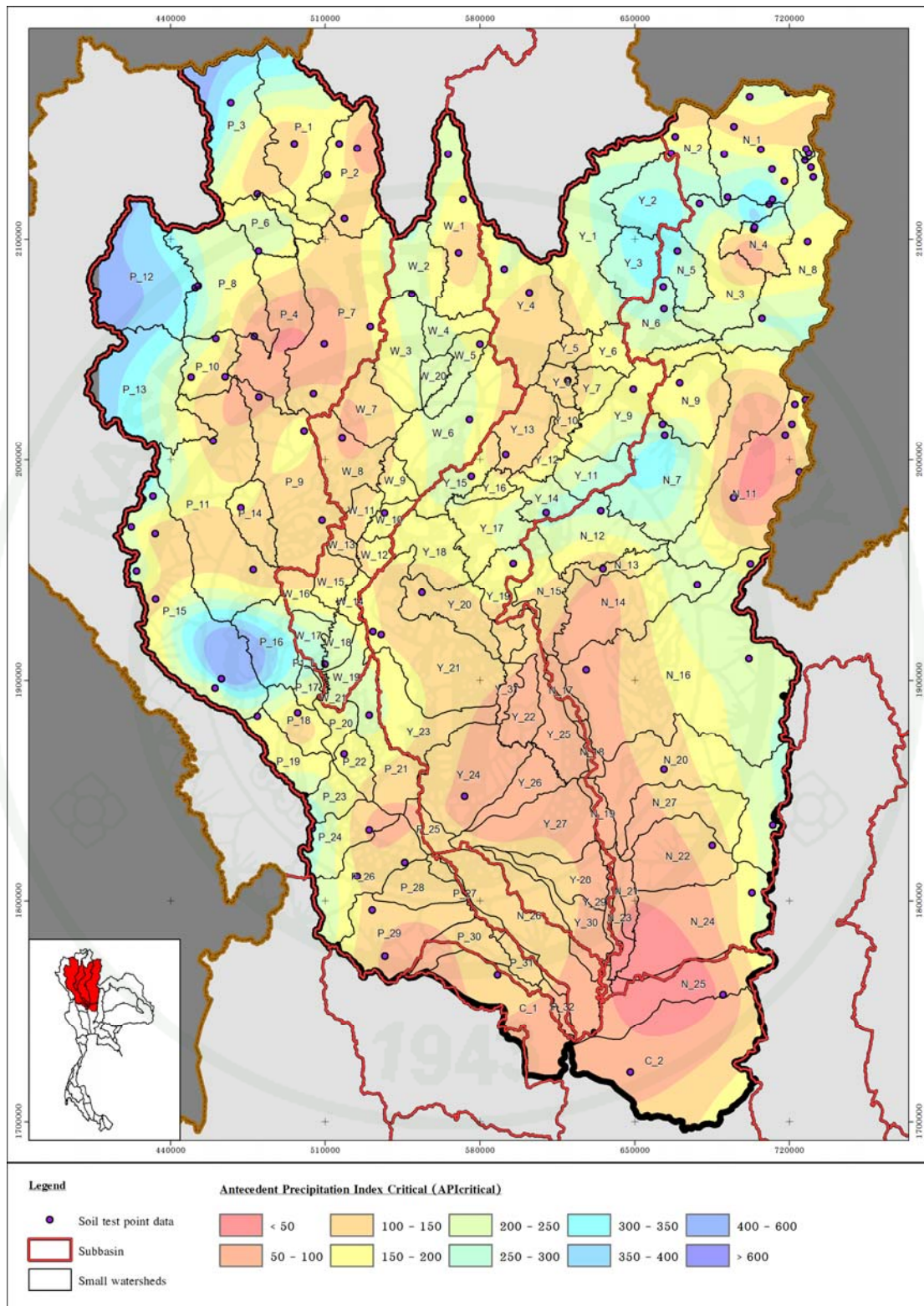


Figure 49 Areal distribution analysis of critical antecedent precipitation index

4. Watershed runoff prediction

The result of watershed runoff prediction is composed of the results of rainfall-runoff model selection, *API* rainfall-runoff model parameters, watershed runoff prediction in an ungauged basin, sensitivity analysis and watershed runoff prediction by *API* model as shown below.

4.1 Rainfall-Runoff model selection

1) Runoff estimation by original *API* model

The results of daily watershed runoff estimation of 36 representative stream gauging stations by using 6 models of relationship between areal daily rainfall and daily antecedent precipitation index (*API*) are show statistical measures of the similarity between simulated hydrograph and observed hydrographs using model-1 to model-6 as shown in Table 21 and Figure 50. The finding shows that model-3 equation (49) which is a nonlinear multiple cubic regression is more appropriate for estimating watershed runoff than other models given that the best of Nash-Sutcliffe efficiency (*NSE*) is 0.366-0.776 with the average of 0.539, correlation coefficient (*r*) is 0.605-0.881 with the average of 0.731 and root mean square error (*RMSE*) is 2.603-191.256 cms with the average of 29.617 cms; thus it indicates that the model predictions are satisfactorily reliable.

2) Runoff estimation by *API* adjusted model by *ET*

The results of daily watershed runoff estimation of 36 representative stream gauging stations by using 6 models of relationship between areal daily rainfall and daily *API* adjust model by evapotranspiration (API_{adj}) show statistical measures of the similarity between simulated hydrograph and observed hydrographs using model-1 to model-6 as shown in Table 22 and Figure 51.

Table 21 Statistical measures of the similarity between simulated and observed hydrographs using original API model 1 to 6

Discharge Station	Model Test								
	Model 1			Model 2			Model 3		
	Linear (Plan)		Quadratic (Paraboloid)			Cubic			
	r	NSE	RMSE	r	NSE	RMSE	r	NSE	RMSE
1. P.24A	0.689	0.467	6.477	0.728	0.529	6.088	0.730	0.532	6.070
2. P.64	0.656	0.430	7.896	0.673	0.453	7.736	0.690	0.475	7.575
3. P.21	0.691	0.477	4.000	0.692	0.479	3.995	0.696	0.484	3.973
4. P.47	0.597	0.340	11.490	0.648	0.420	10.771	0.656	0.429	10.681
5. P.20	0.626	0.392	13.238	0.671	0.451	12.588	0.672	0.452	12.576
6. P.71	0.702	0.481	13.715	0.705	0.498	13.497	0.719	0.517	13.231
7. P.4A	0.603	0.364	15.465	0.630	0.397	15.065	0.630	0.396	15.069
8. P.14	0.718	0.516	25.611	0.723	0.523	25.415	0.725	0.525	25.358
9. P.67	0.753	0.568	24.347	0.772	0.597	23.515	0.774	0.599	23.454
10. P.1	0.683	0.466	42.577	0.690	0.476	42.197	0.691	0.478	42.109
11. W.17	0.699	0.474	6.673	0.745	0.554	6.145	0.746	0.557	6.134
12. W.20	0.699	0.478	6.959	0.715	0.512	6.729	0.714	0.509	6.751
13. W.16A	0.755	0.558	12.299	0.769	0.591	11.835	0.768	0.588	11.872
14. W.3A	0.694	0.476	47.730	0.698	0.487	47.204	0.698	0.487	47.201
15. Y.30	0.581	0.329	2.676	0.599	0.358	2.618	0.605	0.366	2.603
16. Y.34	0.729	0.474	5.709	0.751	0.564	5.194	0.773	0.597	4.996
17. Y.24	0.595	0.349	10.106	0.631	0.398	9.713	0.636	0.404	9.663
18. Y.26	0.604	0.360	10.612	0.599	0.358	10.625	0.613	0.373	10.505
19. Y.31	0.740	0.543	24.443	0.748	0.560	23.970	0.750	0.562	23.916
20. Y.20	0.785	0.608	53.843	0.812	0.660	50.162	0.813	0.661	50.104
21. Y.1C	0.789	0.613	69.287	0.804	0.646	66.230	0.806	0.649	65.996
22. N.66	0.694	0.474	3.358	0.739	0.546	3.121	0.739	0.546	3.122
23. N.49	0.655	0.425	15.163	0.657	0.432	15.073	0.664	0.440	14.969
24. N.62	0.688	0.473	6.888	0.690	0.476	6.870	0.690	0.475	6.872
25. N.59	0.686	0.470	8.865	0.713	0.508	8.539	0.777	0.603	18.370
26. N.65	0.598	0.358	23.877	0.600	0.360	23.840	0.612	0.374	23.584
27. N.63	0.689	0.464	7.710	0.720	0.518	7.309	0.754	0.568	6.923
28. N.55	0.771	0.590	18.667	0.769	0.592	18.629	0.777	0.603	18.370
29. N.36	0.745	0.556	24.875	0.759	0.577	24.272	0.764	0.583	24.094
30. N.24	0.780	0.604	30.465	0.800	0.639	29.063	0.801	0.641	28.980
31. N.42	0.765	0.585	56.732	0.788	0.620	54.262	0.792	0.628	53.727
32. N.64	0.872	0.745	69.709	0.882	0.779	64.936	0.881	0.776	65.287
33. N.40	0.738	0.543	62.221	0.744	0.553	61.551	0.744	0.553	61.538
34. N.1	0.841	0.695	86.348	0.859	0.737	80.066	0.859	0.737	80.133
35. N.22	0.708	0.499	75.228	0.709	0.503	74.942	0.711	0.505	74.794
36. N.13A	0.839	0.690	200.847	0.845	0.714	192.802	0.848	0.719	191.256

Note: Model 1 : $Q = a + b.P + c.API$

Model 2 : $Q = a + b.P + c.P^2 + d.API + e.API^2$

Model 3 : $Q = a + b.P + c.P^2 + d.P^3 + e.API + f.API^2 + g.API^3$

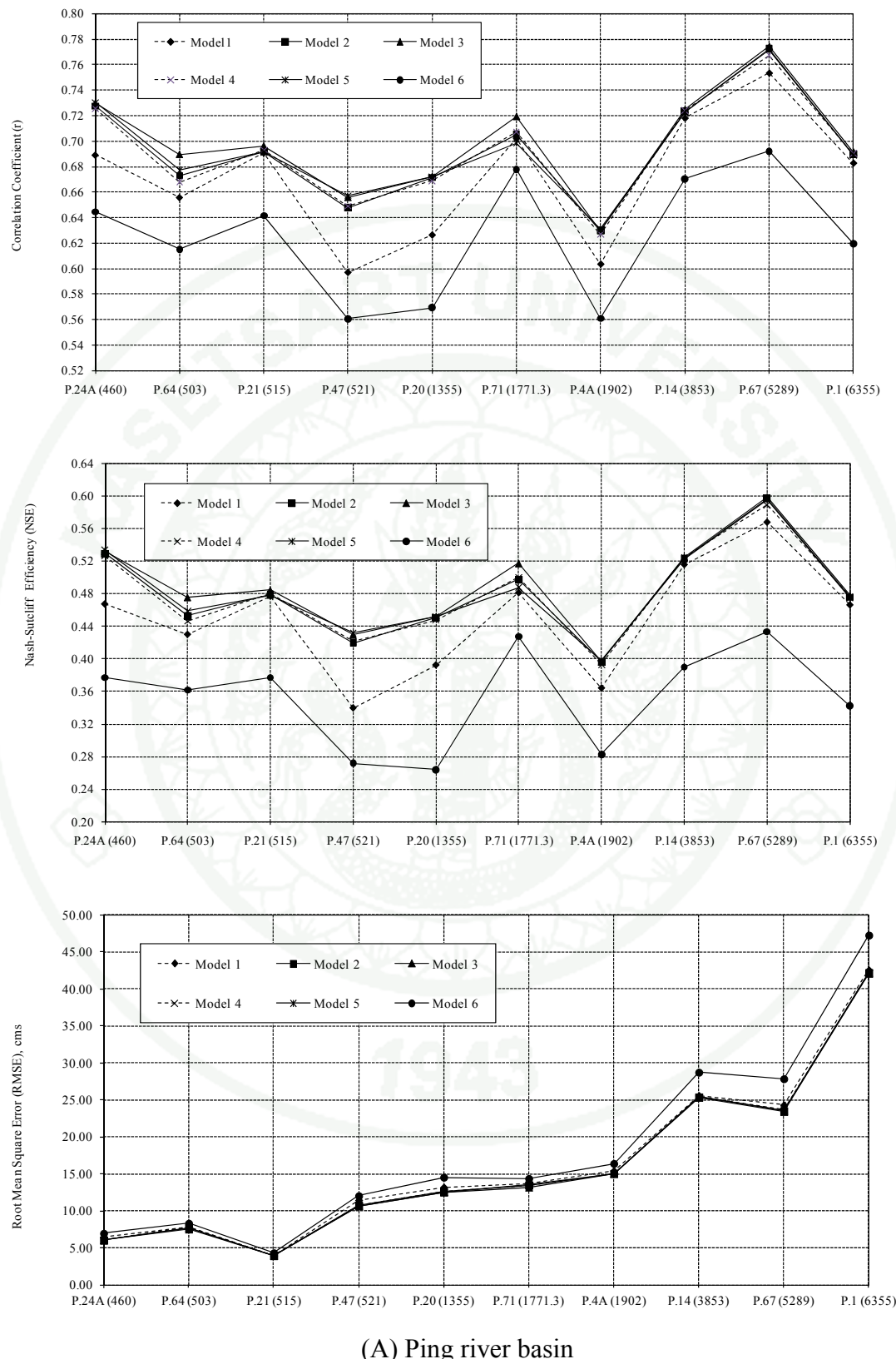
Table 21 (Continued)

Discharge Station	Model Test								
	Model 4 Power			Model 5 Exponential			Model 6 Logarithm		
	r	NSE	RMSE	r	NSE	RMSE	r	NSE	RMSE
1. P.24A	0.725	0.526	6.107	0.730	0.533	6.062	0.645	0.377	7.004
2. P.64	0.668	0.446	7.783	0.677	0.459	7.695	0.615	0.362	8.356
3. P.21	0.693	0.480	3.988	0.691	0.478	3.998	0.642	0.377	4.367
4. P.47	0.649	0.421	10.758	0.657	0.432	10.658	0.561	0.272	12.068
5. P.20	0.669	0.447	12.624	0.672	0.452	12.575	0.569	0.264	14.571
6. P.71	0.707	0.500	13.461	0.698	0.488	13.629	0.678	0.428	14.406
7. P.4A	0.627	0.393	15.110	0.631	0.398	15.046	0.561	0.283	16.428
8. P.14	0.724	0.524	25.382	0.723	0.522	25.433	0.670	0.390	28.749
9. P.67	0.767	0.589	23.748	0.772	0.596	23.550	0.692	0.433	27.872
10. P.1	0.690	0.476	42.166	0.689	0.475	42.236	0.620	0.342	47.266
11. W.17	0.743	0.552	6.164	0.745	0.555	6.144	0.638	0.368	7.315
12. W.20	0.715	0.511	6.732	0.712	0.508	6.759	0.661	0.417	7.351
13. W.16A	0.769	0.591	11.831	0.765	0.584	11.931	0.691	0.450	13.724
14. W.3A	0.700	0.489	47.118	0.698	0.484	47.369	0.650	0.410	50.653
15. Y.30	0.601	0.361	2.612	0.602	0.363	2.609	0.554	0.288	2.759
16. Y.34	0.768	0.590	5.041	0.774	0.599	4.981	0.712	0.437	5.904
17. Y.24	0.631	0.398	9.712	0.640	0.410	9.620	0.547	0.287	10.574
18. Y.26	0.600	0.360	10.610	0.604	0.360	10.608	0.579	0.328	10.876
19. Y.31	0.749	0.562	23.930	0.747	0.557	24.046	0.685	0.454	26.712
20. Y.20	0.812	0.659	50.247	0.811	0.658	50.319	0.717	0.494	61.213
21. Y.1C	0.804	0.646	66.293	0.803	0.643	66.555	0.728	0.516	75.089
22. N.66	0.732	0.536	3.155	0.733	0.537	3.150	0.651	0.396	3.600
23. N.49	0.660	0.436	15.019	0.657	0.430	15.108	0.631	0.384	15.701
24. N.62	0.690	0.476	6.866	0.689	0.475	6.877	0.646	0.404	7.324
25. N.59	0.707	0.500	8.609	0.710	0.505	8.566	0.636	0.386	9.539
26. N.65	0.602	0.363	23.793	0.600	0.360	23.851	0.590	0.326	24.470
27. N.63	0.689	0.466	7.694	0.704	0.495	7.482	0.663	0.418	8.031
28. N.55	0.772	0.597	18.518	0.769	0.591	18.654	0.729	0.510	20.417
29. N.36	0.756	0.571	24.424	0.762	0.580	24.170	0.686	0.454	27.574
30. N.24	0.798	0.637	29.173	0.801	0.641	28.988	0.725	0.512	33.811
31. N.42	0.784	0.615	54.636	0.792	0.627	53.809	0.711	0.472	63.989
32. N.64	0.883	0.779	64.865	0.881	0.776	65.290	0.834	0.664	80.062
33. N.40	0.744	0.553	61.530	0.743	0.551	61.661	0.680	0.448	68.392
34. N.1	0.859	0.738	80.030	0.856	0.733	80.711	0.795	0.596	99.252
35. N.22	0.711	0.505	74.771	0.708	0.501	75.058	0.661	0.422	80.837
36. N.13A	0.847	0.717	191.698	0.841	0.707	195.135	0.796	0.602	227.433

Note: Model 4 : $Q = a + b.P^c + d.API^e$

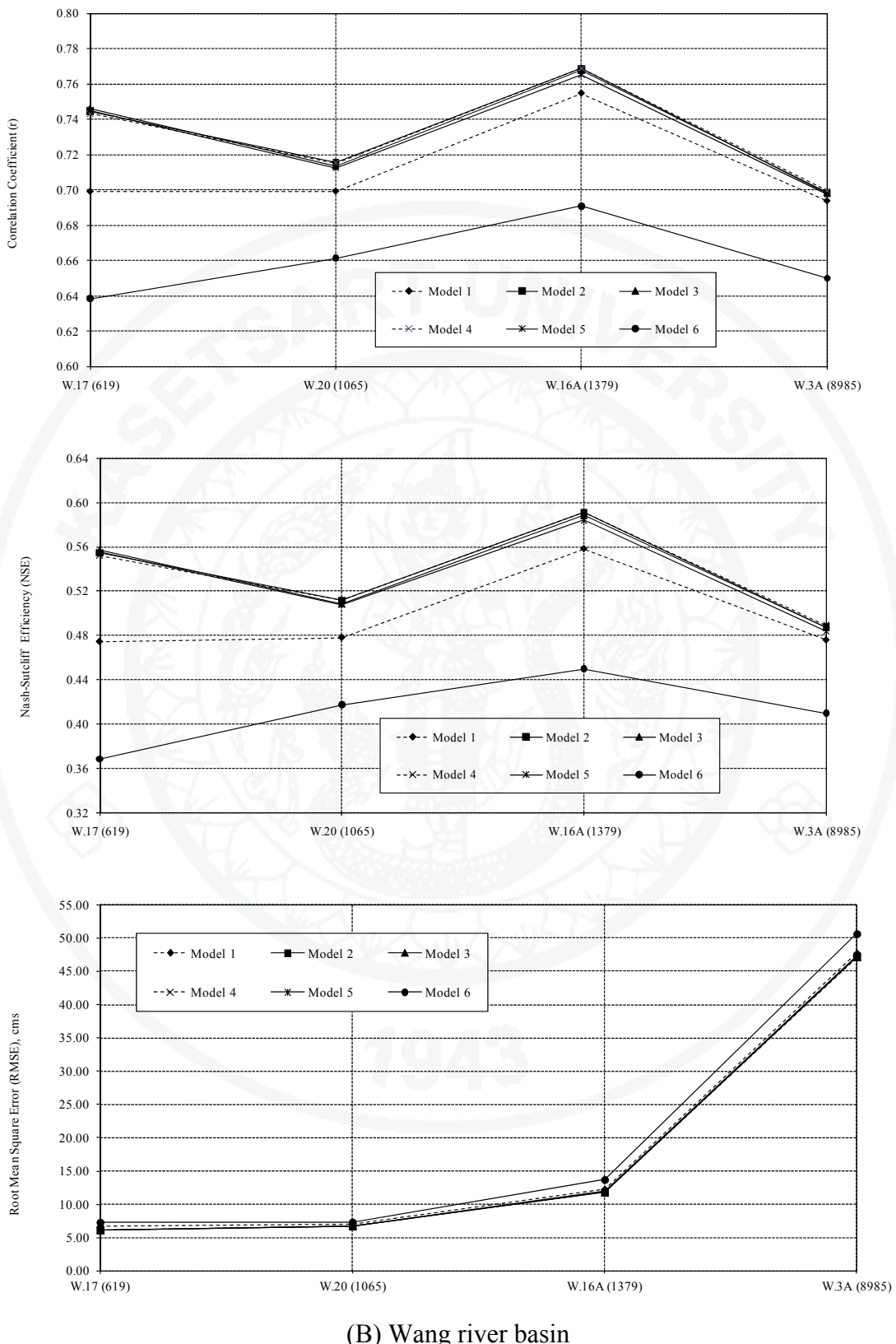
Model 5 : $Q = a + b.exp^{c.P} + d.exp^{e.API}$

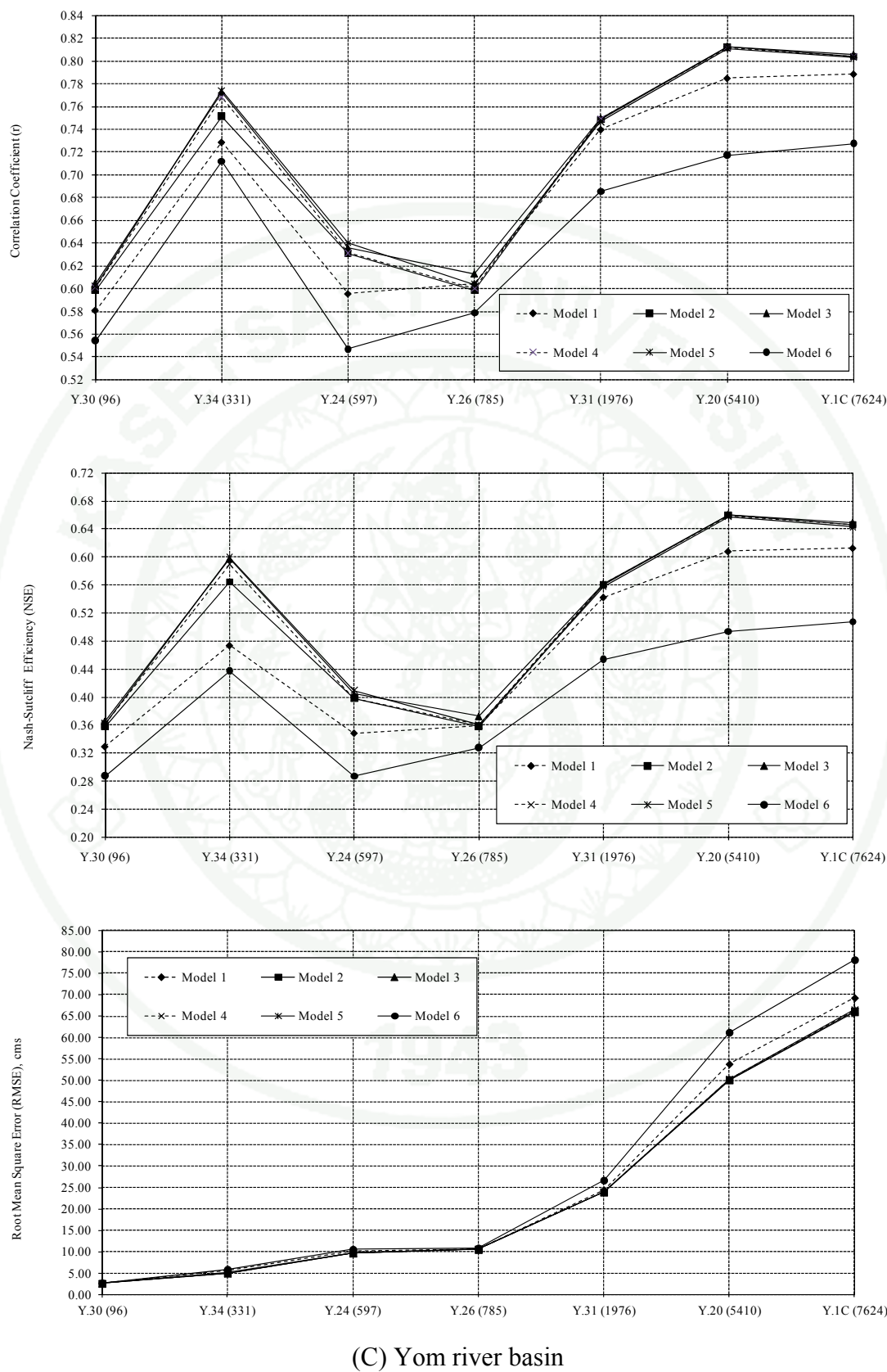
Model 6 : $Q = a + b.\ln(P) + c.\ln(API)$

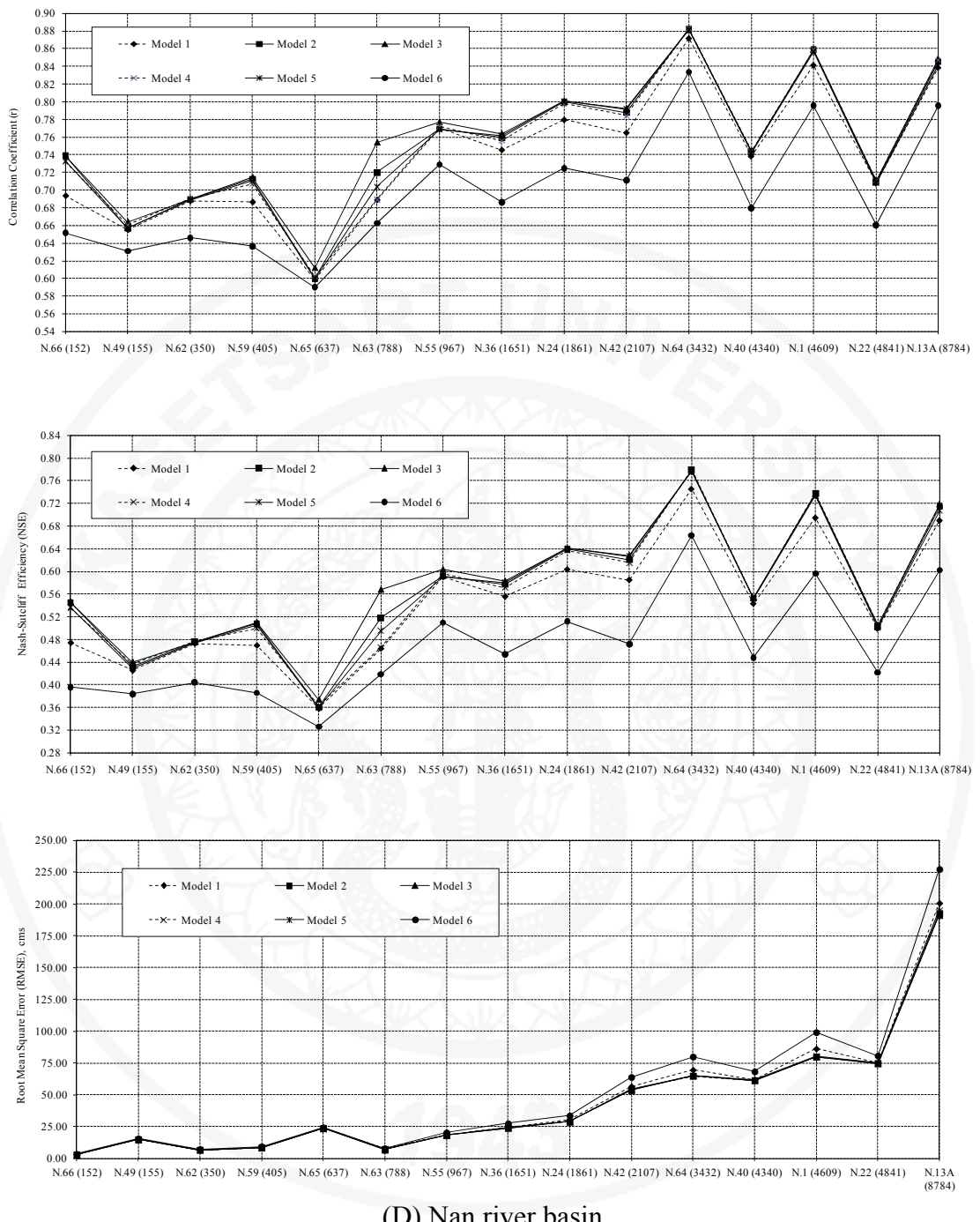


(A) Ping river basin

Figure 50 Statistical measures of the similarity between simulated and observed hydrographs using original API model 1 to 6.

**Figure 50** (Continued)

**Figure 50** (Continued)



(D) Nan river basin

Figure 50 (Continued)

Table 22 Statistical measures of the similarity between simulated and observed hydrographs using *API* adjust model 1 to 6.

Discharge Station	Model Test								
	Model 1			Model 2			Model 3		
	Linear (Plan)			Quadratic (Paraboloid)			Cubic	NSE	RMSE
	r	NSE	RMSE	r	NSE	RMSE	r	NSE	RMSE
1. P.24A	0.569	0.324	7.296	0.579	0.336	7.233	0.589	0.346	7.174
2. P.64	0.389	0.151	9.636	0.409	0.167	9.543	0.298	0.064	10.117
3. P.21	0.429	0.184	4.997	0.442	0.195	4.963	0.447	0.200	4.950
4. P.47	0.664	0.412	10.841	0.703	0.494	10.055	0.702	0.489	10.103
5. P.20	0.485	0.235	14.851	0.490	0.240	14.801	0.492	0.241	14.790
6. P.71	0.276	0.076	18.300	0.296	0.088	18.186	0.306	0.091	18.150
7. P.4A	0.571	0.326	15.928	0.581	0.337	15.788	0.582	0.339	15.770
8. P.14	0.409	0.167	33.580	0.452	0.205	32.820	0.434	0.186	33.200
9. P.67	0.603	0.364	29.539	0.612	0.375	29.273	0.605	0.365	29.508
10. P.1	0.486	0.236	50.924	0.488	0.238	50.868	0.488	0.238	50.865
11. W.17	0.311	0.097	8.749	0.368	0.135	8.560	0.370	0.137	8.559
12. W.20	0.258	0.067	9.304	0.392	0.152	8.870	0.393	0.152	8.867
13. W.16A	0.267	0.071	17.832	0.332	0.110	17.456	0.332	0.110	17.455
14. W.3A	0.248	0.061	63.872	0.345	0.119	61.889	0.347	0.120	61.836
15. Y.30	0.255	0.065	3.160	0.333	0.110	3.083	0.335	0.112	3.079
16. Y.34	0.363	0.132	7.333	0.395	0.156	7.230	0.405	0.162	7.205
17. Y.24	0.229	0.053	12.188	0.290	0.083	11.992	0.290	0.083	11.992
18. Y.26	0.299	0.089	12.658	0.313	0.098	12.598	0.272	0.073	12.770
19. Y.31	0.241	0.058	35.074	0.387	0.147	33.383	0.392	0.150	33.330
20. Y.20	0.244	0.060	83.408	0.381	0.143	79.611	0.387	0.148	79.392
21. Y.1C	0.254	0.065	107.708	0.361	0.127	104.066	0.361	0.129	103.938
22. N.66	0.659	0.433	3.487	0.692	0.479	3.343	0.697	0.482	3.331
23. N.49	0.463	0.214	17.730	0.464	0.215	17.717	0.465	0.215	17.720
24. N.62	0.691	0.477	6.859	0.692	0.478	6.854	0.687	0.464	6.944
25. N.59	0.654	0.427	9.213	0.668	0.446	9.058	0.642	0.359	23.346
26. N.65	0.565	0.317	24.630	0.573	0.323	24.518	0.572	0.322	24.544
27. N.63	0.669	0.436	7.910	0.702	0.493	7.495	0.726	0.519	7.305
28. N.55	0.832	0.688	16.287	0.832	0.692	16.189	0.830	0.685	16.352
29. N.36	0.776	0.599	23.636	0.781	0.609	23.319	0.780	0.598	23.647
30. N.24	0.759	0.570	31.723	0.778	0.606	30.374	0.780	0.608	30.309
31. N.42	0.639	0.408	67.776	0.672	0.452	65.220	0.689	0.474	63.878
32. N.64	0.836	0.680	78.113	0.845	0.713	73.912	0.845	0.713	74.020
33. N.40	0.813	0.656	54.004	0.821	0.674	52.592	0.814	0.658	53.835
34. N.1	0.784	0.595	99.371	0.806	0.649	92.515	0.806	0.648	92.702
35. N.22	0.810	0.650	62.926	0.815	0.664	61.580	0.809	0.651	62.760
36. N.13A	0.609	0.368	286.653	0.640	0.409	277.226	0.641	0.411	276.704

Note: Model 1 : $Q = a + b.P + c.API$

Model 2 : $Q = a + b.P + c.P^2 + d.API + e.API^2$

Model 3 : $Q = a + b.P + c.P^2 + d.P^3 + e.API + f.API^2 + g.API^3$

Table 22 (Continued)

Discharge Station	Model Test								
	Model 4 Power			Model 5 Exponential			Model 6 Logarithm		
	r	NSE	RMSE	r	NSE	RMSE	r	NSE	RMSE
1. P.24A	0.582	0.339	7.217	0.578	0.334	7.244	0.520	0.235	7.764
2. P.64	0.443	0.197	9.375	0.427	0.182	9.460	0.384	0.142	9.685
3. P.21	0.434	0.188	4.984	0.429	0.184	4.999	0.407	0.155	5.086
4. P.47	0.708	0.502	9.981	0.703	0.494	10.055	0.655	0.372	11.207
5. P.20	0.490	0.240	14.804	0.489	0.239	14.813	0.418	0.150	15.660
6. P.71	0.302	0.091	18.149	0.299	0.089	18.169	0.288	0.080	18.267
7. P.4A	0.581	0.338	15.781	0.580	0.336	15.806	0.534	0.263	16.654
8. P.14	0.453	0.205	32.806	0.431	0.185	33.213	0.428	0.181	33.299
9. P.67	0.611	0.373	29.319	0.613	0.376	29.243	0.553	0.281	31.408
10. P.1	0.488	0.239	50.851	0.486	0.236	50.941	0.452	0.182	52.715
11. W.17	0.363	0.132	8.584	0.310	0.096	8.760	0.327	0.106	8.703
12. W.20	0.327	0.106	9.106	0.341	0.116	9.054	0.314	0.098	9.149
13. W.16A	0.328	0.104	17.514	0.266	0.071	17.836	0.302	0.088	17.668
14. W.3A	0.326	0.104	62.399	0.247	0.061	63.891	0.308	0.093	62.776
15. Y.30	0.291	0.085	3.127	0.290	0.084	3.128	0.234	0.051	3.183
16. Y.34	0.374	0.140	7.299	0.368	0.135	7.319	0.265	0.069	7.595
17. Y.24	0.284	0.081	12.006	0.285	0.081	12.004	0.257	0.064	12.112
18. Y.26	0.319	0.101	12.574	0.298	0.089	12.661	0.315	0.097	12.601
19. Y.31	0.347	0.120	33.899	0.340	0.115	33.993	0.267	0.071	34.841
20. Y.20	0.343	0.118	80.787	0.348	0.121	80.637	0.279	0.075	82.729
21. Y.1C	0.338	0.112	104.919	0.254	0.064	107.730	0.311	0.110	101.777
22. N.66	0.685	0.469	3.374	0.652	0.422	3.520	0.626	0.380	3.647
23. N.49	0.473	0.224	17.622	0.464	0.215	17.719	0.437	0.186	18.052
24. N.62	0.692	0.478	6.852	0.692	0.479	6.851	0.679	0.454	7.012
25. N.59	0.656	0.427	9.211	0.673	0.453	8.999	0.620	0.375	9.623
26. N.65	0.579	0.333	24.348	0.565	0.316	24.641	0.569	0.313	24.698
27. N.63	0.644	0.348	8.502	0.692	0.479	7.603	0.649	0.401	8.150
28. N.55	0.833	0.695	16.116	0.830	0.688	16.277	0.820	0.655	17.119
29. N.36	0.781	0.610	23.291	0.775	0.598	23.664	0.759	0.559	24.791
30. N.24	0.774	0.599	30.637	0.762	0.573	31.618	0.741	0.536	32.976
31. N.42	0.667	0.445	65.594	0.685	0.470	64.127	0.584	0.314	72.960
32. N.64	0.846	0.715	73.677	0.841	0.707	74.769	0.805	0.614	85.735
33. N.40	0.821	0.675	52.521	0.820	0.672	52.740	0.791	0.610	57.479
34. N.1	0.806	0.650	92.389	0.800	0.640	93.721	0.746	0.518	108.506
35. N.22	0.816	0.666	61.462	0.814	0.662	61.788	0.792	0.611	66.333
36. N.13A	0.639	0.408	277.518	0.635	0.403	278.473	0.580	0.310	299.563

Note: Model 4 : $Q = a + b.P^c + d.API^e$

Model 5 : $Q = a + b.exp^{c.P} + d.exp^{e.API}$

Model 6 : $Q = a + b.\ln(P) + c.\ln(API)$

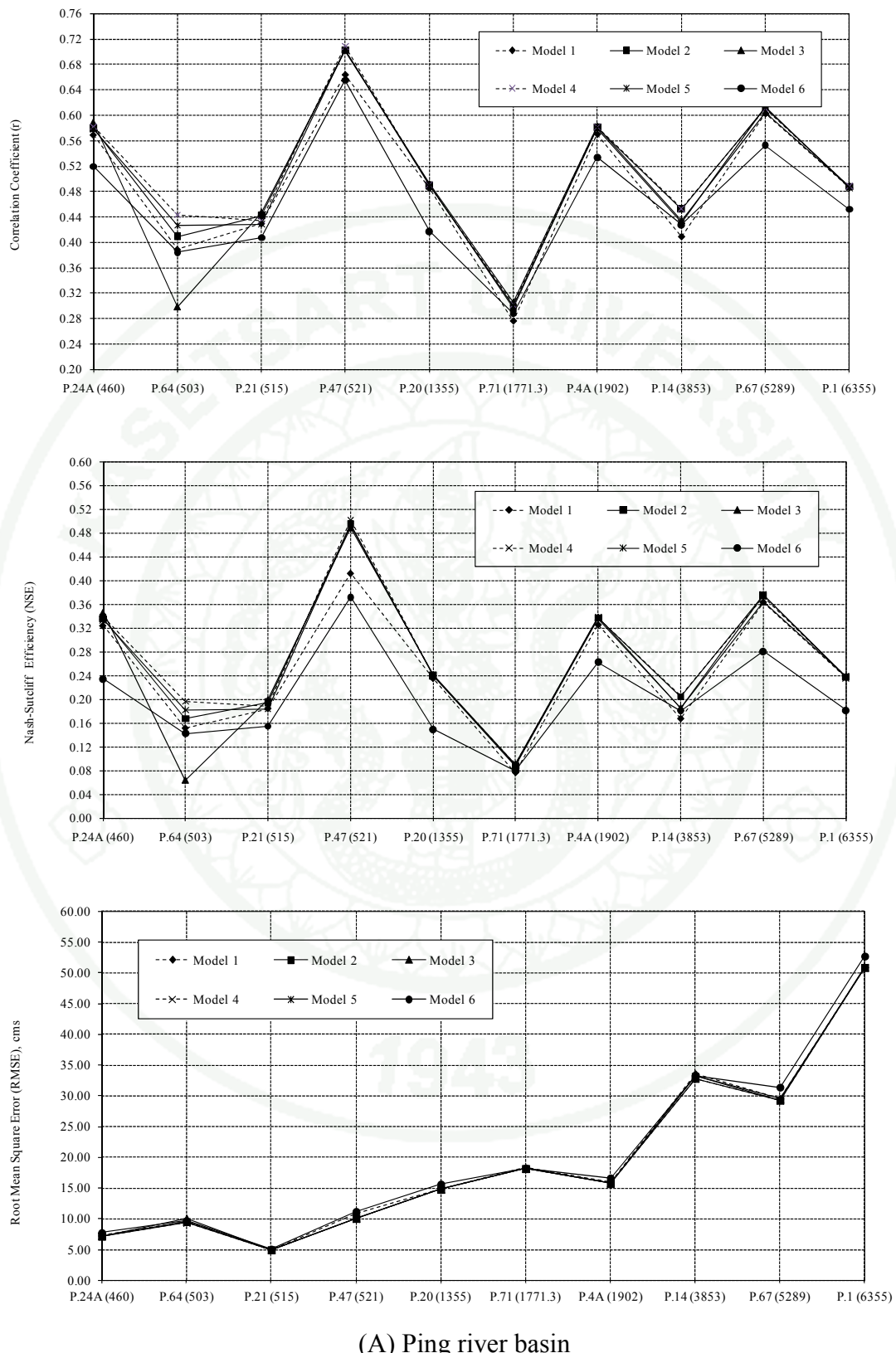
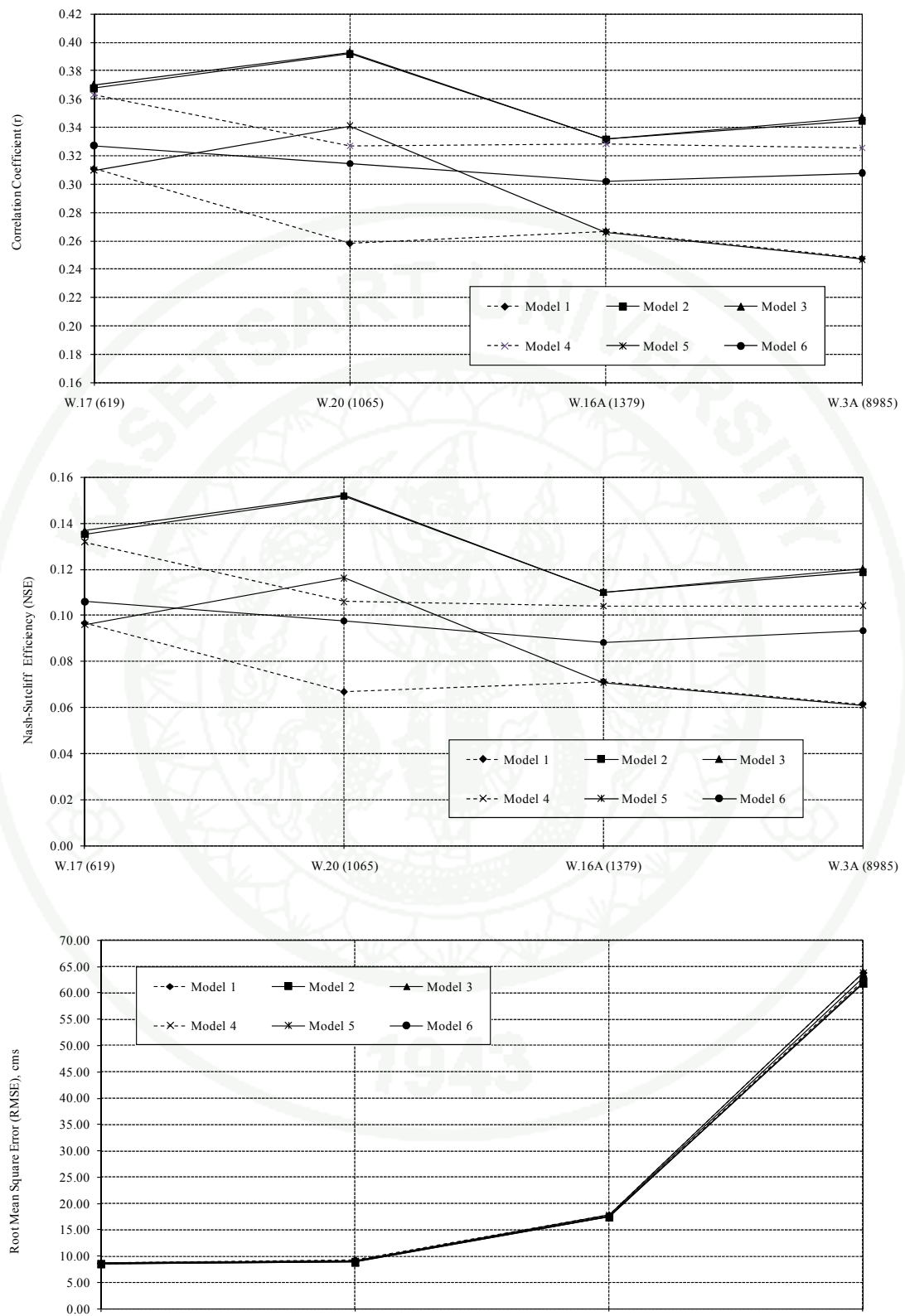
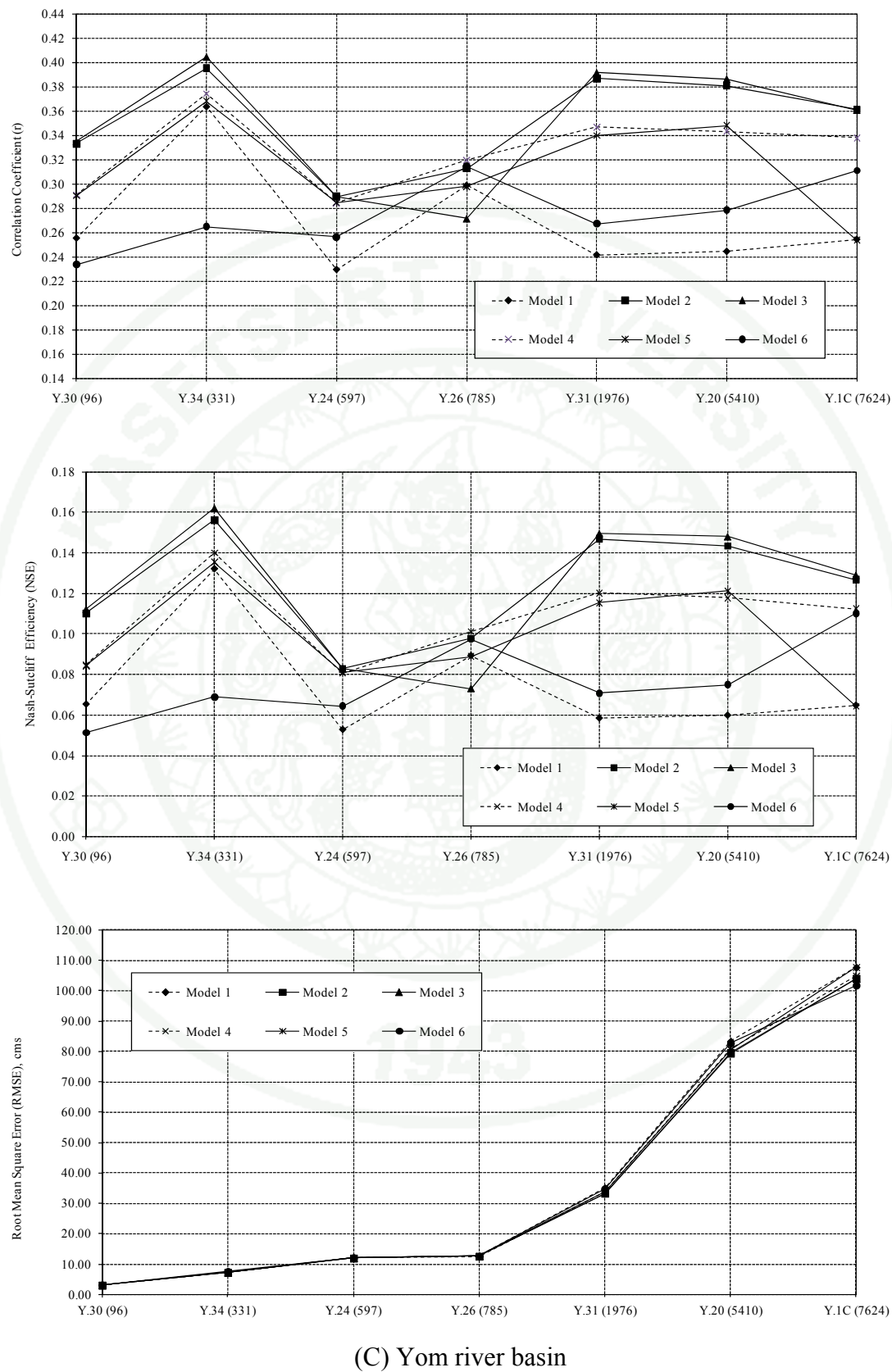


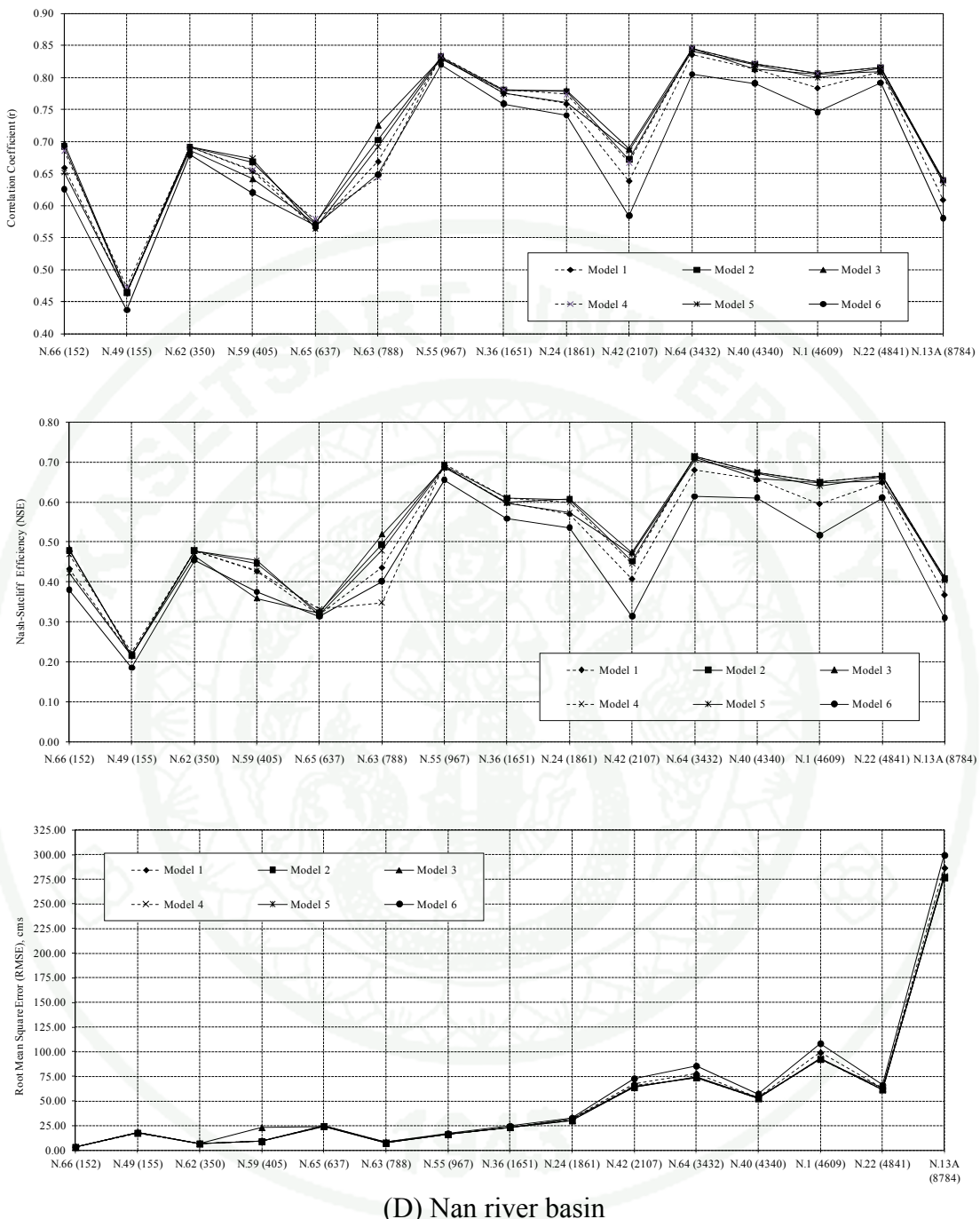
Figure 51 Statistical measures of the similarity between simulated and observed hydrographs using API adjust model 1 to 6.



(B) Wang river basin

Figure 51 (Continued)

**Figure 51** (Continued)



(D) Nan river basin

Figure 51 (Continued)

The finding shows that model-2 equation (57) which is a nonlinear multiple quadratic regression is more appropriate for estimating watershed runoff than other models given that the best of Nash-Sutcliffe efficiency (NSE) is 0.083-0.713 with the average of 0.332, correlation coefficient (r) is 0.290-0.845 with the average

of 0.548 and root mean square error (*RMSE*) is 3.083-277.226 cms with the average of 36.227 cms; thus it indicates that the model are more accurate than the arithmetic mean of the observed data.

3) Comparison of performances of original *API* model and adjusted *API* model by evapotranspiration (API_{adj})

After the daily watershed runoff was simulated by using original *API* model and adjusted *API* model by evapotranspiration (API_{adj}), goodness of fit was evaluated by using statistical measures of the similarity between simulated and observed hydrographs of original *API* model-1 to model-6 (equation 47 to 52) and adjusted *API* model by evapotranspiration (API_{adj}) model-1 to model-6 (equation 56 to 61). The finding shows that the daily runoff estimated by original *API* model-1 to model-6 has given the Nash-Sutcliffe efficiency (*NSE*) and correlation coefficient (*r*) higher than adjusted *API* model by evapotranspiration (API_{adj}) model-1 to model-6, but has given the root mean square error (*RMSE*) lower than adjusted *API* model by evapotranspiration (API_{adj}) model-1 to model-6 as shown in Table 23 and Figure 52. Moreover, the results show that the original *API* model-3 equation (49) which is a nonlinear multiple cubic regression is more appropriate for estimating watershed runoff than other models.

4) Runoff estimation by critical *API* range model

The results of daily watershed runoff estimation of 36 representative stream gauging stations by using 6 models of relationship between areal daily rainfall and daily antecedent precipitation index (*API*) are improved by using the range of critical *API*. The ranges are defined by percentage of critical *API* which is divided into 10 ranges (10, 20, 30, 40, 50, 60, 70, 80, 90 and 100 percentage of critical *API*). For each percentage range, the critical *API* models will have 3 sets of model parameters by comparing daily *API* with critical *API* as shown in statistical measures of the similarity between simulated and observed hydrographs using model-1 to model-6 in Appendix Table C1 to Appendix Table C6.

Table 23 Compare performances of original *API* model and *API* adjust model by evapotranspiration (*ET*)

Model Test	NSE			<i>r</i>			RMSE		
	Average	Maximum	Minimum	Average	Maximum	Minimum	Average	Maximum	Minimum
<i>API</i> original model for runoff estimation									
Model 1	0.498	0.745	0.329	0.707	0.581	0.872	30.725	200.847	2.676
Model 2	0.530	0.779	0.358	0.724	0.599	0.882	29.627	192.802	2.618
Model 3	0.539	0.776	0.366	0.731	0.605	0.881	29.774	191.256	2.603
Model 4	0.528	0.779	0.360	0.724	0.600	0.883	29.617	191.698	2.612
Model 5	0.529	0.776	0.360	0.725	0.600	0.881	29.732	195.135	2.609
Model 6	0.416	0.664	0.264	0.662	0.547	0.834	33.991	227.433	2.759
<i>API</i> adjust model by <i>ET</i> for runoff estimation									
Model 1	0.300	0.688	0.053	0.511	0.229	0.836	37.430	286.653	3.160
Model 2	0.332	0.713	0.083	0.548	0.290	0.845	36.227	277.226	3.083
Model 3	0.326	0.713	0.064	0.545	0.272	0.845	36.679	276.704	3.079
Model 4	0.324	0.715	0.081	0.540	0.284	0.846	36.350	277.518	3.127
Model 5	0.319	0.707	0.061	0.530	0.247	0.841	36.596	278.473	3.128
Model 6	0.272	0.655	0.051	0.500	0.234	0.820	38.653	299.563	3.183

Note: Model 1 : $Q = a + b.P + c.API$

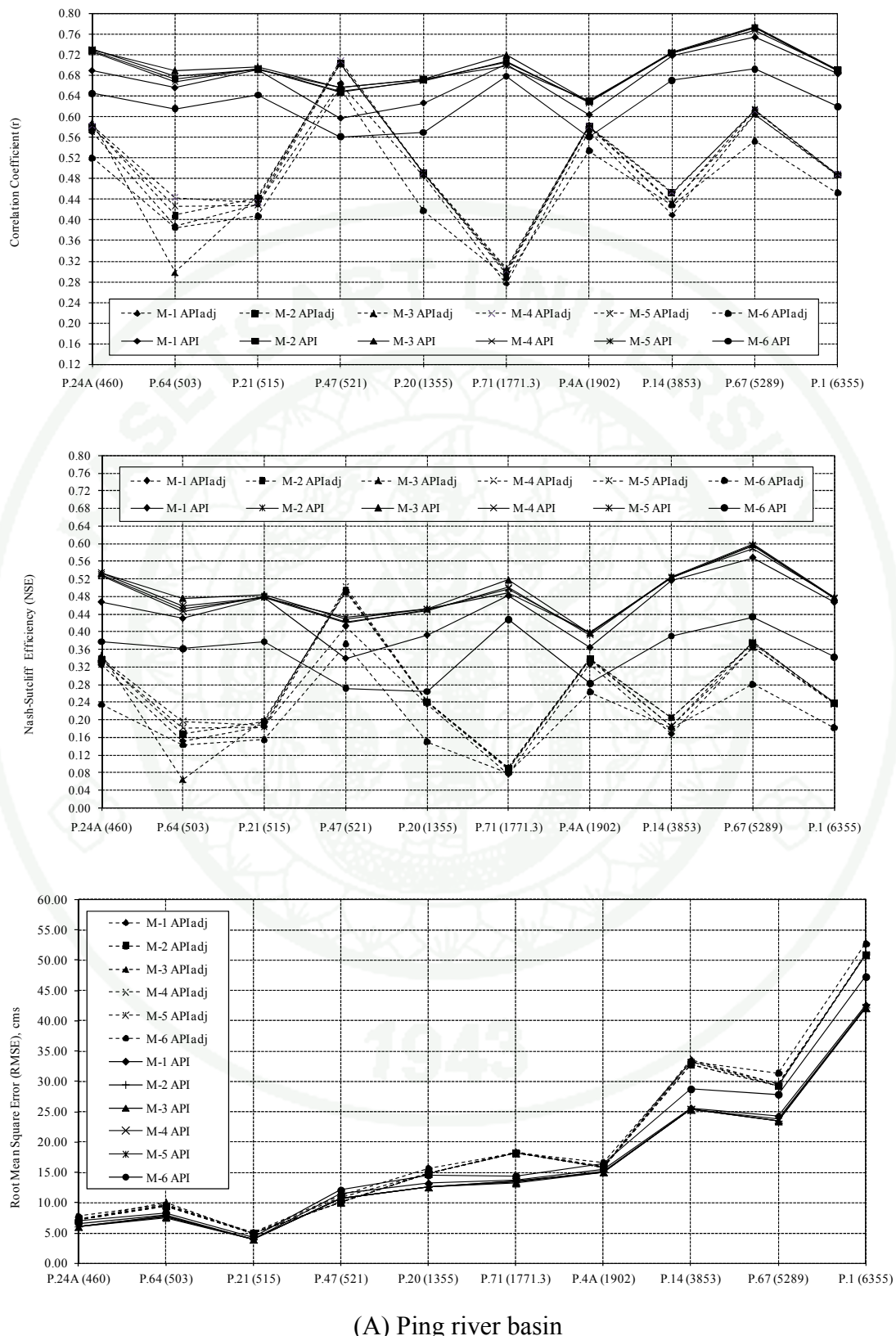
Model 2 : $Q = a + b.P + c.P^2 + d.API + e.API^2$

Model 3 : $Q = a + b.P + c.P^2 + d.P^3 + e.API + f.API^2 + g.API^3$

Model 4 : $Q = a + b.P^c + d.API^e$

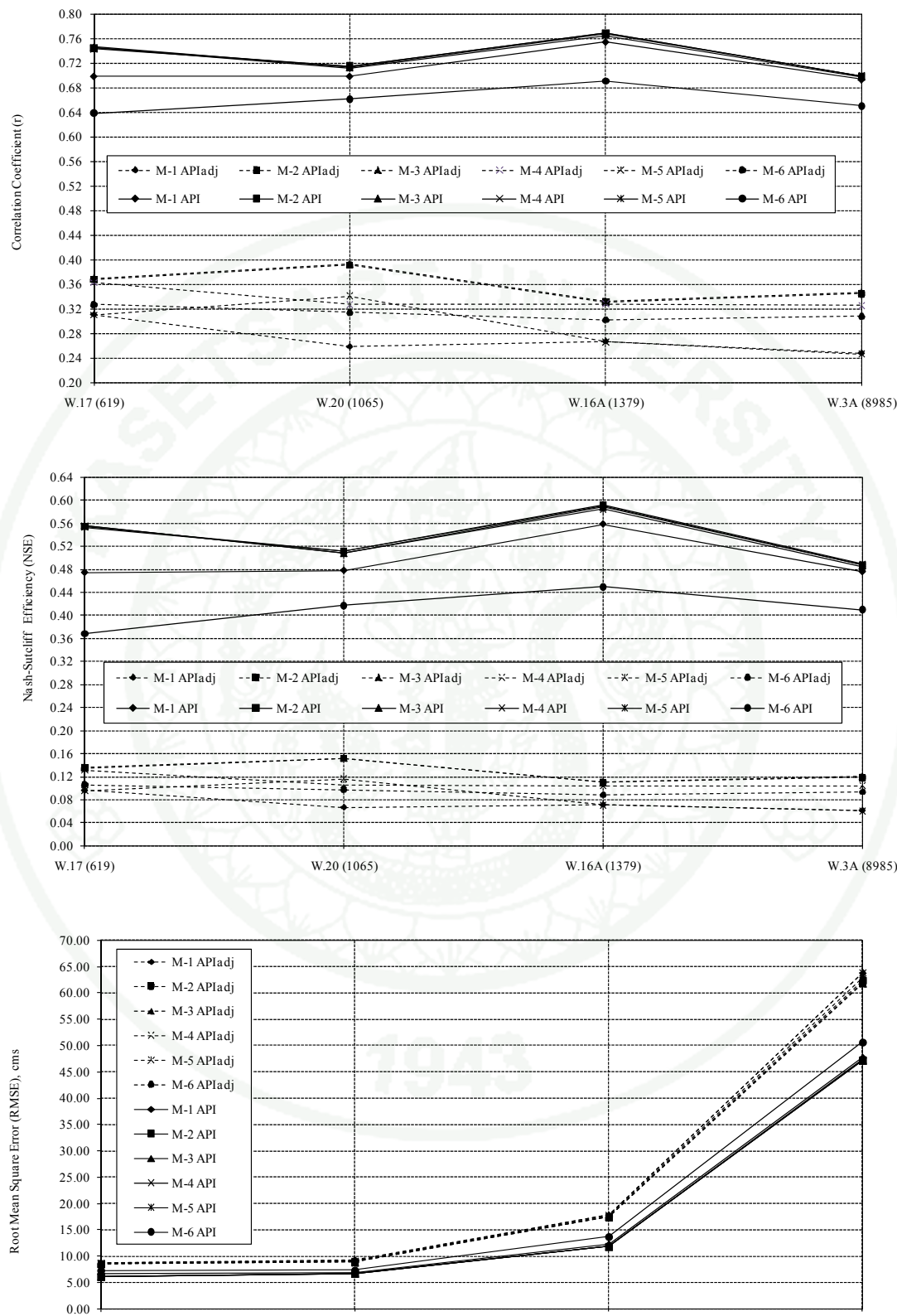
Model 5 : $Q = a + b.exp^{c.P} + d.exp^{e.API}$

Model 6 : $Q = a + b.\ln(P) + c.\ln(API)$



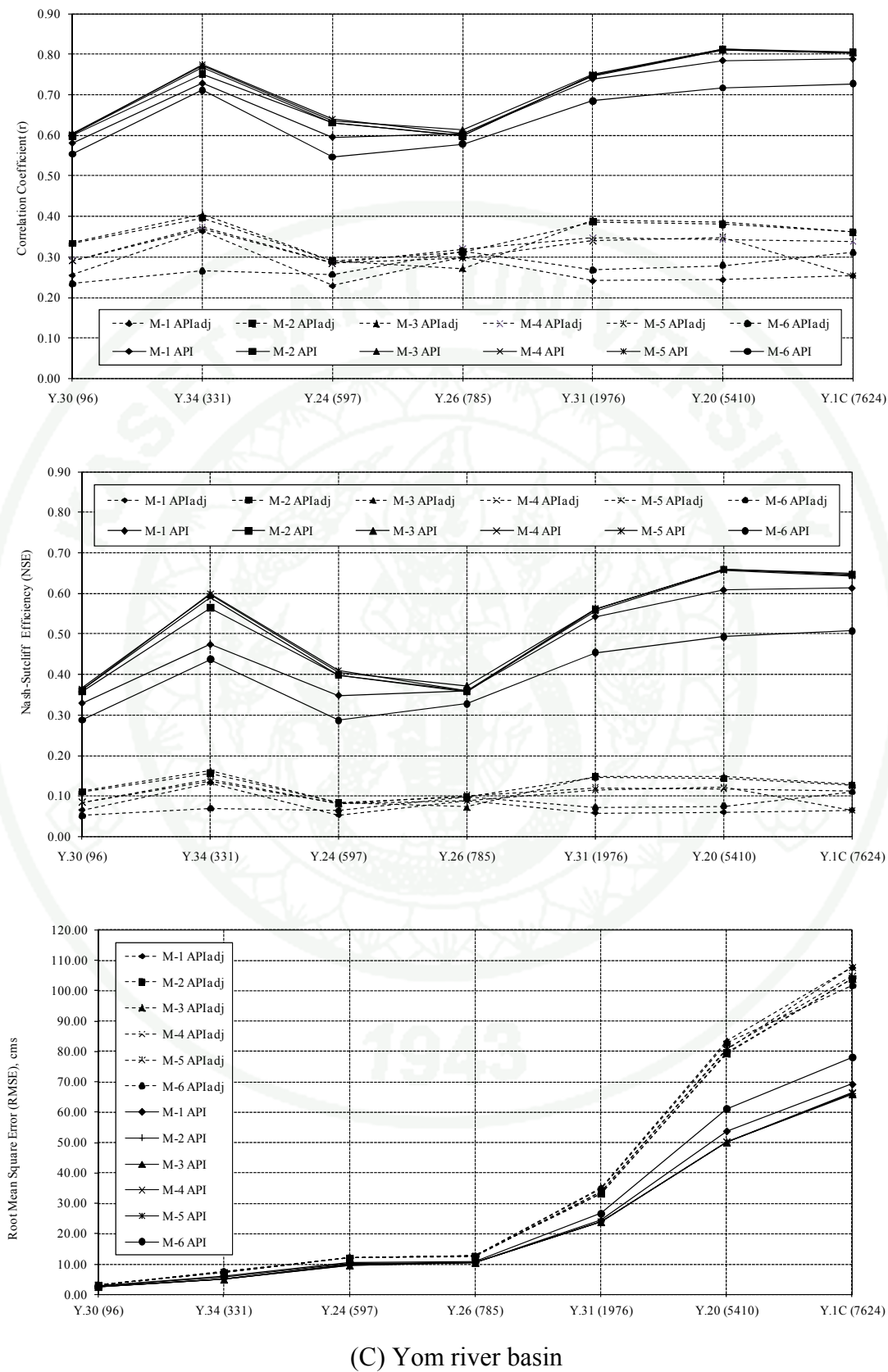
(A) Ping river basin

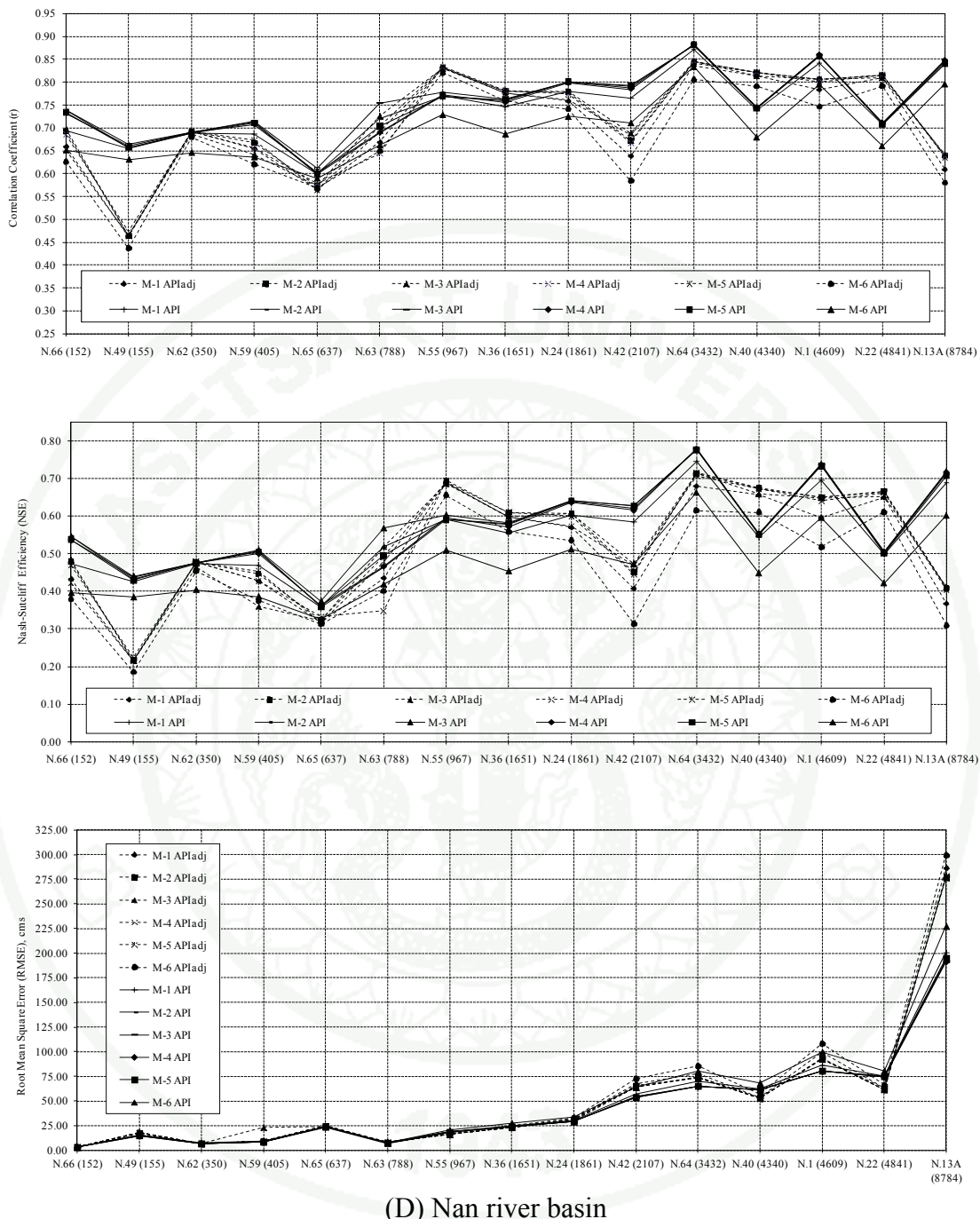
Figure 52 Compare performances of original *API* model and *API* adjust model by evapotranspiration (*ET*)



(B) Wang river basin

Figure 52 (Continued)

**Figure 52** (Continued)



(D) Nan river basin

Figure 52 (Continued)

At the best model performances, all 6 models show the results as follow; model-1 shows the range of 30%, model-2 shows the range of 40%, model-3 shows the range of 60%, model 4 shows the range of 40%, model 5 shows the range of 40% and model 6 shows the range of 20% as shown in Table 24.

The comparison of model-1 to model-6 in every percentage range of critical *API* has shown that 60 percentage range of critical *API* range in model-3, which is a nonlinear multiple cubic regression, is more appropriate for estimating watershed runoff than the other percentage ranges of critical *API* range model given that the best of Nash-Sutcliffe efficiency (*NSE*) of 0.366-0.784 with average of 0.543, correlation coefficient (*r*) of 0.605-0.885 with average of 0.734 and root mean square error (*RMSE*) of 2.603-191.527 cms with average of 29.405 cms are applied as shown in Table 24. The results indicate that the model predictions are correspond to a satisfactory prediction.

In addition, the comparison of critical *API* range model-1 to model-6 (Table 10) and original *API* model-1 to model-6 (equation 47 to 52) shows that 60 percentage range of critical *API* range in model-3 gives the best of model performances as shown in Figure 53. For this reason, critical *API* range model-3 with the range of 60% was chosen for estimating the runoff of small watershed in the upper Chao Phraya river basin as shown in the equation below.

If $API < 60\% \text{ of } API_{critical}$

$$Q = a_1 + b_1.P + c_1.P^2 + d_1.P^3 + e_1.API + f_1.API^2 + g_1.API^3 \quad (62)$$

If $60\% \text{ of } API_{critical} < API < API_{critical}$

$$Q = a_2 + b_2.P + c_2.P^2 + d_2.P^3 + e_2.API + f_2.API^2 + g_2.API^3 \quad (63)$$

If $API > API_{critical}$

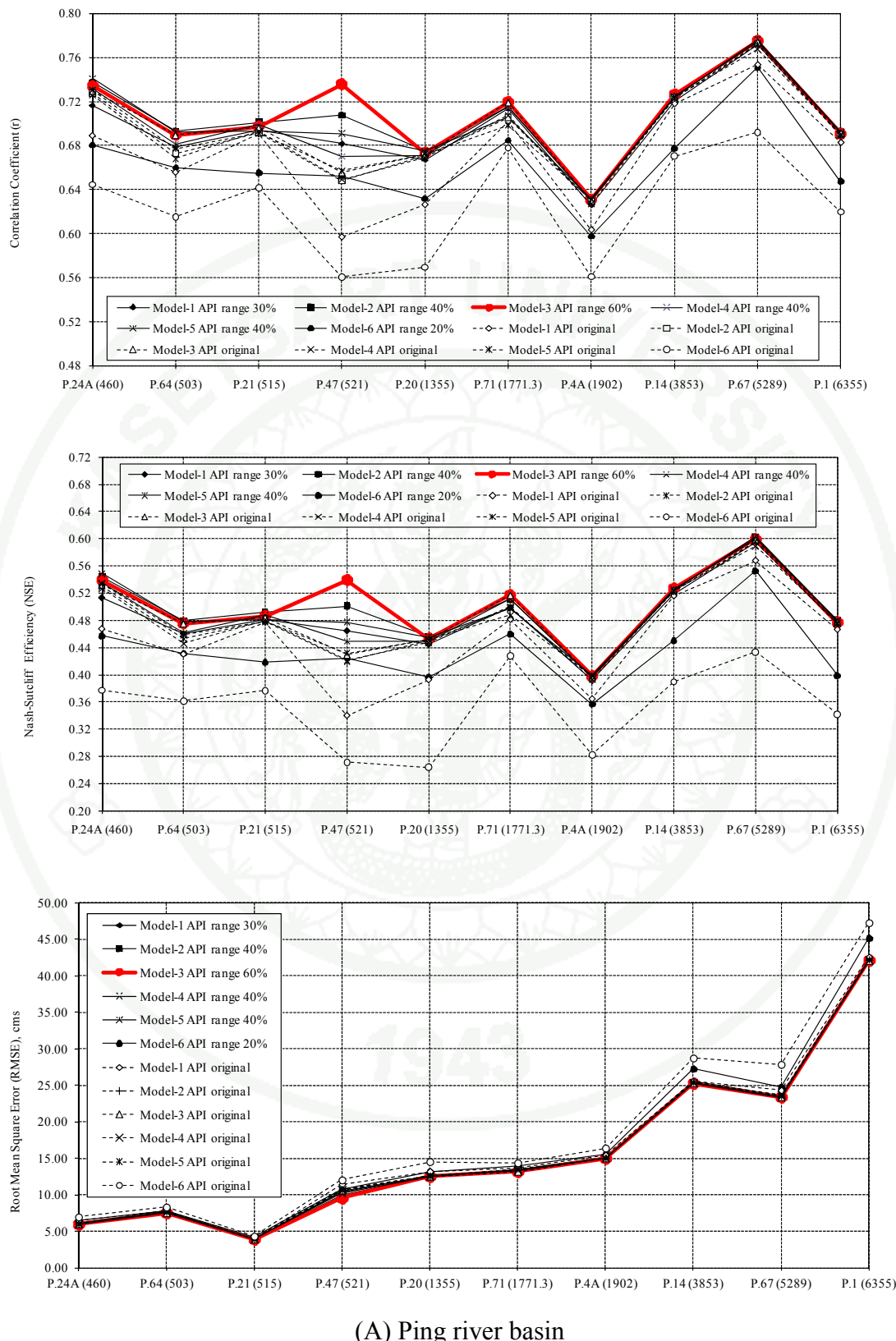
$$Q = a_3 + b_3.P + c_3.P^2 + d_3.P^3 + e_3.API + f_3.API^2 + g_3.API^3 \quad (64)$$

Table 24 Compare performances of various range of critical API range model

Model Test	NSE			r			RMSE (cms)		
	Avg	Max	Min	Avg	Max	Min	Avg	Max	Min
<i>Model 1</i>									
10% of $API_{critical}$	0.519	0.771	0.342	0.718	0.878	0.585	29.84	191.98	2.65
20% of $API_{critical}$	0.524	0.773	0.338	0.722	0.879	0.588	29.68	190.48	2.66
30% of $API_{critical}$	0.526	0.768	0.329	0.723	0.876	0.581	29.82	194.08	2.68
40% of $API_{critical}$	0.522	0.766	0.329	0.721	0.875	0.581	30.05	197.87	2.68
50% of $API_{critical}$	0.521	0.763	0.329	0.721	0.876	0.581	30.22	199.24	2.68
60% of $API_{critical}$	0.516	0.765	0.329	0.718	0.878	0.581	30.30	199.68	2.68
70% of $API_{critical}$	0.513	0.763	0.329	0.716	0.879	0.581	30.32	199.39	2.68
80% of $API_{critical}$	0.506	0.749	0.329	0.712	0.874	0.581	30.50	200.74	2.68
90% of $API_{critical}$	0.506	0.745	0.329	0.712	0.872	0.581	30.53	200.85	2.68
100% of $API_{critical}$	0.501	0.745	0.329	0.709	0.872	0.581	30.68	200.85	2.68
<i>Model 2</i>									
10% of $API_{critical}$	0.537	0.781	0.365	0.730	0.884	0.604	29.43	190.39	2.60
20% of $API_{critical}$	0.540	0.782	0.365	0.732	0.884	0.604	29.36	189.95	2.60
30% of $API_{critical}$	0.542	0.782	0.358	0.733	0.884	0.599	29.34	190.38	2.62
40% of $API_{critical}$	0.543	0.782	0.358	0.734	0.884	0.599	29.32	190.49	2.62
50% of $API_{critical}$	0.543	0.781	0.358	0.734	0.884	0.599	29.37	190.90	2.62
60% of $API_{critical}$	0.542	0.785	0.358	0.733	0.886	0.599	29.40	191.86	2.62
70% of $API_{critical}$	0.538	0.782	0.358	0.731	0.884	0.599	29.42	191.90	2.62
80% of $API_{critical}$	0.535	0.780	0.358	0.728	0.883	0.599	29.45	192.19	2.62
90% of $API_{critical}$	0.535	0.779	0.358	0.728	0.882	0.599	29.48	192.80	2.62
100% of $API_{critical}$	0.532	0.779	0.358	0.726	0.882	0.599	29.59	192.80	2.62
<i>Model 3</i>									
10% of $API_{critical}$	0.539	0.777	0.363	0.732	0.882	0.607	29.43	190.50	2.59
20% of $API_{critical}$	0.538	0.781	0.370	0.730	0.884	0.608	29.44	190.33	2.59
30% of $API_{critical}$	0.539	0.775	0.366	0.731	0.880	0.605	29.43	190.62	2.60
40% of $API_{critical}$	0.542	0.780	0.366	0.733	0.883	0.605	29.38	190.76	2.60
50% of $API_{critical}$	0.543	0.781	0.366	0.734	0.884	0.605	29.39	191.14	2.60
60% of $API_{critical}$	0.543	0.784	0.366	0.734	0.885	0.605	29.40	191.53	2.60
70% of $API_{critical}$	0.542	0.785	0.366	0.733	0.886	0.605	29.37	191.06	2.60
80% of $API_{critical}$	0.539	0.780	0.366	0.732	0.883	0.605	29.42	191.33	2.60
90% of $API_{critical}$	0.540	0.778	0.366	0.732	0.882	0.605	29.41	191.05	2.60
100% of $API_{critical}$	0.539	0.777	0.366	0.732	0.882	0.605	29.47	191.05	2.60

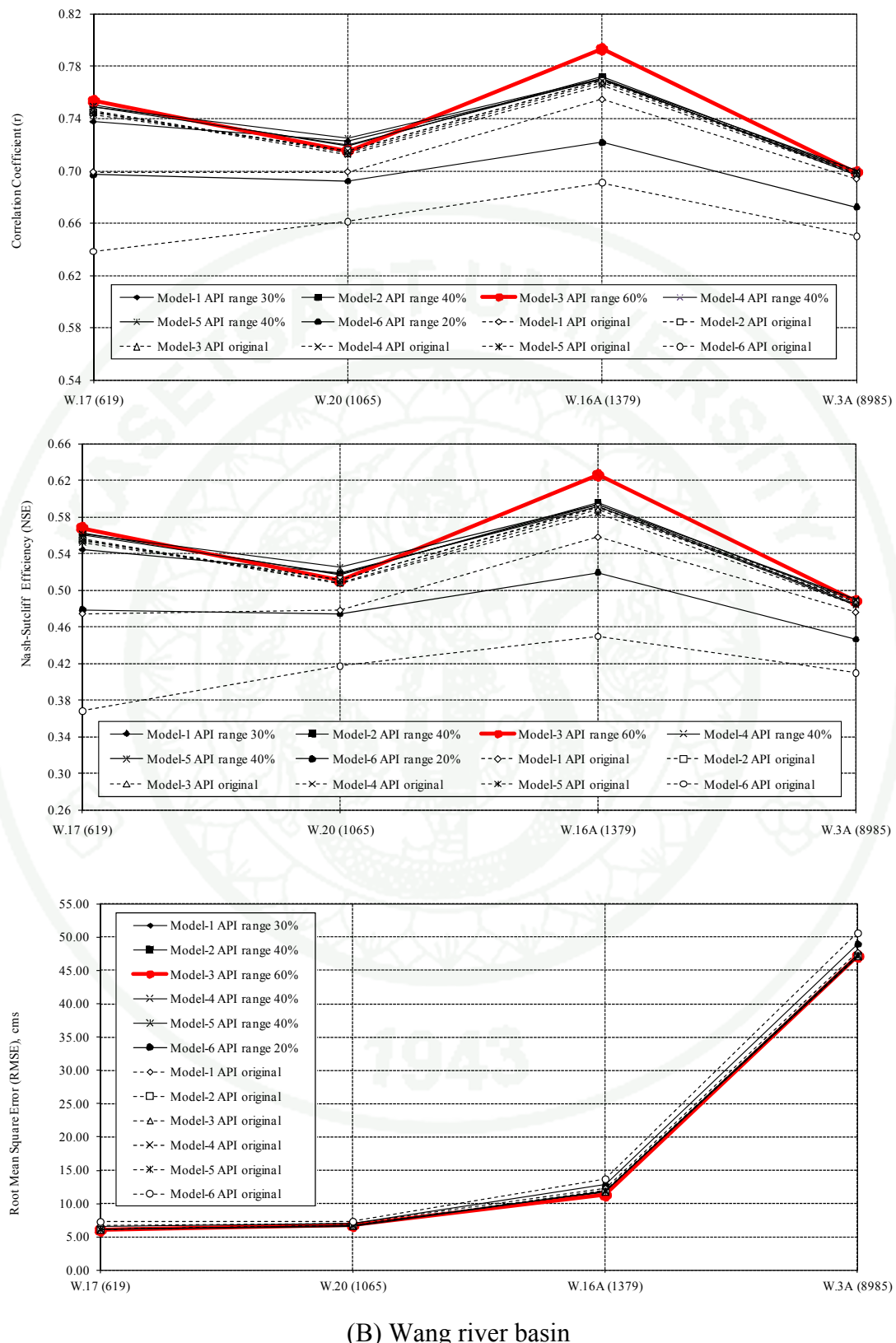
Table 24 (Continued)

Model Test	NSE			r			RMSE (cms)		
	Avg	Max	Min	Avg	Max	Min	Avg	Max	Min
<i>Model 4</i>									
10% of $API_{critical}$	0.534	0.781	0.366	0.728	0.884	0.605	29.47	190.31	2.60
20% of $API_{critical}$	0.536	0.781	0.363	0.729	0.884	0.603	29.41	190.14	2.61
30% of $API_{critical}$	0.537	0.781	0.361	0.730	0.884	0.601	29.40	190.56	2.61
40% of $API_{critical}$	0.537	0.782	0.361	0.730	0.884	0.601	29.38	190.67	2.61
50% of $API_{critical}$	0.537	0.782	0.361	0.730	0.884	0.601	29.43	190.91	2.61
60% of $API_{critical}$	0.536	0.786	0.361	0.729	0.886	0.601	29.45	191.41	2.61
70% of $API_{critical}$	0.535	0.783	0.361	0.728	0.885	0.601	29.46	191.07	2.61
80% of $API_{critical}$	0.532	0.780	0.360	0.726	0.883	0.600	29.50	191.21	2.61
90% of $API_{critical}$	0.532	0.779	0.360	0.726	0.883	0.600	29.50	191.70	2.61
100% of $API_{critical}$	0.530	0.779	0.360	0.725	0.883	0.600	29.60	191.70	2.61
<i>Model 5</i>									
10% of $API_{critical}$	0.535	0.782	0.364	0.728	0.884	0.603	29.46	190.61	2.60
20% of $API_{critical}$	0.536	0.782	0.363	0.729	0.885	0.603	29.41	190.26	2.61
30% of $API_{critical}$	0.538	0.782	0.363	0.730	0.884	0.602	29.38	190.44	2.61
40% of $API_{critical}$	0.539	0.780	0.363	0.731	0.883	0.602	29.38	191.16	2.61
50% of $API_{critical}$	0.538	0.779	0.363	0.731	0.883	0.602	29.46	192.21	2.61
60% of $API_{critical}$	0.537	0.783	0.363	0.730	0.885	0.602	29.52	194.50	2.61
70% of $API_{critical}$	0.535	0.778	0.363	0.729	0.882	0.602	29.56	194.57	2.61
80% of $API_{critical}$	0.533	0.777	0.360	0.727	0.882	0.600	29.62	195.27	2.61
90% of $API_{critical}$	0.533	0.776	0.361	0.727	0.881	0.601	29.63	195.27	2.61
100% of $API_{critical}$	0.530	0.776	0.360	0.725	0.881	0.601	29.71	195.13	2.61
<i>Model 6</i>									
10% of $API_{critical}$	0.460	0.690	0.287	0.678	0.832	0.547	32.67	218.95	2.71
20% of $API_{critical}$	0.476	0.710	0.290	0.691	0.843	0.552	31.91	208.64	2.74
30% of $API_{critical}$	0.475	0.709	0.288	0.694	0.846	0.554	32.09	211.89	2.76
40% of $API_{critical}$	0.460	0.716	0.288	0.687	0.856	0.554	32.58	217.15	2.76
50% of $API_{critical}$	0.450	0.715	0.288	0.683	0.857	0.554	32.95	218.17	2.76
60% of $API_{critical}$	0.440	0.723	0.288	0.677	0.863	0.554	33.17	220.92	2.76
70% of $API_{critical}$	0.435	0.712	0.287	0.675	0.858	0.554	33.39	222.48	2.76
80% of $API_{critical}$	0.425	0.671	0.264	0.668	0.837	0.547	33.83	227.34	2.76
90% of $API_{critical}$	0.424	0.664	0.264	0.668	0.833	0.547	33.86	227.43	2.76
100% of $API_{critical}$	0.418	0.664	0.264	0.664	0.833	0.547	34.03	227.43	2.76



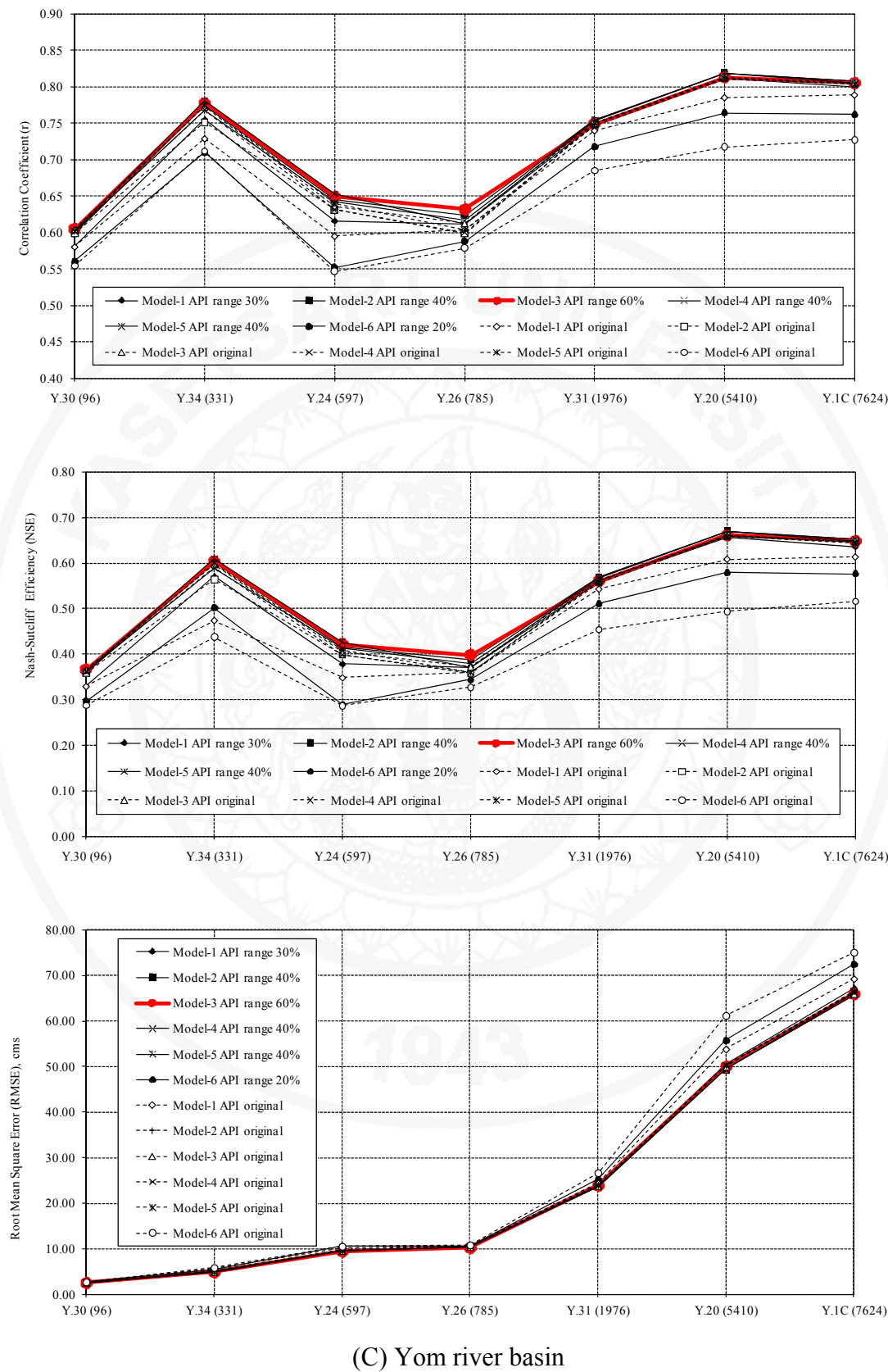
(A) Ping river basin

Figure 53 Compare performances of critical *API* range model and original *API* model



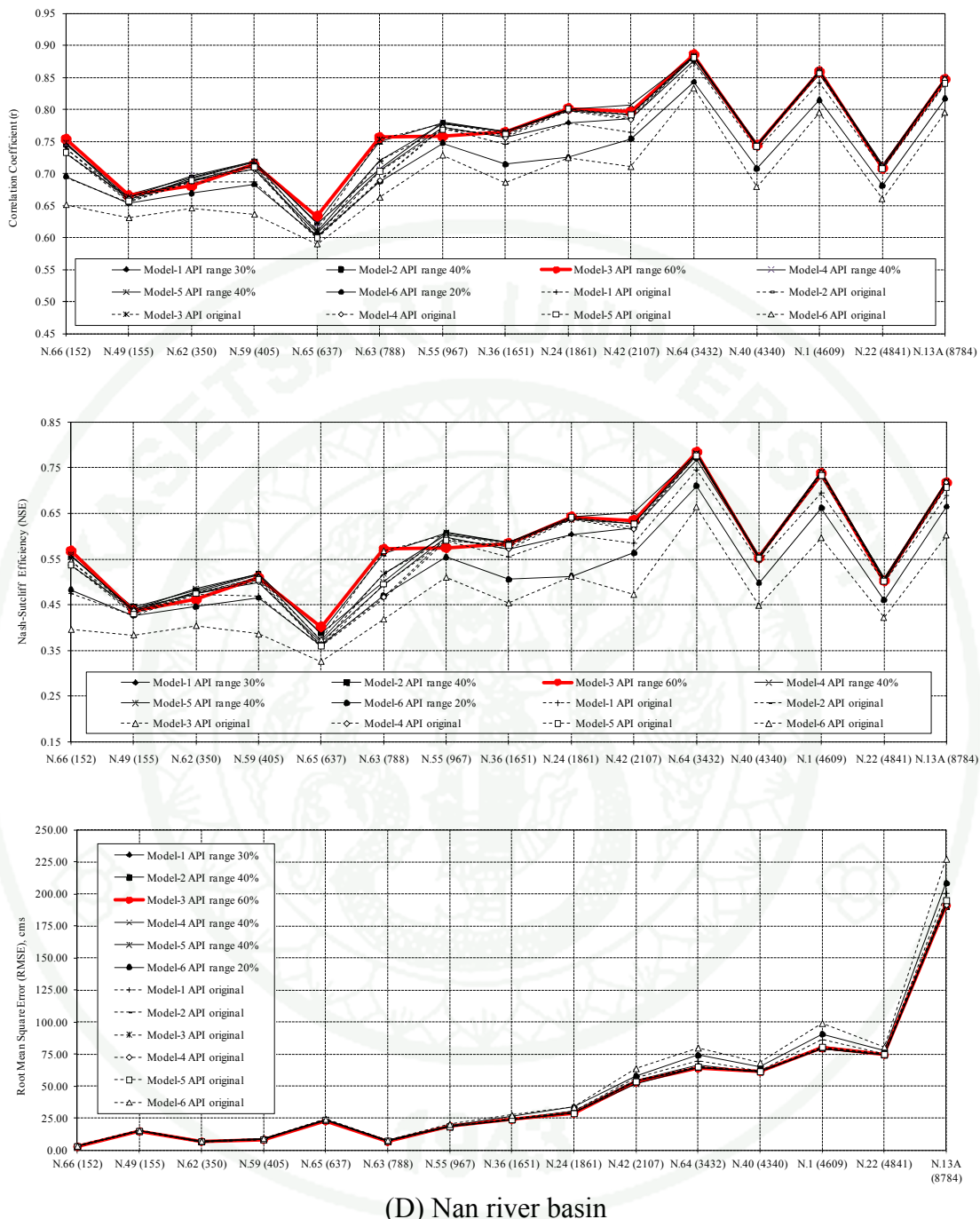
(B) Wang river basin

Figure 53 (Continued)



(C) Yom river basin

Figure 53 (Continued)



(D) Nan river basin

Figure 53 (Continued)

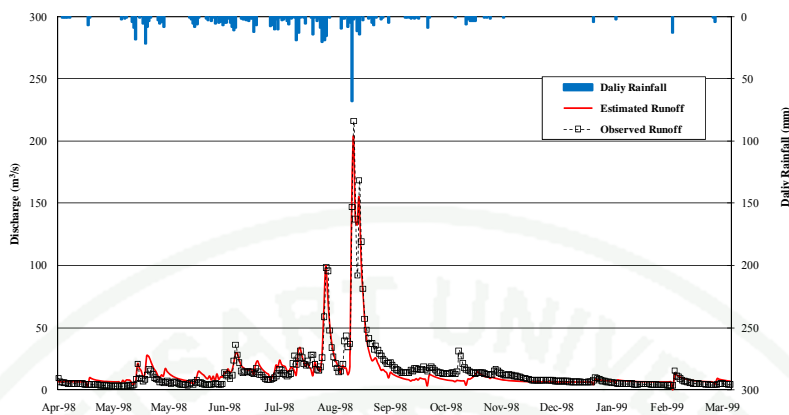
4.2 API rainfall-runoff model parameters

According to the results of *API* rainfall-runoff selection as presented above, the critical *API* range in model-3 with the range of 60% was used to analyze daily watershed runoff of 36 representative stream gauging stations during year 1977 to 2002. The stream gauging stations were selected to be used for model calibration. The results of model calibration were used to determine suitable value of each model parameter. Examples of the model calibration results for stream gauging station are shown in Figure 54; and the summary of parameter range of critical *API* range model-3 range of 60% is shown in Table 25. Moreover, the summary of model parameters was divided by sub-basins as shown below.

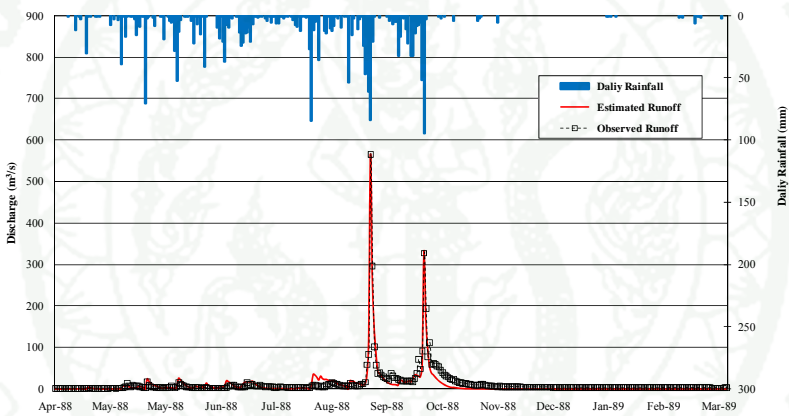
No.	Subbasin	<i>a</i>		<i>b</i>		<i>c</i>	
1.	Ping	-0.02833	-	0.64770	-0.65374	-	0.18221
2.	Wang	-0.22283	-	0.49106	-0.37323	-	0.06510
3.	Yom	-58.5312	-	0.80365	-101.779	-	1.05385
4.	Nan	-82.9189	-	1.24150	-2.01018	-	1.78326

No.	Subbasin	<i>d</i>		<i>e</i>		<i>f</i>	
1	Ping	-0.11362	-	0.00068	-0.03668	-	0.12113
2	Wang	-0.00376	-	0.00032	-0.02578	-	0.13111
3	Yom	-0.25216	-	0.08591	-134.616	-	1.87640
4	Nan	-0.35111	-	0.01566	-0.26534	-	5.48934

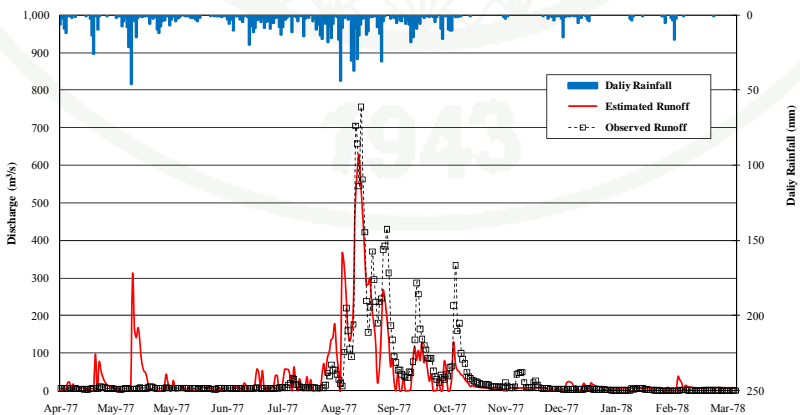
No.	Subbasin	<i>g</i>	
1	Ping	-0.00006	-
2	Wang	-0.00002	-
3	Yom	-0.03251	-
4	Nan	-0.00140	-
		0.00005	
		0.00005	
		0.00221	
		0.01085	



(a) Runoff station P.14 in year 1998 ($NSE = 0.917$, $r = 0.958$, $RMSE = 6.098 \text{ cms}$)

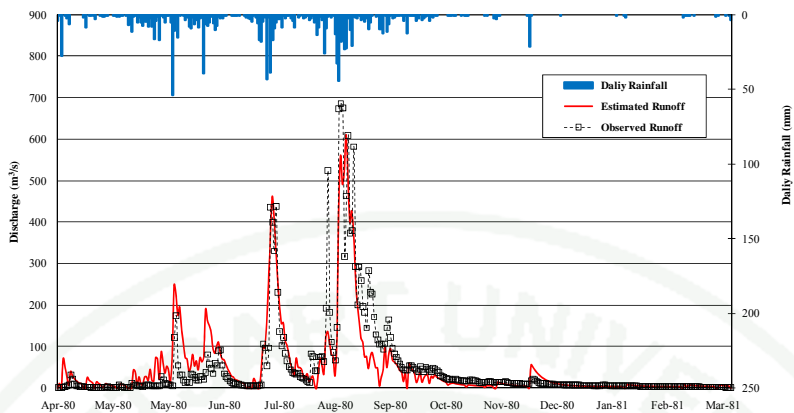


(b) Runoff station P.47 in year 1988 ($NSE = 0.945$, $r = 0.973$, $RMSE = 9.530 \text{ cms}$)

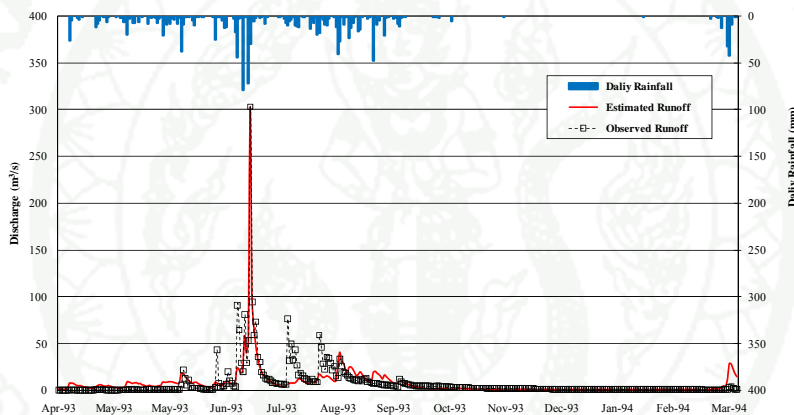


(c) Runoff station W.3A in year 1977 ($NSE = 0.701$, $r = 0.838$, $RMSE = 54.560 \text{ cms}$)

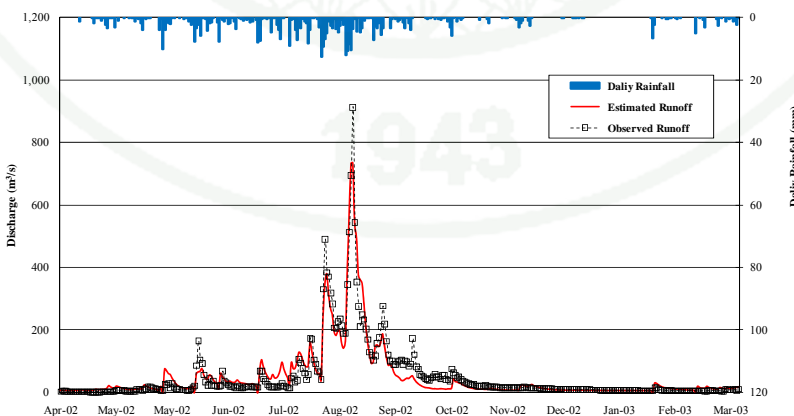
Figure 54 The model calibration results for the runoff station.



(d) Runoff station Y.20 in year 1980 ($NSE = 0.770$, $r = 0.878$, $RMSE = 49.985$ cms)



(e) Runoff station N.49 in year 1993 ($NSE = 0.805$, $r = 0.897$, $RMSE = 9.015$ cms)



(f) Runoff station N.24 in year 2002 ($NSE = 0.907$, $r = 0.953$, $RMSE = 29.653$ cms)

Figure 54 (Continued)

Table 25 Guideline for parameters of critical API range model-3 range of 60%

No.	Discharge Station	Parameters of critical API range model 3 with the range of 60%						
		a	b	c	d	e	f	g
1.	P.1	0.00000 - 0.45512	-0.26851 - 0.00129	-0.00350 - 0.05009	-0.00059 - 0.00133	-0.02121 - 0.04112	-0.00055 - 1.06881	-0.00688 - 0.00001
2.	P.14	0.00000 - 0.42628	-0.10335 - 0.03335	-0.00540 - 0.08390	-0.00036 - 0.62236	-0.00418 - 0.04531	-0.00093 - 0.82190	-0.01630 - 0.00002
3.	P.20	0.00000 - 0.57252	-0.21449 - 0.04073	-0.00737 - 0.72156	-0.00030 - 1.04964	-0.01424 - 0.07377	-0.00199 - 4.13711	-0.08082 - 0.00003
4.	P.21	0.00000 - 0.48126	-0.08956 - 0.05548	-0.01007 - 1.77891	-0.00015 - 0.51616	-0.01667 - 0.07589	-0.00238 - 5.23861	-0.14156 - 0.00002
5.	P.24A	-0.00007 - 0.48217	-0.11437 - 0.18221	-0.02233 - 0.20766	-0.11362 - 1.59861	-0.03668 - 0.10675	-0.00128 - 0.50003	-0.04877 - 0.00003
6.	P.47	-0.02159 - 0.64770	-0.21165 - 0.89456	-0.02083 - 0.47212	-0.00008 - 2.28703	-1.73078 - 0.08805	-0.00094 - 3.00339	-0.16090 - 0.00001
7.	P.4A	-0.02833 - 0.47725	-0.25223 - 0.05366	-0.00315 - 0.40710	-0.00355 - 0.14591	-0.02129 - 0.04835	-0.00151 - 2.55549	-0.01669 - 0.00002
8.	P.64	0.00000 - 0.54923	-0.08642 - 0.14599	-0.00976 - 0.01227	-0.00029 - 0.00019	-0.01747 - 0.12113	-0.00270 - 0.00230	-0.00002 - 0.00003
9.	P.67	0.00000 - 0.25607	-0.10076 - 0.00000	-0.00120 - 0.00439	-0.00009 - 0.00000	0.00000 - 0.03951	-0.00081 - 0.00059	0.00000 - 0.00001
10.	P.71	0.00000 - 0.22097	-0.65374 - 0.00000	-0.00473 - 0.04559	-0.00083 - 0.00010	-0.02090 - 0.05888	-0.00268 - 0.00257	-0.00003 - 0.00005
11.	Bhumiphol Dam	0.00000 - 0.29661	-0.32567 - 0.02989	-0.01348 - 0.04144	-0.00186 - 0.00068	-0.02535 - 0.05535	-0.00122 - 0.00379	-0.00006 - 0.00003
12.	W.16A	-0.00032 - 0.07738	-0.16576 - 0.02012	-0.00785 - 0.36907	-0.00503 - 0.00011	-0.02457 - 0.04962	-0.00185 - 0.03252	-0.00022 - 0.00003
13.	W.17	0.00000 - 0.49106	-0.34547 - 0.06510	-0.00808 - 0.35463	-0.00376 - 7.86767	-0.02322 - 0.13111	-0.00418 - 1.56932	-1.41606 - 0.00005
14.	W.20	-0.01499 - 0.14573	-0.03125 - 0.04457	-0.00960 - 0.00000	-0.00007 - 0.00022	-0.00304 - 0.03919	-0.00152 - 0.00139	-0.00001 - 0.00002
15.	W.3A	-0.22283 - 0.15112	-0.37323 - 0.02576	-0.00972 - 0.02876	-0.00060 - 0.00032	-0.02578 - 0.01550	-0.00019 - 0.00210	-0.00002 - 0.00001
16.	Y.1C	-0.03332 - 0.14705	-0.21560 - 0.03441	-0.02016 - 0.01341	-0.00048 - 0.00055	-0.03439 - 0.05175	-0.00140 - 0.00324	-0.00003 - 0.00003
17.	Y.20	0.00000 - 0.29729	-0.21009 - 0.03146	-0.01454 - 0.02555	-0.00232 - 0.00033	-0.02121 - 0.05876	-0.00141 - 0.00323	-0.00003 - 0.00004
18.	Y.24	-58.5312 - 0.48217	-101.779 - 0.51321	-0.03841 - 10.0650	-0.23194 - 1.20590	-51.0998 - 0.03106	-0.00052 - 1.52559	-0.03508 - 0.00001
19.	Y.26	-21.5268 - 0.29675	-41.8251 - 1.05385	-0.09229 - 7.32817	-0.25216 - 30.4740	-134.616 - 0.20615	-0.00071 - 23.1453	-0.83542 - 0.00002

Table 25 (Continued)

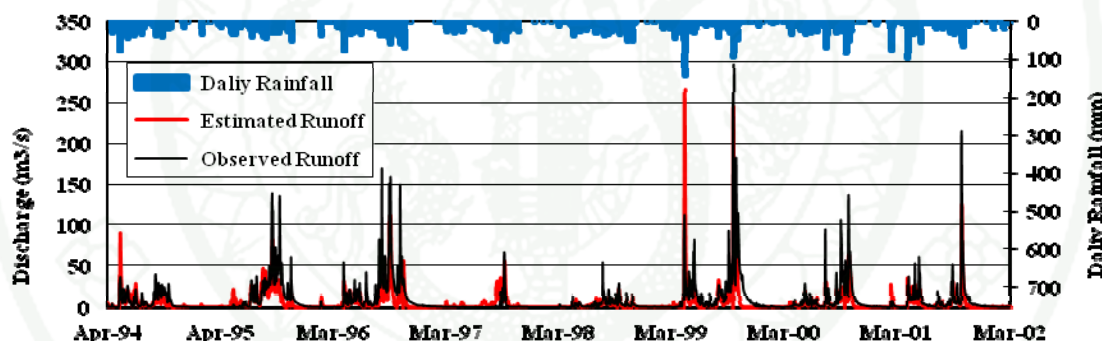
No.	Discharge Station	Parameters of critical API range model 3 with the range of 60%						
		a	b	c	d	e	f	g
20.	Y.30	-9.40784 - 0.80365	-1.31129 - 0.28356	-1.21439 - 0.55403	-0.04919 - 0.08591	-0.24595 - 1.87640	-0.09794 - 0.03654	-0.00070 - 0.00221
21.	Y.31	0.00000 - 0.27062	-0.13625 - 0.02552	-0.00717 - 0.00745	-0.00022 - 0.00006	-0.02022 - 0.04745	-0.00004 - 0.00243	-0.00001 - 0.00001
22.	Y.34	0.00000 - 0.61872	-0.51178 - 0.04620	-0.00642 - 0.16473	-0.00272 - 0.00029	-0.00021 - 0.06654	-0.00755 - 1.41012	-0.00769 - 0.00004
23.	N.1	-0.01208 - 0.67338	-0.45258 - 0.11517	-0.04522 - 0.61042	-0.00266 - 10.6790	-0.89878 - 0.13990	-0.00326 - 9.27120	-0.20314 - 0.00004
24.	N.13A	-0.01064 - 0.91348	-0.49309 - 0.16019	-0.03182 - 0.02413	-0.00017 - 0.18063	-0.77679 - 0.09686	-0.00045 - 0.89706	-0.03480 - 0.00001
25.	N.22	-0.00408 - 0.48218	-2.01018 - 0.05597	-0.00923 - 1.79511	-0.35111 - 0.30393	-0.34282 - 0.07960	-0.00077 - 0.60751	-0.08292 - 0.00000
26.	N.24	-13.1204 - 0.34971	-0.89313 - 0.58269	-0.26849 - 0.38554	-0.05252 - 0.01566	-0.04339 - 4.00222	-0.35115 - 0.03621	-0.00140 - 0.01085
27.	N.36	-0.00046 - 0.48216	-0.20111 - 0.07311	-0.00945 - 2.06684	-0.00008 - 9.87229	-0.04486 - 0.09016	-0.00111 - 5.07544	-2.58850 - 0.00001
28.	N.40	-0.00075 - 0.48216	-0.15783 - 0.05609	-0.00856 - 0.22368	-0.00038 - 0.37333	-0.07580 - 0.06870	-0.00092 - 0.54841	-0.10043 - 0.00001
29.	N.42	0.00000 - 0.45512	-0.26851 - 0.00129	-0.00350 - 0.05009	-0.00059 - 0.00133	-0.02121 - 0.04112	-0.00055 - 1.06881	-0.00688 - 0.00001
30.	N.49	-82.9189 - 1.24150	-1.43406 - 1.78326	-0.24442 - 1.12892	-0.04882 - 3.21143	-0.96169 - 5.48934	-0.10309 - 16.4575	-0.15127 - 0.00065
31.	N.55	0.00000 - 0.50882	-0.39332 - 0.14301	-0.01252 - 0.19691	-0.00013 - 0.35028	-0.07170 - 0.09246	-0.00048 - 0.48328	-0.09401 - 0.00000
32.	N.59	0.00000 - 0.39299	-0.00836 - 0.07349	-0.01105 - 0.18447	0.00000 - 0.76191	-0.00022 - 0.03988	0.00000 - 0.45269	-0.20020 - 0.00000
33.	N.62	0.00000 - 0.46186	-0.31367 - 0.02373	-0.00644 - 2.45323	-0.00029 - 1.73979	-0.01752 - 0.12611	-0.00123 - 5.92605	-0.49225 - 0.00001
34.	N.63	0.00000 - 0.13504	-0.15917 - 0.11166	-0.01231 - 0.12312	-0.00041 - 0.00538	-0.02963 - 0.02885	-0.00084 - 1.87987	-0.01197 - 0.00002
35.	N.64	-0.01086 - 0.65895	-0.39420 - 0.02043	-0.01247 - 0.05166	-0.00027 - 0.00308	-0.81111 - 0.13051	-0.00288 - 0.85887	-0.00661 - 0.00003
36.	N.65	-0.01364 - 1.01088	-0.32692 - 0.85522	-0.08769 - 6.47857	-0.05830 - 6.08215	-0.88567 - 0.06432	-0.00074 - 2.57566	-0.15568 - 0.00001
37.	N.66	-0.01919 - 0.34280	-0.27691 - 0.13423	-0.01199 - 0.16813	-0.00005 - 0.75210	-0.09483 - 0.05491	-0.00040 - 0.41346	-0.19739 - 0.00001
38.	Sirikit Dam	-0.00047 - 0.53969	-0.12587 - 0.05107	-0.01644 - 0.04914	-0.00012 - 2.41121	-0.03735 - 0.04499	-0.00013 - 0.71997	-0.08756 - 0.00000

Note: Model 3 : $Q = a + b.P + c.P^2 + d.P^3 + e.API + f.API^2 + g.API^3$

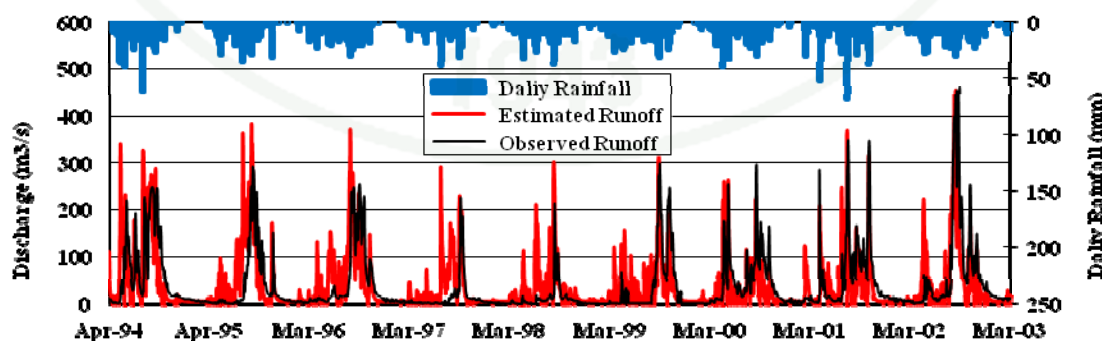
4.3 Watershed runoff prediction in an ungauged basin

The critical API range in model-3 with the range of 60% and API rainfall-runoff model parameters from topic 4.2 were used to analyze daily watershed runoff of 4 stream gauging stations. The stream gauging stations were selected to be used to determine model performance for ungauged basin runoff prediction. The results of model performances are shown in Figure 55 and below.

No.	Stream Gauging Station	Year	NSE	r	RMSE (cms)
1.	P.47	1994 - 2001	0.423	0.679	14.92
2.	W.3A	1994 - 2002	0.368	0.668	52.70
3.	Y.34	1999 - 2001	0.699	0.863	6.16
4.	N.66	1998 - 2003	0.301	0.677	6.02

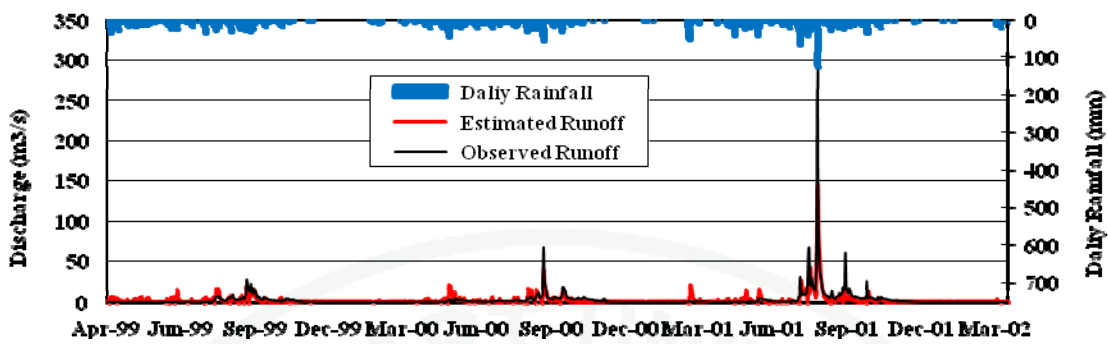


(a) Runoff station P.47 in year 1994-2001 ($NSE = 0.423$, $r = 0.679$, $RMSE = 14.92$ cms)

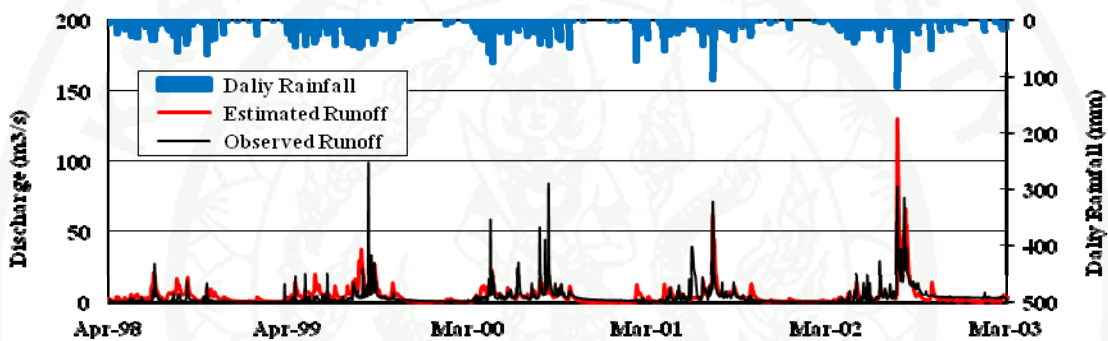


(b) Runoff station W.3A in year 1994-2002 ($NSE = 0.368$, $r = 0.668$, $RMSE = 52.70$ cms)

Figure 55 The model performance for ungauged basin.



(c) Runoff station Y.34 in year 1999-2001 ($NSE = 0.699$, $r = 0.863$, $RMSE = 6.16$ cms)



(d) Runoff station N.6 in year 1998-2003 ($NSE = 0.301$, $r = 0.677$, $RMSE = 6.02$ cms)

Figure 55 (Continued)

The finding shows that the critical API range in model-3 with the range of 60% and API rainfall-runoff model parameters from topic 4.2 is appropriate for estimating watershed runoff given that the best of Nash-Sutcliffe efficiency (NSE) is 0.301-0.699, correlation coefficient (r) is 0.668-0.863 and root mean square error ($RMSE$) is 6.02-52.70 cms; thus it indicates that the model predictions correspond to a satisfactory prediction.

4.4 Sensitivity analysis

Sensitivity analysis of critical *API* range in model-3 with the range of 60% parameters was evaluated in order to understand the characteristics of the hydrograph outputs of model are affected by the 7 significant model parameters (a, b, c, d, e, f and g) of representative stream gauging stations as shown in Table 26, which were used as initial parameters of sensitivity analysis. The results are shown as percentage difference of peak discharge, time to peak and discharge volume compare with model paremeters in Table 26. The results are shown in Table 27 to Table 30 and in the summary below.

The finding shows that if the a parameter value is increased from 10% to 30%, it will affect the peak discharge to increase from 0.09% to 1.10%, and the discharge volume to increase from 1.28% to 19.14%. On the other hand, if the a parameter value is decrease from 10% to 30%, it will affect the peak discharge decreasing 0.09% to 1.10%, and the discharge volume to decrease from 1.28% to 12.17%. Howerver, both increasing and decreasing of a parameter have an insignificant effect on time to peak.

Table 26 Model parameters of representative stream gauging stations.

Station	Year	Model Parameters						
		a	b	c	d	e	f	g
P.14	1998	0.145511	-0.028485	0.000533	-0.000013	0.015746	-0.000332	0.000011
W.17	1985	0.314383	0.013126	-0.003368	0.000001	0.009346	0.000348	0.000010
Y.20	1987	0.136684	-0.129144	0.008348	-0.000198	0.007133	0.000777	0.000002
N.24	2002	0.292782	-0.001446	-0.056624	0.000321	0.104771	0.007614	0.000253

Table 27 Sensitivity results on critical API range model parameters at P.14 station.

No.	Parameter <i>a</i>	Peak discharge (cms)	Difference of peak discharge (%)	Time to peak (day)	Difference of time to peak (%)	Discharge volume (mcm)	Difference of discharge volume (%)
1	0.101858	201.77	-0.96	160.00	0.00	448.08	4.78
2	0.116409	202.42	-0.64	160.00	0.00	386.82	-9.54
3	0.130960	203.07	-0.32	160.00	0.00	407.23	-4.77
4	0.145511	203.72	0.00	160.00	0.00	427.64	0.00
5	0.160062	204.37	0.32	160.00	0.00	468.54	9.56
6	0.174613	205.02	0.64	160.00	0.00	489.00	14.35
7	0.189164	205.67	0.96	160.00	0.00	509.47	19.14

No.	Parameter <i>b</i>	Peak discharge (cms)	Difference of peak discharge (%)	Time to peak (day)	Difference of time to peak (%)	Discharge volume (mcm)	Difference of discharge volume (%)
1	-0.037031	202.78	-0.46	160.00	0.00	427.72	-4.54
2	-0.034182	203.09	-0.31	160.00	0.00	434.50	-3.03
3	-0.031334	203.41	-0.15	160.00	0.00	441.27	-1.52
4	-0.028485	203.72	0.00	160.00	0.00	448.08	0.00
5	-0.025637	204.04	0.15	160.00	0.00	455.00	1.54
6	-0.022788	204.35	0.31	160.00	0.00	461.92	3.09
7	-0.019940	204.67	0.46	160.00	0.00	468.84	4.63

No.	Parameter <i>c</i>	Peak discharge (cms)	Difference of peak discharge (%)	Time to peak (day)	Difference of time to peak (%)	Discharge volume (mcm)	Difference of discharge volume (%)
1	0.000373	203.68	-0.02	160.00	0.00	442.00	-1.36
2	0.000426	203.69	-0.01	160.00	0.00	444.01	-0.91
3	0.000480	203.71	-0.01	160.00	0.00	446.03	-0.46
4	0.000533	203.72	0.00	160.00	0.00	448.08	0.00
5	0.000586	203.74	0.01	160.00	0.00	450.13	0.46
6	0.000640	203.75	0.01	160.00	0.00	452.18	0.92
7	0.000693	203.77	0.02	160.00	0.00	454.23	1.37

No.	Parameter <i>d</i>	Peak discharge (cms)	Difference of peak discharge (%)	Time to peak (day)	Difference of time to peak (%)	Discharge volume (mcm)	Difference of discharge volume (%)
1	-0.000017	203.72	0.00	160.00	0.00	442.40	-1.27
2	-0.000015	203.72	0.00	160.00	0.00	444.29	-0.84
3	-0.000014	203.72	0.00	160.00	0.00	446.18	-0.42
4	-0.000013	203.72	0.00	160.00	0.00	448.08	0.00
5	-0.000012	203.72	0.00	160.00	0.00	449.97	0.42
6	-0.000010	203.72	0.00	160.00	0.00	451.86	0.84
7	-0.000009	203.72	0.00	160.00	0.00	453.76	1.27

Table 27 (Continued)

No.	Parameter <i>e</i>	Peak discharge (cms)	Difference of peak discharge (%)	Time to peak (day)	Difference of time to peak (%)	Discharge volume (mcm)	Difference of discharge volume (%)
1	0.011022	187.19	-8.11	160.00	0.00	375.94	-16.10
2	0.012596	192.70	-5.41	160.00	0.00	399.97	-10.74
3	0.014171	198.21	-2.70	160.00	0.00	424.01	-5.37
4	0.015746	203.72	0.00	160.00	0.00	448.08	0.00
5	0.017320	209.23	2.70	160.00	0.00	472.19	5.38
6	0.018895	214.74	5.41	160.00	0.00	496.31	10.76
7	0.020469	220.25	8.11	160.00	0.00	520.43	16.15

No.	Parameter <i>f</i>	Peak discharge (cms)	Difference of peak discharge (%)	Time to peak (day)	Difference of time to peak (%)	Discharge volume (mcm)	Difference of discharge volume (%)
1	-0.000431	176.40	-13.41	160.00	0.00	402.40	-10.19
2	-0.000398	185.51	-8.94	160.00	0.00	417.61	-6.80
3	-0.000365	194.61	-4.47	160.00	0.00	432.84	-3.40
4	-0.000332	203.72	0.00	160.00	0.00	448.08	0.00
5	-0.000299	212.83	4.47	160.00	0.00	463.32	3.40
6	-0.000265	221.94	8.94	160.00	0.00	478.55	6.80
7	-0.000232	231.05	13.41	160.00	0.00	493.79	10.20

No.	Parameter <i>g</i>	Peak discharge (cms)	Difference of peak discharge (%)	Time to peak (day)	Difference of time to peak (%)	Discharge volume (mcm)	Difference of discharge volume (%)
1	0.000008	132.85	-34.79	160.00	0.00	381.40	-14.88
2	0.000009	156.48	-23.19	160.00	0.00	403.62	-9.92
3	0.000010	180.10	-11.60	160.00	0.00	425.85	-4.96
4	0.000011	203.72	0.00	160.00	0.00	448.08	0.00
5	0.000012	227.34	11.60	160.00	0.00	470.30	4.96
6	0.000013	250.97	23.19	160.00	0.00	492.53	9.92
7	0.000014	274.59	34.79	160.00	0.00	514.76	14.88

Table 28 Sensitivity results on critical API range model parameters at W.17 station.

No.	Parameter <i>a</i>	Peak discharge (cms)	Difference of peak discharge (%)	Time to peak (day)	Difference of time to peak (%)	Discharge volume (mcm)	Difference of discharge volume (%)
1	0.220068	60.86	-1.10	166.00	0.00	152.46	-12.17
2	0.251506	61.09	-0.73	166.00	0.00	159.49	-8.12
3	0.282945	61.31	-0.37	166.00	0.00	166.54	-4.06
4	0.314383	61.54	0.00	166.00	0.00	173.58	0.00
5	0.345821	61.76	0.37	166.00	0.00	180.63	4.06
6	0.377260	61.99	0.73	166.00	0.00	187.68	8.12
7	0.408698	62.21	1.10	166.00	0.00	194.75	12.19

No.	Parameter <i>b</i>	Peak discharge (cms)	Difference of peak discharge (%)	Time to peak (day)	Difference of time to peak (%)	Discharge volume (mcm)	Difference of discharge volume (%)
1	0.009188	61.15	-0.62	166.00	0.00	171.27	-1.33
2	0.010501	61.28	-0.42	166.00	0.00	172.03	-0.90
3	0.011813	61.41	-0.21	166.00	0.00	172.80	-0.45
4	0.013126	61.54	0.00	166.00	0.00	173.58	0.00
5	0.014439	61.67	0.21	166.00	0.00	174.36	0.45
6	0.015751	61.79	0.42	166.00	0.00	175.14	0.90
7	0.017064	61.92	0.62	166.00	0.00	175.93	1.35

No.	Parameter <i>c</i>	Peak discharge (cms)	Difference of peak discharge (%)	Time to peak (day)	Difference of time to peak (%)	Discharge volume (mcm)	Difference of discharge volume (%)
1	-0.004379	60.20	-2.17	166.00	0.00	164.41	-5.28
2	-0.004042	60.65	-1.45	166.00	0.00	167.19	-3.68
3	-0.003705	61.09	-0.72	166.00	0.00	170.31	-1.89
4	-0.003368	61.54	0.00	166.00	0.00	173.58	0.00
5	-0.003032	61.98	0.72	166.00	0.00	177.03	1.99
6	-0.002695	62.43	1.45	166.00	0.00	180.57	4.03
7	-0.002358	62.87	2.17	166.00	0.00	184.13	6.07

No.	Parameter <i>d</i>	Peak discharge (cms)	Difference of peak discharge (%)	Time to peak (day)	Difference of time to peak (%)	Discharge volume (mcm)	Difference of discharge volume (%)
1	0.0000006	61.53	-0.01	166.00	0.00	173.51	-0.04
2	0.0000007	61.53	-0.01	166.00	0.00	173.53	-0.03
3	0.0000008	61.54	0.00	166.00	0.00	173.56	-0.01
4	0.0000009	61.54	0.00	166.00	0.00	173.58	0.00
5	0.0000010	61.54	0.00	166.00	0.00	173.60	0.01
6	0.0000011	61.54	0.01	166.00	0.00	173.63	0.03
7	0.0000012	61.54	0.01	166.00	0.00	173.65	0.04

Table 28 (Continued)

No.	Parameter <i>e</i>	Peak discharge (cms)	Difference of peak discharge (%)	Time to peak (day)	Difference of time to peak (%)	Discharge volume (mcm)	Difference of discharge volume (%)
1	0.006543	59.89	-2.67	166.00	0.00	164.08	-5.47
2	0.007477	60.44	-1.78	166.00	0.00	167.23	-3.66
3	0.008412	60.99	-0.89	166.00	0.00	170.40	-1.83
4	0.009346	61.54	0.00	166.00	0.00	173.58	0.00
5	0.010281	62.09	0.89	166.00	0.00	176.76	1.83
6	0.011216	62.63	1.78	166.00	0.00	179.93	3.66
7	0.012150	63.18	2.67	166.00	0.00	183.12	5.49

No.	Parameter <i>f</i>	Peak discharge (cms)	Difference of peak discharge (%)	Time to peak (day)	Difference of time to peak (%)	Discharge volume (mcm)	Difference of discharge volume (%)
1	0.000243	56.53	-8.14	166.00	0.00	161.33	-7.06
2	0.000278	58.20	-5.42	166.00	0.00	165.40	-4.71
3	0.000313	59.87	-2.71	166.00	0.00	169.48	-2.36
4	0.000348	61.54	0.00	166.00	0.00	173.58	0.00
5	0.000382	63.21	2.71	166.00	0.00	177.69	2.36
6	0.000417	64.88	5.42	166.00	0.00	181.79	4.73
7	0.000452	66.54	8.14	166.00	0.00	185.90	7.10

No.	Parameter <i>g</i>	Peak discharge (cms)	Difference of peak discharge (%)	Time to peak (day)	Difference of time to peak (%)	Discharge volume (mcm)	Difference of discharge volume (%)
1	0.000007	49.45	-19.64	166.00	0.00	156.86	-9.64
2	0.000008	53.48	-13.09	166.00	0.00	162.42	-6.43
3	0.000009	57.51	-6.55	166.00	0.00	167.98	-3.23
4	0.000010	61.54	0.00	166.00	0.00	173.58	0.00
5	0.000011	65.57	6.55	166.00	0.00	179.18	3.23
6	0.000012	69.59	13.09	166.00	0.00	184.79	6.46
7	0.000013	73.62	19.64	166.00	0.00	190.39	9.69

Table 29 Sensitivity results on critical API range model parameters at Y.20 station.

No.	Parameter <i>a</i>	Peak discharge (cms)	Difference of peak discharge (%)	Time to peak (day)	Difference of time to peak (%)	Discharge volume (mcm)	Difference of discharge volume (%)
1	0.095679	835.51	-0.31	145.00	0.00	1,056.80	-6.61
2	0.109347	836.36	-0.20	145.00	0.00	1,081.57	-4.42
3	0.123016	837.22	-0.10	145.00	0.00	1,106.50	-2.22
4	0.136684	838.07	0.00	145.00	0.00	1,131.58	0.00
5	0.150353	838.93	0.10	145.00	0.00	1,156.75	2.22
6	0.164021	839.78	0.20	145.00	0.00	1,182.09	4.46
7	0.177689	840.64	0.31	145.00	0.00	1,207.46	6.71

No.	Parameter <i>b</i>	Peak discharge (cms)	Difference of peak discharge (%)	Time to peak (day)	Difference of time to peak (%)	Discharge volume (mcm)	Difference of discharge volume (%)
1	-0.167887	828.07	-1.19	145.00	0.00	1,021.61	-9.72
2	-0.154973	831.41	-0.80	145.00	0.00	1,052.72	-6.97
3	-0.142058	834.74	-0.40	145.00	0.00	1,088.19	-3.83
4	-0.129144	838.07	0.00	145.00	0.00	1,131.58	0.00
5	-0.116229	841.41	0.40	145.00	0.00	1,180.44	4.32
6	-0.103315	844.74	0.80	145.00	0.00	1,235.92	9.22
8	-0.090401	848.07	1.19	145.00	0.00	1,294.50	14.40

No.	Parameter <i>c</i>	Peak discharge (cms)	Difference of peak discharge (%)	Time to peak (day)	Difference of time to peak (%)	Discharge volume (mcm)	Difference of discharge volume (%)
1	0.005844	835.41	-0.32	145.00	0.00	1,018.98	-9.95
2	0.006678	836.30	-0.21	145.00	0.00	1,048.05	-7.38
3	0.007513	837.18	-0.11	145.00	0.00	1,083.45	-4.25
4	0.008348	838.07	0.00	145.00	0.00	1,131.58	0.00
5	0.009183	838.96	0.11	145.00	0.00	1,193.23	5.45
6	0.010018	839.85	0.21	145.00	0.00	1,260.68	11.41
7	0.010852	969.27	15.65	144.00	-0.69	1,343.01	18.68

No.	Parameter <i>d</i>	Peak discharge (cms)	Difference of peak discharge (%)	Time to peak (day)	Difference of time to peak (%)	Discharge volume (mcm)	Difference of discharge volume (%)
1	-0.000257	837.81	-0.03	145.00	0.00	1,043.56	-7.78
2	-0.000237	837.90	-0.02	145.00	0.00	1,067.27	-5.68
3	-0.000218	837.99	-0.01	145.00	0.00	1,096.26	-3.12
4	-0.000198	838.07	0.00	145.00	0.00	1,131.58	0.00
5	-0.000178	838.16	0.01	145.00	0.00	1,174.36	3.78
6	-0.000158	889.25	6.11	144.00	-0.69	1,229.92	8.69
7	-0.000139	1051.13	25.42	144.00	-0.69	1,296.14	14.54

Table 29 (Continued)

No.	Parameter <i>e</i>	Peak discharge (cms)	Difference of peak discharge (%)	Time to peak (day)	Difference of time to peak (%)	Discharge volume (mcm)	Difference of discharge volume (%)
1	0.004993	822.97	-1.80	145.00	0.00	1,074.20	-5.07
2	0.005706	828.01	-1.20	145.00	0.00	1,093.29	-3.38
3	0.006420	833.04	-0.60	145.00	0.00	1,112.40	-1.69
4	0.007133	838.07	0.00	145.00	0.00	1,131.58	0.00
5	0.007846	843.11	0.60	145.00	0.00	1,150.80	1.70
6	0.008560	848.14	1.20	145.00	0.00	1,170.07	3.40
7	0.009273	853.17	1.80	145.00	0.00	1,189.38	5.11

No.	Parameter <i>f</i>	Peak discharge (cms)	Difference of peak discharge (%)	Time to peak (day)	Difference of time to peak (%)	Discharge volume (mcm)	Difference of discharge volume (%)
1	0.000544	652.84	-22.10	145.00	0.00	880.02	-22.23
2	0.000621	714.58	-14.73	145.00	0.00	963.11	-14.89
3	0.000699	776.33	-7.37	145.00	0.00	1,046.78	-7.49
4	0.000777	838.07	0.00	145.00	0.00	1,131.58	0.00
5	0.000854	899.82	7.37	145.00	0.00	1,216.66	7.52
6	0.000932	961.56	14.73	145.00	0.00	1,302.30	15.09
7	0.001010	1023.31	22.10	145.00	0.00	1,388.27	22.68

No.	Parameter <i>g</i>	Peak discharge (cms)	Difference of peak discharge (%)	Time to peak (day)	Difference of time to peak (%)	Discharge volume (mcm)	Difference of discharge volume (%)
1	0.0000015	781.95	-6.70	145.00	0.00	1,089.98	-3.68
2	0.0000017	800.66	-4.46	145.00	0.00	1,103.85	-2.45
3	0.0000019	819.37	-2.23	145.00	0.00	1,117.71	-1.23
4	0.0000021	838.07	0.00	145.00	0.00	1,131.58	0.00
5	0.0000023	856.78	2.23	145.00	0.00	1,145.45	1.23
6	0.0000025	875.49	4.46	145.00	0.00	1,159.31	2.45
7	0.0000027	894.19	6.70	145.00	0.00	1,173.18	3.68

Table 30 Sensitivity results on critical API range model parameters at N.24 station.

No.	Parameter <i>a</i>	Peak discharge (cms)	Difference of peak discharge (%)	Time to peak (day)	Difference of time to peak (%)	Discharge volume (mcm)	Difference of discharge volume (%)
1	0.204947	733.21	-0.26	157.00	0.00	1,471.55	-3.85
2	0.234225	733.84	-0.17	157.00	0.00	1,491.17	-2.56
3	0.263504	734.47	-0.09	157.00	0.00	1,510.78	-1.28
4	0.292782	735.10	0.00	157.00	0.00	1,530.40	0.00
5	0.322060	735.73	0.09	157.00	0.00	1,550.01	1.28
6	0.351338	736.36	0.17	157.00	0.00	1,569.63	2.56
7	0.380616	736.99	0.26	157.00	0.00	1,589.25	3.85

No.	Parameter <i>b</i>	Peak discharge (cms)	Difference of peak discharge (%)	Time to peak (day)	Difference of time to peak (%)	Discharge volume (mcm)	Difference of discharge volume (%)
1	-0.001880	735.06	-0.005	157.00	0.00	1,530.11	-0.02
2	-0.001736	735.08	-0.003	157.00	0.00	1,530.21	-0.01
3	-0.001591	735.09	-0.002	157.00	0.00	1,530.30	-0.01
4	-0.001446	735.10	0.00	157.00	0.00	1,530.40	0.00
5	-0.001302	735.11	0.002	157.00	0.00	1,530.50	0.01
6	-0.001157	735.12	0.003	157.00	0.00	1,530.59	0.01
7	-0.001012	735.13	0.005	157.00	0.00	1,530.69	0.02

No.	Parameter <i>c</i>	Peak discharge (cms)	Difference of peak discharge (%)	Time to peak (day)	Difference of time to peak (%)	Discharge volume (mcm)	Difference of discharge volume (%)
1	-0.073611	729.86	-0.71	157.00	0.00	1,475.73	-3.57
2	-0.067948	731.61	-0.48	157.00	0.00	1,492.24	-2.49
3	-0.062286	733.35	-0.24	157.00	0.00	1,511.21	-1.25
4	-0.056624	735.10	0.00	157.00	0.00	1,530.40	0.00
5	-0.050961	746.20	1.51	156.00	-0.64	1,550.09	1.29
6	-0.045299	759.31	3.29	156.00	-0.64	1,570.57	2.62
7	-0.039637	772.43	5.08	156.00	-0.64	1,591.41	3.99

No.	Parameter <i>d</i>	Peak discharge (cms)	Difference of peak discharge (%)	Time to peak (day)	Difference of time to peak (%)	Discharge volume (mcm)	Difference of discharge volume (%)
1	0.000225	734.99	-0.02	157.00	0.00	1,528.00	-0.16
2	0.000257	735.02	-0.01	157.00	0.00	1,528.80	-0.10
3	0.000289	735.06	-0.01	157.00	0.00	1,529.60	-0.05
4	0.000321	735.10	0.00	157.00	0.00	1,530.40	0.00
5	0.000353	735.14	0.01	157.00	0.00	1,531.20	0.05
6	0.000385	735.17	0.01	157.00	0.00	1,532.00	0.10
7	0.000417	735.40	0.04	156.00	-0.64	1,532.80	0.16

Table 30 (Continued)

No.	Parameter <i>e</i>	Peak discharge (cms)	Difference of peak discharge (%)	Time to peak (day)	Difference of time to peak (%)	Discharge volume (mcm)	Difference of discharge volume (%)
1	0.073340	707.30	-3.78	157.00	0.00	1,384.67	-9.52
2	0.083817	716.57	-2.52	157.00	0.00	1,433.25	-6.35
3	0.094294	725.83	-1.26	157.00	0.00	1,481.82	-3.17
4	0.104771	735.10	0.00	157.00	0.00	1,530.40	0.00
5	0.115248	744.37	1.26	157.00	0.00	1,579.03	3.18
6	0.125725	753.63	2.52	157.00	0.00	1,627.85	6.37
7	0.136202	762.90	3.78	157.00	0.00	1,676.75	9.56

No.	Parameter <i>f</i>	Peak discharge (cms)	Difference of peak discharge (%)	Time to peak (day)	Difference of time to peak (%)	Discharge volume (mcm)	Difference of discharge volume (%)
1	0.005330	652.15	-11.28	157.00	0.00	1,356.06	-11.39
2	0.006091	679.80	-7.52	157.00	0.00	1,414.18	-7.59
3	0.006852	707.45	-3.76	157.00	0.00	1,472.29	-3.80
4	0.007614	735.10	0.00	157.00	0.00	1,530.40	0.00
5	0.008375	763.94	3.92	156.00	-0.64	1,588.54	3.80
6	0.009136	794.80	8.12	156.00	-0.64	1,646.88	7.61
7	0.009898	825.65	12.32	156.00	-0.64	1,705.21	11.42

No.	Parameter <i>g</i>	Peak discharge (cms)	Difference of peak discharge (%)	Time to peak (day)	Difference of time to peak (%)	Discharge volume (mcm)	Difference of discharge volume (%)
1	0.0001769	622.05	-15.38	157.00	0.00	1,394.72	-8.87
2	0.0002022	659.73	-10.25	157.00	0.00	1,439.95	-5.91
3	0.0002274	697.42	-5.13	157.00	0.00	1,485.17	-2.96
4	0.0002527	735.10	0.00	157.00	0.00	1,530.40	0.00
5	0.0002780	777.50	5.77	156.00	-0.64	1,575.63	2.96
6	0.0003032	821.92	11.81	156.00	-0.64	1,620.85	5.91
7	0.0003285	866.33	17.85	156.00	-0.64	1,666.16	8.87

The finding shows that if the b parameter value is increased from 10% to 30%, it will affect the peak discharge to increase from 0.002% to 1.19%, and the discharge volume to increase from 0.01% to 14.40%. On the other hand, if the b parameter value is decreased from 10% to 30%, it will affect the peak discharge to decrease from 0.002% to 1.19%, and the discharge volume to decrease from 0.01% to 9.72%. However, both increasing and decreasing of b parameter have an insignificant effect on time to peak.

The finding shows that if the c parameter value is increased from 10% to 30%, it will affect the peak discharge to increase from 0.01% to 15.65%, and the discharge volume to increase from 0.46% to 18.68%. On the other hand, if the c parameter value is decrease from 10% to 30%, it will affect the peak discharge to decrease from 0.01% to 2.17%, and the discharge volume to decrease from 0.46% to 9.95%. However, both increasing and decreasing of c parameter have an insignificant effect on time to peak.

The finding shows that if the d parameter value is increased from 10% to 30%, it will affect the peak discharge to increase from 0.01% to 25.42% except at P.14 station, and the discharge volume to increase from 0.01% to 14.54%. On the other hand, if the d parameter value is decrease from 10% to 30%, it will affect the peak discharge to decrease from 0.01% to 0.03% except at P.14 station, and the discharge volume to decrease from 0.01% to 7.78%. However, both increasing and decreasing of d parameter have an insignificant effect on time to peak.

The finding shows that if the e parameter value is increased from 10% to 30%, it will affect the peak discharge to increase from 0.06% to 8.11%, and the discharge volume to increase from 1.70% to 16.15%. On the other hand, if the e parameter value is decrease from 10% to 30%, it will affect the peak discharge to decrease from 0.06% to 8.11%, and the discharge volume to decrease from 1.69% to 16.10%. However, both increasing and decreasing of e parameter have an insignificant effect on time to peak.

The finding shows that if the f parameter value is increased from 10% to 30%, it will affect the peak discharge to increase from 2.71% to 22.10%, and the discharge volume to increase from 2.36% to 22.68%. On the other hand, if the f parameter value is decrease from 10% to 30%, it will affect the peak discharge to decrease from 2.71% to 22.10%, and the discharge volume to decrease from 2.36% to 22.23%. However, both increasing and decreasing of f parameter have an insignificant effect on time to peak.

The finding shows that if the g parameter value is increased from 10% to 30%, it will affect the peak discharge to increase from 2.23% to 34.79%, and the discharge volume to increase from 1.23% to 14.88%. On the other hand, if the g parameter value is decrease from 10% to 30%, it will affect the peak discharge to decrease from 2.23% to 34.79%, and the discharge volume to decrease from 1.23% to 14.88%. However, both increasing and decreasing of g parameter have an insignificant effect on time to peak.

4.5 Watershed runoff prediction by *API* model

The results of areal daily rainfall and daily antecedent precipitation index (*API*) of small watersheds in the upper Chao Phraya river basin (Figure 18 and Appendix Table C7) and model parameters were used to predict watershed runoff of 112 small watersheds by using critical *API* range in model-3 with the range of 60% as shown in equation (62) to (64) as shown in Figure 56. The results of watershed runoff prediction were used as input data for hydrologic routing model.

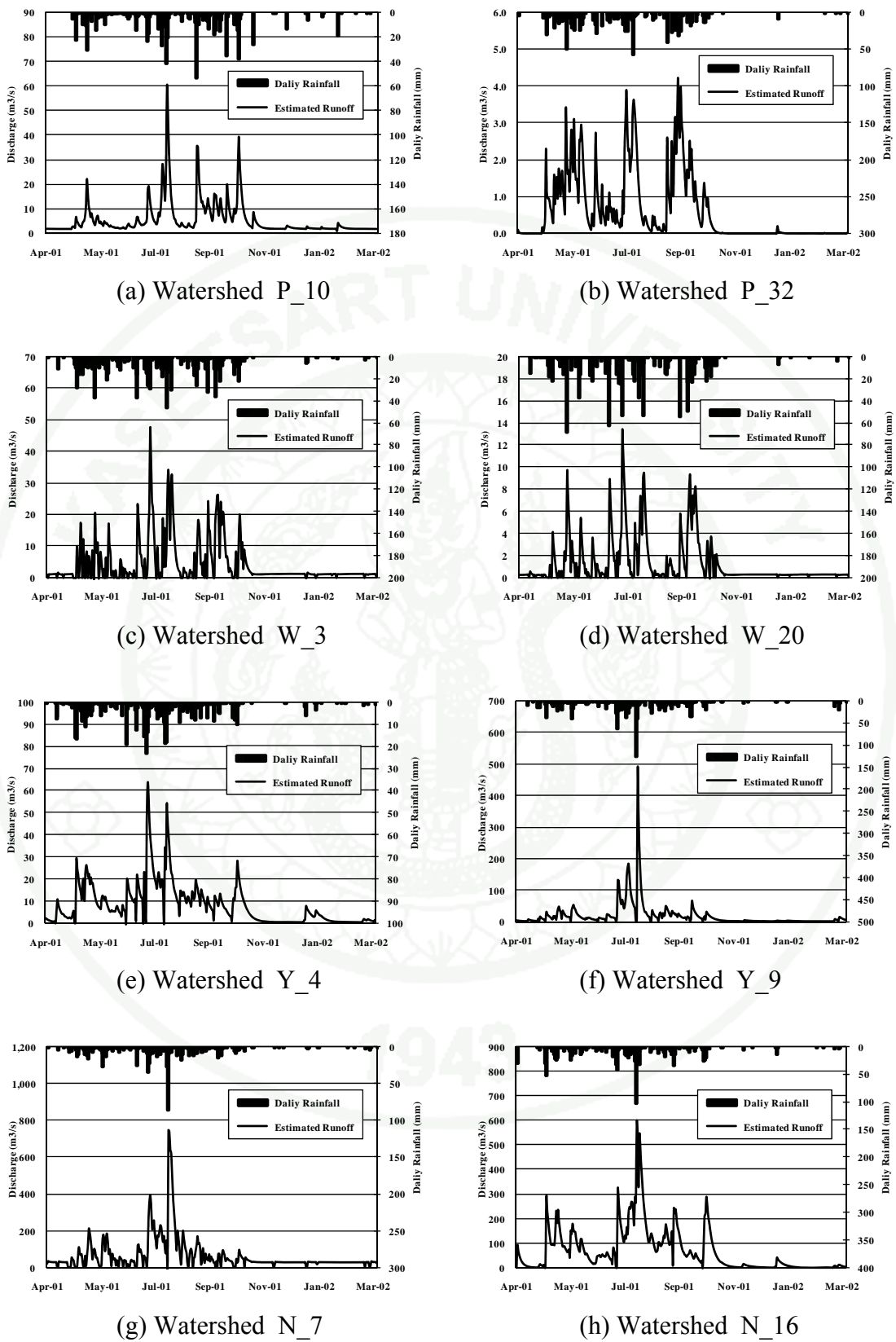


Figure 56 Examples of watershed runoff estimation in year 2001.

5. Hydrological routing

HEC-HMS model was set up by using input data and schematic diagram of the upper Chao Phraya river network which was divided into upper Ping river network, upper Nan river network and downstream of Bhumibol dam and Sirikit dam as shown in Figure 57 to 59 respectively.

The results of outflow hydrographs routing of 112 small watersheds by using Muskingum routing model of HEC-HMS model during year 1994 to 2002 and the calibration and verification on 12 stream gauging stations and inflow of Bhumibol dam and Sirikit dam at the major reach of the upper Chao Phraya river network are shown in Figure 60. The statistical values resulting from model calibration and verification are shown below.

No.	Calibration Point	Year 1994-2002		
		NSE	r	RMSE (cms)
1.	P.1	0.677	0.823	33.62
2.	P.2A	0.610	0.802	83.00
3.	P.7A	0.409	0.763	121.76
4.	P.16	0.490	0.771	152.62
5.	W.3A	0.632	0.796	48.73
6.	Y.1C	0.579	0.769	95.57
7.	Y.3A	0.633	0.815	118.90
8.	Y.17	0.473	0.801	153.62
9.	N.5A	0.686	0.853	134.19
10.	N.12A	0.919	0.960	46.92
11.	N.13A	0.759	0.872	214.19
12.	C.2	0.636	0.817	419.28
13.	Bhumibol Dam	0.684	0.840	141.88
14.	Sirikit Dam	0.523	0.945	211.15

The length of main channel (L) and the average channel slope (S_{avg}) of major reach were used as input data for channel routing models. Major reach length varies from 2.90 to 139.92 kilometer, and the average slope varies from 0.000004 to 0.001294 while the average major reach length and the average slope of the upper Chao Phraya river basin are 43.96 and 0.000387 respectively, as shown in Table 31.

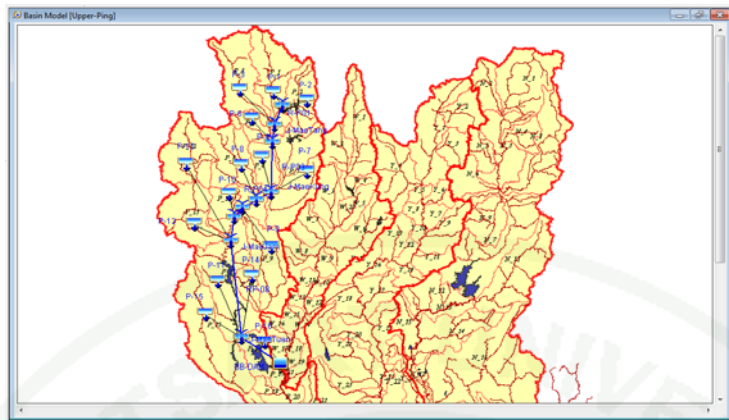


Figure 57 The upper Ping river network model of HEC-HMS model.

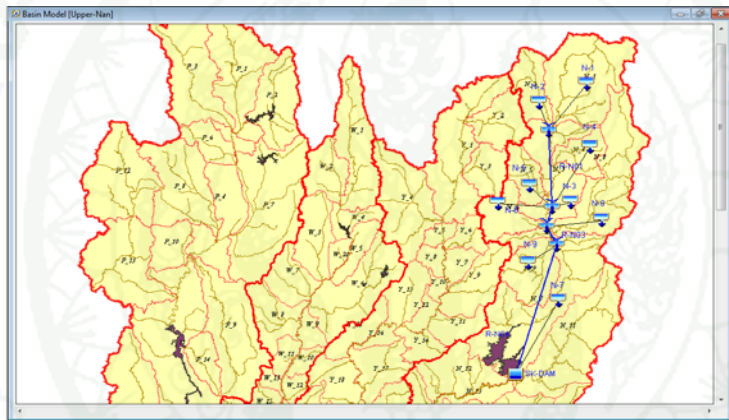


Figure 58 The upper Nan river network model of HEC-HMS model.

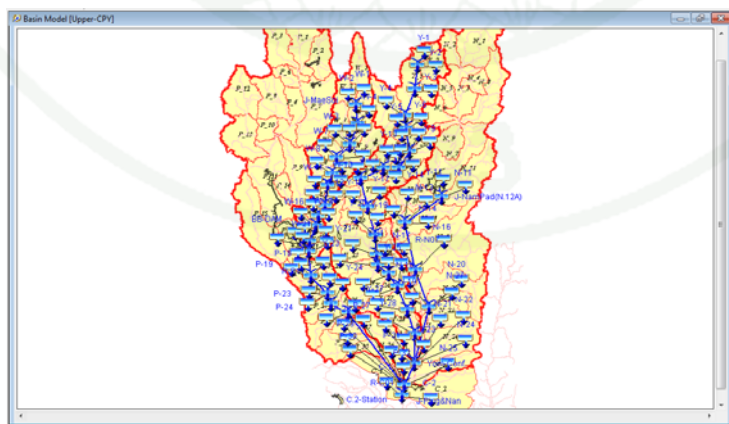
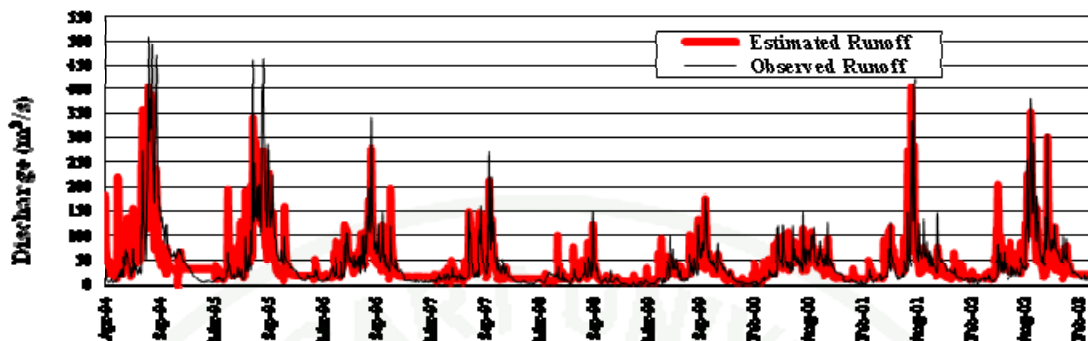
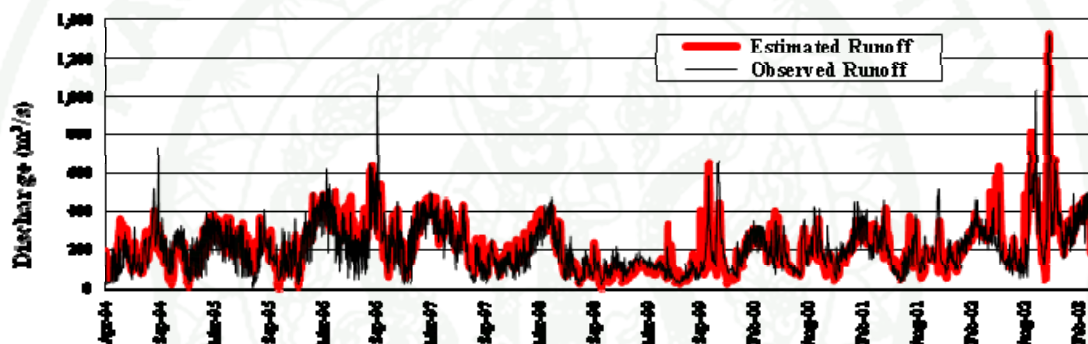


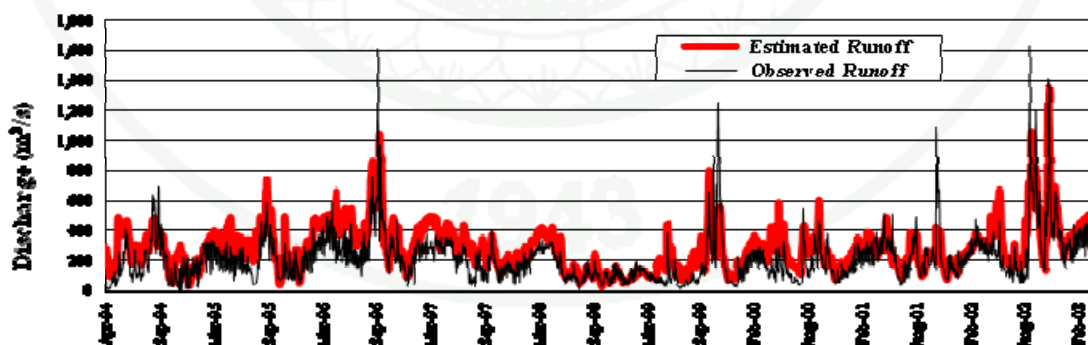
Figure 59 The upper Chao Phraya river network model of HEC-HMS model (downstream of Bhumibol dam and Sirikit dam).



(a) Runoff station P.1 in year 1994-2002 ($NSE = 0.677$, $r = 0.823$, $RMSE = 33.62$ cms)

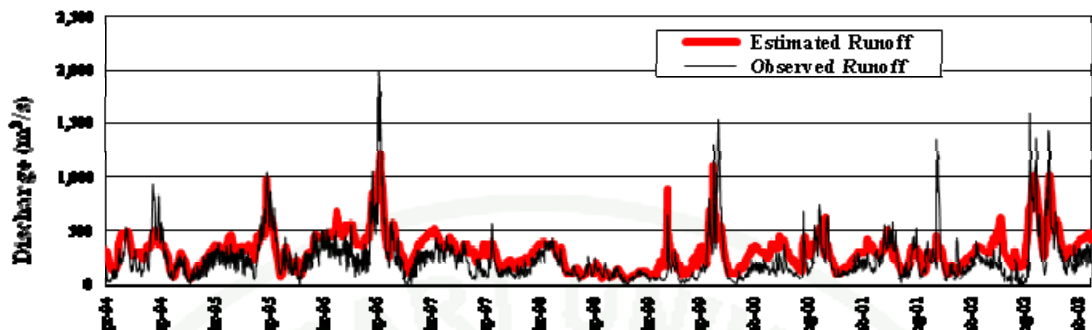


(b) Runoff station P.2A in year 1994-2002 ($NSE = 0.610$, $r = 0.802$, $RMSE = 83.00$ cms)

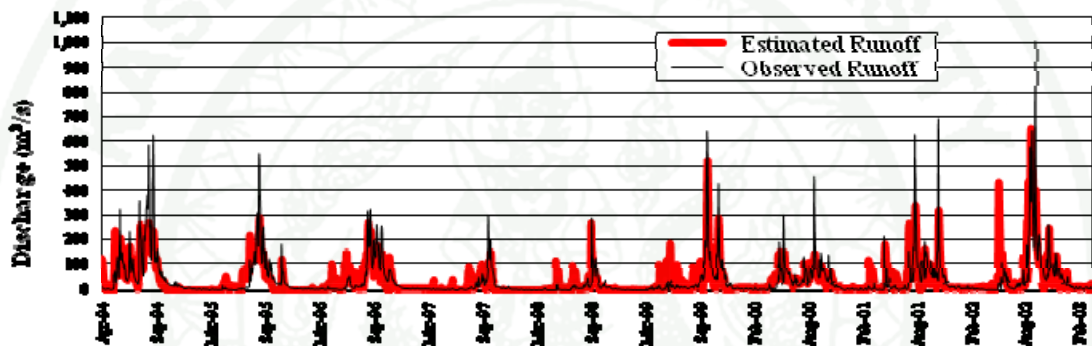


(c) Runoff station P.7A in year 1994-2002 ($NSE = 0.409$, $r = 0.763$, $RMSE = 121.76$ cms)

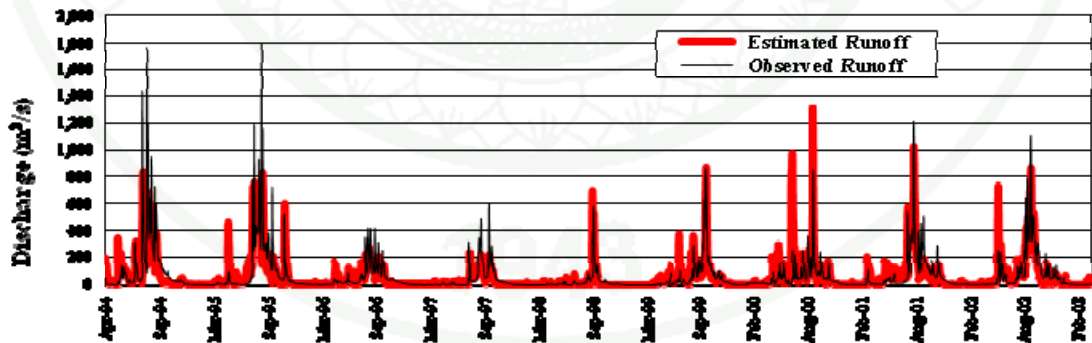
Figure 60 Comparison of the calculate and observed outflow hydrographs at major reach of the upper Chao Phraya river network



(d) Runoff station P.16 in year 1994-2002 ($NSE = 0.490$, $r = 0.771$, $RMSE = 152.62$ cms)

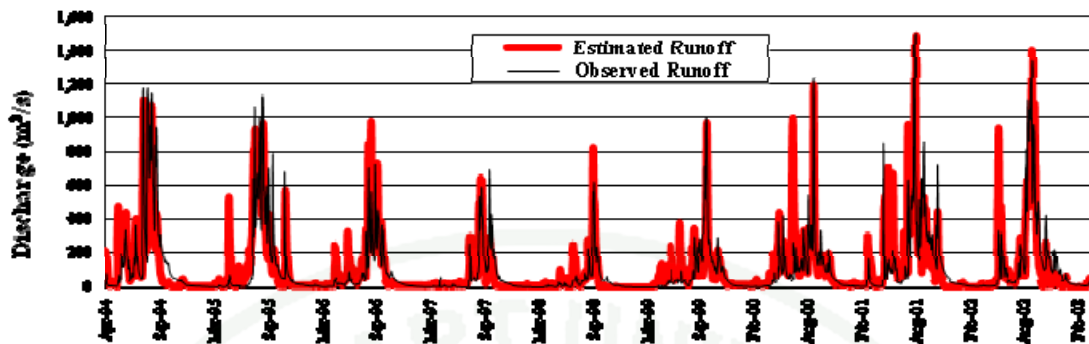


(e) Runoff station W.3A in year 1994-2002 ($NSE = 0.632$, $r = 0.796$, $RMSE = 48.73$ cms)

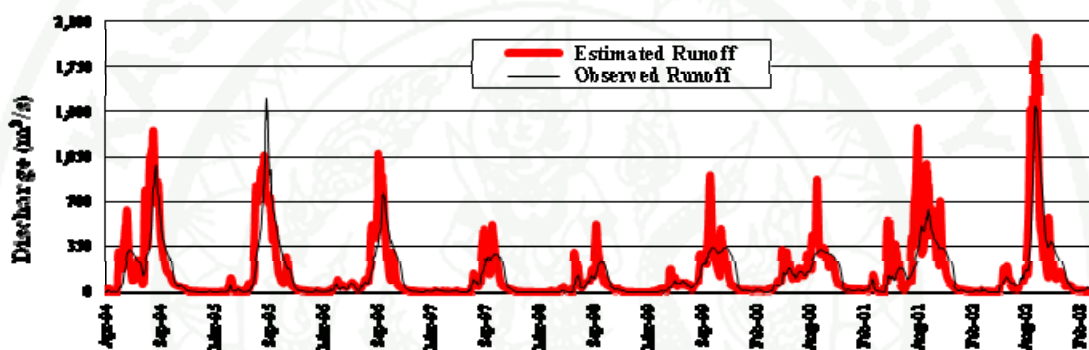


(f) Runoff station Y.1C in year 1994-2002 ($NSE = 0.579$, $r = 0.769$, $RMSE = 95.57$ cms)

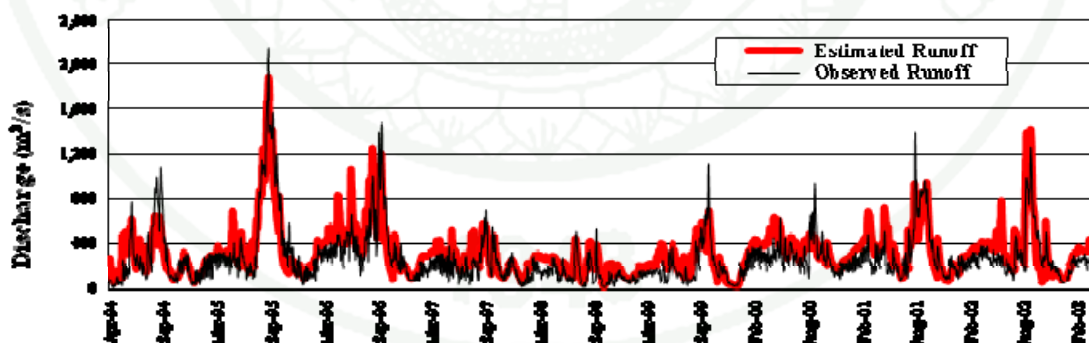
Figure 60 (Continued)



(g) Runoff station Y.3A in year 1994-2002 ($NSE = 0.633$, $r = 0.815$, $RMSE = 118.90$ cms)

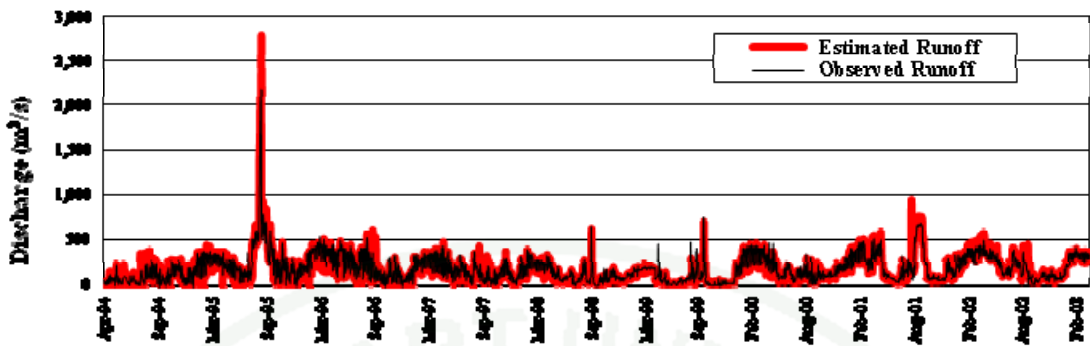


(h) Runoff station Y.17 in year 1994-2002 ($NSE = 0.473$, $r = 0.801$, $RMSE = 153.62$ cms)

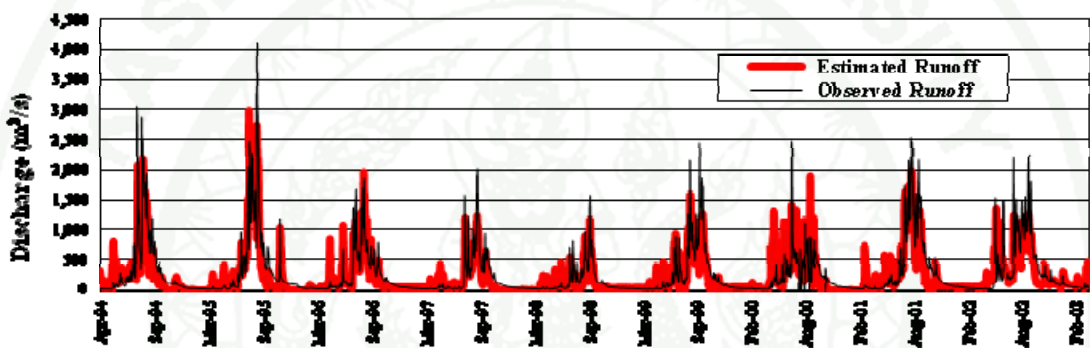


(i) Runoff station N.5A in year 1994-2002 ($NSE = 0.686$, $r = 0.853$, $RMSE = 134.19$ cms)

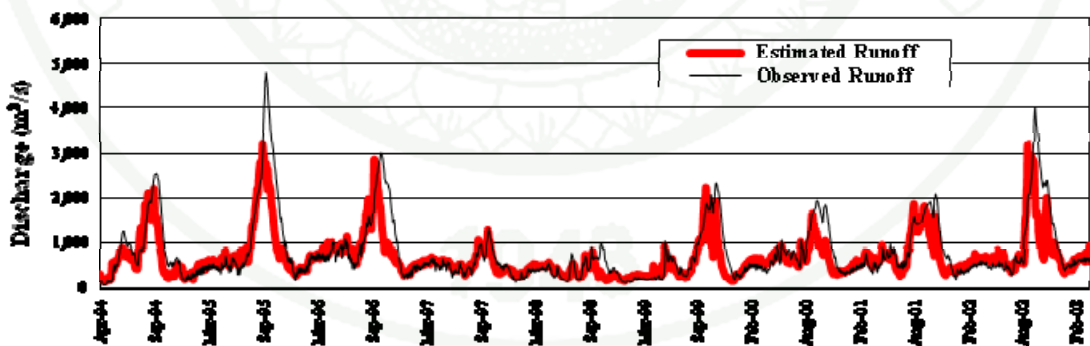
Figure 60 (Continued)



(j) Runoff station N.12A in year 1994-2002 ($NSE = 0.919$, $r = 0.906$, $RMSE = 46.92$ cms)

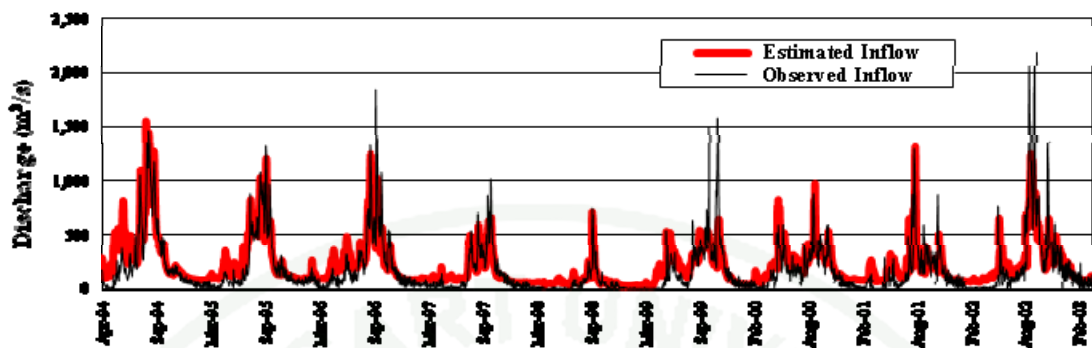


(k) Runoff station N.13A in year 1994-2002 ($NSE = 0.759$, $r = 0.872$, $RMSE = 214.19$ cms)

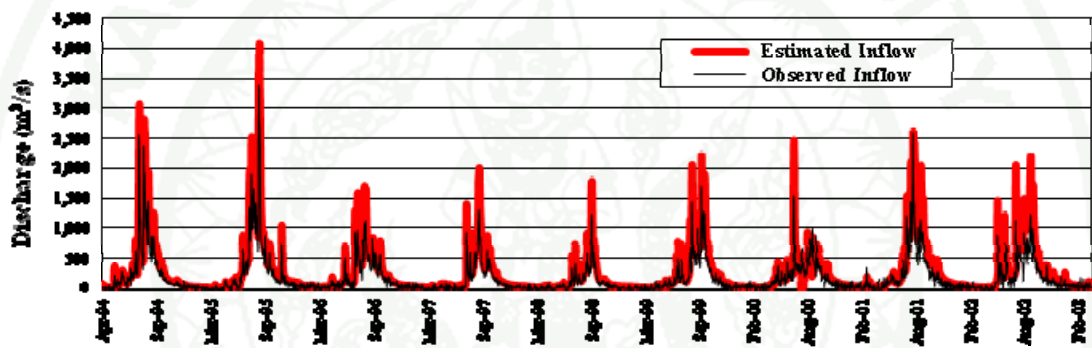


(l) Runoff station C.2 in year 1994-2002 ($NSE = 0.636$, $r = 0.817$, $RMSE = 419.28$ cms)

Figure 60 (Continued)



(m) Bhumibol Dam in year 1994-2002 ($NSE = 0.684$, $r = 0.840$, $RMSE = 141.88 \text{ cms}$)



(n) Sirikit Dam in year 1994-2002 ($NSE = 0.523$, $r = 0.945$, $RMSE = 211.15 \text{ cms}$)

Figure 60 (Continued)

Table 31 Summary parameters of HEC-HMS model

No.	Reach	<i>L</i> (km.)	Slope (<i>S_{avg}</i>)	Major Reach		Muskingum	
				Upstream	Downstream	<i>K</i>	<i>X</i>
1.	R-P01	15.32	0.00031	Mae Ngad	Mae Tang	2.18	0.20
2.	R-P02	28.50	0.00044	Mae Tang	Mae Rim	6.09	0.20
3.	R-P03	55.11	0.00046	Mae Rim	Mae Kung	9.29	0.30
4.	R-P04	12.08	0.00064	Mae Kung	Mae Khan	1.98	0.30
5.	R-P05	24.25	0.00020	Mae Khan	Mae Li	4.21	0.30
6.	R-P06	10.07	0.00022	Mae Li	Mae Khlang	1.75	0.30
7.	R-P07	32.73	0.00049	Mae Khlang	Mae Jam	5.51	0.30
8.	R-P08	128.18	0.00017	Mae Jam	Mae Tuen	18.75	0.30
9.	R-P09	59.56	0.00021	Mae Tuen	Bhumibol Dam	10.35	0.30
10.	R-P10	24.31	0.00129	Bhumibol Dam	Mae Wang	19.31	0.15
11.	R-P11	37.45	0.00050	Mae Wang	Huai Mae Thor	23.14	0.15
12.	R-P12	27.49	0.00028	Huai Mae Thor	Khlong Wang Jao	25.47	0.10
13.	R-P13	18.84	0.00034	Khlong Wang Jao	Khlong Mae Raka	13.10	0.10
14.	R-P14	19.59	0.00052	Khlong Mae Raka	Khlong Sua Mak	13.62	0.10
15.	R-P15	139.92	0.00027	Khlong Sua Mak	Nan River	129.66	0.05
16.	R-W01	31.99	0.00067	Mae Soi	Kiu Lom Dam	11.86	0.20
17.	R-W02	53.32	0.00078	Kiu Lom Dam	Mae Tui	19.76	0.20
18.	R-W03	22.61	0.00050	Mae Tui	Mae Jang	9.67	0.20
19.	R-W04	15.02	0.00022	Mae Jang	Mae Tam	7.59	0.20
20.	R-W05	32.84	0.00035	Mae Tam	Amphoe Sop Prab	16.60	0.20
21.	R-W06	15.24	0.00096	Amphoe Sop Prab	Huai Mae Pa	5.65	0.20
22.	R-W07	30.47	0.00096	Huai Mae Pa	Amphoe Thern	15.40	0.15
23.	R-W08	33.62	0.00006	Amphoe Thern	Amphoe Mae Prik	18.69	0.15
24.	R-W09	51.40	0.00033	Amphoe Mae Prik	Huai Mae Chiang Rai	25.98	0.15
25.	R-W10	34.27	0.00033	Huai Mae Chiang Rai	Ping River	17.32	0.15
26.	R-Y01	57.02	0.00087	Khan River	Pee River	15.10	0.20
27.	R-Y02	49.11	0.00093	Pee River	Ngaow River	13.00	0.20
28.	R-Y03	24.74	0.00052	Ngaow River	Song River	6.55	0.20
29.	R-Y04	47.50	0.00037	Song River	Kum Me	13.90	0.20
30.	R-Y05	4.29	0.00034	Kum Me	Amphoe Sung Men	0.90	0.15
31.	R-Y06	65.38	0.00047	Amphoe Sung Men	Mae Tar	13.67	0.15
32.	R-Y07	54.50	0.00044	Mae Tar	Huai Mae Bong	11.39	0.15
33.	R-Y08	54.50	0.00044	Huai Mae Bong	Huai Mae Sin	11.39	0.15
34.	R-Y09	63.43	0.00024	Huai Mae Sin	Huai Tha Pair	13.26	0.15
35.	R-Y10	41.71	0.00017	Huai Tha Pair	Huai Mae Mok	28.99	0.10
36.	R-Y11	8.87	0.00015	Huai Mae Mok	Huai Mae Rampan	6.16	0.10
37.	R-Y12	66.71	0.00011	Huai Mae Rampan	Huai Bong	46.36	0.10
38.	R-Y13	66.71	0.00011	Huai Bong	Khong Bang Kaow	46.36	0.10
39.	R-Y14	42.89	0.00008	Khong Bang Kaow	Huai Yai	39.74	0.10
40.	R-Y15	43.92	0.00009	Huai Yai	Khlong Nong Sano	40.70	0.10

Table 31 (Continued)

No.	Reach Code	L (km.)	Slope (S_{avg})	Major Reach		Muskingum	
				Upstream	Downstream	K	X
41.	R-Y16	44.45	0.000004	Khlong Nong Sano	Nan River	41.19	0.10
42.	R-N01	99.55	0.00036	Yao River	Sa River	42.58	0.20
43.	R-N02	3.44	0.00026	Sa River	Na Wa River	1.47	0.20
44.	R-N03	5.87	0.00092	Na Wa River	Hang River	0.96	0.10
45.	R-N04	34.32	0.00072	Hang River	Sirikit Dam	5.61	0.10
46.	R-N05	2.90	0.00052	Sirikit Dam	Pad River	1.79	0.10
47.	R-N06	105.19	0.00024	Pad River	Khlong Tron	97.48	0.10
48.	R-N07	110.22	0.00008	Khlong Tron	Kaew Noi River	102.14	0.10
49.	R-N08	83.77	0.00004	Kaew Noi River	Wang Thong River	116.44	0.05
50.	R-N09	108.96	0.00004	Wang Thong River	Yom River	121.16	0.05
51.	R-N10	35.88	0.00003	Yom River	Ping River	66.50	0.10
52.	R-C01	5.72	0.00010	Ping and Nan River	C.2 stations	10.60	0.10

The finding shows that parameter of travel time of the flood wave through routing reach (K) of Muskingum routing model varies from 1.75 to 129.66 with the average of 18.96 for Ping river basin; it varies from 5.65 to 25.98 with the average of 14.85 for Wang river basin; it varies from 0.90 to 46.36 with the average of 21.79 for Yom river basin; it varies from 0.96 to 121.16 with the average of 55.61 for Nan river basin and overall of the upper Chao Phraya river basin varies from 0.90 to 129.66 with the average of 25.93 as shown in Table 31.

In addition, the finding shows that parameter of dimensionless weighting factor (X) of Muskingum routing model varies from 0.05 to 0.30 with the average of 0.21 for Ping river basin; it varies from 0.15 to 0.20 with the average of 0.18 for Wang river basin; it varies from 0.10 to 0.20 with the average of 0.14 for Yom river basin; it varies from 0.05 to 0.20 with the average of 0.11 for Nan river basin and overall of the upper Chao Phraya river basin varies from 0.05 to 0.30 with the average of 0.16 as shown in Table 31.

CONCLUSION AND RECOMMENDATION

This study show that the rainfall-runoff model by using relationship between antecedent precipitation index (API), daily rainfall and daily discharge has the capacity of predicting daily watershed runoff of both gauged basin and ungauged basin. API rainfall-runoff model has its strong points because it is easy to apply, time-saving; and lastly, it doesn't require a lot of data inputs, and only requires existing data. However, this model also has a weak point which is the fact that it can't adjust the parameter of model in order to calibrate time to peak of hydrograph. Therefore, it should be further developed in the future in order to fix its weakness, and to improve its capability of estimating hourly watershed runoff.

The conclusion and recommendation for the study on “watershed runoff prediction, streamflow analysis and river modeling in the Chao Phraya river basin” is described as follows.

Objective 1: *Using long-term period of weather data to evaluate reference evapotranspiration (ET_o) and using Mann-Kendall statistical test, determine the trends of weather variables, reference evapotranspiration parameters and reference evapotranspiration in the upper Chao Phraya river basin.*

The FAO Penman-Monteith method was used to estimate reference evapotranspiration (ET_o) of the upper Chao Phraya river basin by using weather parameters were collected by Thailand Meteorological Department (TMD) from 1977 to 2006. The results show that the daily average of reference evapotranspiration (ET_o) varies from 2.86 mm/day in December to 5.35 mm/day in April.

The Mann-Kendall was applied to detect trends of weather variables, ET_o parameters and reference evapotranspiration (ET_o), which has resulted in the identification of significant trends in the upper Chao Phraya river basin. The trends have various directions which are both increasing and decreasing, only decreasing trends, only increasing trends, and insignificant trends.

Trend analysis of weather variables showed decreasing trends in wind speed while the increasing trends were shown in air temperature and relative humidity. Moreover, both increasing and decreasing trends were shown in evaporation, sunshine and rainfall.

Trend analysis of the ET_o parameters showed increasing trends in soil heat flux and the actual vapor pressure while the decreasing trends were shown in vapor pressure deficit and net radiation.

The weather variables and ET_o parameters decrease the trends of reference evapotranspiration (ET_o) in the upper Chao Phraya river basin which is composed of relative humidity, wind speed, actual vapour pressure, vapour pressure deficit and net radiation. In addition, reference evapotranspiration (ET_o) trends conform to the trends of relative humidity and wind speed which are the most sensitive variables.

A comparison between trend of pan evaporation and the estimated reference evapotranspiration (ET_o) shows that the evaporation values increase rapidly with increasing air temperatures but the ET_o values significantly increase with decreasing relative humidity and increasing wind speed.

Objective 2: *Using daily rainfall data and soil moisture data with reference evapotranspiration information to evaluate antecedent precipitation index (API) relationship for the upper Chao Phraya river basin.*

The results of reference evapotranspiration (ET_o), areal daily rainfall and soil water recession coefficient (K) were used to calculate daily antecedent precipitation index (API) in the upper Chao Phraya river basin.

The areal daily rainfall was analysed by using daily rainfall data from 116 rainfall stations of Thai Meteorological Department (TMD) in the upper Chao Phraya river basin for a 30-year period (1974-2003) by Thiessen technique.

The soil moisture data was used to calculate maximum soil moisture available for evaporation (W_m) of surface soil (0-10 cm) in the upper Chao Phraya river basin that varies from 18.18 to 26.75 mm with the average of 23.05 mm. Therefore, W_m and reference evapotranspiration (ET_o) were used to analyse soil water recession coefficient (K) that varies from 0.791 to 0.883 mm/day with the average of 0.842 mm.

Daily antecedent precipitation index (*API*) from 1977 to 2003 of 112 small watersheds in the upper Chao Phraya river basin was evaluated by using the relationship between antecedent precipitation index (*API*) and daily rainfall of Kohler & Linsley (1951). The finding shows that *API* varies from 2.55 mm/day in December to 54.63 mm/day in September with the average of 17.27 mm/day.

Soil data was collected from 197 soil testing results. Most of the soil boring test site were located in highland and upstream of watershed. For this reason, it is recommended that the soil testing should have more testing sites in lower land and flat plain area in order to be suitable of calculating the maximum soil moisture available for evaporation (W_m) and antecedent precipitation index (*API*); thus improving *API* rainfall-runoff model accuracy.

Objective 3: *Using land use data and crop coefficient (K_c), adjust the recession coefficient (K) of antecedent precipitation index (*API*) and using adjusted K to evaluate antecedent precipitation index (*API*) relationship.*

The agriculture landuse data, crop coefficient (K_c) and reference evapotranspiration (ET_o) were used to calculate evapotranspiration (ET). Thereafter, evapotranspiration (ET) was used to improve the soil water recession coefficient (K) of antecedent precipitation index (*API*) by using evapotranspiration (K_{adj}) instead of reference evapotranspiration (ET_o) for calculating adjusted soil water recession coefficient. After that K_{adj} was used to analyse *API* adjusted by evapotranspiration (API_{adj}).

In the upper Chao Phraya river basin, soil water recession coefficient adjusted by evapotranspiration (K_{adj}) varies from 0.810 – 0.978 mm/day with the average of 0.889 mm/day. The results show that adjusted K is higher than original K from 1.32 to 16.17 percentages in March to September while original K is higher than adjusted K from 0.73 to 3.41 percentage in October to February. In addition, soil water recession coefficient adjusted by evapotranspiration (K_{adj}) was used to analyse daily API adjusted by evapotranspiration (API_{adj}) of 112 small watersheds during year 1977 to 2003. The results show that the average of API_{adj} in the upper Chao Phraya river basin is 30.90 mm/day which varies from 10.00 mm/day in December to 62.47 mm/day in May.

Comparison between the results of daily original API and daily API adjusted by evapotranspiration (API_{adj}) shows that the daily average of API adjusted is higher than original API of the same time from 7.82 to 481.64 percentage. Furthermore, the values of API adjusted by evapotranspiration (API_{adj}) are higher in May and September while the value of original API is the highest in September.

The results of critical antecedent precipitation index ($API_{critical}$) were used to improve API rainfall-runoff model of the upper Chao Phraya river basin that varies from 199.41 – 293.23 mm with the average of 237.90 mm

Objective 4: *Using antecedent precipitation index (API) to develop a rainfall-runoff model and to compare the result from the original recession coefficient (K) and adjusted K (K_{adj}).*

Comparison between daily watershed runoff of representative stream gauging stations by using the 6 models of relationship between antecedent precipitation index (API) and daily rainfall is shown in equation (47) to (52) and daily watershed runoff by using the 6 models of relationship between daily rainfall and API adjusted by evapotranspiration (API_{adj}) using adjusted soil water recession coefficient (K_{adj}) is shown in equation (56) to (61). The finding shows that the daily runoff estimated by original API uses original K given that the Nash-Sutcliffe efficiency (NSE), correlation

coefficient (r) and root mean square error ($RMSE$) are better than API adjusted model by evapotranspiration (API_{adj}). Moreover, the results show that a nonlinear multiple cubic regressions ($Q = a + b.P + c.P^2 + d.P + e.API + f.API^2 + g.API^3$) are more appropriate for estimating watershed runoff than other models.

In this thesis, the relationship between antecedent precipitation index (API) and daily rainfall for watershed runoff prediction is improved by using the range of critical API . The ranges are defined by percentage of critical API ; which are divided into 10 ranges (10, 20, 30, 40, 50, 60, 70, 80, 90 and 100 percentage of critical API). For each percentage range, the critical API models will have 3 sets of model parameters. Each set of parameters is derived by comparing daily API with critical API . The first set of parameters is $API < \text{percentage of } API_{critical}$; the second set is $\text{percentage of } API_{critical} < API < API_{critical}$; and the third set is $API > API_{critical}$.

The results show that the range of 60% of $API_{critical}$ of model-3, which is a nonlinear multiple cubic regression, is more appropriate for estimating watershed runoff than the other percentage ranges of critical API range model given that the best of Nash-Sutcliffe efficiency (NSE) is 0.366-0.784 with the average of 0.543, correlation coefficient (r) is 0.605-0.885 with the average of 0.734 and root mean square error ($RMSE$) is 2.603-191.527 cms with the average of 29.405 cms. In this study, critical API range model-3 with the range of 60% is chosen for estimating runoff of small watershed in the upper Chao Phraya river basin as shown in equation below.

If $API < 60\% \text{ of } API_{critical}$

$$Q = a_1 + b_1.P + c_1.P^2 + d_1.P^3 + e_1.API + f_1.API^2 + g_1.API^3$$

If $60\% \text{ of } API_{critical} < API < API_{critical}$

$$Q = a_2 + b_2.P + c_2.P^2 + d_2.P^3 + e_2.API + f_2.API^2 + g_2.API^3$$

If $API > API_{critical}$

$$Q = a_3 + b_3.P + c_3.P^2 + d_3.P^3 + e_3.API + f_3.API^2 + g_3.API^3$$

The selected model is used to analyse daily watershed runoff of 36 representative stream gauging stations during year 1977 to 2002. The results of model calibration are used to determine suitable value of each model parameter in the upper Chao Phraya river basin with a parameter value varies from -82.9189 to 1.24150, b parameter value varies from -2.01018 to 1.78326, c parameter value varies from -1.21439 to 1.79511, d parameter value varies from -0.35111 to 0.08591, e parameter value varies from -134.616 to 5.48934, f parameter value varies from -0.35115 to 4.15849 and g parameter value varies from -0.03251 to 0.01085.

In addition, this model produces satisfactory watershed runoff prediction in an ungauged basin given that the best of Nash-Sutcliffe efficiency (NSE) is 0.301-0.699, correlation coefficient (r) is 0.668-0.863 and root mean square error ($RMSE$) is 6.02-52.70 cms of 4 stream gauging stations.

Sensitivity analysis of 7 significant model parameters (a, b, c, d, e, f and g) by increasing and decreasing parameter values from -30% to 30% of parameter values (-30%, -20%, -10%, +10%, +20% and +30%) was done. The finding shows that increasing and decreasing of g parameter value has the most significant effect by increasing and decreasing the peak discharge, while increasing and decreasing of f parameter value has the most significant effect on increasing the discharge volume.

Objective 5: *To predict (forecast) outflow hydrographs for each of the watershed and each major reach of the upper Chao Phraya river channel network.*

Critical API range in model-3 with the range of 60%, and daily rainfall and daily antecedent precipitation index (API) were used to predict outflow hydrograph of 112 small watersheds in the upper Chao Phraya river basin. Thereafter, HEC-HMS model was used to analyse outflow hydrographs routing during year 1994 to 2002, the calibration and verification on 8 stream gauging stations, and inflow of Bhumibol dam and Sirikit dam at the major reach of the upper Chao Phraya river network.

The finding shows that parameter of travel time of the flood wave through routing reach (K) of Muskingum routing model varies from 0.90 to 129.66 with the average of 25.93, and parameter of dimensionless weighting factor (X) of Muskingum routing model varies from 0.05 to 0.30 with the average of 0.16. The statistical values resulting from model calibration and verification show the Nash-Sutcliffe efficiency (NSE) is 0.409-0.919, correlation coefficient (r) is 0.763-0.960 and root mean square error ($RMSE$) is 33.62-419.28 cms. Furthermore, the outflow hydrograph at upper major reach of river network shows higher accuracy than the outflow hydrograph at lower major reach of upper Chao Phraya river network.

The concept of antecedent precipitation index (*API*) rainfall-runoff model uses the vertical water budget of soil water, soil moisture index and relationship between *API*, daily rainfall and daily discharge, for transforming rainfall value to unit of discharge depth. Consequently, the recommendation for the improvement of model accuracy is that the river basin should be divided into a lot of small watersheds then the outflow hydrograph of each watershed is analyzed. After that route and combine outflow hydrograph of small watersheds to the river basin outlet which eventually gives a better representative outflow hydrograph of river basin.

LITERATURE CITED

- Abbott, M.B., J.C. Bathurst, J.A. Cunge, P.E. O'Connell and J. Rasmussen. 1986. An introduction to the European Hydrological System – Système Hydrologique Européan, (SHE), 1: History and philosophy of a physically-based distributed modelling system. **Journal of Hydrology** 87: 45-59.
- AIMWATER (European research project Analysis, Investigation, and Monitoring of Water Resources). 1999. **WP4100 Survey of modelling approaches of Intermediate Report.** AIMWATER, n.p.
- Alikhan, M.A., D.N. Contract and J.M. Wiggart. 1972. Modelling of low flows in rivers using antecedent precipitation index. **Transactions - American Geophysical Union** 53: 984.
- Allen, R.G., L.S. Pereiro, D. Raes and M. Smith. 1998. **Crop evapotranspiration: Guidelines for computing crop requirements. Irrigation and Drainage paper No. 56.** FAO, Rome.
- Ambroise, B. 1998. **La dynamique du cycle de l'eau dans un bassin versant-Processus.** Facteurs, Modèles. EPFL, HGA (Ed.), Buchares.
- Atthaporn, B. 1999. Water Information System and Flood Disaster in Thailand. **Proc. of IDNDR Symposium.** Tijuana, Mexico.
- Bell, V.A. and R.J. Moore. 1998. A grid-based distributed flood forecasting model for use with weather radar data: 1: Formulation, 2: Case Studies. **Hydrology and Earth Science** 2(2-3): 265-298.
- Bergstrom, S. and A. Forsman. 1973. Development of conceptual deterministic rainfall-runoff model. **Nordic Hydrology** 4: 47-70.

Beschta, R.L. 1990. Peakflow estimation using an antecedent precipitation index (*API*) model in tropical environments, pp. 128-137. **IAHS-AISH Publication No. 192.** IAHS, France.

Biswas, A.K. 1970. **History of hydrology.** North-Holland Publishing Company, Amsterdam.

Blanchard, B.J., M.J. McFarland, T.J Schmugge and E. Rhoades. 1981. Estimation of soil moisture with *API* algorithms and microwave emission. **Water Resources Bulletin** 17: 767-774.

Burnash, R.J.C., R.L. Ferral. and R.A. McGuire. 1973. **A generalized streamflow simulation system-conceptual modeling for digital computers.** Joint Federal-State River Forecast Center, Sacramento.

Calder, I.R., 1996. Dependence of rainfall interception on drop size: 1. Development of the two-layer stochastic model. **Journal of Hydrology** 185: 363-378.

Chadwick, A. and J. Morfett. 1986. **Hydraulic in Civil and Environmental Engineering.** Roulledge. n.p.

Cheng, S.J. and V.P. Singh. 1986. Derivation of a new variable instantaneous unit hydrograph. **Journal of Hydrology** 88: 25-42.

Cheng, S.J. and R.Y. Wang. 2002. An approach for evaluating the hydrological effects of urbanization and its application. **Hydrological Processes** 16: 1403-1418.

Chiew, F. and T. McMahon. 1994. Application of the daily rainfall runoff model MODHYDROLOG to 28 Australian catchments. **Journal of Hydrology** 153: 383-416.

- Choudhury, B.J. and B.J. Blanchard. 1983. Simulating soil water recession coefficients for agricultural watersheds. **Water Resources Bulletin** 19: 241-247.
- Crawford, N.H. and R.K. Linsley. 1966. Digital simulation in hydrology: Stanford Watershed Model IV. **Technical Report 39**. Stanford University, California.
- Cunge, J. A. 1969. On the subject of a flood propagation computation method (Muskingum method). **Journal of Hydraulic Research** 7 (2): 205-230.
- Danish Hydraulics Institute (DHI). 2003. **MIKE11 A Modelling System for Rivers and Channels: Reference Manual**, Hørsholm, Denmark.
- Descroix, L., J.F. Nouvelot and M. Vauclin. 2002. Evaluation of an antecedent precipitation index to model runoff yield in the west Sierra Madre (North-west Mexico). **Journal of Hydrology** 263: 114-130.
- Ding, J.Y. 1974. Variable unit hydrograph. **Journal of Hydrology** 22: 53-69.
- Dodge, J.C.I. 1957. The rational method for estimating flood peaks. **Engineering** 184: 311-313, 374-377.
- Duan, Q., S. Soroosh and V.K. Gupta. 1994. Optimal use of the SCE-UA global optimization method for calibrating watershed models. **Journal of Hydrology** 158: 265-284.
- Franchini, M. and M. Pacciani. 1991. Comparative analysis of several conceptual rainfall-runoff models. **Journal of Hydrology** 122: 161-219.
- Francis, C. and L. Siriwardena. 2005. **Trend/ change detection software**. CRC for Catchment Hydrology, Australia.

Fread, D.L. 1992. **Flow routing.** In: Maidment, D.R. (Ed.), *Handbook of Hydrology*. McGraw-Hill Book Company, New York.

Granger, R.J., 1995. A feedback approach for the estimation of evapotranspiration using remotely sensed data, pp. 211-222. In **Applications of Remote Sensing in Hydrology, Proceedings of the Second International Workshop**. 18-20 October 1994, by G.W. Kite, A. Pietroniro and T. Pultz (eds.), Symposium No. 14, NHRI, Saskatoon, Saskatchewan.

Green, W.H. and G.A. Ampt. 1911. Studies in soil physics. 1. Flow of air and water through soils. **J. Agric. Science** 4: 1-24.

Gosh, S.N., 1997. **Flood Control and Drainage Engineering.** Taylor & Francis. n.p.

Hamed, K.H. 2008. Trend detection in hydrologic data: The Mann–Kendall trend test under the scaling hypothesis. **Journal of Hydrology** 349: 350-363.

Irmak, S. and Z.H. Dorota. n.d. **Evapotranspiration: Potential or Reference?**. ABE 343, University of Florida, Institute of Food and Agricultural Sciences (UF/IFAS), Available Source: <http://edis.ifas.ufl.edu/AE256>, January 16, 2006.

Jian, L., B. Gabor and G. Balazs. 2004. Runoff Simulation of Three Gorges Area in the Upper Yangtze River during 1998 Flood Season. **Acta Meteorologica Sinica** 19 (2): 241-252.

Kahya, E. and S. Kalayci. 2004. Trend analysis of streamflow in Turkey. **Journal of Hydrology** 289:128-144.

Kendall, M.G., 1975. **Rank Correlation Methods.** Griffin, London.

Khatibi, R.H. 2001. Some Issues in Computational Hydraulics Practice. **J. Hydraulic Engineering** 127 (6): 438-442.

Khatibi, R.H. and J. Haywood. 2002. The Role of Flood Forecasting and Warning in Sustainability of Flood Defence. **Proceedings of the ICE - Municipal Engineer** 151 (4): 313-320

Khatibi, R. H., R.J. Moore, M.J.Booij, D. Cadman, and G. Boyce. 2002.

Parsimonious Catchment and River Flow Modeling. Available Source:
http://www.iemss.org/iemss2002/pdf/volumeno/72_khatibi.pdf, January 07, 2005.

Kite, G.W. 1975. Performance of two deterministic hydrological models. **IASH-AISH Publication** 115: 136-142.

Kite, G.W. 1978. Development of a hydrologic model for a Canadian Watershed. **Canadian Journal of Civil Engineering** 5 (1): 126-134.

Kite, G.W., 1989. Using NOAA data for hydrological modeling, pp. 553-557. In **Quantitative Remote Sensing: An Economic Tool for the Nineties.** IGARSS'89, 12th Canadian Symposium on Remote Sensing, IEEE, 10-14 July 1989, Vancouver, British Columbia.

Kite, G.W. 1995. Scaling of input data for macroscale hydrologic modeling. **Water Resources Research** 31 (11): 2769-2781.

Kite, G.W. and C. Spence, 1995. Land cover, NDVI, LAI and evapotranspiration in hydrologic modeling, pp. 223-240. In **Applications of Remote Sensing in Hydrology, Proceedings of the Second International Workshop.** 18-20 October, 1994, by G.W. Kite, A. Pietroniro and T. Pultz (eds.), Symposium No. 14, NHRI, Saskatoon, Saskatchewan.

- Kite, G.W., E. Ellehoj and A. Dalton. 1996. GIS for large-scale watershed modeling. In V.P. Singh and M. Fiorentino, eds. **Geographical Information Systems in Hydrology**. Kluwer Academic Publishers, Netherlands.
- Kite, G.W. 2000. **Manual for The SLURP Hydrological Model, V.11.4.** International Water Management Institute, Colombo, Sri Lanka.
- Kohler, M.A. and R.K. Linsley. 1951. **Predicting the runoff from storm rainfall.** U.S. Weather Bureau Research Paper 34, Washington.
- Kundzewicz, Z.W. and A. Robson. 2000. **Detecting Trend and Other Changes in Hydrological Data.** World Climate Program – Water, WMO/UNESCO, WCDMP- 45, WMO/TD 1013, Geneva.
- Lacroix M. and Martz L.W. 1998. **The Application of Digital Terrain Analysis Modelling Techniques for the Parameterization of a Hydrological Model in the Wolf Creek Research Basin.** Wolf Creek Research Basin Planning Workshop, Whitehorse.
- Linsley, R.K. and N.H. Crawford. 1960. **Computation of a synthetic streamflow record on a digital computer.** Publication 51, International Association of Scientific Hydrology, Stanford.
- Linsley, R.K., M.A. Kohler. and J.L.H. Paulhus. 1982. **Hydrology for engineers.** McGraw-Hill, New York.
- Littlewood, I. 2001. Practical aspects of calibrating and selecting unit hydrograph-based models for continuous river flow simulation. **Hydrological Sciences Journal** 46: 795-811.

- Malek, M.B.A. 2002. Watershed analysis – rainfall - runoff model, pp. 780-789. **International Conference on Urban Hydrology for the 21st Century**. Kuala Lumpur.
- Mann, H.B., 1945. Nonparametric tests against trend. **Econometrica** 13: 245–259.
- Minshall, N.E. 1960. Predicting storm runoff on small experimental watersheds. **Journal of the Hydraulics Division** 86: 7-38.
- Morton, F.I., 1983. Operational estimates of areal evapotranspiration and their significance to the science and practice of hydrology. **Journal of Hydrology** 66: 77-100.
- Mustonen, S. 1963. **Kesäsateiden aiheuttamasta valunnasta (in Finnish)**. Tiedotus 3/1963, Maataloushallituksen insinööritoimisto, Maa-ja vesiteknillinen tutkimustoitomisto, Helsinki.
- Nash, J.E. 1957. The form of the instantaneous unit hydrograph. **Publication 45 International Association of Scientific Hydrology**. Wallingford, n.p.
- Nutchanat, S. 2002. **Flood Modeling**. Lecture document Department of Water Resources Engineering, Kasetsart University, Bangkok.
- ONWRC (The Working Group of the office of Natural Water Resources Committee). 1999. **Chao Phraya River Basin**. ONWRC, Thailand.
- Papadakis, C.N. and H.C. Pruel. 1973. Infiltration and antecedent precipitation. **J. Hydraul. Div.** 99: 1235-1245.
- Patra, K.C. 2000. **Hydrology and Water Resources Engineering**. CRC Press LLC, India.

Pilgrim, D.H. 1986. Bridging the gap between flood research and design practice. **Water Resources Research** 22: 165-176.

Pilgrim, D.H. and I. Cordery. 1992. **Flood runoff**. In: Maidment, D.R. (Ed.), Handbook of Hydrology. McGraw-Hill, New York.

Ponce, V. M., 1983. **Development of physically based coefficients for the diffusion method of flood routing, Final Report to the USDA**. Soil Conservation Service, Maryland.

Pongput, K., C. Theprasit. and T. Chaturabul. 2008. **A flash flood watch and warning systems:** Warning system and participation of upper nan watershed community network for flood and landslide protection. The National Research Council of Thailand, Bangkok.

Priestley, C.H.B. and R.J. Taylor. 1972. On the assessment of surface heat flux and evaporation using large-scale parameters. **Monthly Weather Review** 100: 81-92.

Rallison, R. E., 1980. Origin and evolution of the SCS runoff equation. Proc. **Irrigation and Drainage Symposium on Watershed Mgmt.** 2: 912–924.

Richard, J.H., 2001. Normalized antecedent precipitation index. **Journal of Hydrologic Engineering** 13 (5): 377-381.

Rosenthal, W.D., J.C. Harlan and T.J. Blanchard. 1982. Case study: estimating antecedent precipitation index from Heat Capacity Mapping Mission day thermal infrared data. **Hydrological Sciences Journal** 27: 415-426.

Royal Irrigation Department (RID). 2000. **The study of Water allocation in the Chao Phraya River Basin Project.** RID, Bangkok.

Saint-Venant, B.D. 1871. Theory of unsteady water flow, with application to river floods and to propagation of tides in river channels. **Comptes rendus** 73: 148-154, 237-240.

Sherman, L.K. 1932. Streamflow from rainfall by the unit-hydrograph method. **Engineering News Record** 108: 501-505.

Singh, V.P. 1995. **Computer Models of Watershed Hydrology**. Water Resources Publications Book, Littleton, Colorado.

Smith, M. 1990. **Expert consultation on revision of FAO methodologies for crop water requirements**. FAO, Rome.

Spittlehouse, D.L., 1989. Estimating evapotranspiration from land surfaces in British Columbia, In: Estimation of Areal Evapotranspiration. **IAHS Publication No. 177**. IAHS, France.

Subramanya, K., 2002. **Engineering Hydrology**. 2nd ed., McGraw Hills, Tata.

Thiemann, M., M. Trosset, H. Gupta and S. Sorooshian. 2001. Bayesian recursive parameter estimation for hydrologic models. **Water Resources Research** 37: 2521-2535.

Todini, E. 1996. The ARNO rainfall-runoff model. **Journal of Hydrology** 175: 339-382.

US Army Crops of Engineers (USACE). 2000. **Hydrologic Modeling System, HEC-HMS: Technical Reference Manual**, Hydrologic Engineering Center, California.

- Vakkilainen, P. and T. Karvonen. 1982. Adaptive Rainfall-Runoff Model, SATT-I. **Civil Engineering and Building Construction Series NO. 81.** University of Technology, Helsinki.
- Vanclooster, M., P. Viaene, J. Diels and K. Christiaen., 1994. **WAVE, Reference and User Manual (release 2).** Institute for Land and Water Management, Katholieke Universiteit, Leuven, Belgium.
- Vehvilainen, B. 1992. Snow Cover Models in Operational Watershed Forecasting. **Publications of Water and Environment Research Institute 11.** National Board of Waters and the Environment, Helsinki.
- Verhoef, A. and R.A. Feddes, 1991. **Preliminary review of revised FAO radiation and temperature methods, Report 16.** Landbouwuniversiteit Wageningen, Wageningen, Netherlands.
- Viessman, Jr. W., G.L. Lewis and J.W. Knapp. 1989. **Introduction to Hydrology.** Harper & Row Publishers, Singapore.
- Viraphol, T. n.d. **Advance Hydrology for Water Resources Engineering.** Lecture document Department of Water Resources Engineering, Kasetsart University, Bangkok.
- Vudhivanich, V. 2010. Accurate analysis of model by Nash-Sutcliffe Efficiency and R^2 . pp.1-10. **In Proceedings Seminar on Chuchart Day. Irrigation Engineering Alumni Association under H.M. The King's Patronage.** Thailand.
- Watson, I.C. 1983. **Hydrology: An Environmental Approach.** CRC Press, n.p.

Withhawatchutikul, P. 1985. Watershed research at rayong, Thailand. pp.57-68. In **Proceedings Seminar on Watershed Research and Management Practices Theme: Towards More Effective Watershed Management. ASEAN-US Watershed Project.** Laguna, Philippines.

Withhawatchutikul, P., A. Boosaner. and S. Sucharit. 2005. Hydrological model for integrated water resource assessment and management. **International Conference on Simulation & Modeling.** Nakorn Pathom, Thailand.

Xia, J., K.M. O'Connor, R.K. Kachroo and G.C. Liang. 1997. A non-linear perturbation model considering catchment wetness and its application in river flow forecasting. **Journal of Hydrology** 200: 164-178.

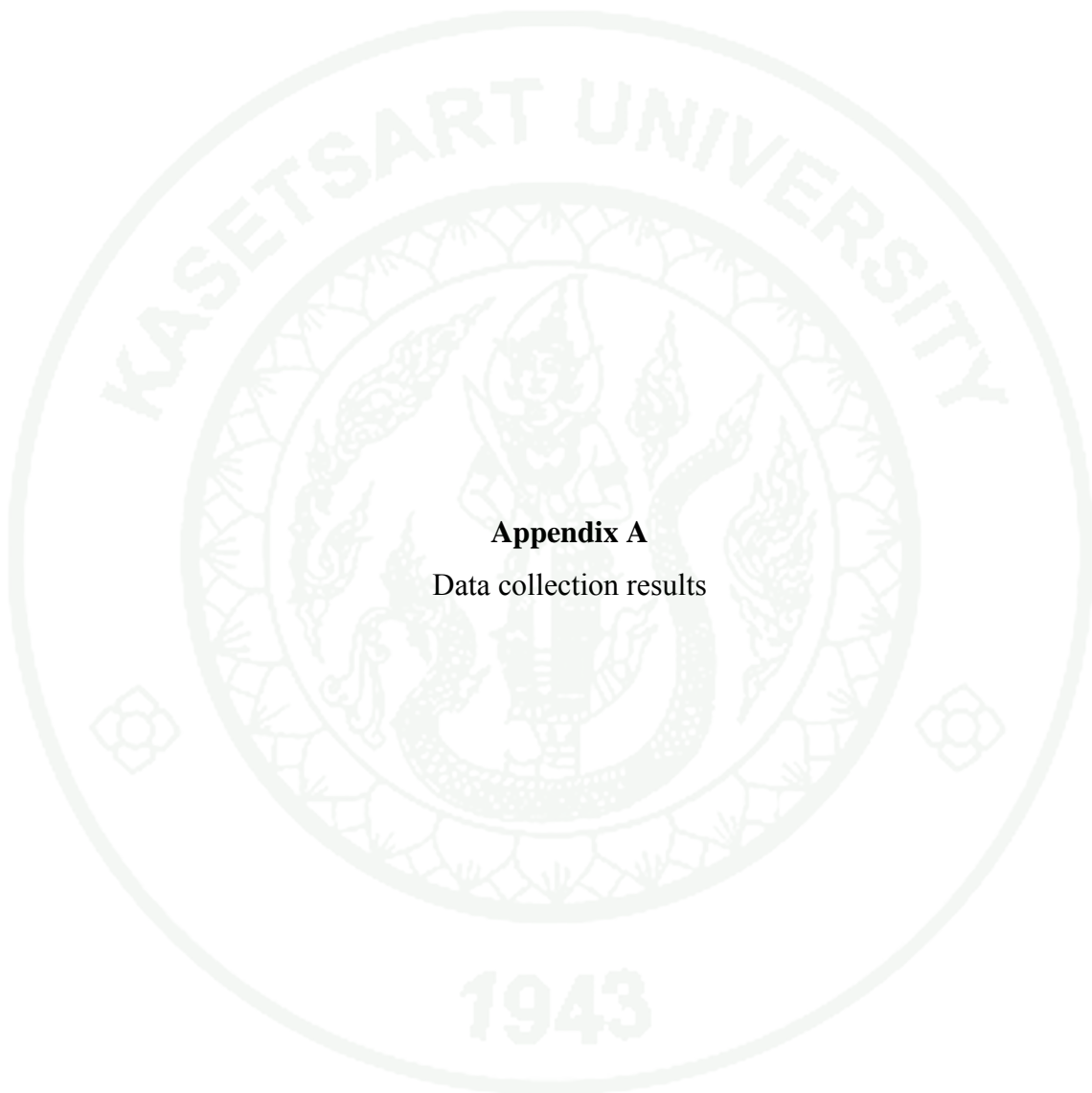
Yin, Z. and T.H.L. Williams, 1997. Obtaining spatial and temporal vegetation data from Landsat MSS and AVHRR/NOAA satellite images for a hydrologic model. **Photogrammetric Engineering & Remote Sensing** 63 (1): 69-77.

Yu, Y.S., S. Zou and D. Whittemore. 1993. Non-parametric trend analysis of water quality data of rivers in Kansas. **Journal of Hydrology** 150: 61–80.

Yue, S. and C. Wang. 2004. The Mann-Kendall Test Modified by Effective Sample Size to Detect Trend in Serially Correlated Hydrological Series. **J. Water Resources Management** 18: 201-218.

Zoch, R.T. 1934. On the relation between rainfall and stream flow. **Monthly Weather Review** 62: 315-322.





Appendix A
Data collection results

Appendix Table A1 List of rainfall stations used in this study.

No.	Station Code	Station Name	Province	Agencies	Latitude	Longitude
1.	07013	A. Muang	Chiang Mai	TMD	18-50-23	98-58-32
2.	07022	A. Sarapi	Chiang Mai	TMD	18-42-48	99-02-29
3.	07032	A. San Kamphaeng	Chiang Mai	TMD	18-44-39	99-07-28
4.	07042	A. San Sai	Chiang Mai	TMD	18-50-51	99-02-54
5.	07052	A. Doi Saket	Chiang Mai	TMD	18-52-08	99-08-22
6.	07062	A. Mae Rim	Chiang Mai	TMD	18-54-47	99-56-52
7.	07072	A. Hang Dong	Chiang Mai	TMD	18-41-10	98-55-19
8.	07082	A. San Pa Tong	Chiang Mai	TMD	18-37-37	98-53-56
9.	07092	A. Hot	Chiang Mai	TMD	18-11-26	98-36-52
10.	07112	A. Mae Taeng	Chiang Mai	TMD	19-07-08	98-56-52
11.	07122	A. Phrao	Chiang Mai	TMD	19-21-52	99-12-17
12.	07132	A. Chiang Dao	Chiang Mai	TMD	19-21-53	98-58-00
13.	07142	A. Samoeng	Chiang Mai	TMD	18-50-52	98-44-09
14.	07152	A. Mae Chaem	Chiang Mai	TMD	18-29-54	98-21-54
15.	07162	A. Omkoi	Chiang Mai	TMD	17-47-45	98-21-36
16.	07182	A. Chom Thong	Chiang Mai	TMD	18-24-57	98-40-47
17.	07242	Doi Suthep-Pui National Park	Chiang Mai	TMD	18-48-10	98-55-30
18.	07252	Doi Chiang Dao Watershed Research	Chiang Mai	TMD	19-16-07	98-58-32
19.	07282	Doi Bo Kaeo Seed-Multiplication, A. Hot	Chiang Mai	TMD	18-09-01	98-23-35
20.	07292	San Pa Tong Rice Experimental Station	Chiang Mai	TMD	18-36-40	98-54-02
21.	07391	R.I.D. Office Unit 1, A. Muang	Chiang Mai	RID	18-47-21	99-01-01
22.	07472	Bhumiphol Dam Development Settlement	Chiang Mai	TMD	17-55-00	98-41-00
23.	07502	Mae Ho Phra Forest Plantation, A. Mae Taeng	Chiang Mai	TMD	19-04-00	99-13-00
24.	12012	A. Muang	Kamphaeng Phet	TMD	16-28-56	99-31-26
25.	12032	A. Phran Kratai	Kamphaeng Phet	TMD	16-39-48	99-35-31
26.	12042	A. Khanu Woralakburi	Kamphaeng Phet	TMD	16-03-37	99-51-49
27.	12052	Thung Pho Thale Self-Supporting Settlement	Kamphaeng Phet	TMD	16-28-00	99-39-00
28.	12091	Ban Pang Wai (P.35), A. Khlong Khlung	Kamphaeng Phet	RID	16-04-22	99-24-18
29.	12102	A. Sai Ngam	Kamphaeng Phet	TMD	16-27-00	99-53-00
30.	12121	Ban Pong Nam Ron (P.47), A. Khlong Lan	Kamphaeng Phet	RID	16-20-03	99-16-29
31.	16013	A. Muang	Lampang	TMD	18-17-23	99-30-27
32.	16022	A. Chae Hom	Lampang	TMD	18-42-07	99-34-13
33.	16032	A. Ko Kha	Lampang	TMD	18-11-21	99-23-50
34.	16042	A. Sop Prap	Lampang	TMD	17-52-45	99-20-26

Appendix Table A1 (Continued)

No.	Station Code	Station Name	Province	Agencies	Latitude	Longitude
35.	16052	A. Mae Tha	Lampang	TMD	18-07-58	99-31-00
36.	16062	A. Hang Chat	Lampang	TMD	18-25-00	99-13-00
37.	16072	A. Thoen	Lampang	TMD	17-36-39	99-13-08
38.	16082	A. Mae Phrik	Lampang	TMD	17-26-49	99-07-04
39.	16092	A. Ngao	Lampang	TMD	18-42-25	99-58-20
40.	16102	Huat Thak Plantation, A. Ngao	Lampang	TMD	18-40-00	99-55-00
41.	16112	A. Wang Nua	Lampang	TMD	19-08-42	99-37-20
42.	16180	Mae Suk (W.16), A. Chae Hom	Lampang	RID	18-48-12	99-38-45
43.	16194	Mae Moh Forest Plantation, A. Muang	Lampang	TMD	18-24-45	99-43-24
44.	16214	Mae Sai Kham Forest Plantation, A. Chae Hom	Lampang	TMD	18-30-00	99-32-00
45.	17012	A. Muang	Lamphun	TMD	18-34-38	99-00-34
46.	17022	A. Li	Lamphun	TMD	17-48-01	98-57-17
47.	17032	A. Pa Sang (Pak Bong)	Lamphun	TMD	18-31-25	98-56-38
48.	17042	A. Mae Tha	Lamphun	TMD	18-27-35	99-08-14
49.	17052	A. Ban Hong	Lamphun	TMD	18-18-52	98-49-21
50.	17062	Ban Ko, A. Li	Lamphun	TMD	17-39-20	98-46-30
51.	17080	Ban Don Mun (P.42), A. Thung Hua Chang	Lamphun	RID	17-53-16	99-05-20
52.	17093	Lamphun Agrometeorological Station	Lamphun	TMD	18-35-00	99-02-00
53.	26013	A. Muang	Nakhon Sawan	TMD	15-42-11	100-08-28
54.	26022	A. Chumsaeng	Nakhon Sawan	TMD	15-52-48	100-18-22
55.	26032	A. Tha Tako	Nakhon Sawan	TMD	15-38-20	100-29-10
56.	26042	A. Krok Phra	Nakhon Sawan	TMD	15-33-16	100-04-34
57.	26062	A. Banphot Phisai	Nakhon Sawan	TMD	15-56-01	99-59-08
58.	26092	Animal Food Division Unit 2, A. Muang	Nakhon Sawan	TMD	15-39-00	100-10-01
59.	26122	A. Phaisali	Nakhon Sawan	TMD	15-35-43	100-39-40
60.	28013	A. Muang	Nan	TMD	18-46-35	100-46-26
61.	28022	A. Sa	Nan	TMD	18-34-10	100-45-14
62.	28032	A. Na Noi	Nan	TMD	18-19-34	100-43-01
63.	28042	A. Pua	Nan	TMD	19-10-57	100-55-01
64.	28053	A. Thung Chang	Nan	TMD	19-23-11	100-52-48
65.	28062	Mae Sakhon Forest Protected Station Unit 5, A. Sa	Nan	TMD	18-32-00	100-45-00
66.	28073	A. Tha Wang Pha	Nan	TMD	19-07-04	100-48-47
67.	28102	A. Chiang Klang	Nan	TMD	19-17-33	100-51-58
68.	28142	Nan Agrometeorological Station	Nan	TMD	18-52-00	100-45-00
69.	28152	A. Mae Charim	Nan	TMD	18-44-00	101-01-01
70.	38012	A. Muang	Phichit	TMD	16-26-12	100-21-14

Appendix Table A1 (Continued)

No.	Station Code	Station Name	Province	Agencies	Latitude	Longitude
71.	38022	A. Bang Mun Nak	Phichit	TMD	16-01-35	100-23-56
72.	38032	A. Pho Thale	Phichit	TMD	16-05-28	100-15-54
73.	38042	A. Taphan Hin	Phichit	TMD	16-12-44	100-25-34
74.	38052	A. Sam Ngam	Phichit	TMD	16-30-25	100-12-32
75.	38062	A. Pho Prathap Chang	Phichit	TMD	16-18-27	100-16-48
76.	38072	A. Wang Sai Phun	Phichit	TMD	16-25-00	100-33-00
77.	39013	A. Muang	Phitsanulok	TMD	16-49-24	100-15-43
78.	39022	A. Bang Rakam	Phitsanulok	TMD	16-45-23	100-07-19
79.	39032	A. Wang Thong	Phitsanulok	TMD	16-49-25	100-25-59
80.	39042	A. Nakhon Thai	Phitsanulok	TMD	17-05-56	100-50-31
81.	39052	A. Phrom Phiram	Phitsanulok	TMD	17-02-56	100-12-14
82.	39072	A. Wat Bot	Phitsanulok	TMD	16-59-34	100-18-43
83.	39101	Wang Nok Aen (N.24), A. Wang Thong	Phitsanulok	RID	16-50-35	100-31-19
84.	39132	Khao Krayang Forest Plantation	Phitsanulok	TMD	16-52-00	100-45-00
85.	39142	A. Chatrakan	Phitsanulok	TMD	17-17-00	100-33-00
86.	39161	Ban Nong Bon (N.40), A. Wat Bot	Phitsanulok	RID	17-13-14	100-21-11
87.	40013	A. Muang	Phrae	TMD	18-08-44	100-08-42
88.	40022	A. Sung Men	Phrae	TMD	18-02-58	100-06-54
89.	40032	A. Rong Kwang	Phrae	TMD	18-20-21	100-19-12
90.	40043	A. Song	Phrae	TMD	18-28-06	100-11-10
91.	40052	A. Long	Phrae	TMD	18-04-25	99-50-10
92.	40062	A. Wang Chin	Phrae	TMD	17-53-56	99-36-24
93.	40092	A. Den Chai	Phrae	TMD	17-58-56	100-03-14
94.	40111	Yom River (Y.20), A. Song	Phrae	RID	18-35-03	100-09-18
95.	40124	Khun Mae Khammi Forest Plantation, A. Rong Kwang	Phrae	TMD	18-23-00	100-22-01
96.	59012	A. Muang	Sukhothai	TMD	17-00-21	99-49-36
97.	59022	A. Si Satchanalai	Sukhothai	TMD	17-30-55	99-45-52
98.	59032	A. Sawankhalok	Sukhothai	TMD	17-18-55	99-50-08
99.	59042	A. Kong Krailat	Sukhothai	TMD	16-57-04	99-58-46
100.	59062	A. Ban Dan Lan Hoi	Sukhothai	TMD	17-00-16	99-34-38
101.	59082	A. Kirimat	Sukhothai	TMD	16-49-55	99-48-20
102.	59092	A. Thung Saliam	Sukhothai	TMD	17-19-12	99-33-50
103.	59121	Kaeng Luang (Y.6), A. Si Satchanalai	Sukhothai	RID	17-26-03	99-47-32
104.	63013	A. Muang	Tak	TMD	16-52-50	99-07-36
105.	63022	A. Ban Tak	Tak	TMD	17-02-46	99-04-34
106.	63062	A. Sam Ngao	Tak	TMD	17-14-32	99-01-28
107.	63075	Bhumibol Dam	Tak	EGAT	17-14-30	99-03-45
108.	70013	A. Muang	Uttaradit	TMD	17-37-32	100-05-56

Appendix Table A1 (Continued)

No.	Station Code	Station Name	Province	Agencies	Latitude	Longitude
109.	70022	A. Nam Pat	Uttaradit	TMD	17-43-35	100-41-17
110.	70032	A. Laplae	Uttaradit	TMD	17-39-00	100-02-33
111.	70042	A. Phichai	Uttaradit	TMD	17-17-04	100-05-28
112.	70052	A. Tron	Uttaradit	TMD	17-28-53	100-07-01
113.	70062	A. Tha Pla	Uttaradit	TMD	17-47-26	100-22-52
114.	70072	A. Fak Tha	Uttaradit	TMD	17-59-25	100-52-55
115.	70151	Hat Phai (N.12A), A. Tha Pla	Uttaradit	RID	17-44-10	100-32-28
116.	73032	A. Pong	Phayao	TMD	19-08-32	100-16-41

Remark: EGAT = Electricity Generating Authority of Thailand

RID = Royal Irrigation Department

TMD = Thai Meteorological Department

Appendix Table A2 List of stream gauging stations used in this study.

No.	Station Code	Station Name	Province	Agencies	Latitude	Longitude
1.	P.1	Ping River at Nawarat Bridge	Chiang Mai	RID	18-47-09	99-00-29
2.	P.14	Nam Mae Chaem at Kaeng Ob Luang	Chiang Mai	RID	18-13-49	98-33-35
3.	P.15	Ping River at Khlong Khlung	Kamphaeng Phet	RID	16-12-50	99-43-26
4.	P.16	Ping River at Khanu Woralaksaburi	Kamphaeng Phet	RID	16-03-42	99-51-51
5.	P.20	Ping River at Chiang Dao	Chiang Mai	RID	19-21-09	98-58-25
6.	P.21	Nam Mae Rim at Mae Rim	Chiang Mai	RID	18-55-29	98-56-34
7.	P.24A	Nam Mae Klang at Pracha	Chiang Mai	RID	18-25-01	98-40-29
8.	P.2A	Ping River at Ban Tha Khae	Tak	RID	16-51-14	99-07-50
9.	P.47	Ping River at Ban Pong Nam Ron	Kamphaeng	RID	16-20-03	99-16-29
10.	P.4A	Mae Taeng at Mae Taeng	Chiang Mai	RID	19-07-15	98-56-51
11.	P.64	Ping River at Highway Bridge (Ban Luang)	Chiang Mai	RID	17-47-01	98-22-31
12.	P.67	Ping River at Ban Mae Tae	Chiang Mai	RID	19-01-11	98-57-42
13.	P.71	Ping River at Ban Sop Wang	Chiang Mai	RID	18-32-14	98-51-47
14.	P.7A	Ping River at Ban Huai Yang	Kamphaeng Phet	RID	16-28-38	99-31-06
15.	PE.2	Nam Mae Ping at Ban Kong Hin	Chiang Mai	EGAT	18-10-30	98-36-00
16.	W.16A	Wang River at Ban Hai	Lampang	RID	18-46-45	99-37-52
17.	W.17	Nam Mae Soi at Highway Bridge	Lampang	RID	18-43-16	99-34-12
18.	W.20	Nam Mae Tui at Ban Tha Lo	Lampang	RID	18-18-35	99-27-29
19.	W.3A	Wang River at Ban Don Chai	Lampang	RID	17-38-29	99-14-04
20.	W.4A	Wang River at Ban Wang Man	Tak	RID	17-12-22	99-06-08
21.	Y.14	Yom River at Ban Don Rabiang	Sukhothai	RID	17-35-42	99-43-08
22.	Y.16	Yom River at Bang Rakam	Phitsanulok	RID	16-45-35	100-07-40
23.	Y.17	Yom River at Sam Ngam	Phichit	RID	16-30-50	100-12-40
24.	Y.1C	Yom River at Ban Nam Khong	Phrae	RID	18-07-59	100-07-39
25.	Y.20	Yom River at Ban Ngao Sak	Phrae	RID	18-35-03	100-09-17
26.	Y.24	Nam Pi at Highway Bridge	Phayao	RID	18-53-04	100-17-24
27.	Y.26	Yom River at Ban Mae Phu	Lampang	RID	17-19-45	99-27-42
28.	Y.30	Yom River at Highway Bridge (Ban Pong)	Lampang	RID	18-42-59	99-57-40
29.	Y.31	Yom River at Highway Bridge (Ban Thung Nong)	Phayao	RID	18-57-27	100-16-08
30.	Y.34	Yom River at Ban Mae Lai	Phrae	RID	18-13-11	100-12-36
31.	Y.3A	Yom River at Sawankhalok	Sukhothai	RID	17-18-29	99-49-43
32.	Y.4	Yom River at Talat Thani	Sukhothai	RID	17-00-18	99-49-31

Appendix Table A2 (Continued)

No.	Station Code	Station Name	Province	Agencies	Latitude	Longitude
33.	N.1	Nan River at Forestry Office	Nan	RID	18-46-23	100-46-51
34.	N.12A	Nan River at Ban Hat Phai	Uttaradit	RID	17-44-10	100-32-28
35.	N.13A	Nan River at Highway Bridge	Nan	RID	18-33-12	100-46-08
36.	N.14A	Nan River at Wat Luang Pho Kaeo	Nakhon Sawan	RID	15-53-56	100-18-34
37.	N.22	Nan River at Ban Yang	Phitsanulok	RID	17-01-57	100-22-23
38.	N.24	Nan River at Ban Wang Nok Aen	Phitsanulok	RID	16-50-35	100-31-20
39.	N.27A	Nan River at Phrom Phiram	Phitsanulok	RID	17-01-54	100-11-05
40.	N.36	Nan River at Ban Nong Krathao	Phitsanulok	RID	17-04-59	100-49-55
41.	N.40	Nan River at Ban Nong Bon	Phitsanulok	RID	17-13-14	100-21-10
42.	N.42	Nan River at Ban Hat Khao San	Nan	RID	18-34-08	100-52-28
43.	N.49	Nan River at Highway Bridge (Ban Nam Yao)	Nan	RID	18-59-29	100-56-32
44.	N.55	Nan River at Ban Tha Sakae	Phitsanulok	RID	17-15-10	100-37-51
45.	N.59	Khwae Noi River at Ban Na Chan	Phitsanulok	RID	17-01-43	100-50-44
46.	N.5A	Nan River at Muang Phisanulok	Phitsanulok	RID	16-49-15	100-15-49
47.	N.60	Nan River at Ban Hat Song Khwae	Uttaradit	RID	17-24-50	100-07-50
48.	N.62	Khwae Noi River at Ban Huai Tha Nua	Phitsanulok	RID	17-14-25	100-33-11
49.	N.63	Nan River at Highway Bridge (Ban Hua Muang)	Nan	RID	18-21-48	100-43-41
50.	N.64	Nan River at Ban Pha Khwang	Nan	RID	19-00-31	100-47-18
51.	N.65	Nan River at Ban Pang Sa	Nan	RID	19-13-47	100-45-26
52.	N.66	Nan River at Ban Om Sing Nua	Phitsanulok	RID	17-07-17	100-53-51
53.	N.7	Nan River at Phichit	Phichit	RID	16-26-31	100-21-11
54.	C.2	Chao Phraya River at Khai Chirat Prawat	Nakhon Sawan	RID	15-40-15	100-06-45

Appendix Table A3 Soil test data.

No.	Village	Subdistrict	District	Province	Bulk Density (B.D.)	Water Holding Capacity, (WHC) (g./cu.cm.)	Saturation Percentage (%)
1.	Khao Lek	Khao Chot	Si Sawat	Kanchanaburi	1.37	15.19	24.44
2.	Huai Rai	Pang Tru	Tha Muang	Kanchanaburi	1.61	9.22	13.63
3.	U Song	Tha Kanun	Thong Pha Phum	Kanchanaburi	1.42	14.35	18.34
4.	Mai Phatthana	Nong Lu Buri	Sangkhla	Kanchanaburi	1.36	16.50	22.28
5.	Nong Bua Thong	Tha Khun Ram	Mueang	Kamphaeng Phet	1.26	12.67	24.49
6.	Lom Chai	Khlong Nam Lai	Khlong Lan	Kamphaeng Phet	1.28	12.64	26.17
7.	Khlong Samui Ron	Pong Nam Ron	Khlong Lan	Kamphaeng Phet	1.31	12.46	25.79
8.	Non Po Daeng	Sakhon Bat	Khanu Woralaksaburi	Kamphaeng Phet	1.16	17.10	37.74
9.	Wang Maka	Wang Tabaek	Phran Kratai	Kamphaeng Phet	1.54	11.85	18.89
10.	Pang Nuea	Pang Ta Wai	Pang Sila Thong	Kamphaeng Phet	1.36	12.73	18.43
11.	Nong Bua Samakkhi	Kosamphi	Kosamphi	Kamphaeng Phet	1.42	9.20	18.54
12.	Ka Bok Tai	Tha Kadan	Sanam Chai Khet	Chachoengsao	1.73	9.10	13.63
13.	Kao Loy	Khlong Takrao	Tha Takiap	Chachoengsao	1.34	11.64	20.66
14.	Tha Rabad	Phraek Si Racha	Mueang	Chainat	1.40	20.64	18.66
15.	Huai Mak Daeng	Tha Hin Ngom	Mueang	Chaiyaphum	1.27	15.40	25.26
16.	Tad Rin Thong	That Thong	Phu Khiao	Chaiyaphum	1.37	10.30	21.34
17.	Khong Sai	Ban Chiang	Phakdi Chumphon	Chaiyaphum	1.45	12.99	19.96
18.	Huai Muag San Chareun	Mae Chedi Mai	Wiang Pa Pao	Chiang Rai	1.27	15.77	28.40
19.	Mueang Ong	Ban Luang	Chom Thong	Chiang Mai	1.27	17.27	25.14
20.	Nam Lad	Ban Luang	Chom Thong	Chiang Mai	1.31	8.41	22.59
21.	Den	Ban Luang	Chom Thong	Chiang Mai	1.20	21.52	25.76

Appendix Table A3 (Continued)

No.	Village	Subdistrict	District	Province	Bulk Density (B.D.)	Water Holding Capacity, (WHC) (g./cu.cm.)	Saturation Percentage (%)
22.	Mae Hae Nuea	Mae Na Chon	Mae Chaem	Chiang Mai	1.06	21.20	32.63
23.	Huai Hoy	Mae Na Chon	Mae Chaem	Chiang Mai	1.15	19.03	28.98
24.	Pa Fon	Pang Hin	Mae Chaem	Chiang Mai	0.96	26.06	37.79
25.	Chiang Dao	Chiang Dao	Chiang Dao	Chiang Mai	1.45	16.61	21.46
26.	Aru No Thai	Mueang Na	Chiang Dao	Chiang Mai	0.70	32.20	46.45
27.	Iak	San Pa Yang	Mae Taeng	Chiang Mai	1.23	21.89	26.68
28.	Lao	Mueang Kai	Mae Taeng	Chiang Mai	1.14	22.27	27.94
29.	Nong Hoy Mai	Mae Ram	Mae Rim	Chiang Mai	1.11	24.50	32.15
30.	Thung Ha	Pa Tum	Phrao	Chiang Mai	1.66	10.98	15.69
31.	Pa Hin	Ban Pong	Phrao	Chiang Mai	1.24	21.48	26.24
32.	Mon Hin Lai	Mae Pang	Phrao	Chiang Mai	1.25	25.55	29.21
33.	Luang	Long Khot	Phrao	Chiang Mai	1.38	15.02	25.52
34.	Hang Dong	Hang Dong	Hot	Chiang Mai	1.32	10.38	24.00
35.	Doi Tao	Doi Tao	Doi Tao	Chiang Mai	1.39	16.02	22.26
36.	Yong Kue	Omkoi	Omkoi	Chiang Mai	1.18	45.10	28.77
37.	Tung Ting	Omkoi	Omkoi	Chiang Mai	1.27	18.81	27.01
38.	Mae Ra	Omkoi	Omkoi	Chiang Mai	1.39	15.49	23.72
	Meed Luang						
39.	Luang	Yang Piang	Omkoi	Chiang Mai	1.25	17.29	25.52
40.	Huai Tong	Yang Piang	Omkoi	Chiang Mai	1.20	46.95	25.79
41.	Huai Lo Duk	Mae Tuen	Omkoi	Chiang Mai	1.34	15.93	16.20
42.	Mae Ra Ar Nai	Mae Tuen	Omkoi	Chiang Mai	1.18	17.66	25.74
43.	Thung Ton Ngiu	Mae Tuen	Omkoi	Chiang Mai	1.09	20.99	30.47
44.	Sam Muen	Mueang Haeng	Wiang Haeng	Chiang Mai	0.91	26.08	38.08
45.	Mae Tae	Mueang Haeng	Wiang Haeng	Chiang Mai	1.05	23.00	29.63
46.	Na Sai	Thung Pi	Mae Wang	Chiang Mai	1.46	5.62	14.05
47.	Tha Mon	Mae Tha	Mae On	Chiang Mai	1.43	9.84	22.41
48.	Thung Phu Mian	Khane Chue	Mae Ramat	Tak	1.28	16.36	21.62
49.	Huai Phlu	Mae Tuen	Mae Ramat	Tak	1.29	17.80	24.56
50.	Huai Ma Ba	Mae Tuen	Mae Ramat	Tak	1.44	14.51	21.50

Appendix Table A3 (Continued)

No.	Village	Subdistrict	District	Province	Bulk Density (B.D.)	Water Holding Capacity, (WHC) (g./cu.cm.)	Saturation Percentage (%)
51.	Khun Huai Mae Tho	Sam Muen	Mae Ramat	Tak	1.42	13.88	20.15
52.	Yang Huai Ya-U	Dan Mae La Mao	Mae Sot	Tak	1.30	15.83	19.57
53.	Hauai Nam Nak	Phop Phra	Phop Phra	Tak	1.45	41.86	117.33
54.	Chong Khaep	Chong Khaep	Phop Phra	Tak	1.29	19.45	27.40
55.	Huai Laeng	Chong Khaep	Phop Phra	Tak	1.29	15.23	19.05
56.	Um Piem	Khiri Rat	Phop Phra	Tak	1.37	16.19	22.77
57.	Umphang	Umphang	Umphang	Tak	1.19	21.87	23.01
58.	Mae Klong Yai	Mokro	Umphang	Tak	1.23	19.28	29.67
59.	Mae Klong Noi	Mokro	Umphang	Tak	1.16	22.58	35.28
60.	Nong Prue	Si Chula	Mueang	Nakhon Nayok	1.13	23.72	27.97
61.	Suan Hong	Sarika	Mueang	Nakhon Nayok	1.31	19.34	30.92
62.	Lam Hoei	Lam Hoei	Don Tum	Nakhon Phathom	1.36	13.42	22.45
63.	Han	Dan Khun Thot	Dan Khun Thot	Nakhon Ratchasima	1.52	6.06	17.32
64.	Huai Pong	Huai Bong	Dan Khun Thot	Nakhon Ratchasima	1.44	7.78	23.53
65.	Khok Tong	Tha Lat	Chum Phuang	Nakhon Ratchasima	1.40	11.67	19.92
66.	Khao Yai Tiang	Khlong Pai	Sikhio	Nakhon Ratchasima	1.20	14.44	25.85
67.	Pa Kluai	Wang Katha	Pak Chong	Nakhon Ratchasima	1.43	12.95	20.27
68.	Poahu	Pong Talong	Pak Chong	Nakhon Ratchasima	1.24	19.73	22.38
69.	Sap Tai	Phaya Yen	Pak Chong	Nakhon Ratchasima	1.46	90.22	18.90
70.	Non Rawiang	Bueng Phalai	Kaeng Sanam Nang	Nakhon Ratchasima	1.50	9.33	18.26
71.	Khlong Hin Pun	Nong Bua	Nong Bua	Nakhon Sawan	1.40	15.99	20.03
72.	Chong Khiri	Takhro	Phaisali	Nakhon Sawan	1.19	18.77	29.00

Appendix Table A3 (Continued)

No.	Village	Subdistrict	District	Province	Bulk Density (B.D.)	Water Holding Capacity, (WHC) (g./cu.cm.)	Saturation Percentage (%)
73.	Khao Sam Yot	Khao Kala	Phayuha Khiri	Nakhon Sawan	1.21	16.61	26.04
74.	Kra Thum Thong	Mae Wong	Mae Wong	Nakhon Sawan	1.47	10.67	20.01
75.	Mai Ratchasima	Khao Chon Kan	Mae Wong	Nakhon Sawan	1.62	6.95	14.66
76.	Huai Ra Pe	Sa Nian	Mueang	Nan	1.16	16.87	31.36
77.	Nam Pai	Nam Pai	Mae Charim	Nan	1.25	18.94	23.27
78.	Wang Kok	Nam Tok	Na Noi	Nan	1.30	17.08	24.40
79.	Kok	Ouan	Pua	Nan	1.35	13.41	23.47
80.	Thung Mai	Ouan	Pua	Nan	1.19	20.01	30.74
81.	Na Wong	Chedi Chai	Pua	Nan	1.24	19.38	25.48
82.	Khun Kun	Phu Kha	Pua	Nan	1.14	25.04	29.31
83.	Pha Weang	Phu Kha	Pua	Nan	1.02	24.57	36.49
84.	Toey Kio Hen	Phu Kha	Pua	Nan	1.08	24.88	32.27
85.	Sakat Nuea	Sakat	Pua	Nan	1.00	29.33	35.86
86.	San ti Suk	Saen Thong	Tha Wang Pha	Nan	1.13	24.29	28.66
87.	Hak Han	Yap Hua Na	Wiang Sa	Nan	1.08	19.38	29.98
88.	Pa Phae	Mae Khaning	Wiang Sa	Nan	1.17	23.62	28.96
89.	Huai Na Ngiu	Mae Khaning	Wiang Sa	Nan	1.13	22.63	29.70
90.	Chaloem Rat	Pon	Thung Chang	Nan	1.09	25.30	34.43
91.	Nam Sod	Lae	Thung Chang	Nan	1.16	21.95	27.41
92.	Nam Muet	Puea	Chiang Klang	Nan	1.40	18.41	22.52
93.	Nong Pla	Phra That	Chiang Klang	Nan	1.12	20.21	32.46
94.	Tha Kwauy	Mueang Le	Na Muen	Nan	1.10	24.33	31.65
95.	Huai Yen	Ping Luang	Na Muen	Nan	1.11	22.38	28.96
96.	Wen	Bo Kluea Nuea	Bo Kluea	Nan	1.36	19.32	25.15
97.	Bo Yuak Tai	Bo Kluea Nuea	Bo Kluea	Nan	1.13	20.34	28.09

Appendix Table A3 (Continued)

No.	Village	Subdistrict	District	Province	Bulk Density (B.D.)	Water Holding Capacity, (WHC) (g./cu.cm.)	Saturation Percentage (%)
98.	Na Kuen	Bo Kluea Nuea	Bo Kluea	Nan	1.29	19.91	24.41
99.	Huai Por	Bo Kluea Nuea	Bo Kluea	Nan	1.21	21.70	31.51
100.	Na Bong	Bo Kluea Tai	Bo Kluea	Nan	1.23	17.74	29.46
101.	Huai Lom	Phu Fa	Bo Kluea	Nan	1.19	19.58	26.42
102.	Sawa Tai	Dong Phaya	Bo Kluea	Nan	1.30	19.11	24.63
103.	Pha Sing	Yot	Song Khwae	Nan	1.22	23.54	25.94
104.	Nam Ko	Yot	Song Khwae	Nan	1.09	24.37	34.75
105.	Huai Sai	Huai Kon	Chaloem	Nan	1.07	25.21	32.22
	Khao		Phra Kiat				
106.	Nam Chang	Khun Nan	Chaloem	Nan	1.29	20.32	22.87
			Phra Kiat				
107.	Huai Kaeo	Huai Khao Kam	Chun	Phayao	1.44	13.78	19.59
108.	Pha Hao	Thung Pha Suk	Chiang Kham	Phayao	1.33	7.68	23.27
109.	Nam Jaeng	Na Bua	Nakhon Thai	Phitsanulok	1.31	15.59	25.45
	Phattana						
110.	Rak Thai	Bo Phak	Chat Trakan	Phitsanulok	1.37	13.11	22.77
111.	Huai Dua	Wang Nok	Wang Thong	Phitsanulok	1.32	14.15	24.27
	Aen						
112.	Lam Phat	Ban Mung	Noen Maprang	Phitsanulok	1.28	15.87	25.31
113.	Pang Yao	Phai Thon	Rong Kwang	Phrae	1.20	19.13	27.88
114.	Thung Ta	Ban Pin	Long	Phrae	1.39	11.88	21.33
	Kla						
115.	Mae Khaem	Bo Lek Long	Long	Phrae	1.22	13.25	29.29
116.	Khuang Buk	Huai Rai	Den Chai	Phrae	1.29	18.88	26.99
117.	Huai Khon	Huai Mai	Song	Phrae	1.29	16.10	25.45
118.	Sob Soi	Pang Mu	Mueang	Mae Hong Son	1.31	19.60	23.61
119.	Mahin Luang	Mueang Pon	Khun Yuam	Mae Hong Son	1.28	18.23	25.61
120.	Huai Pong	Mae Ki	Khun Yuam	Mae Hong Son	1.32	19.03	27.66
	Lao						
121.	Tha Pai	Mae Hi	Pai	Mae Hong Son	1.78	10.10	15.35
122.	Mae Ping	Mae Hi	Pai	Mae Hong Son	1.66	13.46	18.23
123.	Mueang	Mueang	Pai	Mae Hong Son	1.74	9.46	15.35
	Paeng	Paeng					

Appendix Table A3 (Continued)

No.	Village	Subdistrict	District	Province	Bulk Density (B.D.)	Water Holding Capacity, (WHC) (g./cu.cm.)	Saturation Percentage (%)
124.	Mai Don Tan	Mueang Paeng	Pai	Mae Hong Son	1.74	10.15	14.09
125.	Pong Sa	Pong Sa	Pai	Mae Hong Son	1.47	14.58	22.31
126.	Huai Rai	Pong Sa	Pai	Mae Hong Son	1.27	20.08	13.63
127.	Khun Sa Nai	Pong Sa	Pai	Mae Hong Son	1.18	19.66	31.19
128.	Pong Tak	Pong Sa	Pai	Mae Hong Son	1.52	17.63	21.11
129.	Pang Tong	Pong Sa	Pai	Mae Hong Son	1.43	20.15	23.57
130.	Mae Sawan Luang	Mae Ho	Mae Sariang	Mae Hong Son	1.20	23.69	28.75
131.	Hua Mae Tho	Mae Tho	Mae La Noi	Mae Hong Son	1.45	14.74	23.58
132.	Mae Cho	Mae Tho	Mae La Noi	Mae Hong Son	1.31	18.73	27.30
133.	Mae Mu Liso Soppong		Pang Mapha	Mae Hong Son	1.19	24.64	31.48
134.	Pang Kham	Pang Mapha	Pang Mapha	Mae Hong Son	1.15	23.29	30.69
135.	Na Pu Pom	Napu Pom	Pang Mapha	Mae Hong Son	1.30	20.00	24.54
136.	Pho Ngam	Huai Pong	Khok Samrong	Lopburi	1.48	15.59	18.65
137.	Nong Phak Chi	Chai Narai	Chai Badan	Lopburi	1.31	17.01	19.73
138.	Nong Krathum	Maha Phot	Sa Bot	Lopburi	1.38	14.71	19.38
139.	Klang	Ban Dong	Mae Mo	Lampang	1.18	21.03	29.12
140.	Sob Moh	Sop Pat	Mae Mo	Lampang	1.13	25.73	32.26
141.	Mae Liang Phatthana	Soem Khwa	Some Ngam	Lampang	1.09	15.94	30.17
142.	Huai Nam Tuen	Pong Tao	Ngao	Lampang	1.16	22.28	30.28
143.	Nong Hiang	Nakae	Ngao	Lampang	1.34	13.61	24.08
144.	Hua Fai	Thung Phueng	Chae Hom	Lampang	1.26	15.02	21.97
145.	Pa Lan	Wang Thong	Wang Nuea	Lampang	1.27	15.18	27.18
146.	Mae Heed	Wang Kaeo	Wang Nuea	Lampang	1.13	18.37	31.65
147.	Mae Salem	Wiang Mok	Thoen	Lampang	1.26	9.66	24.12
148.	Chai Chompu	Wiang Mok	Thoen	Lampang	1.16	12.15	30.39
149.	Phae	Sop Prap	Sop Prap	Lampang	1.36	18.47	25.10
150.	Pang Ai	Mueang Pan	Mueang Pan	Lampang	1.09	13.68	32.57
151.	Si Chum	Ban Klang	Mueang	Lamphun	1.61	14.58	12.82
152.	Pha Dan	Tha Kat	Mae Tha	Lamphun	1.32	11.82	22.73

Appendix Table A3 (Continued)

No.	Village	Subdistrict	District	Province	Bulk Density (B.D.)	Water Holding Capacity, (WHC) (g./cu.cm.)	Saturation Percentage (%)
153.	Huai Hom Nok	Tha Mae Lop	Mae Tha	Lamphun	1.37	16.69	23.89
154.	Pak Thang Mung Ton	Lao Yao	Ban Hong	Lamphun	1.69	12.76	11.72
155.	Ko Jok	Ko	Li	Lamphun	1.25	23.40	21.69
156.	Nong Kok	Ban Puang	Thung Hua Chang	Lamphun	1.48	10.33	22.58
157.	Nam Huay	Na Pong	Thung Hua Chang	Lamphun	1.36	15.18	23.17
158.	Hau Nareang	Ban Pa	Kaeng Khoi	Saraburi	1.39	15.36	22.37
159.	Lam Bua	Kum Hak	Nong Khae	Saraburi	1.27	20.73	23.24
160.	Nong Samak	Khok Yae	Nong Khae	Saraburi	1.39	17.28	24.34
161.	Nong Dok	Phu Krang	Phra Phutthabat	Saraburi	1.31	19.35	25.44
162.	Pak Khlong	Muak Lek	Muak Lek	Saraburi	1.35	18.03	28.84
163.	Dong Ya Pa	Ban Tuek	Si Satchanalai	Sukhothai	1.20	18.54	28.94
164.	Pa Ka	Ban Kaeng	Si Satchanalai	Sukhothai	1.32	19.15	26.12
165.	Huai Ta Yang	Nong Ong	U Thong	Suphan Buri	1.36	12.52	21.37
166.	Nam Wang Luang	Ban Dan	Mueang	Uttaradit	1.45	12.90	21.56
167.	Nam Li	Nam Man	Tha Pla	Uttaradit	1.18	19.32	27.84
168.	Kok Mon	Nam Pai	Nam Pat	Uttaradit	1.37	16.00	24.32
	Kiew						
169.	Wang O	Ban Siao	Fak Tha	Uttaradit	1.57	8.34	15.29
170.	Nam Phae	Ban Khok	Ban Khok	Uttaradit	1.40	13.17	21.40
171.	Bo Bia	Bo Bia	Ban Khok	Uttaradit	1.40	14.66	20.32
172.	Pang Com	Bo Bia	Ban Khok	Uttaradit	1.44	14.45	19.25
173.	Huai Yang	Bo Bia	Ban Khok	Uttaradit	1.33	15.99	21.19
174.	Pang Hi	Bo Bia	Ban Khok	Uttaradit	1.53	10.00	16.01
175.	Pak Mueang	Na In	Phi Chai	Uttaradit	1.51	10.06	16.39
176.	Khao Keow	Rabam	Lan Sak	Uthai Thani	1.30	13.49	25.49
177.	Dong Chat Kom	Pong Daeng	Mueang	Tak	1.45	14.72	22.36
178.	Kholng Sak	Nam Ruem	Mueang	Tak	1.40	15.46	21.60
179.	Thong Fa	Thong Fa	Ban Tak	Tak	1.39	15.54	23.08
180.	Wang Po	Wang Chan	Sam Ngao	Tak	1.31	18.14	24.95

Appendix Table A3 (Continued)

No.	Village	Subdistrict	District	Province	Bulk Density (B.D.)	Water Holding Capacity, (WHC) (g./cu.cm.)	Saturation Percentage (%)
181.	Khun Huai Mae Kha Ho Ma	Mae Tan	Tha Song Yang	Tak	1.43	14.34	20.87
182.	Mae Pha Deang	Mae Song	Tha Song Yang	Tak	1.43	13.65	21.72
183.	Khun Huai Nok Kok	Mae La	Tha Song Yang	Tak	1.58	11.95	15.10
184.	Ra Ka Ti	Mae U-su	Tha Song Yang	Tak	1.44	15.03	22.96
185.	Pha Phueng	Chiang Thong	Wang Chao	Tak	1.18	19.52	24.45
186.	Khao Khat	Tabo	Mueang	Phetchabun	1.31	17.74	25.01
187.	Nam Phu	Phutthabat	Chon Daen	Phetchabun	1.31	19.29	25.83
188.	Pong Chet	Phutthabat	Chon Daen	Phetchabun	1.45	14.00	20.27
	Hua						
189.	Wang Rong	Sak Long	Lom Sak	Phetchabun	1.32	18.87	25.57
190.	Ta Rub Lan	Bug Khla	Lom Sak	Phetchabun	1.33	16.99	23.46
191.	Sak Nga	Sila	Lom Kao	Phetchabun	1.40	16.85	22.40
192.	Thap Boek	Wang Ban	Lom Kao	Phetchabun	1.14	21.48	31.91
193.	Nong Mu	Pradu Ngam	Si Thep	Phetchabun	1.34	20.92	26.81
194.	Pong Nok	Wang Kaeo	Nam Nao Kwang	Phetchabun	1.40	15.83	21.75
195.	Pa Ruak	Khok Mon	Nam Nao	Phetchabun	1.29	18.01	26.04
196.	Thang Deang	Khaem Son	Khao Kho	Phetchabun	1.22	19.55	27.60
197.	Kong Niam	Khao Kho	Khao Kho	Phetchabun	1.32	17.53	25.50

Appendix Table A4 Major land use of small watersheds.

No.	Small Watersheds Code	Catchment Area (sq.km)	Major land use (sq.km)				
			Urban	Agriculture	Forest	Water Bodies	Other
1.	C_1	1,545.83	271.41	1,229.83	53.37	25.39	15.90
2.	C_2	3,401.69	91.61	3,844.45	213.04	55.70	117.03
3.	N_1	2,228.40	24.56	950.12	1,184.01	5.93	26.77
4.	N_2	790.12	2.87	390.89	433.31	1.06	26.25
5.	N_3	1,536.76	36.93	636.62	781.28	10.88	96.59
6.	N_4	600.56	4.16	250.52	325.00	1.82	6.84
7.	N_5	591.43	9.63	202.94	249.80	0.19	9.96
8.	N_6	781.25	3.64	124.70	606.25	3.19	20.22
9.	N_7	3,195.67	18.41	468.30	2,439.37	233.71	15.68
10.	N_8	2,206.21	2.74	586.01	1,477.45	8.64	5.53
11.	N_9	1,046.72	9.47	410.06	664.25	1.53	12.37
12.	N_11	2,429.65	22.44	728.36	1,569.69	5.47	7.82
13.	N_12	1,095.06	71.93	532.61	492.64	0.78	2.69
14.	N_13	339.67	17.13	83.89	237.95		5.07
15.	N_14	1,727.56	38.99	1,094.99	634.61	19.38	11.37
16.	N_15	688.24	48.61	606.20	65.89	63.86	8.03
17.	N_16	5,583.44	116.19	3,054.60	2,146.65	18.98	170.15
18.	N_17	219.89	25.77	110.13	0.53	0.64	1.91
19.	N_18	158.46	30.08	93.48	0.53	1.53	4.35
20.	N_19	259.45	970.65	297.17	0.53	0.78	4.25
21.	N_20	2,615.91	448.92	592.02	1,365.07	8.32	22.57
22.	N_21	271.77	68.44	107.04	0.62	20.63	11.59
23.	N_22	1,226.22	18.03	157.10	13.41	1.03	9.41
24.	N_23	205.20	6.73	255.68	0.53	0.28	2.34
25.	N_24	2,208.96	84.90	2,492.66	282.15	0.76	99.08
26.	N_25	1,426.18	51.72	227.79	70.55	1.57	38.57
27.	N_26	2,142.74	76.74	1,100.18	8.96	9.35	8.40
28.	N_27	988.53	0.58	143.38	516.20	0.95	6.16
29.	P_1	1,912.74	24.50	286.41	1,580.21	0.45	7.36
30.	P_2	1,286.47	25.37	223.43	1,039.96	12.41	11.05
31.	P_3	1,961.74	24.06	331.20	1,551.53	1.85	2.55
32.	P_4	1,530.67	247.76	553.64	606.13	11.60	83.47
33.	P_5	53.44	5.51	12.18	1.49	0.19	1.91
34.	P_6	562.05	16.32	89.24	481.78		1.91
35.	P_7	2,894.30	216.83	908.29	1,699.61	24.58	52.86
36.	P_8	1,745.75	47.26	198.51	1,507.38	0.48	18.82
37.	P_9	2,100.52	61.03	406.53	1,615.08	4.04	95.73
38.	P_10	620.93	5.97	88.04	465.32	0.30	15.25
39.	P_11	3,194.35	37.57	193.04	2,781.42	125.56	85.13
40.	P_12	1,971.02	6.94	96.94	1,871.00	0.15	5.71

Appendix Table A4 (Continued)

No.	Small Watersheds Code	Catchment Area (sq.km)	Major land use (sq.km)				
			Urban	Agriculture	Forest	Water Bodies	Other
41.	P_13	1,935.41	9.62	185.84	1,723.74	0.80	6.34
42.	P_14	522.07	9.10	96.73	420.81	1.11	8.89
43.	P_15	3,179.69	5.68	201.64	3,157.00	14.91	2.80
44.	P_16	845.40	0.45	0.97	624.44	140.06	1.91
45.	P_17	166.08	1.84	17.47	152.53	0.48	5.91
46.	P_18	527.90	6.91	116.74	307.24	0.23	17.26
47.	P_19	654.36	4.59	37.31	623.38	62.49	1.91
48.	P_20	274.51	18.66	35.45	186.14	2.09	39.05
49.	P_21	959.53	10.69	339.98	407.22	3.69	18.12
50.	P_22	367.57	16.67	62.79	321.39	1.47	41.48
51.	P_23	383.54	12.64	119.11	239.81	0.81	2.17
52.	P_24	759.00	1.86	168.12	592.48		1.91
53.	P_25	293.50	12.26	716.71	46.95		3.35
54.	P_26	1,222.97	16.38	431.30	740.41	1.23	7.37
55.	P_27	211.17	6.48	175.63	0.61		3.38
56.	P_28	549.15	24.61	307.34	15.78	0.60	3.09
57.	P_29	1,351.47	18.34	915.37	428.20	27.02	8.06
58.	P_30	532.15	515.70	119.38	5.76	0.04	1.91
59.	P_31	237.67	17.38	275.54	3.04	0.10	1.91
60.	P_32	133.25	24.11	82.87	0.53	0.23	1.91
61.	W_1	1,645.68	21.17	304.48	1,262.11	0.94	40.54
62.	W_2	736.11	9.36	118.84	645.31	0.40	3.73
63.	W_3	967.36	35.16	215.24	647.98	1.20	69.57
64.	W_4	403.91	6.59	52.48	197.85	8.73	7.62
65.	W_5	455.09	14.76	84.70	567.21	0.14	29.56
66.	W_6	1,758.75	108.29	284.11	971.79	20.59	236.91
67.	W_7	736.48	39.59	178.67	433.39	3.68	61.88
68.	W_8	863.30	16.62	110.87	610.04	2.56	104.34
69.	W_9	282.53	3.96	41.11	249.85	2.01	20.61
70.	W_10	232.81	6.17	58.46	90.94	0.54	15.82
71.	W_11	281.77	3.31	20.62	235.88	5.57	10.54
72.	W_12	230.08	1.67	11.19	47.82	0.03	13.80
73.	W_13	149.13	0.90	6.36	36.50		5.05
74.	W_14	182.87	4.79	30.26	52.77		10.94
75.	W_15	362.83	12.08	81.44	171.04	5.02	10.47
76.	W_16	340.06	1.90	13.72	514.05	1.88	2.42
77.	W_17	308.38	7.27	56.01	92.87	5.20	9.18
78.	W_18	256.61	4.02	45.65	235.47	0.28	7.62
79.	W_19	378.76	3.18	35.27	80.28	2.01	16.14
80.	W_20	215.53	11.71	95.45	39.69	0.74	23.60

Appendix Table A4 (Continued)

No.	Small Watersheds Code	Catchment Area (sq.km)	Major land use (sq.km)				
			Urban	Agriculture	Forest	Water Bodies	Other
81.	W_21	22.36	2.62	18.99	0.53	3.05	1.91
82.	Y_1	2,119.68	18.03	381.12	1,991.62	7.03	56.58
83.	Y_2	873.55	4.55	140.40	660.50	0.68	19.88
84.	Y_3	658.84	5.97	44.16	427.58	0.91	50.30
85.	Y_4	1,760.07	18.82	255.87	1,380.08	1.37	15.21
86.	Y_5	214.68	0.55	30.91	26.06	0.44	1.91
87.	Y_6	374.67	7.47	40.23	457.41	4.89	2.22
88.	Y_7	332.06	13.20	237.55	19.83	9.13	4.18
89.	Y_8	246.06	4.69	71.25	32.02	0.80	3.17
90.	Y_9	1,032.13	42.99	371.86	347.11	4.49	12.78
91.	Y_10	149.72	5.45	23.63	460.64	1.02	1.91
92.	Y_11	532.40	14.54	24.81	886.80	1.39	1.91
93.	Y_12	246.04	4.00	108.00	14.01	1.39	2.18
94.	Y_13	710.99	6.46	35.38	545.40	0.84	2.38
95.	Y_14	439.67	9.94	30.41	170.72	0.54	4.18
96.	Y_15	531.06	11.03	145.08	54.10	6.80	1.91
97.	Y_16	214.37	2.42	26.24	28.94		1.91
98.	Y_17	880.08	5.32	141.19	852.00	0.17	1.91
99.	Y_18	832.84	4.26	203.93	1,433.54	0.24	1.91
100.	Y_19	796.77	23.09	624.79	375.24	1.47	3.69
101.	Y_20	768.35	29.72	201.00	161.97	24.45	3.93
102.	Y_21	2,312.65	46.11	1,227.61	1,637.58	4.24	41.06
103.	Y_22	491.33	11.95	999.17	2.05	3.32	18.02
104.	Y_23	1,055.89	23.25	314.36	749.53	0.76	8.20
105.	Y_24	1,572.14	28.54	3,588.68	371.72	3.83	39.56
106.	Y_25	905.78	27.98	225.20	0.90	3.09	18.39
107.	Y_26	545.44	21.09	117.42	0.53	0.25	14.04
108.	Y_27	1,323.37	66.94	64.20	0.96	2.55	7.38
109.	Y_28	656.33	31.33	298.99	0.53	10.41	2.52
110.	Y_29	191.71	22.57	81.44	0.53	0.20	2.37
111.	Y_30	655.33	31.09	117.56	0.86	530.41	5.74
112.	Y_31	169.97	27.98	35.18	0.53	0.45	9.07

Appendix Table A5 Agriculture land use of small watersheds

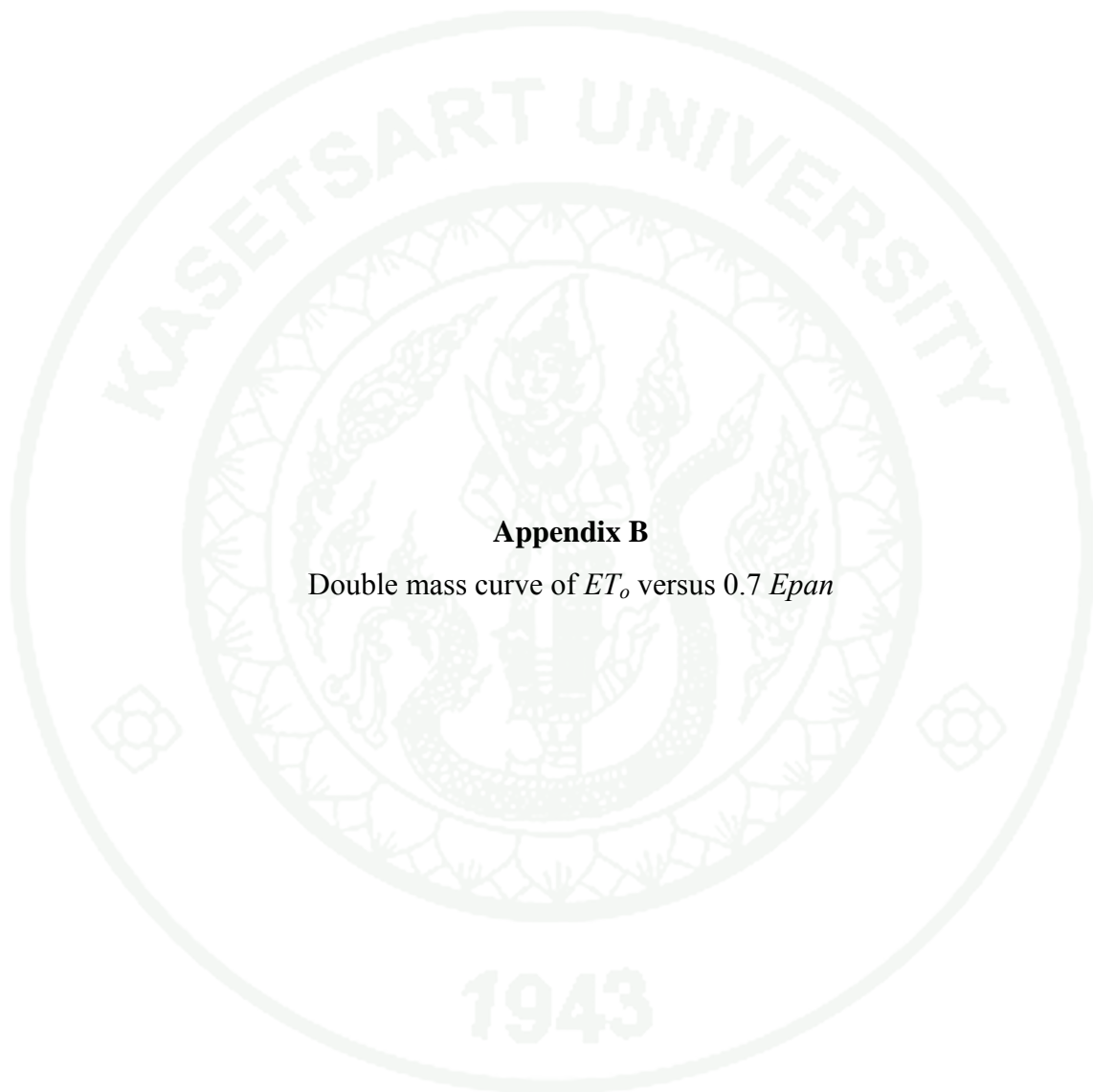
No.	Small Watersheds Code	Agriculture Area (sq.km)	Agriculture land use (sq.km)			
			Paddy	Paddy in irrigation area	Field Crop	Tree
1.	C_1	1,229.8	822.44		397.27	10.11
2.	C_2	3,844.5	2,225.11		1,598.59	20.75
3.	N_1	950.1	84.60		854.93	10.59
4.	N_2	390.9	3.09		387.25	0.56
5.	N_3	636.6	197.56		297.17	141.90
6.	N_4	250.5	26.65		203.42	20.45
7.	N_5	202.9	88.24		80.05	34.65
8.	N_6	124.7	13.48		106.42	4.80
9.	N_7	468.3	25.39	4.24	422.61	16.06
10.	N_8	586.0	14.99		568.30	2.72
11.	N_9	410.1	35.71		366.74	7.61
12.	N_11	728.4		81.07	645.72	1.57
13.	N_12	532.6		110.90	382.04	39.67
14.	N_13	83.9		14.29	69.03	0.57
15.	N_14	1,095.0		204.54	888.19	2.27
16.	N_15	606.2	7.67	338.15	118.43	141.95
17.	N_16	3,054.6	627.84	0.81	2,385.71	40.25
18.	N_17	110.1	92.43	4.29	1.17	12.25
19.	N_18	93.5	77.96		0.16	15.36
20.	N_19	297.2	290.04		0.16	6.97
21.	N_20	592.0	79.00		496.27	16.75
22.	N_21	107.0	104.04		0.16	2.84
23.	N_22	157.1	47.66		68.67	40.77
24.	N_23	255.7	253.77		0.55	1.37
25.	N_24	2,492.7	1,982.13		399.96	110.57
26.	N_25	227.8	35.13		175.27	17.39
27.	N_26	1,100.2	875.87		185.33	38.98
28.	N_27	143.4	24.18		118.80	0.40
29.	P_1	286.4	75.46		106.78	104.17
30.	P_2	223.4	72.61		56.27	94.55
31.	P_3	331.2	35.03	1.22	246.30	48.65
32.	P_4	553.6	304.04		22.67	226.93
33.	P_5	12.2	4.58		6.78	0.82
34.	P_6	89.2	44.00		30.47	14.77
35.	P_7	908.3	583.61		28.42	296.26
36.	P_8	198.5	118.75		61.72	18.04
37.	P_9	406.5	113.89		212.20	80.44
38.	P_10	88.0	12.63		43.05	32.37
39.	P_11	193.0	33.35		49.26	110.43
40.	P_12	96.9	26.02		70.91	

Appendix Table A5 (Continued)

No.	Small Watersheds Code	Agriculture Area (sq.km)	Agriculture land use (sq.km)			Tree
			Paddy	Paddy in irrigation area	Field Crop	
41.	P_13	185.8	36.77		146.40	2.67
42.	P_14	96.7	9.90		67.60	19.23
43.	P_15	201.6	39.54		161.86	0.24
44.	P_16	1.0	0.81		0.16	
45.	P_17	17.5	11.01		6.46	
46.	P_18	116.7	64.07		51.94	0.73
47.	P_19	37.3	18.50		16.64	2.17
48.	P_20	35.4	22.37		13.07	
49.	P_21	340.0	260.48		70.18	9.31
50.	P_22	62.8	55.59		2.77	4.43
51.	P_23	119.1	12.67		102.15	4.29
52.	P_24	168.1	16.89		145.96	5.27
53.	P_25	716.7	18.95		689.95	7.81
54.	P_26	431.3	106.54		304.96	19.79
55.	P_27	175.6	82.21		76.04	17.38
56.	P_28	307.3	32.86		250.30	24.17
57.	P_29	915.4	151.10		748.94	15.34
58.	P_30	119.4	19.63		88.50	11.25
59.	P_31	275.5	106.46		168.54	0.54
60.	P_32	82.9	43.33		39.53	
61.	W_1	304.5	96.42	1.55	199.47	7.04
62.	W_2	118.8	44.60		72.00	2.24
63.	W_3	215.2	89.36		123.50	2.38
64.	W_4	52.5	10.39		37.07	5.02
65.	W_5	84.7	17.51		57.85	9.33
66.	W_6	284.1	197.27		84.59	2.25
67.	W_7	178.7	132.81		45.57	0.29
68.	W_8	110.9	78.13		28.05	4.69
69.	W_9	41.1	10.76		30.35	
70.	W_10	58.5	50.20		8.26	
71.	W_11	20.6	10.50		10.12	
72.	W_12	11.2	5.91		2.54	2.73
73.	W_13	6.4	3.72		0.16	2.48
74.	W_14	30.3	21.18		8.78	0.30
75.	W_15	81.4	62.23		15.54	3.67
76.	W_16	13.7	8.95		4.77	
77.	W_17	56.0	14.37		40.49	1.15
78.	W_18	45.6	24.47		18.16	3.01
79.	W_19	35.3	27.25		7.75	0.26
80.	W_20	95.4	37.94		56.88	0.63

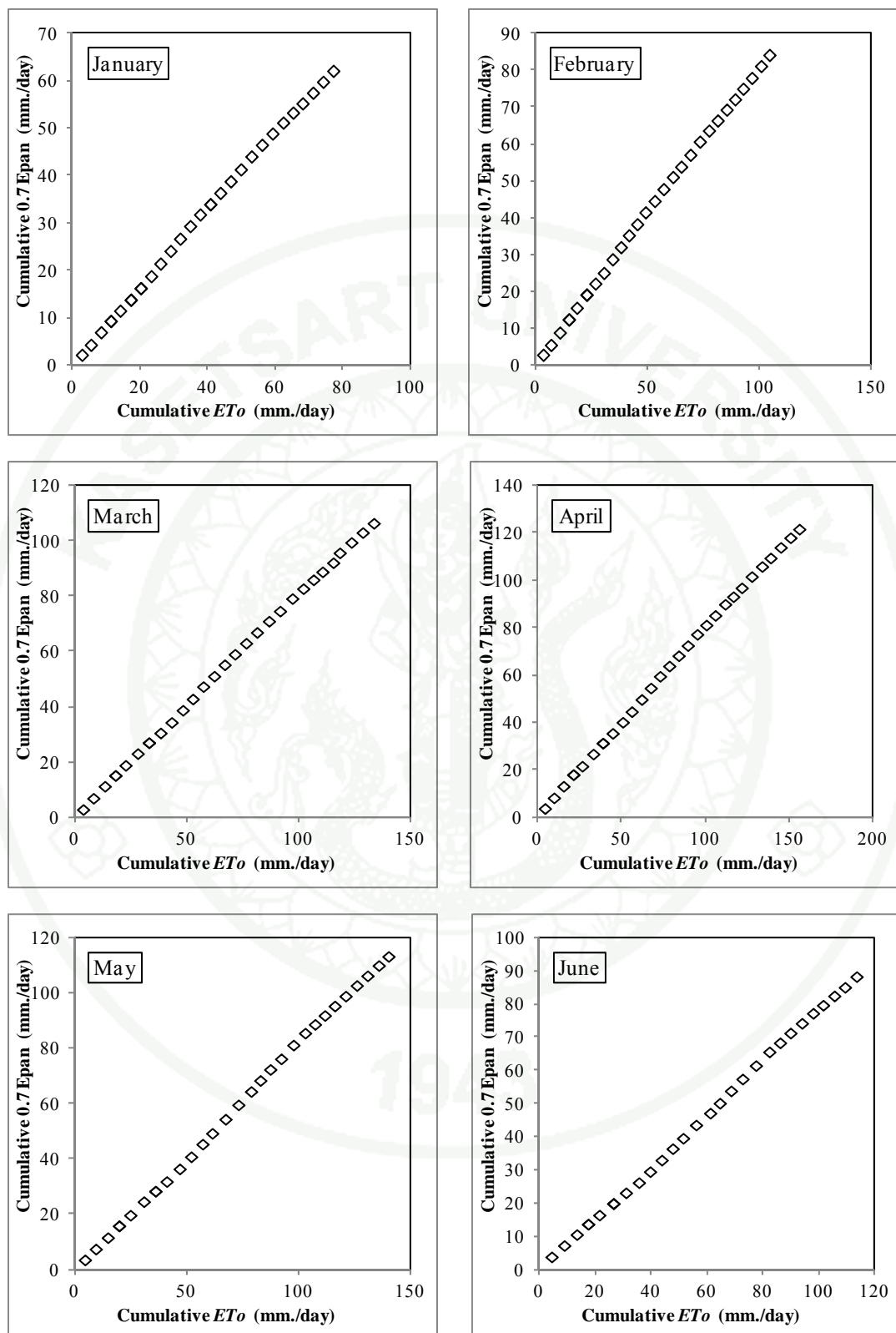
Appendix Table A5 (Continued)

No.	Small Watersheds Code	Agriculture Area (sq.km)	Agriculture land use (sq.km)		
			Paddy	Paddy in irrigation area	Field Crop
81.	W_21	19.0	15.08		3.90
82.	Y_1	381.1	76.44		301.33
83.	Y_2	140.4	20.24		120.16
84.	Y_3	44.2	24.48		19.04
85.	Y_4	255.9	77.48		174.22
86.	Y_5	30.9	2.45		23.18
87.	Y_6	40.2	1.14		35.64
88.	Y_7	237.6	140.98		83.59
89.	Y_8	71.3	25.15		38.58
90.	Y_9	371.9	212.75		133.48
91.	Y_10	23.6			19.87
92.	Y_11	24.8			4.24
93.	Y_12	108.0	88.00		2.28
94.	Y_13	35.4	22.85		8.58
95.	Y_14	30.4	9.68		3.05
96.	Y_15	145.1	74.75		24.30
97.	Y_16	26.2	13.98		0.16
98.	Y_17	141.2	27.67		36.18
99.	Y_18	203.9	18.61		153.29
100.	Y_19	624.8	160.96		426.67
101.	Y_20	201.0	29.44		157.11
102.	Y_21	1,227.6	978.40		173.56
103.	Y_22	999.2		0.78	984.99
104.	Y_23	314.4	181.88		119.68
105.	Y_24	3,588.7	3,388.20		183.95
106.	Y_25	225.2	103.88	69.88	45.20
107.	Y_26	117.4	1.99		111.47
108.	Y_27	64.2	6.72		47.49
109.	Y_28	299.0	261.54		25.33
110.	Y_29	81.4	37.75		0.16
111.	Y_30	117.6	38.41		64.35
112.	Y_31	35.2	19.75		0.81

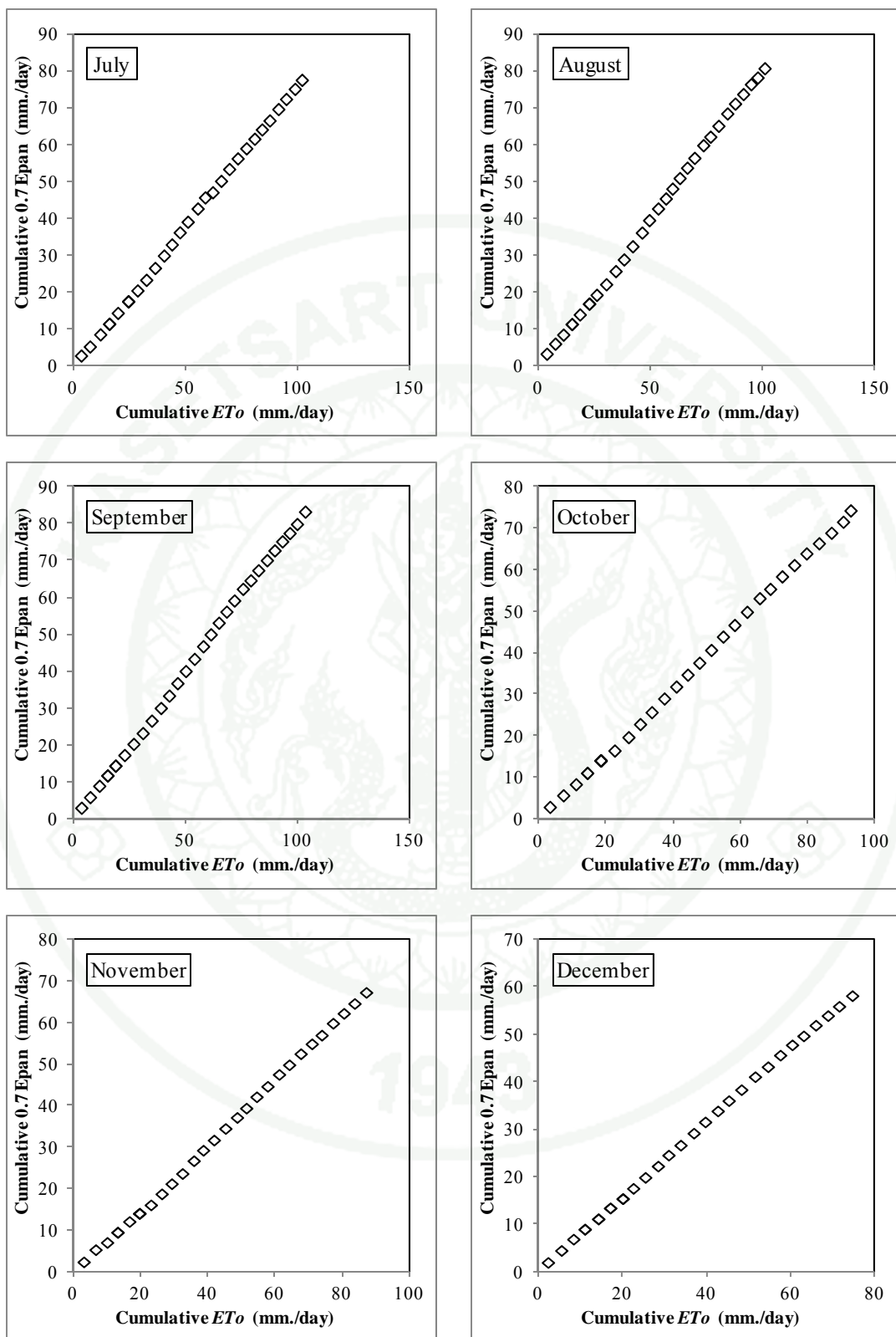


Appendix B

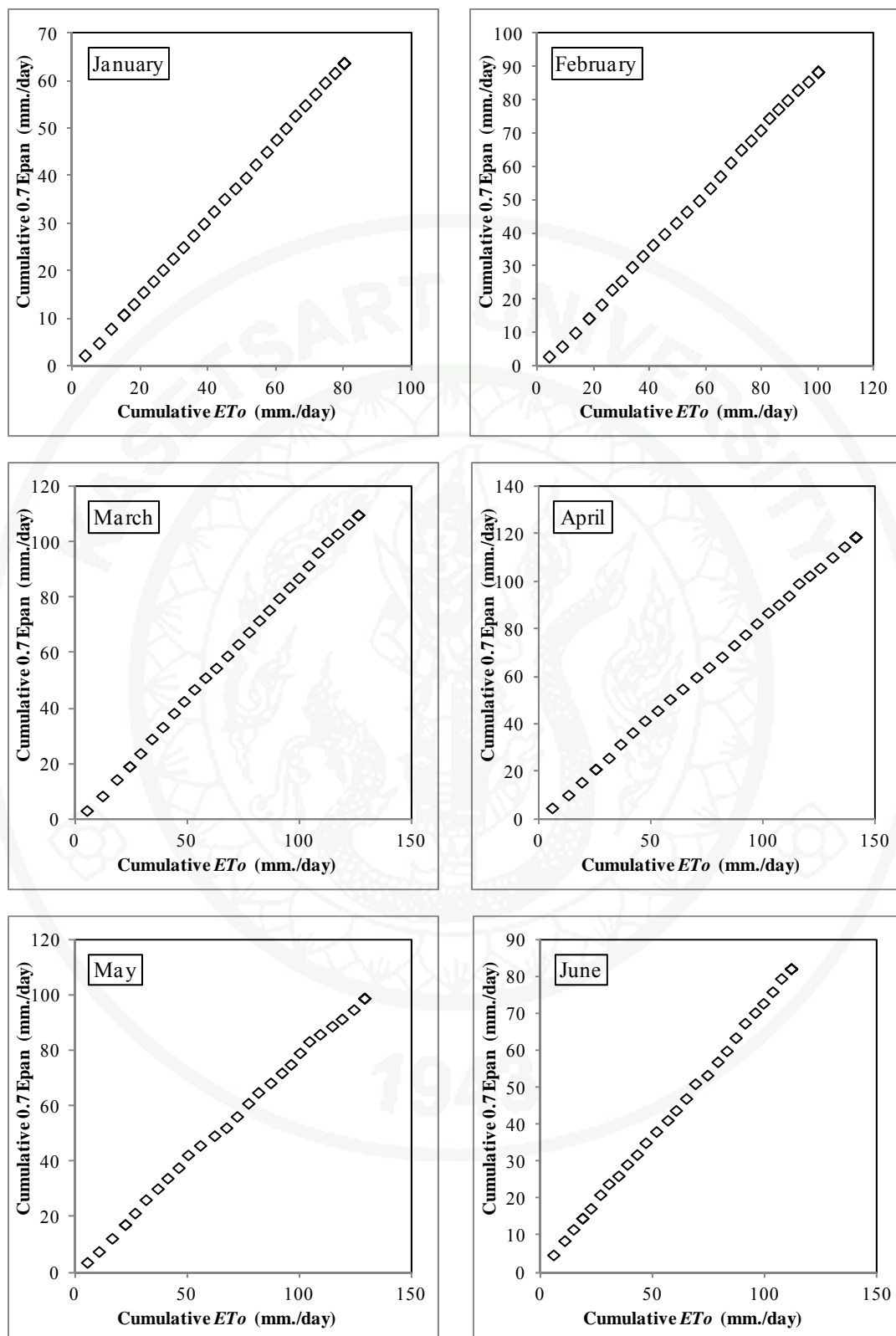
Double mass curve of ET_o versus $0.7 Epan$



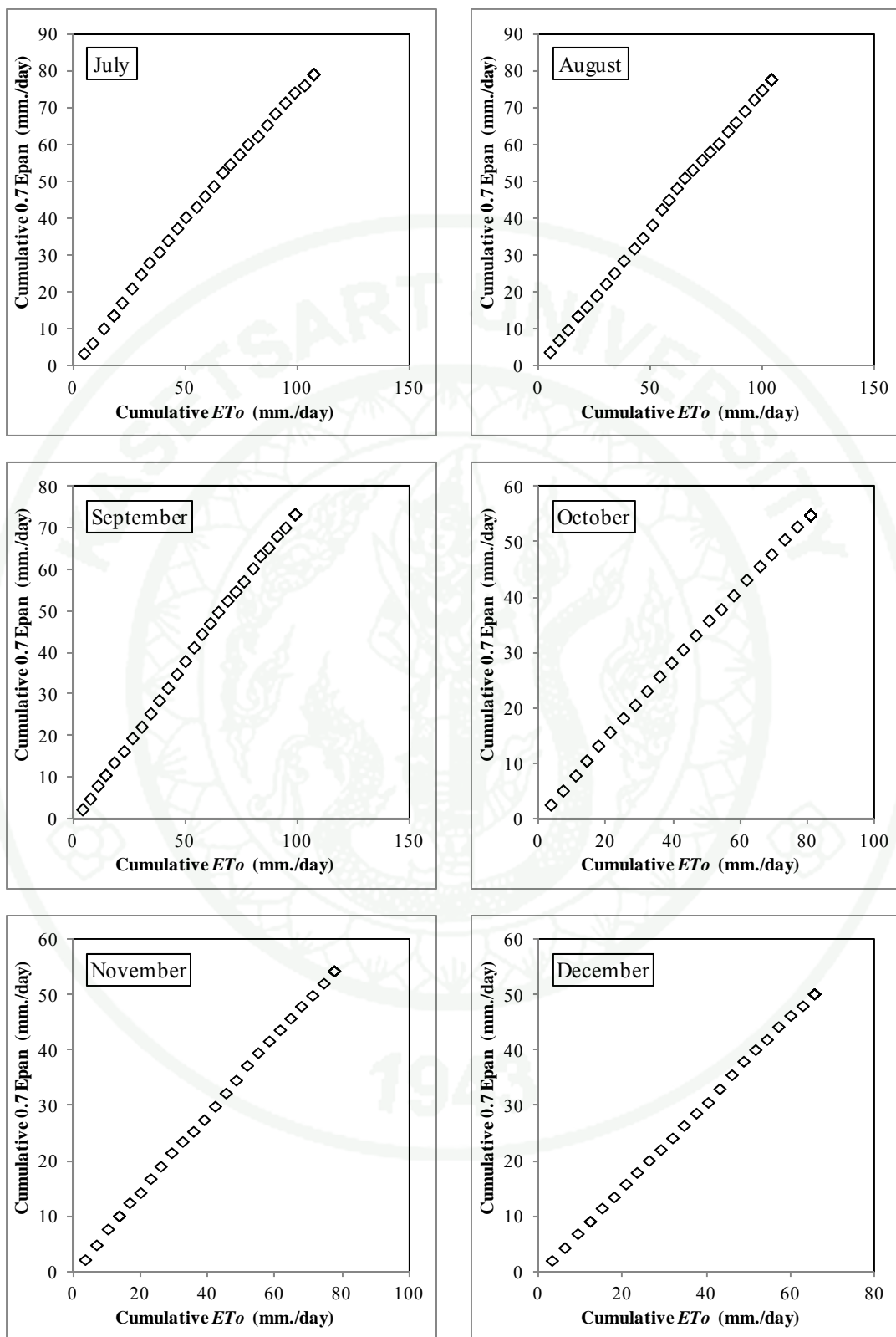
Appendix Figure B1 Double mass curve of ETo and 0.7 Epan at Chiang Mai station during the 1977-2006



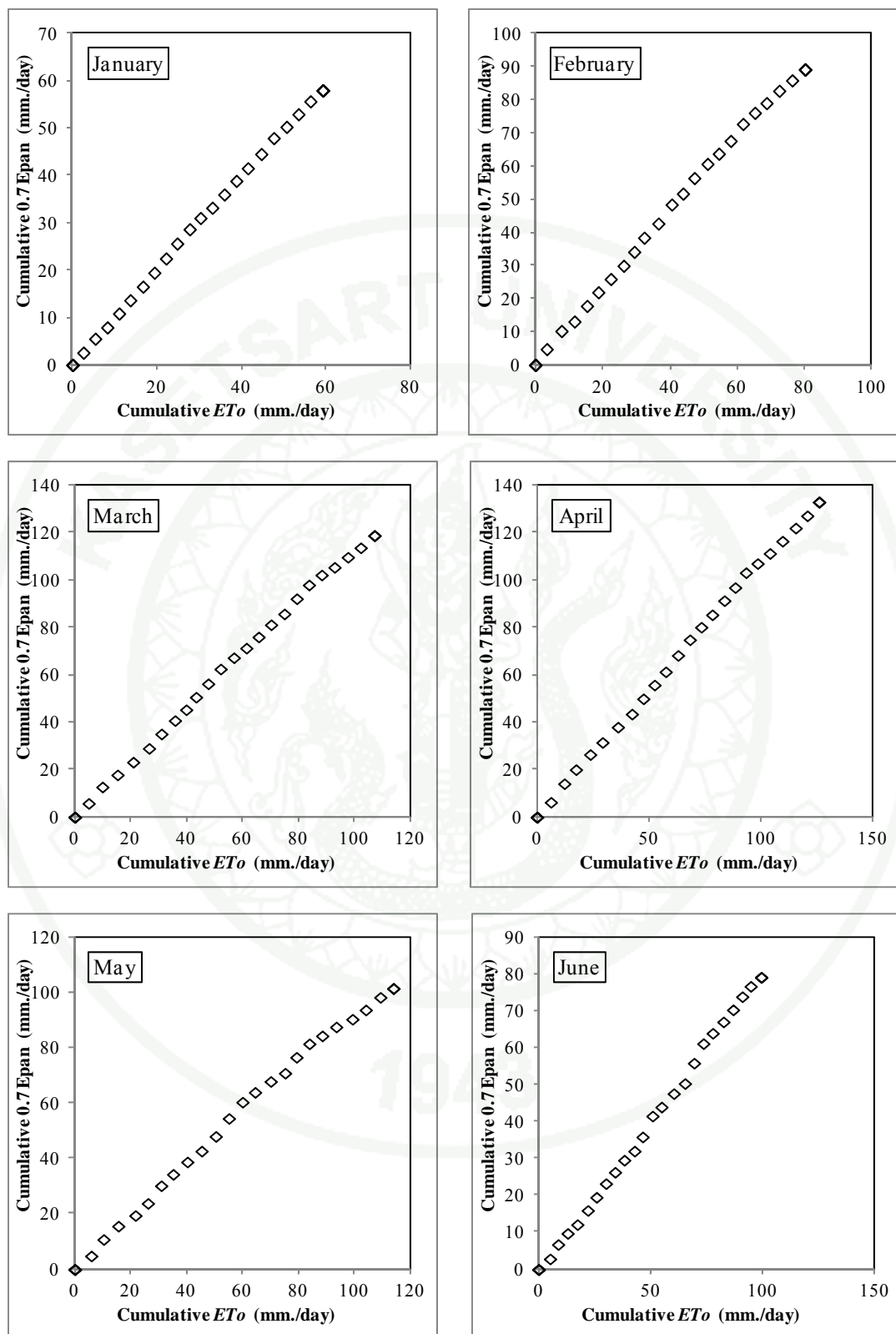
Appendix Figure B1 (Continued)



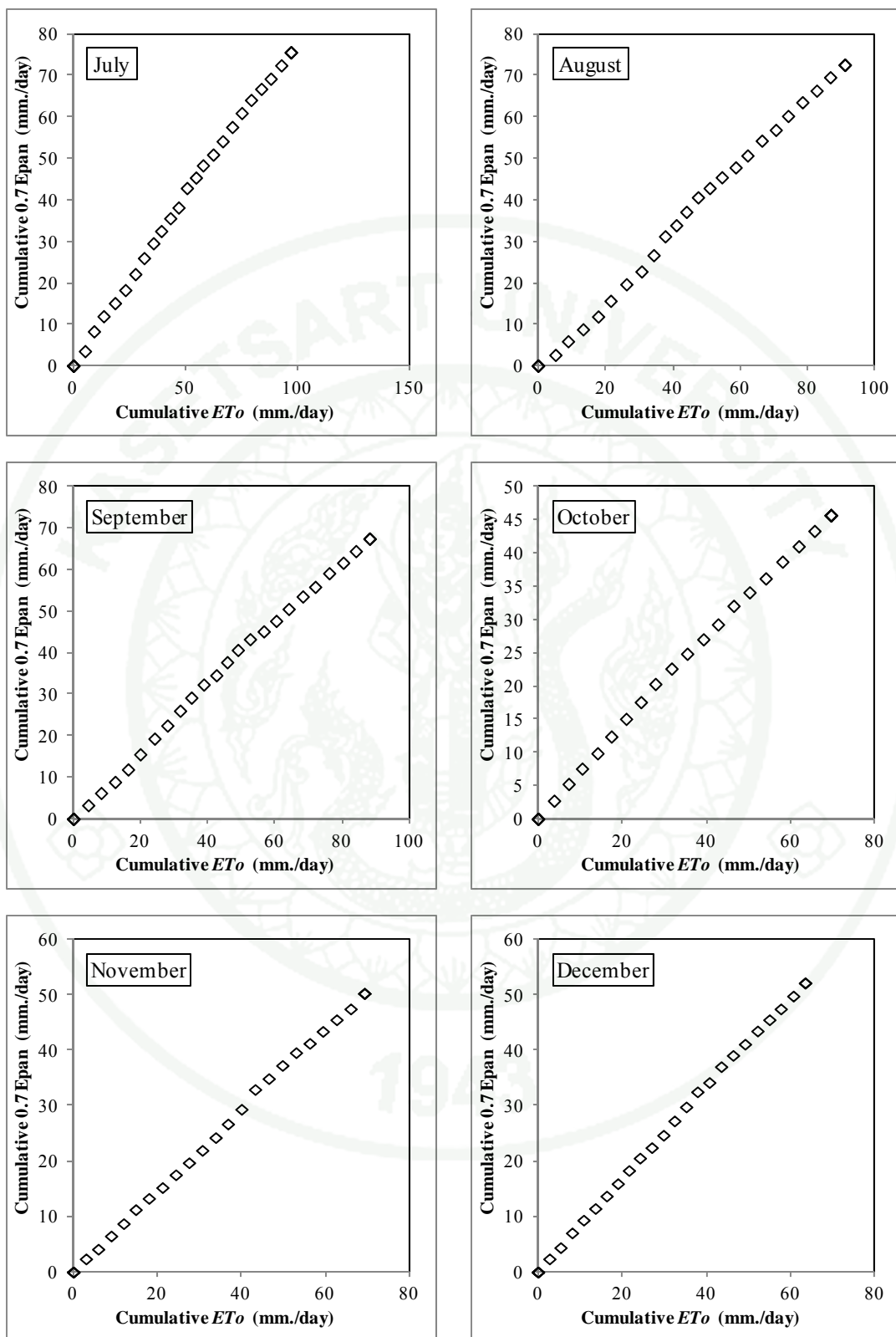
Appendix Figure B2 Double mass curve of ET_o and 0.7 Epan at Bhumibol Dam station during the 1977-2006



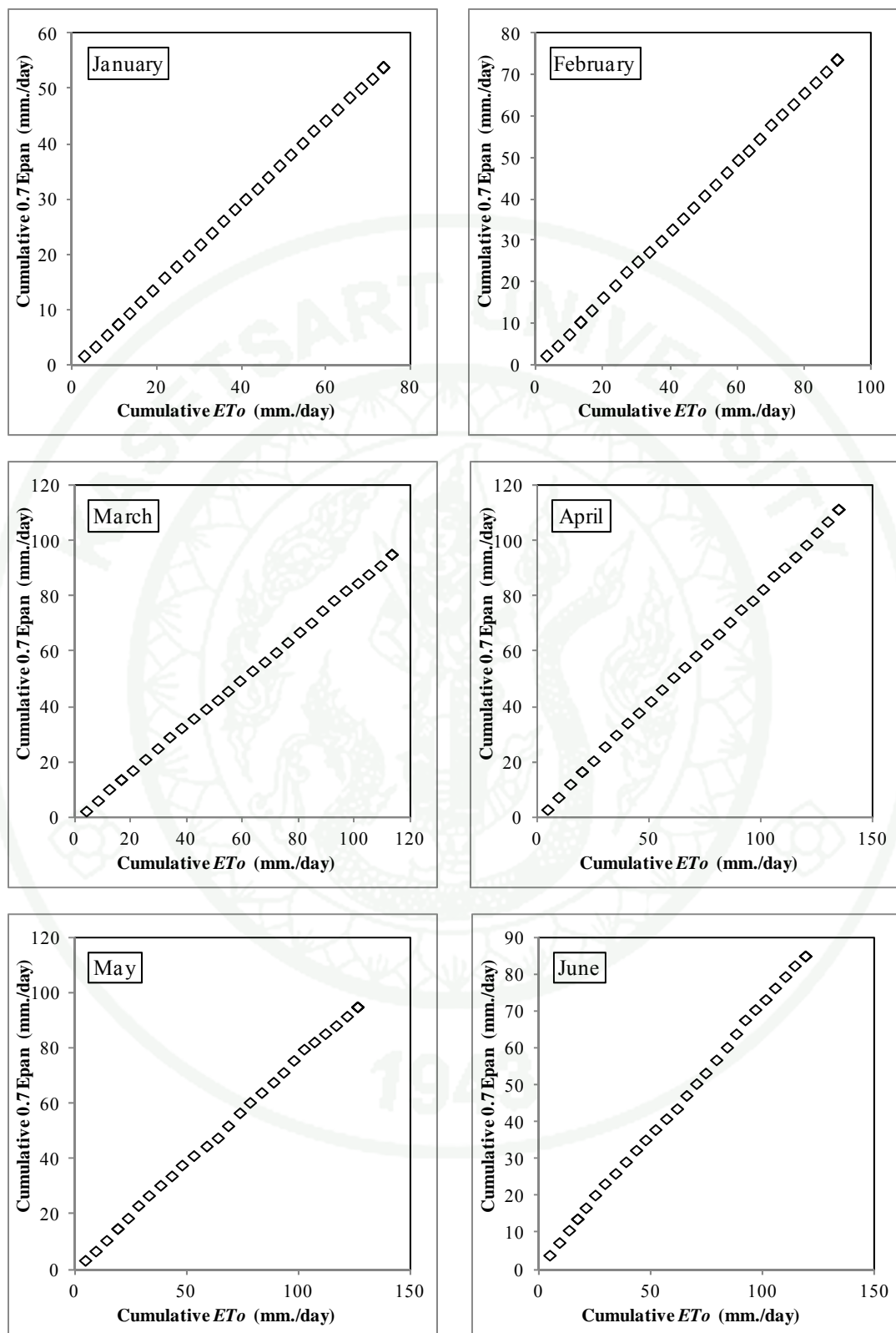
Appendix Figure B2 (Continued)



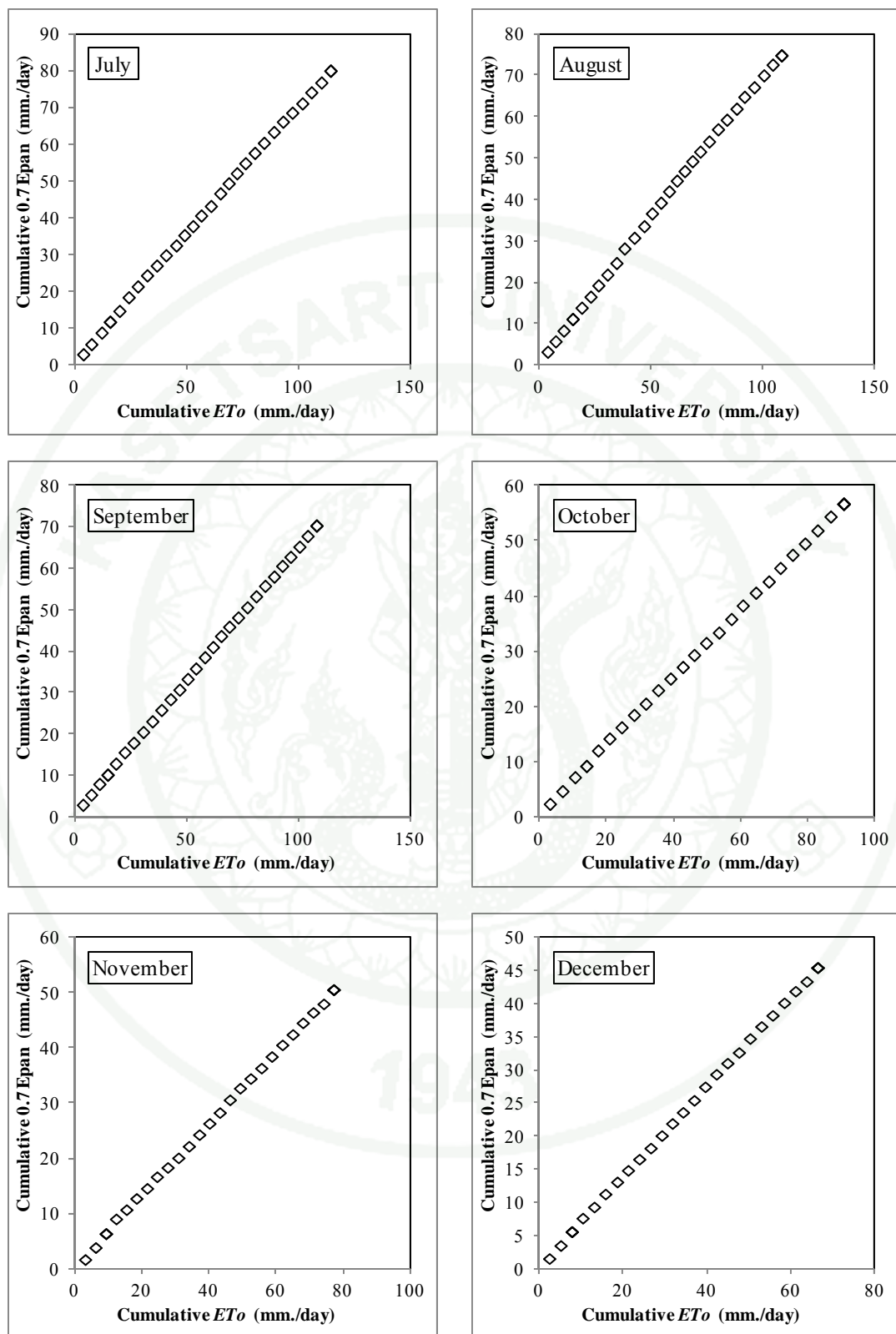
Appendix Figure B3 Double mass curve of ET_o and 0.7 Epan at Tak station during the 1977-2006



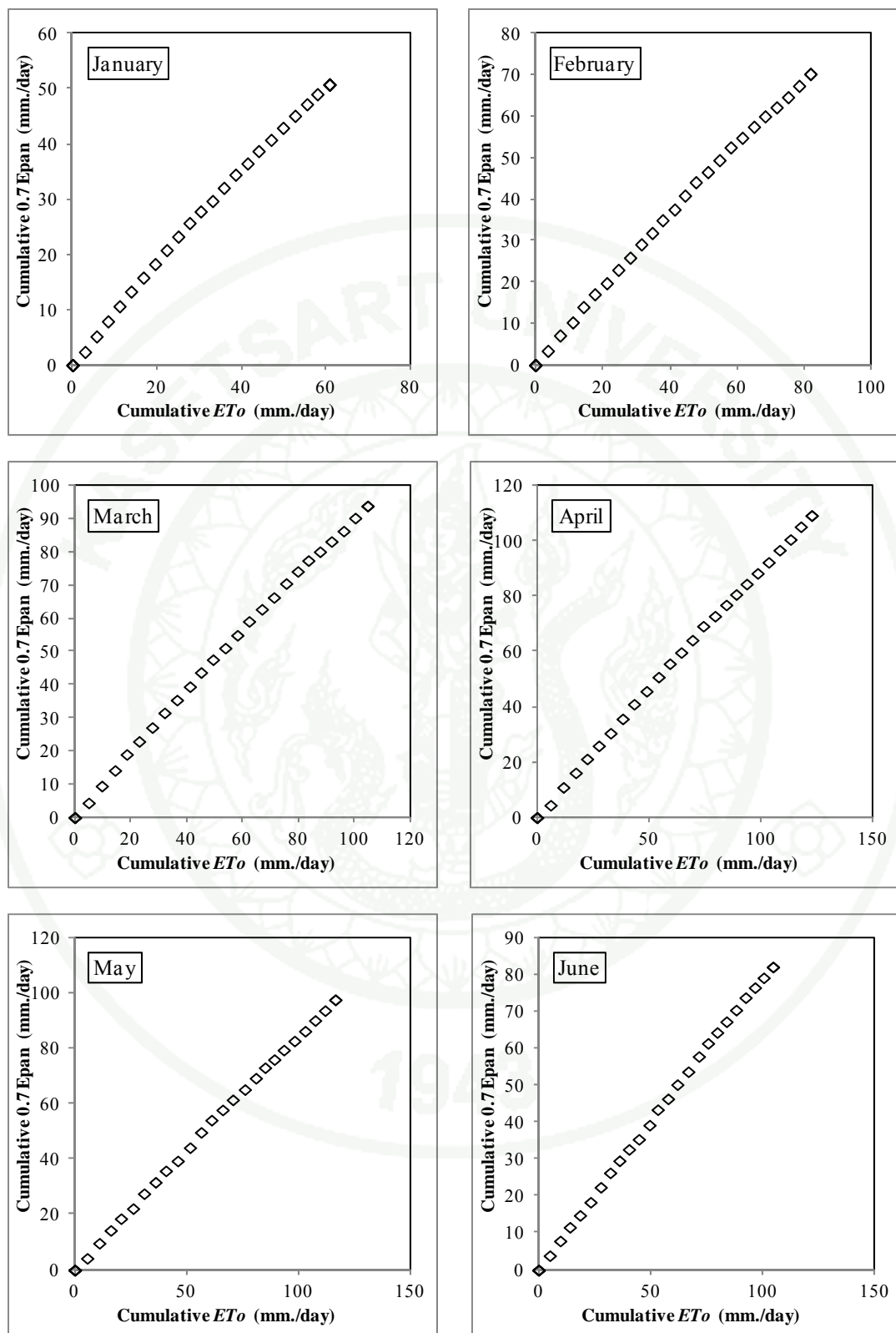
Appendix Figure B3 (Continued)



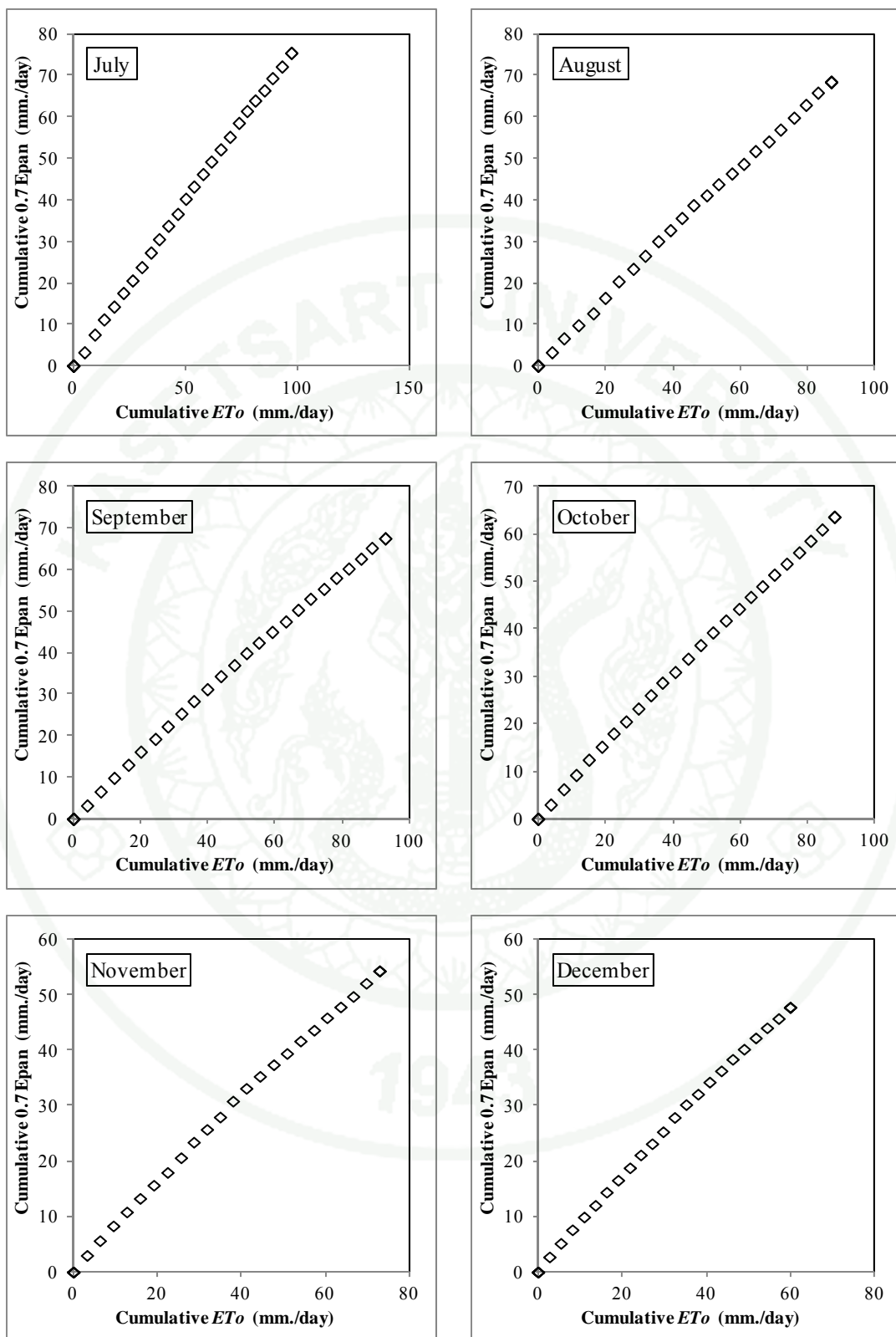
Appendix Figure B4 Double mass curve of ETo and 0.7 Epan at Lampang station during the 1977-2006



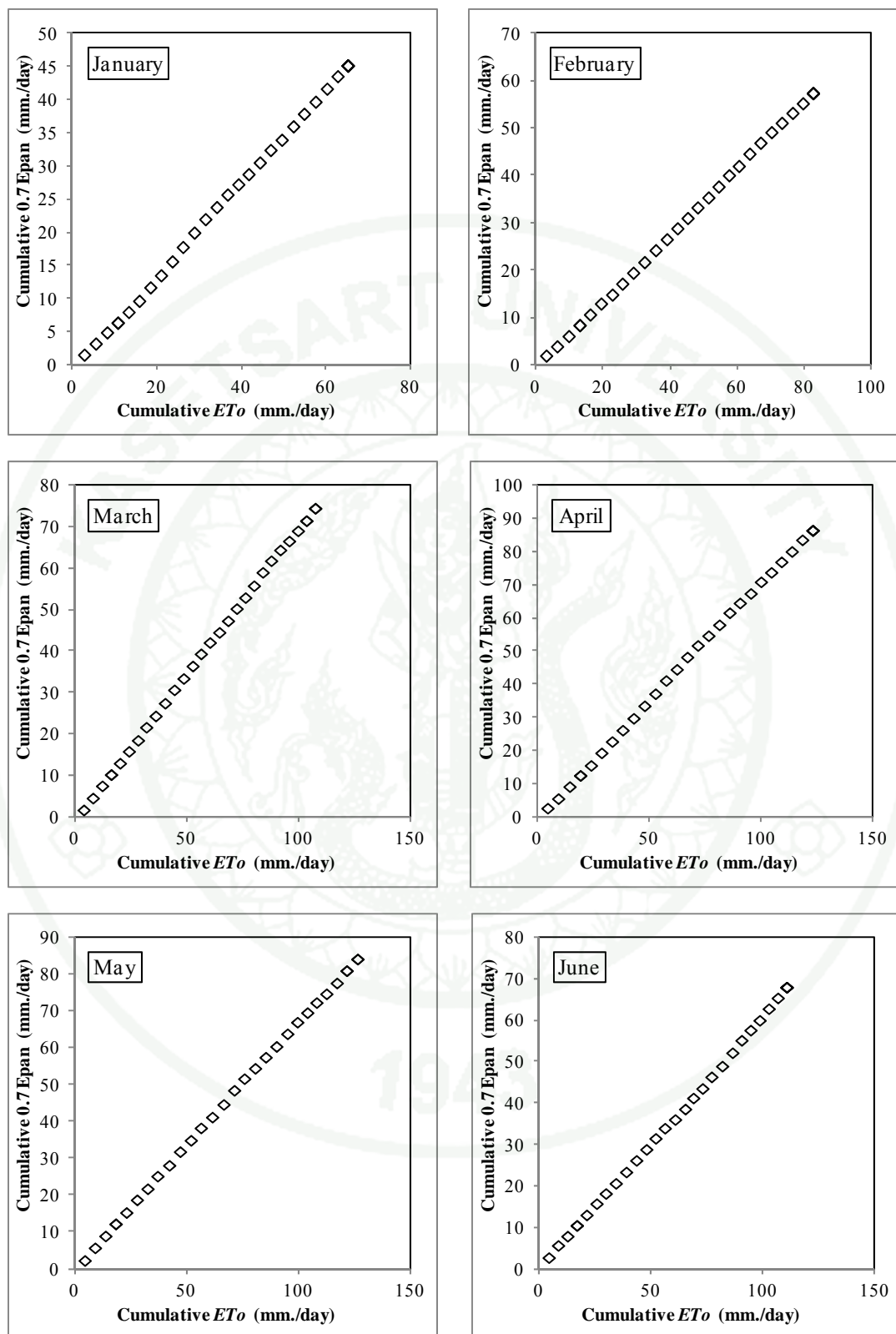
Appendix Figure B4 (Continued)



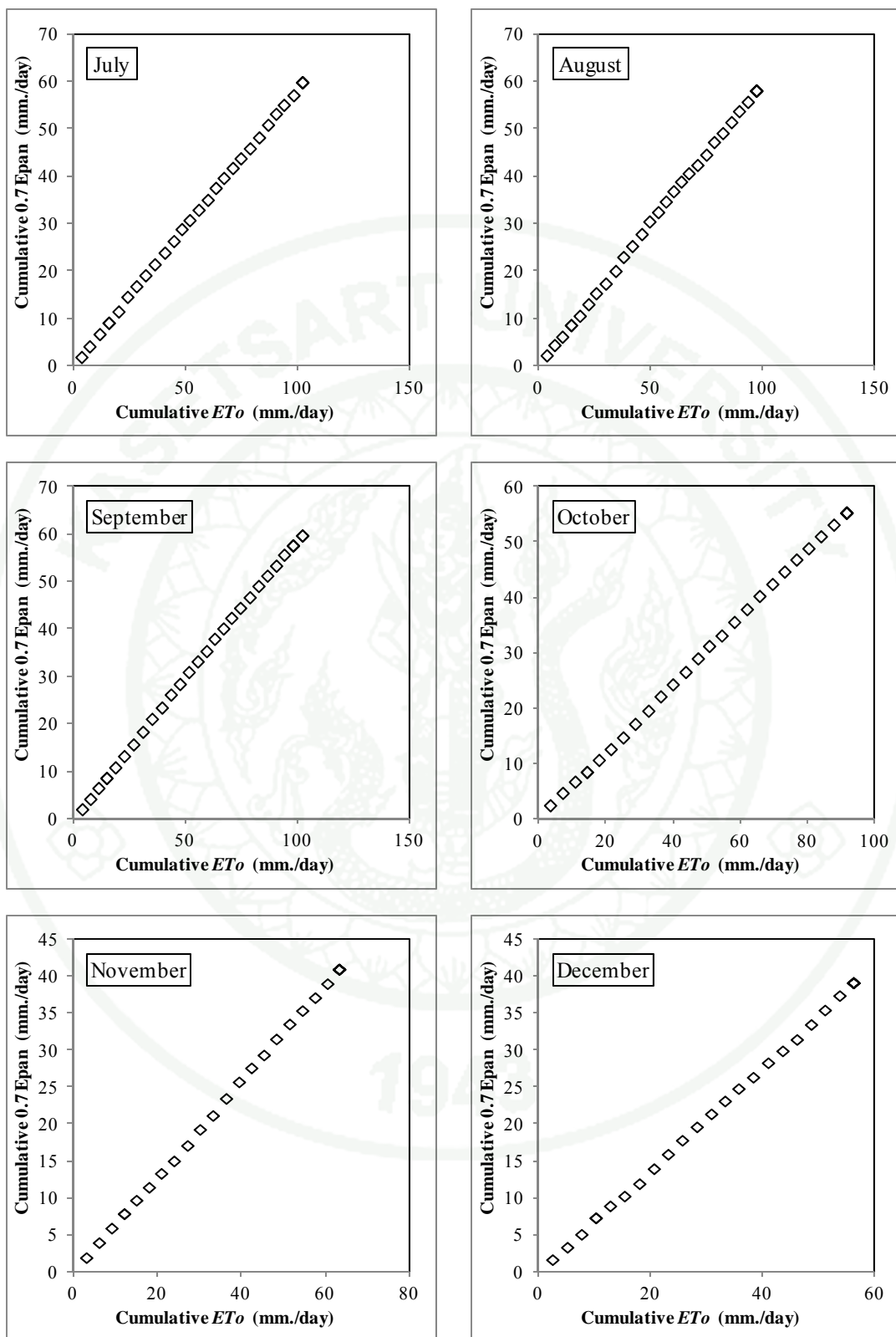
Appendix Figure B5 Double mass curve of ET_o and 0.7 Epan at Phrae station during the 1977-2006



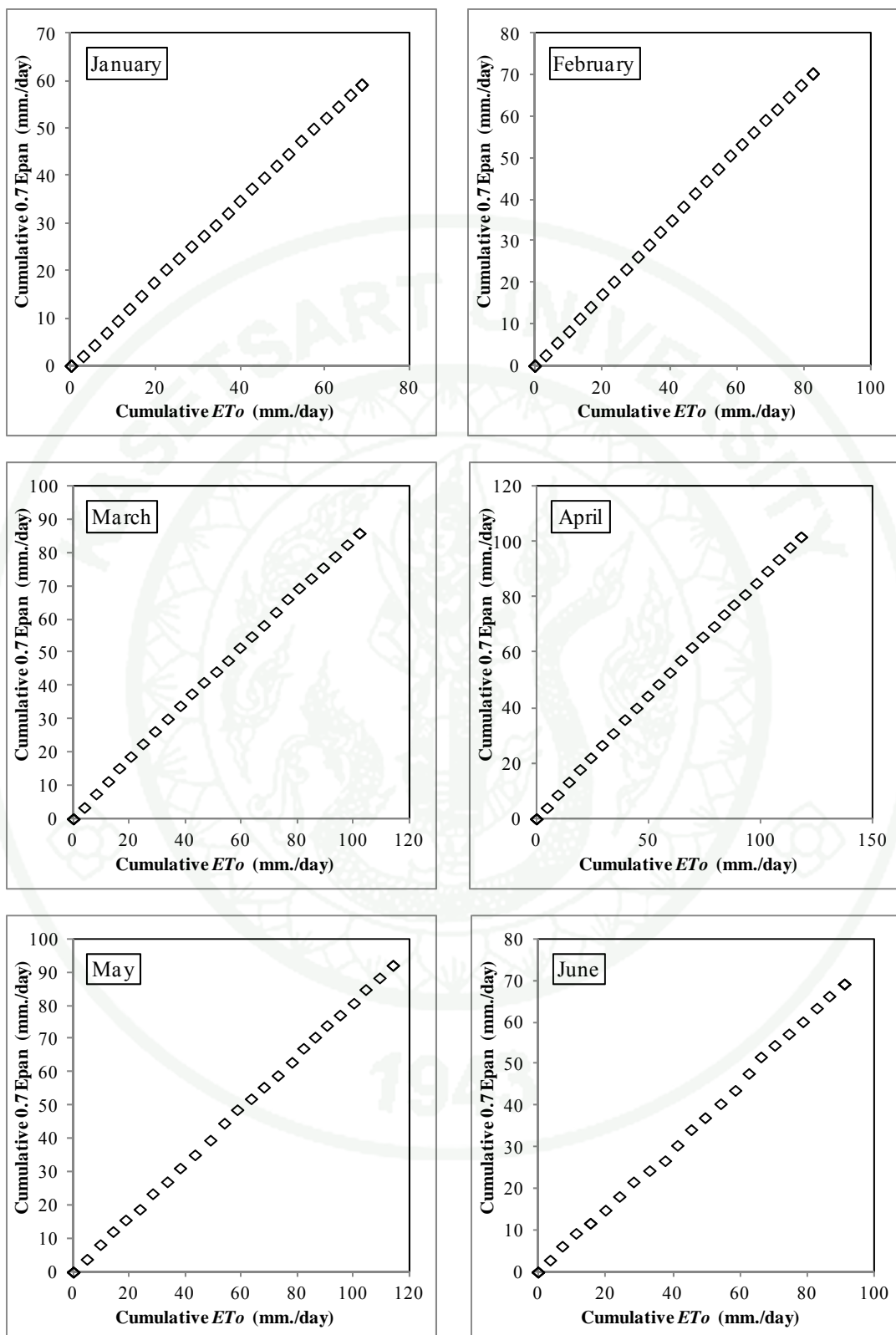
Appendix Figure B5 (Continued)



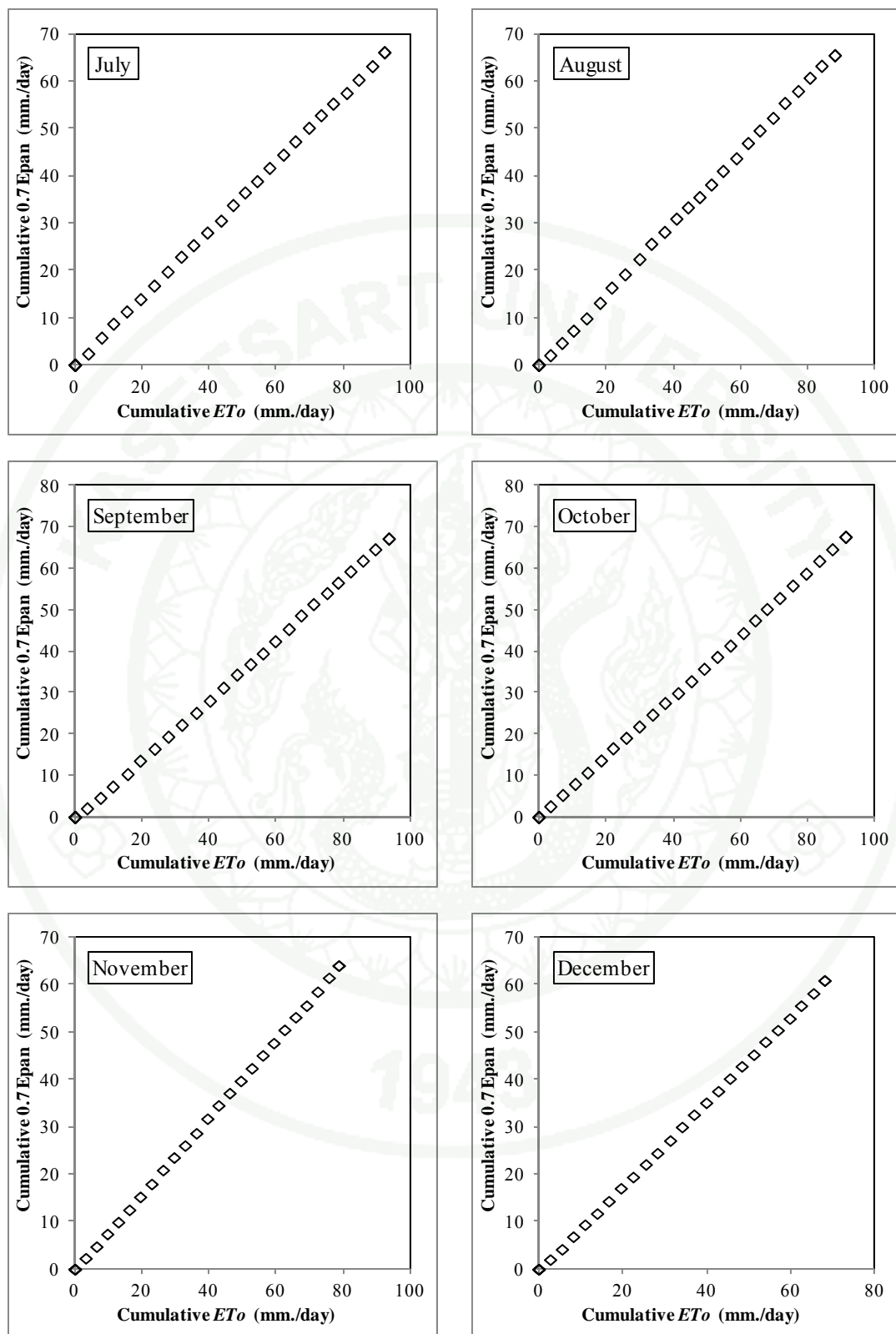
Appendix Figure B6 Double mass curve of ET_o and 0.7 Epan at Nan station during the 1977-2006

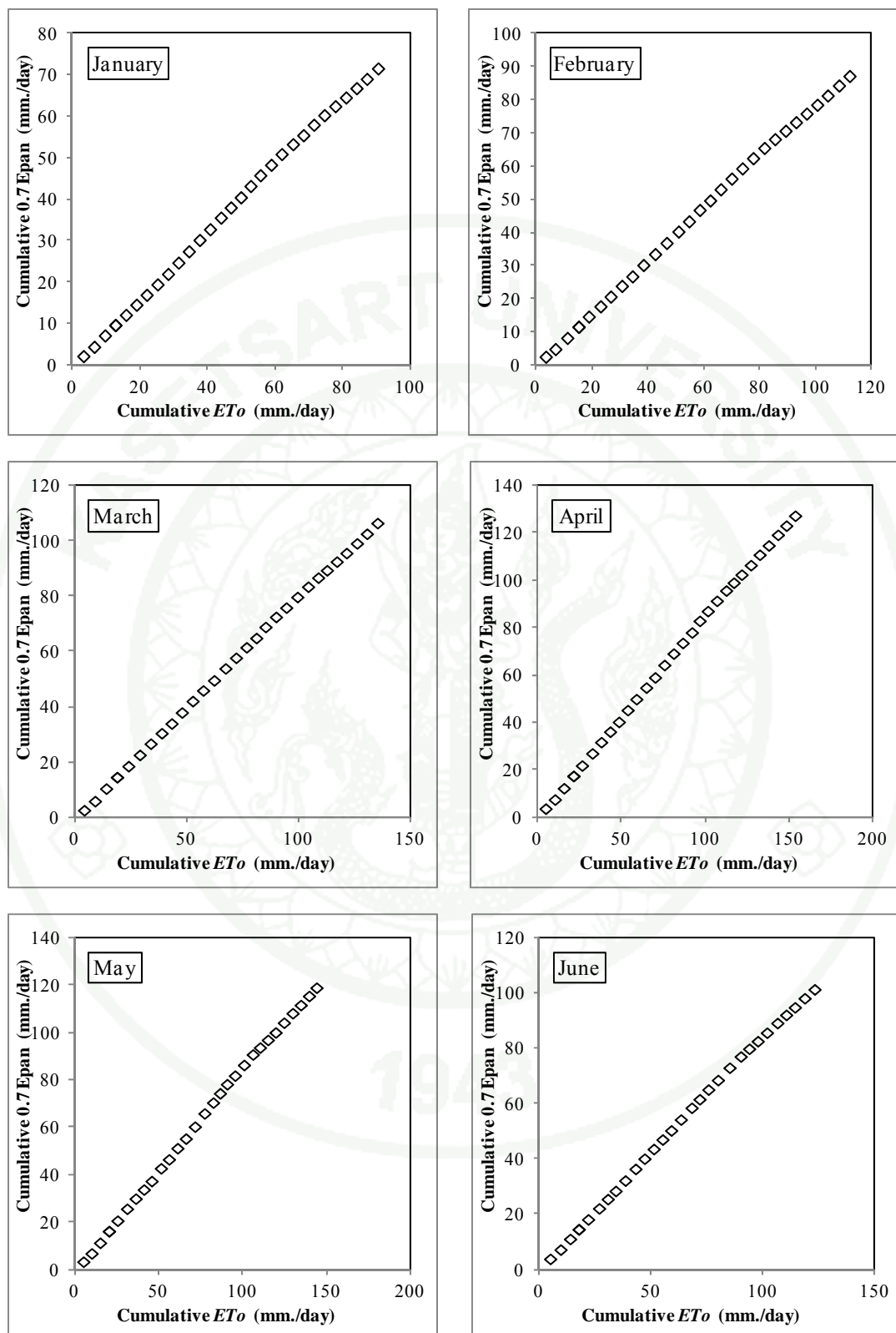


Appendix Figure B6 (Continued)

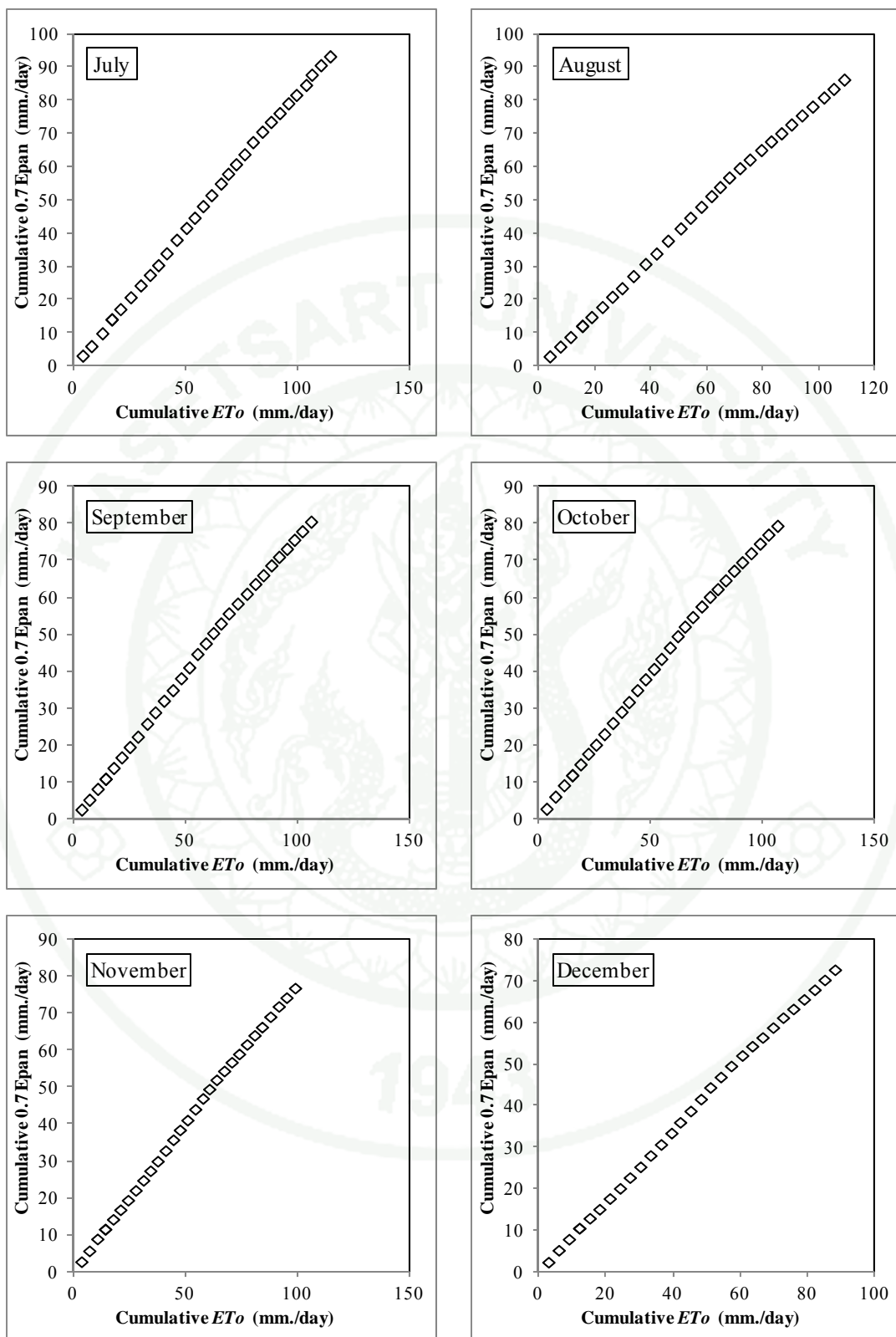


Appendix Figure B7 Double mass curve of ETo and 0.7 Epan at Uttaradit station during the 1977-2006

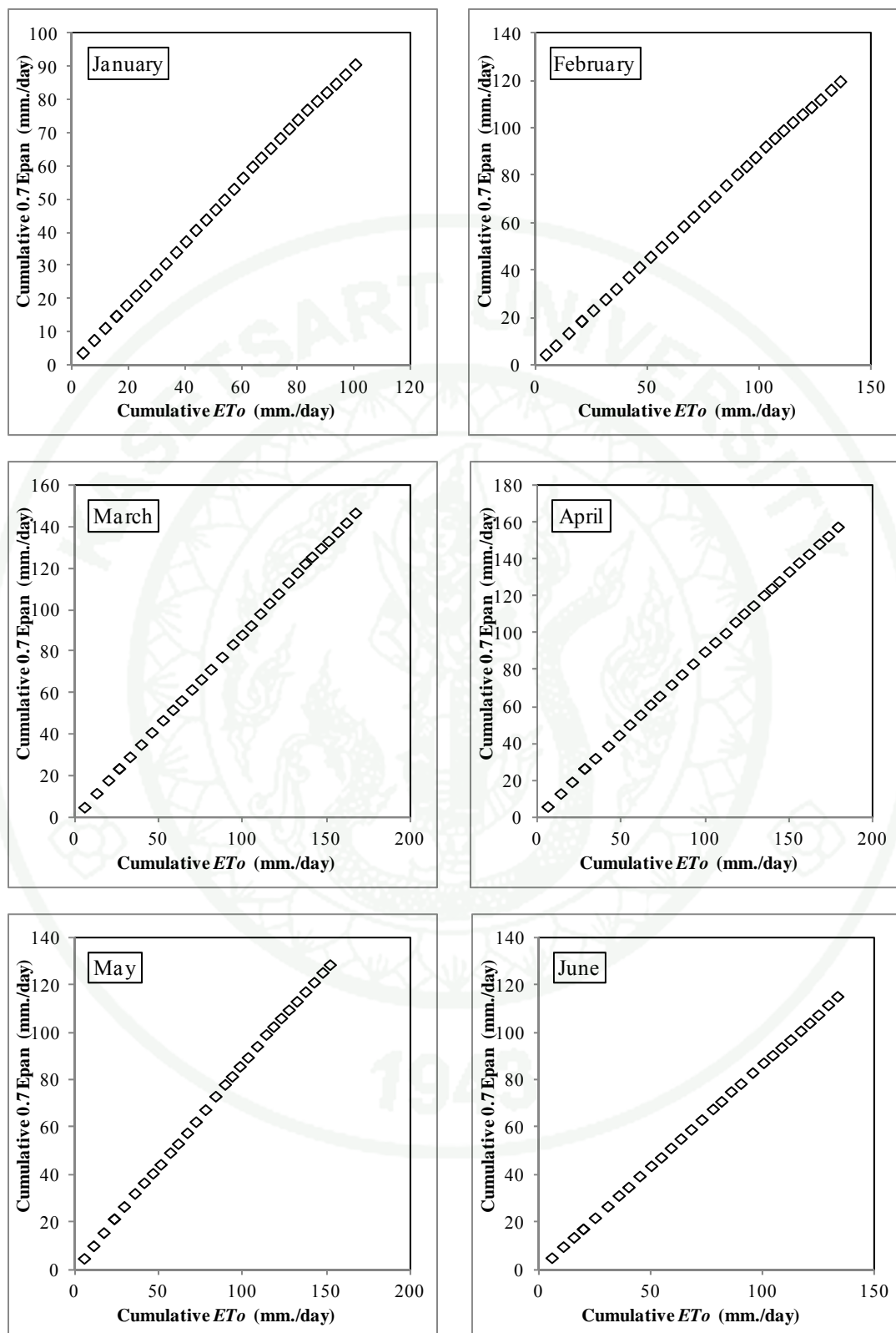
**Appendix Figure B7** (Continued)



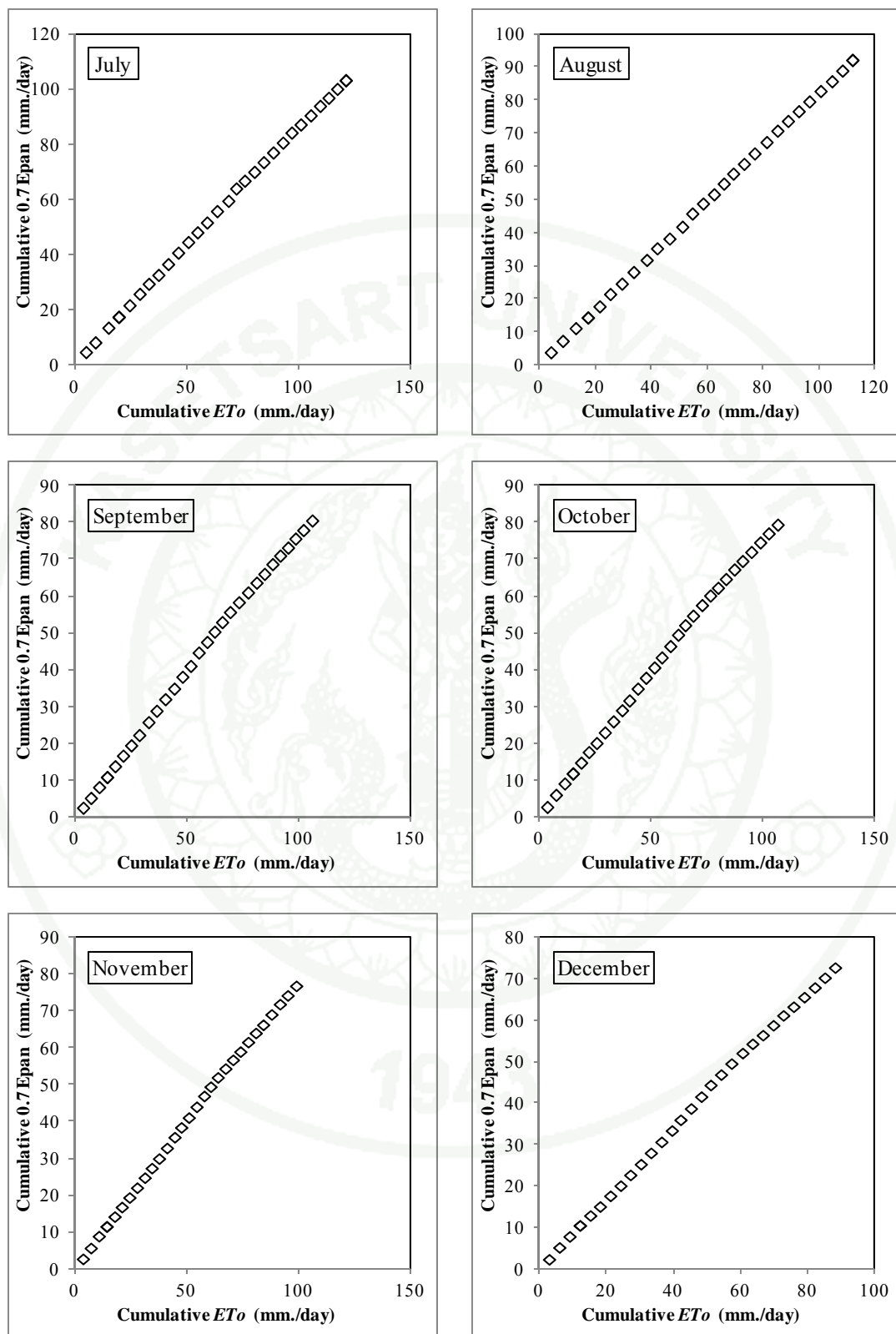
Appendix Figure B8 Double mass curve of ETo and 0.7 Epan at Phitsanulok station during the 1977-2006



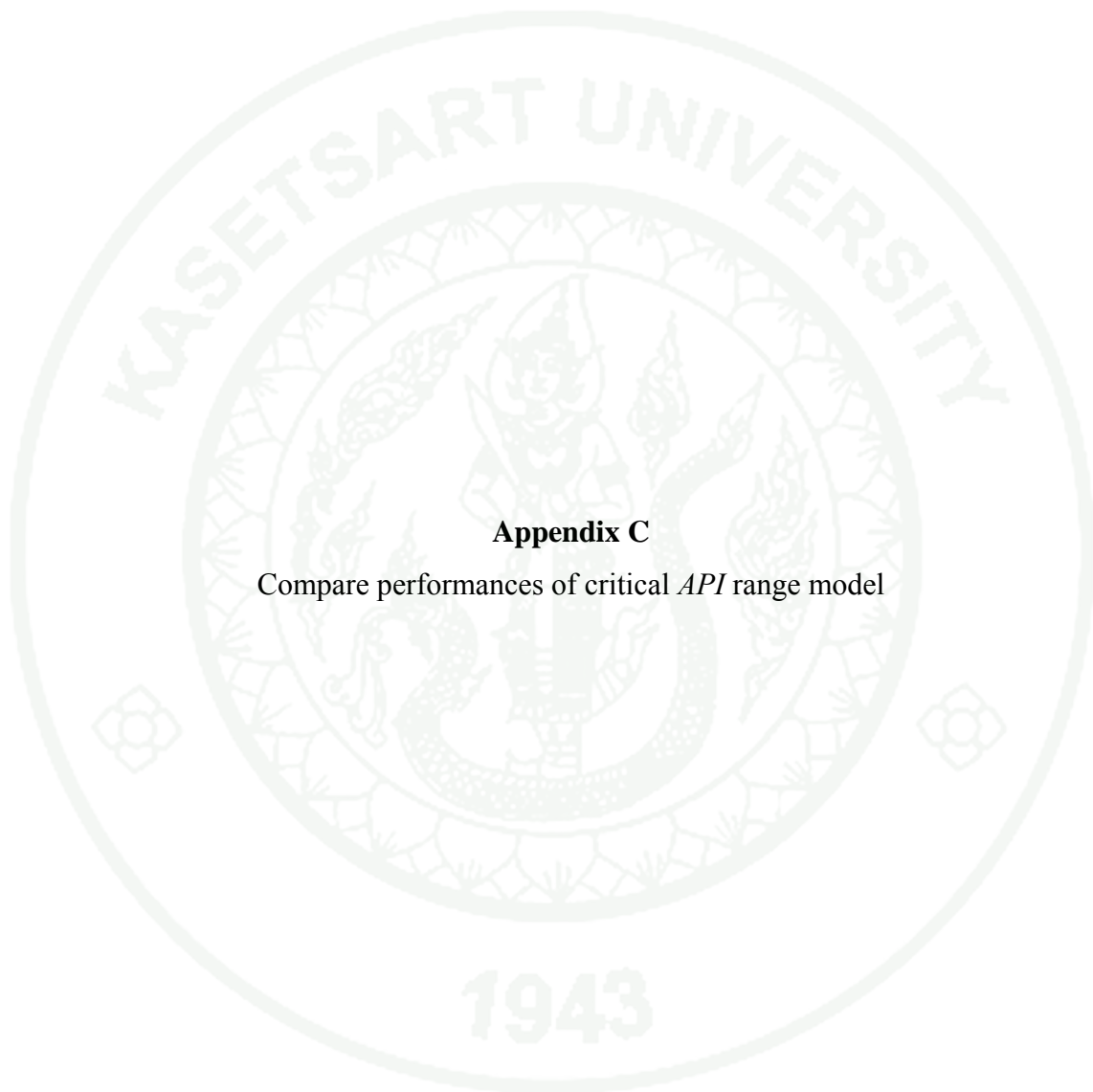
Appendix Figure B8 (Continued)



Appendix Figure B9 Double mass curve of ET_o and 0.7 Epan at Nakhon Sawan station during the 1977-2006



Appendix Figure B9 (Continued)



Appendix C

Compare performances of critical *API* range model

Appendix Table C1 Statistical measures of the similarity between simulated and observed hydrographs using critical API range model 1.

Discharge Station	<i>API</i> critical range model for runoff estimation											
	10% of $API_{critical}$			20% of $API_{critical}$			30% of $API_{critical}$			40% of $API_{critical}$		
	r	NSE	RMSE	r	NSE	RMSE	r	NSE	RMSE	r	NSE	RMSE
1. P.24A	0.708	0.501	6.267	0.716	0.512	6.199	0.716	0.513	6.191	0.712	0.507	6.234
2. P.64	0.660	0.436	7.856	0.674	0.455	7.724	0.679	0.461	7.682	0.684	0.468	7.631
3. P.21	0.693	0.481	3.988	0.694	0.481	3.984	0.694	0.481	3.985	0.692	0.479	3.995
4. P.47	0.669	0.448	10.507	0.677	0.458	10.406	0.682	0.465	10.345	0.686	0.471	10.286
5. P.20	0.658	0.433	12.787	0.669	0.447	12.628	0.667	0.445	12.652	0.656	0.431	12.814
6. P.71	0.715	0.511	13.310	0.710	0.505	13.400	0.714	0.499	13.478	0.706	0.485	13.659
7. P.4A	0.621	0.386	15.201	0.626	0.392	15.120	0.626	0.392	15.124	0.623	0.388	15.173
8. P.14	0.725	0.526	25.334	0.723	0.523	25.417	0.720	0.518	25.536	0.719	0.517	25.563
9. P.67	0.770	0.593	23.612	0.779	0.606	23.241	0.772	0.595	23.559	0.764	0.583	23.907
10. P.1	0.691	0.478	42.116	0.691	0.478	42.104	0.690	0.476	42.168	0.685	0.469	42.470
11. W.17	0.722	0.521	6.372	0.740	0.547	6.196	0.738	0.544	6.213	0.726	0.527	6.331
12. W.20	0.705	0.497	6.828	0.713	0.508	6.757	0.723	0.519	6.681	0.699	0.479	6.955
13. W.16A	0.762	0.581	11.980	0.772	0.595	11.770	0.770	0.591	11.830	0.757	0.567	12.174
14. W.3A	0.698	0.488	47.191	0.698	0.485	47.319	0.698	0.484	47.367	0.696	0.479	47.591
15. Y.30	0.585	0.342	2.652	0.588	0.338	2.659	0.581	0.329	2.676	0.581	0.329	2.676
16. Y.34	0.729	0.474	5.709	0.729	0.474	5.709	0.755	0.571	5.158	0.749	0.561	5.216
17. Y.24	0.599	0.359	10.026	0.608	0.369	9.943	0.616	0.379	9.871	0.623	0.386	9.808
18. Y.26	0.604	0.360	10.612	0.607	0.368	10.544	0.611	0.372	10.512	0.610	0.369	10.539
19. Y.31	0.746	0.557	24.059	0.750	0.562	23.926	0.748	0.559	23.991	0.746	0.554	24.151
20. Y.20	0.797	0.636	51.899	0.807	0.650	50.897	0.812	0.656	50.435	0.807	0.645	51.234
21. Y.1C	0.798	0.637	67.082	0.802	0.641	66.713	0.800	0.636	67.212	0.794	0.623	68.387
22. N.66	0.705	0.497	3.285	0.724	0.524	3.195	0.732	0.535	3.156	0.743	0.552	3.100
23. N.49	0.663	0.439	14.979	0.665	0.443	14.935	0.664	0.441	14.961	0.662	0.437	15.009
24. N.62	0.690	0.477	6.863	0.690	0.475	6.871	0.689	0.475	6.877	0.691	0.477	6.860
25. N.59	0.697	0.486	8.726	0.704	0.495	8.651	0.707	0.499	8.612	0.718	0.515	8.477
26. N.65	0.608	0.369	23.667	0.608	0.369	23.674	0.607	0.368	23.685	0.615	0.378	23.509
27. N.63	0.694	0.482	7.580	0.701	0.492	7.505	0.704	0.493	7.496	0.706	0.493	7.496
28. N.55	0.776	0.602	18.392	0.776	0.603	18.379	0.773	0.597	18.513	0.771	0.591	18.658
29. N.36	0.751	0.564	24.626	0.753	0.567	24.539	0.756	0.572	24.421	0.763	0.582	24.132
30. N.24	0.798	0.636	29.198	0.780	0.604	30.465	0.780	0.604	30.465	0.780	0.604	30.465
31. N.42	0.783	0.613	54.754	0.785	0.617	54.506	0.786	0.618	54.426	0.787	0.620	54.308
32. N.64	0.878	0.771	66.082	0.879	0.773	65.728	0.876	0.768	66.489	0.875	0.766	66.733
33. N.40	0.743	0.551	61.655	0.744	0.553	61.551	0.744	0.553	61.545	0.743	0.552	61.598
34. N.1	0.850	0.722	82.348	0.856	0.733	80.797	0.855	0.730	81.104	0.853	0.727	81.610
35. N.22	0.712	0.507	74.632	0.711	0.505	74.719	0.709	0.503	74.900	0.708	0.501	75.069
36. N.13A	0.846	0.716	191.982	0.849	0.721	190.476	0.843	0.710	194.078	0.839	0.699	197.873

Appendix Table C1 (Continued)

Discharge Station	<i>API</i> critical range model for runoff estimation											
	50% of <i>API_{critical}</i>			60% of <i>API_{critical}</i>			70% of <i>API_{critical}</i>			80% of <i>API_{critical}</i>		
	r	NSE	RMSE	r	NSE	RMSE	r	NSE	RMSE	r	NSE	RMSE
1. P.24A	0.712	0.507	6.232	0.711	0.506	6.240	0.707	0.493	6.316	0.689	0.467	6.477
2. P.64	0.687	0.472	7.602	0.656	0.430	7.896	0.656	0.430	7.896	0.656	0.430	7.896
3. P.21	0.692	0.479	3.993	0.693	0.480	3.990	0.693	0.480	3.988	0.691	0.477	4.000
4. P.47	0.689	0.475	10.244	0.689	0.474	10.251	0.689	0.475	10.248	0.682	0.466	10.335
5. P.20	0.644	0.415	12.988	0.642	0.412	13.027	0.640	0.409	13.052	0.626	0.392	13.238
6. P.71	0.702	0.481	13.715	0.702	0.481	13.715	0.702	0.481	13.715	0.702	0.481	13.715
7. P.4A	0.621	0.386	15.201	0.623	0.388	15.168	0.615	0.378	15.299	0.603	0.364	15.465
8. P.14	0.720	0.519	25.528	0.719	0.517	25.575	0.718	0.516	25.611	0.718	0.516	25.611
9. P.67	0.754	0.568	24.339	0.753	0.568	24.347	0.753	0.568	24.347	0.753	0.568	24.347
10. P.1	0.683	0.467	42.564	0.683	0.466	42.570	0.683	0.466	42.575	0.683	0.466	42.577
11. W.17	0.716	0.503	6.491	0.692	0.478	6.649	0.699	0.474	6.673	0.699	0.474	6.673
12. W.20	0.698	0.478	6.959	0.698	0.478	6.959	0.698	0.478	6.959	0.698	0.478	6.959
13. W.16A	0.760	0.567	12.169	0.774	0.592	11.826	0.769	0.582	11.961	0.755	0.558	12.299
14. W.3A	0.694	0.476	47.719	0.694	0.476	47.730	0.694	0.476	47.730	0.694	0.476	47.730
15. Y.30	0.581	0.329	2.676	0.581	0.329	2.676	0.581	0.329	2.676	0.581	0.329	2.676
16. Y.34	0.748	0.551	5.276	0.754	0.550	5.282	0.753	0.514	5.486	0.729	0.474	5.709
17. Y.24	0.634	0.399	9.705	0.633	0.399	9.704	0.650	0.420	9.539	0.595	0.349	10.106
18. Y.26	0.617	0.375	10.486	0.618	0.377	10.470	0.607	0.364	10.580	0.604	0.360	10.612
19. Y.31	0.741	0.544	24.394	0.740	0.543	24.443	0.740	0.543	24.443	0.740	0.543	24.443
20. Y.20	0.788	0.613	53.524	0.785	0.608	53.843	0.785	0.608	53.843	0.785	0.608	53.843
21. Y.1C	0.790	0.615	69.140	0.789	0.613	69.287	0.789	0.613	69.287	0.789	0.613	69.287
22. N.66	0.753	0.567	3.046	0.728	0.528	3.181	0.712	0.505	3.259	0.712	0.504	3.260
23. N.49	0.661	0.435	15.036	0.658	0.430	15.096	0.658	0.430	15.105	0.658	0.430	15.103
24. N.62	0.691	0.478	6.857	0.691	0.478	6.857	0.692	0.479	6.848	0.689	0.475	6.877
25. N.59	0.720	0.518	8.447	0.707	0.499	8.614	0.702	0.492	8.674	0.701	0.491	8.684
26. N.65	0.627	0.393	23.228	0.601	0.362	23.813	0.603	0.363	23.785	0.601	0.361	23.831
27. N.63	0.714	0.503	7.425	0.717	0.506	7.398	0.692	0.468	7.678	0.689	0.464	7.710
28. N.55	0.772	0.593	18.608	0.772	0.592	18.626	0.772	0.592	18.623	0.772	0.592	18.621
29. N.36	0.764	0.584	24.070	0.761	0.579	24.207	0.760	0.578	24.245	0.760	0.577	24.268
30. N.24	0.780	0.604	30.465	0.780	0.604	30.465	0.780	0.604	30.465	0.780	0.604	30.465
31. N.42	0.788	0.622	54.178	0.790	0.625	53.948	0.798	0.637	53.081	0.807	0.651	51.992
32. N.64	0.876	0.763	67.195	0.878	0.765	66.903	0.879	0.763	67.205	0.874	0.749	69.181
33. N.40	0.745	0.555	61.431	0.740	0.548	61.905	0.738	0.544	62.169	0.737	0.543	62.238
34. N.1	0.850	0.718	82.941	0.849	0.715	83.364	0.849	0.713	83.714	0.843	0.699	85.741
35. N.22	0.709	0.503	74.887	0.708	0.501	75.058	0.707	0.500	75.132	0.707	0.500	75.118
36. N.13A	0.839	0.695	199.237	0.839	0.693	199.678	0.840	0.694	199.386	0.839	0.690	200.740

Appendix Table C1 (Continued)

Discharge Station	<i>API</i> critical range model for runoff estimation					
	90% of $API_{critical}$			100% of $API_{critical}$		
	r	NSE	RMSE	r	NSE	RMSE
1. P.24A	0.689	0.467	6.477	0.689	0.467	6.477
2. P.64	0.656	0.430	7.896	0.656	0.430	7.896
3. P.21	0.691	0.477	4.000	0.691	0.477	4.000
4. P.47	0.696	0.485	10.152	0.651	0.424	10.729
5. P.20	0.626	0.392	13.238	0.626	0.392	13.238
6. P.71	0.702	0.481	13.715	0.702	0.481	13.715
7. P.4A	0.603	0.364	15.465	0.603	0.364	15.465
8. P.14	0.718	0.516	25.611	0.718	0.516	25.611
9. P.67	0.753	0.568	24.347	0.753	0.568	24.347
10. P.1	0.683	0.466	42.577	0.683	0.466	42.577
11. W.17	0.699	0.474	6.673	0.699	0.474	6.673
12. W.20	0.698	0.478	6.959	0.699	0.478	6.959
13. W.16A	0.755	0.558	12.299	0.755	0.558	12.299
14. W.3A	0.694	0.476	47.730	0.694	0.476	47.730
15. Y.30	0.581	0.329	2.676	0.581	0.329	2.676
16. Y.34	0.729	0.474	5.709	0.729	0.474	5.709
17. Y.24	0.595	0.349	10.106	0.595	0.349	10.106
18. Y.26	0.604	0.360	10.612	0.604	0.360	10.612
19. Y.31	0.740	0.543	24.443	0.740	0.543	24.443
20. Y.20	0.785	0.608	53.843	0.785	0.608	53.843
21. Y.1C	0.789	0.613	69.287	0.789	0.613	69.287
22. N.66	0.710	0.501	3.271	0.694	0.474	3.358
23. N.49	0.659	0.431	15.090	0.655	0.425	15.163
24. N.62	0.688	0.474	6.881	0.688	0.473	6.888
25. N.59	0.695	0.482	8.762	0.686	0.470	8.865
26. N.65	0.599	0.359	23.864	0.599	0.359	23.869
27. N.63	0.689	0.464	7.710	0.689	0.464	7.710
28. N.55	0.772	0.591	18.639	0.771	0.590	18.667
29. N.36	0.761	0.579	24.203	0.745	0.556	24.875
30. N.24	0.780	0.604	30.465	0.780	0.604	30.465
31. N.42	0.806	0.650	52.116	0.774	0.599	55.793
32. N.64	0.872	0.745	69.709	0.872	0.745	69.709
33. N.40	0.737	0.543	62.244	0.738	0.543	62.221
34. N.1	0.841	0.695	86.345	0.841	0.695	86.348
35. N.22	0.707	0.499	75.177	0.708	0.499	75.207
36. N.13A	0.839	0.690	200.847	0.839	0.690	200.847

Appendix Table C2 Statistical measures of the similarity between simulated and observed hydrographs using critical API range model 2.

Discharge Station	API critical range model for runoff estimation											
	10% of $API_{critical}$			20% of $API_{critical}$			30% of $API_{critical}$			40% of $API_{critical}$		
	r	NSE	RMSE	r	NSE	RMSE	r	NSE	RMSE	r	NSE	RMSE
1. P.24A	0.729	0.532	6.074	0.730	0.533	6.064	0.731	0.534	6.057	0.738	0.544	5.992
2. P.64	0.688	0.473	7.593	0.689	0.475	7.578	0.693	0.480	7.543	0.693	0.480	7.542
3. P.21	0.696	0.485	3.972	0.697	0.486	3.968	0.697	0.486	3.968	0.701	0.492	3.944
4. P.47	0.704	0.496	10.037	0.706	0.498	10.021	0.707	0.500	9.995	0.708	0.501	9.988
5. P.20	0.673	0.453	12.557	0.673	0.453	12.559	0.673	0.453	12.556	0.675	0.456	12.530
6. P.71	0.719	0.517	13.231	0.729	0.531	13.042	0.738	0.544	12.855	0.715	0.511	13.313
7. P.4A	0.631	0.398	15.048	0.631	0.398	15.044	0.631	0.398	15.045	0.631	0.399	15.041
8. P.14	0.726	0.527	25.322	0.725	0.526	25.350	0.725	0.526	25.332	0.725	0.526	25.337
9. P.67	0.774	0.599	23.458	0.780	0.609	23.168	0.776	0.602	23.362	0.776	0.603	23.345
10. P.1	0.692	0.478	42.091	0.693	0.481	42.000	0.693	0.481	42.003	0.693	0.480	42.004
11. W.17	0.747	0.558	6.118	0.748	0.559	6.114	0.748	0.560	6.109	0.750	0.563	6.083
12. W.20	0.716	0.513	6.721	0.718	0.515	6.704	0.731	0.534	6.576	0.719	0.517	6.692
13. W.16A	0.770	0.593	11.799	0.774	0.599	11.715	0.776	0.603	11.661	0.772	0.596	11.763
14. W.3A	0.701	0.491	47.054	0.702	0.493	46.938	0.701	0.491	47.054	0.699	0.488	47.166
15. Y.30	0.604	0.365	2.604	0.604	0.365	2.604	0.599	0.358	2.618	0.599	0.358	2.618
16. Y.34	0.768	0.590	5.038	0.771	0.594	5.016	0.770	0.593	5.020	0.775	0.601	4.975
17. Y.24	0.632	0.400	9.700	0.637	0.405	9.655	0.642	0.413	9.596	0.645	0.416	9.571
18. Y.26	0.605	0.365	10.565	0.612	0.375	10.489	0.625	0.391	10.349	0.624	0.389	10.369
19. Y.31	0.749	0.562	23.930	0.751	0.565	23.845	0.752	0.565	23.834	0.754	0.568	23.743
20. Y.20	0.813	0.661	50.079	0.814	0.663	49.933	0.817	0.667	49.653	0.819	0.670	49.394
21. Y.1C	0.805	0.648	66.063	0.806	0.650	65.891	0.807	0.651	65.785	0.807	0.652	65.720
22. N.66	0.741	0.549	3.108	0.743	0.552	3.099	0.743	0.552	3.098	0.746	0.557	3.083
23. N.49	0.664	0.441	14.956	0.665	0.442	14.941	0.667	0.445	14.896	0.667	0.445	14.901
24. N.62	0.691	0.478	6.856	0.692	0.479	6.849	0.692	0.478	6.853	0.694	0.481	6.834
25. N.59	0.715	0.511	8.515	0.716	0.512	8.499	0.716	0.513	8.497	0.719	0.517	8.458
26. N.65	0.610	0.372	23.611	0.614	0.376	23.534	0.617	0.380	23.465	0.624	0.389	23.301
27. N.63	0.723	0.522	7.279	0.728	0.531	7.215	0.739	0.546	7.097	0.750	0.563	6.964
28. N.55	0.778	0.605	18.331	0.780	0.609	18.231	0.780	0.609	18.243	0.779	0.607	18.277
29. N.36	0.762	0.580	24.178	0.764	0.584	24.070	0.766	0.586	24.007	0.766	0.586	24.004
30. N.24	0.802	0.644	28.875	0.800	0.639	29.060	0.800	0.639	29.060	0.800	0.639	29.060
31. N.42	0.792	0.627	53.814	0.793	0.629	53.651	0.796	0.634	53.314	0.796	0.634	53.281
32. N.64	0.884	0.781	64.538	0.884	0.782	64.471	0.884	0.782	64.524	0.884	0.782	64.445
33. N.40	0.744	0.554	61.485	0.745	0.555	61.432	0.745	0.555	61.438	0.747	0.558	61.190
34. N.1	0.859	0.739	79.859	0.860	0.740	79.715	0.860	0.740	79.713	0.861	0.741	79.470
35. N.22	0.712	0.507	74.567	0.713	0.508	74.494	0.713	0.508	74.552	0.713	0.508	74.506
36. N.13A	0.849	0.721	190.385	0.850	0.722	189.945	0.849	0.721	190.383	0.849	0.721	190.486

Appendix Table C2 (Continued)

Discharge Station	<i>API</i> critical range model for runoff estimation											
	50% of <i>API_{critical}</i>			60% of <i>API_{critical}</i>			70% of <i>API_{critical}</i>			80% of <i>API_{critical}</i>		
	r	NSE	RMSE	r	NSE	RMSE	r	NSE	RMSE	r	NSE	RMSE
1. P.24A	0.736	0.541	6.010	0.740	0.547	5.970	0.738	0.544	5.992	0.728	0.529	6.088
2. P.64	0.692	0.479	7.547	0.673	0.453	7.736	0.673	0.453	7.736	0.673	0.453	7.736
3. P.21	0.696	0.484	3.973	0.696	0.484	3.973	0.695	0.484	3.975	0.692	0.479	3.995
4. P.47	0.708	0.501	9.984	0.709	0.503	9.971	0.712	0.507	9.933	0.716	0.512	9.874
5. P.20	0.674	0.454	12.547	0.674	0.454	12.547	0.675	0.455	12.534	0.671	0.451	12.584
6. P.71	0.705	0.498	13.497	0.705	0.498	13.497	0.705	0.498	13.497	0.705	0.498	13.497
7. P.4A	0.633	0.401	15.011	0.639	0.408	14.921	0.635	0.403	14.986	0.630	0.397	15.065
8. P.14	0.726	0.527	25.310	0.725	0.526	25.331	0.723	0.523	25.415	0.723	0.523	25.415
9. P.67	0.776	0.602	23.362	0.772	0.597	23.515	0.772	0.597	23.515	0.772	0.597	23.515
10. P.1	0.691	0.478	42.113	0.691	0.477	42.135	0.690	0.476	42.197	0.690	0.476	42.197
11. W.17	0.748	0.560	6.107	0.749	0.561	6.099	0.745	0.554	6.145	0.745	0.554	6.145
12. W.20	0.716	0.512	6.729	0.716	0.512	6.729	0.716	0.512	6.729	0.716	0.512	6.729
13. W.16A	0.773	0.597	11.739	0.788	0.620	11.400	0.773	0.598	11.729	0.769	0.591	11.835
14. W.3A	0.698	0.487	47.203	0.698	0.487	47.205	0.698	0.487	47.205	0.698	0.487	47.205
15. Y.30	0.599	0.358	2.618	0.599	0.358	2.618	0.599	0.358	2.618	0.599	0.358	2.618
16. Y.34	0.779	0.606	4.940	0.776	0.603	4.962	0.769	0.591	5.032	0.751	0.564	5.194
17. Y.24	0.648	0.420	9.536	0.649	0.421	9.525	0.665	0.442	9.354	0.631	0.398	9.713
18. Y.26	0.631	0.399	10.286	0.636	0.405	10.232	0.605	0.366	10.558	0.599	0.358	10.625
19. Y.31	0.751	0.564	23.858	0.748	0.560	23.970	0.748	0.560	23.970	0.748	0.560	23.970
20. Y.20	0.815	0.664	49.883	0.812	0.660	50.162	0.812	0.660	50.162	0.812	0.660	50.162
21. Y.1C	0.805	0.648	66.032	0.804	0.646	66.230	0.804	0.646	66.230	0.804	0.646	66.230
22. N.66	0.756	0.571	3.032	0.746	0.556	3.085	0.741	0.549	3.111	0.739	0.546	3.121
23. N.49	0.667	0.445	14.904	0.669	0.447	14.871	0.669	0.448	14.866	0.667	0.445	14.897
24. N.62	0.693	0.480	6.842	0.693	0.480	6.843	0.695	0.483	6.819	0.691	0.478	6.855
25. N.59	0.721	0.520	8.431	0.714	0.509	8.526	0.717	0.514	8.486	0.718	0.515	8.474
26. N.65	0.638	0.407	22.946	0.625	0.390	23.271	0.611	0.374	23.585	0.605	0.366	23.740
27. N.63	0.749	0.561	6.979	0.753	0.568	6.925	0.721	0.519	7.301	0.720	0.518	7.309
28. N.55	0.775	0.600	18.439	0.774	0.600	18.449	0.775	0.600	18.442	0.774	0.599	18.463
29. N.36	0.765	0.586	24.019	0.764	0.584	24.058	0.764	0.584	24.079	0.764	0.584	24.068
30. N.24	0.800	0.639	29.060	0.800	0.639	29.060	0.800	0.639	29.060	0.800	0.639	29.060
31. N.42	0.796	0.634	53.268	0.798	0.637	53.065	0.807	0.652	51.984	0.813	0.661	51.274
32. N.64	0.884	0.781	64.584	0.886	0.785	64.025	0.884	0.782	64.505	0.883	0.780	64.695
33. N.40	0.748	0.559	61.123	0.746	0.556	61.345	0.746	0.556	61.352	0.746	0.556	61.355
34. N.1	0.859	0.739	79.859	0.860	0.740	79.636	0.860	0.740	79.659	0.859	0.738	79.910
35. N.22	0.712	0.508	74.561	0.712	0.507	74.572	0.713	0.508	74.510	0.712	0.507	74.569
36. N.13A	0.848	0.720	190.898	0.847	0.717	191.862	0.847	0.717	191.903	0.846	0.716	192.193

Appendix Table C2 (Continued)

Discharge Station	<i>API</i> critical range model for runoff estimation					
	90% of $API_{critical}$			100% of $API_{critical}$		
	r	NSE	RMSE	r	NSE	RMSE
1. P.24A	0.728	0.529	6.088	0.728	0.529	6.088
2. P.64	0.673	0.453	7.736	0.673	0.453	7.736
3. P.21	0.692	0.479	3.995	0.692	0.479	3.995
4. P.47	0.731	0.534	9.656	0.702	0.493	10.071
5. P.20	0.671	0.451	12.584	0.671	0.451	12.584
6. P.71	0.705	0.498	13.497	0.705	0.498	13.497
7. P.4A	0.630	0.397	15.065	0.630	0.397	15.065
8. P.14	0.723	0.523	25.415	0.723	0.523	25.415
9. P.67	0.772	0.597	23.515	0.772	0.597	23.515
10. P.1	0.690	0.476	42.197	0.690	0.476	42.197
11. W.17	0.745	0.554	6.145	0.745	0.554	6.145
12. W.20	0.716	0.512	6.729	0.716	0.512	6.729
13. W.16A	0.769	0.591	11.835	0.769	0.591	11.837
14. W.3A	0.698	0.487	47.205	0.698	0.487	47.204
15. Y.30	0.599	0.358	2.618	0.599	0.358	2.618
16. Y.34	0.751	0.564	5.194	0.751	0.564	5.194
17. Y.24	0.631	0.398	9.713	0.631	0.398	9.713
18. Y.26	0.599	0.358	10.625	0.599	0.358	10.625
19. Y.31	0.748	0.560	23.970	0.748	0.560	23.970
20. Y.20	0.812	0.660	50.162	0.812	0.660	50.162
21. Y.1C	0.804	0.646	66.230	0.804	0.646	66.230
22. N.66	0.739	0.546	3.121	0.739	0.546	3.121
23. N.49	0.665	0.442	14.939	0.662	0.438	15.001
24. N.62	0.690	0.476	6.867	0.690	0.476	6.870
25. N.59	0.714	0.509	8.527	0.713	0.508	8.539
26. N.65	0.602	0.362	23.798	0.602	0.362	23.808
27. N.63	0.720	0.518	7.309	0.720	0.518	7.309
28. N.55	0.772	0.596	18.532	0.769	0.592	18.629
29. N.36	0.767	0.588	23.942	0.759	0.577	24.272
30. N.24	0.800	0.639	29.060	0.800	0.639	29.063
31. N.42	0.814	0.663	51.148	0.791	0.626	53.868
32. N.64	0.882	0.779	64.936	0.882	0.779	64.936
33. N.40	0.745	0.555	61.416	0.744	0.553	61.551
34. N.1	0.859	0.738	80.007	0.859	0.737	80.066
35. N.22	0.710	0.505	74.782	0.709	0.503	74.921
36. N.13A	0.845	0.714	192.802	0.845	0.714	192.802

Appendix Table C3 Statistical measures of the similarity between simulated and observed hydrographs using critical API range model 3.

Discharge Station	API critical range model for runoff estimation											
	10% of $API_{critical}$			20% of $API_{critical}$			30% of $API_{critical}$			40% of $API_{critical}$		
	r	NSE	RMSE	r	NSE	RMSE	r	NSE	RMSE	r	NSE	RMSE
1. P.24A	0.730	0.533	6.067	0.729	0.531	6.078	0.729	0.531	6.078	0.734	0.538	6.031
2. P.64	0.691	0.477	7.566	0.693	0.479	7.546	0.689	0.475	7.580	0.697	0.486	7.498
3. P.21	0.696	0.484	3.976	0.697	0.486	3.968	0.696	0.484	3.973	0.696	0.484	3.972
4. P.47	0.736	0.540	9.585	0.734	0.537	9.625	0.726	0.521	9.782	0.733	0.534	9.652
5. P.20	0.672	0.451	12.585	0.673	0.453	12.562	0.671	0.449	12.603	0.671	0.450	12.591
6. P.71	0.726	0.526	13.104	0.727	0.528	13.080	0.727	0.529	13.068	0.720	0.518	13.221
7. P.4A	0.632	0.399	15.040	0.628	0.394	15.097	0.630	0.397	15.056	0.630	0.397	15.064
8. P.14	0.726	0.527	25.316	0.726	0.527	25.300	0.725	0.526	25.346	0.725	0.526	25.336
9. P.67	0.776	0.602	23.367	0.779	0.607	23.207	0.774	0.598	23.482	0.776	0.601	23.383
10. P.1	0.692	0.479	42.075	0.689	0.475	42.242	0.691	0.478	42.112	0.691	0.478	42.111
11. W.17	0.746	0.557	6.127	0.745	0.555	6.140	0.747	0.556	6.130	0.749	0.560	6.108
12. W.20	0.712	0.505	6.773	0.718	0.515	6.704	0.719	0.517	6.695	0.723	0.523	6.655
13. W.16A	0.768	0.588	11.877	0.769	0.592	11.826	0.770	0.593	11.811	0.771	0.593	11.800
14. W.3A	0.699	0.489	47.120	0.699	0.488	47.168	0.700	0.491	47.058	0.699	0.488	47.160
15. Y.30	0.609	0.370	2.593	0.608	0.370	2.594	0.605	0.366	2.603	0.605	0.366	2.603
16. Y.34	0.771	0.594	5.015	0.754	0.566	5.183	0.762	0.580	5.102	0.752	0.563	5.205
17. Y.24	0.637	0.406	9.654	0.637	0.405	9.657	0.640	0.409	9.625	0.644	0.415	9.580
18. Y.26	0.614	0.376	10.478	0.619	0.383	10.416	0.617	0.377	10.467	0.629	0.394	10.321
19. Y.31	0.749	0.561	23.951	0.747	0.558	24.029	0.752	0.566	23.817	0.752	0.565	23.848
20. Y.20	0.813	0.661	50.074	0.813	0.661	50.084	0.817	0.668	49.556	0.819	0.671	49.348
21. Y.1C	0.807	0.650	65.842	0.806	0.650	65.921	0.808	0.653	65.620	0.807	0.651	65.819
22. N.66	0.740	0.547	3.115	0.740	0.548	3.114	0.743	0.552	3.099	0.753	0.567	3.048
23. N.49	0.666	0.438	14.990	0.666	0.441	14.955	0.667	0.441	14.955	0.665	0.438	14.999
24. N.62	0.689	0.475	6.875	0.690	0.476	6.866	0.691	0.477	6.859	0.686	0.471	6.900
25. N.59	0.714	0.510	8.518	0.715	0.510	8.517	0.711	0.505	8.567	0.719	0.516	8.467
26. N.65	0.610	0.371	23.630	0.612	0.374	23.576	0.613	0.376	23.549	0.614	0.375	23.570
27. N.63	0.755	0.570	6.907	0.756	0.571	6.895	0.758	0.574	6.875	0.757	0.574	6.877
28. N.55	0.777	0.603	18.371	0.776	0.601	18.407	0.773	0.596	18.524	0.772	0.596	18.539
29. N.36	0.764	0.583	24.092	0.766	0.587	23.983	0.762	0.581	24.159	0.765	0.584	24.055
30. N.24	0.803	0.644	28.858	0.801	0.642	28.944	0.801	0.642	28.937	0.801	0.642	28.937
31. N.42	0.793	0.627	53.773	0.797	0.634	53.250	0.797	0.636	53.162	0.797	0.635	53.180
32. N.64	0.882	0.777	65.135	0.884	0.781	64.644	0.880	0.775	65.468	0.883	0.780	64.818
33. N.40	0.743	0.551	61.677	0.744	0.554	61.485	0.744	0.553	61.521	0.747	0.558	61.210
34. N.1	0.859	0.737	80.135	0.859	0.738	79.944	0.860	0.739	79.857	0.859	0.738	80.009
35. N.22	0.712	0.506	74.649	0.711	0.505	74.775	0.712	0.507	74.591	0.712	0.506	74.652
36. N.13A	0.849	0.721	190.495	0.850	0.721	190.329	0.849	0.720	190.619	0.849	0.720	190.765

Appendix Table C3 (Continued)

Discharge Station	API critical range model for runoff estimation											
	50% of $API_{critical}$			60% of $API_{critical}$			70% of $API_{critical}$			80% of $API_{critical}$		
	r	NSE	RMSE	r	NSE	RMSE	r	NSE	RMSE	r	NSE	RMSE
1. P.24A	0.733	0.537	6.037	0.734	0.539	6.027	0.738	0.545	5.987	0.729	0.532	6.072
2. P.64	0.698	0.488	7.486	0.690	0.476	7.574	0.690	0.476	7.574	0.690	0.476	7.574
3. P.21	0.694	0.482	3.982	0.697	0.486	3.966	0.697	0.486	3.965	0.697	0.486	3.967
4. P.47	0.727	0.524	9.757	0.736	0.539	9.600	0.734	0.532	9.668	0.749	0.557	9.411
5. P.20	0.676	0.456	12.520	0.673	0.453	12.558	0.675	0.456	12.531	0.673	0.452	12.570
6. P.71	0.720	0.518	13.224	0.720	0.518	13.224	0.720	0.518	13.224	0.720	0.518	13.224
7. P.4A	0.629	0.395	15.082	0.631	0.398	15.043	0.627	0.393	15.115	0.630	0.397	15.058
8. P.14	0.727	0.528	25.276	0.726	0.528	25.292	0.725	0.526	25.339	0.725	0.526	25.339
9. P.67	0.773	0.596	23.524	0.775	0.600	23.429	0.775	0.600	23.429	0.775	0.600	23.429
10. P.1	0.689	0.474	42.263	0.691	0.477	42.142	0.691	0.477	42.141	0.690	0.476	42.167
11. W.17	0.751	0.563	6.087	0.754	0.568	6.050	0.746	0.557	6.129	0.746	0.557	6.129
12. W.20	0.715	0.511	6.736	0.715	0.511	6.736	0.715	0.511	6.736	0.715	0.511	6.736
13. W.16A	0.772	0.595	11.771	0.793	0.626	11.318	0.783	0.610	11.562	0.770	0.591	11.835
14. W.3A	0.699	0.488	47.162	0.699	0.488	47.172	0.699	0.488	47.172	0.698	0.486	47.252
15. Y.30	0.605	0.366	2.603	0.605	0.366	2.603	0.605	0.366	2.603	0.605	0.366	2.603
16. Y.34	0.784	0.614	4.889	0.777	0.604	4.956	0.778	0.606	4.942	0.772	0.596	5.006
17. Y.24	0.649	0.421	9.527	0.649	0.421	9.526	0.665	0.442	9.354	0.637	0.405	9.657
18. Y.26	0.634	0.401	10.265	0.632	0.398	10.295	0.616	0.375	10.484	0.616	0.374	10.492
19. Y.31	0.751	0.563	23.885	0.749	0.561	23.960	0.749	0.561	23.960	0.749	0.561	23.960
20. Y.20	0.815	0.665	49.785	0.813	0.661	50.084	0.813	0.661	50.084	0.813	0.661	50.084
21. Y.1C	0.806	0.649	65.998	0.806	0.649	66.001	0.806	0.649	66.001	0.806	0.649	66.001
22. N.66	0.753	0.567	3.046	0.754	0.569	3.041	0.747	0.557	3.082	0.741	0.548	3.115
23. N.49	0.668	0.440	14.965	0.666	0.437	15.014	0.666	0.435	15.032	0.664	0.434	15.053
24. N.62	0.687	0.472	6.896	0.690	0.475	6.871	0.692	0.479	6.848	0.689	0.474	6.881
25. N.59	0.719	0.516	8.465	0.714	0.509	8.529	0.715	0.511	8.513	0.715	0.511	8.514
26. N.65	0.638	0.398	23.115	0.634	0.401	23.068	0.609	0.370	23.651	0.612	0.371	23.644
27. N.63	0.755	0.570	6.908	0.757	0.572	6.889	0.755	0.570	6.909	0.755	0.570	6.908
28. N.55	0.766	0.586	18.757	0.778	0.601	18.420	0.777	0.599	18.470	0.770	0.569	19.144
29. N.36	0.766	0.587	23.987	0.764	0.584	24.058	0.764	0.584	24.071	0.764	0.584	24.059
30. N.24	0.801	0.642	28.937	0.801	0.642	28.937	0.801	0.642	28.937	0.801	0.642	28.937
31. N.42	0.797	0.635	53.172	0.797	0.635	53.244	0.809	0.654	51.840	0.814	0.663	51.126
32. N.64	0.884	0.781	64.645	0.885	0.784	64.188	0.886	0.785	63.959	0.883	0.780	64.823
33. N.40	0.748	0.559	61.133	0.744	0.553	61.519	0.743	0.552	61.629	0.743	0.552	61.623
34. N.1	0.859	0.737	80.122	0.859	0.737	80.057	0.860	0.739	79.743	0.859	0.736	80.264
35. N.22	0.713	0.508	74.513	0.710	0.504	74.850	0.711	0.504	74.811	0.711	0.505	74.750
36. N.13A	0.848	0.719	191.138	0.847	0.718	191.527	0.848	0.719	191.063	0.848	0.718	191.329

Appendix Table C3 (Continued)

Discharge Station	<i>API</i> critical range model for runoff estimation					
	90% of $API_{critical}$			100% of $API_{critical}$		
	r	NSE	RMSE	r	NSE	RMSE
1. P.24A	0.729	0.532	6.072	0.729	0.532	6.071
2. P.64	0.690	0.476	7.574	0.689	0.475	7.578
3. P.21	0.697	0.486	3.967	0.697	0.486	3.967
4. P.47	0.759	0.572	9.251	0.735	0.537	9.619
5. P.20	0.673	0.452	12.570	0.673	0.452	12.570
6. P.71	0.720	0.518	13.224	0.720	0.518	13.224
7. P.4A	0.630	0.397	15.058	0.630	0.397	15.066
8. P.14	0.725	0.526	25.339	0.725	0.525	25.356
9. P.67	0.775	0.600	23.429	0.775	0.600	23.429
10. P.1	0.690	0.476	42.167	0.690	0.476	42.167
11. W.17	0.746	0.557	6.129	0.746	0.557	6.128
12. W.20	0.715	0.511	6.736	0.715	0.511	6.736
13. W.16A	0.770	0.591	11.835	0.770	0.591	11.835
14. W.3A	0.698	0.486	47.252	0.698	0.486	47.252
15. Y.30	0.605	0.366	2.603	0.605	0.366	2.603
16. Y.34	0.772	0.596	5.006	0.773	0.597	4.995
17. Y.24	0.637	0.405	9.657	0.637	0.405	9.657
18. Y.26	0.616	0.374	10.492	0.616	0.374	10.492
19. Y.31	0.749	0.561	23.960	0.749	0.561	23.960
20. Y.20	0.813	0.661	50.084	0.813	0.661	50.084
21. Y.1C	0.806	0.649	66.001	0.806	0.649	66.001
22. N.66	0.739	0.545	3.122	0.738	0.545	3.124
23. N.49	0.664	0.433	15.056	0.666	0.437	15.004
24. N.62	0.689	0.474	6.884	0.687	0.471	6.898
25. N.59	0.717	0.514	8.486	0.714	0.510	8.522
26. N.65	0.610	0.371	23.646	0.613	0.375	23.562
27. N.63	0.755	0.570	6.908	0.755	0.570	6.908
28. N.55	0.774	0.596	18.544	0.776	0.602	18.399
29. N.36	0.767	0.589	23.934	0.762	0.581	24.143
30. N.24	0.801	0.642	28.937	0.801	0.642	28.937
31. N.42	0.813	0.661	51.303	0.794	0.631	53.516
32. N.64	0.882	0.778	65.090	0.882	0.777	65.166
33. N.40	0.743	0.552	61.638	0.742	0.550	61.767
34. N.1	0.859	0.736	80.241	0.859	0.736	80.231
35. N.22	0.711	0.505	74.738	0.710	0.505	74.773
36. N.13A	0.848	0.719	191.046	0.848	0.719	191.046

Appendix Table C4 Statistical measures of the similarity between simulated and observed hydrographs using critical API range model 4.

Discharge Station	API critical range model for runoff estimation											
	10% of $API_{critical}$			20% of $API_{critical}$			30% of $API_{critical}$			40% of $API_{critical}$		
	r	NSE	RMSE	r	NSE	RMSE	r	NSE	RMSE	r	NSE	RMSE
1. P.24A	0.728	0.530	6.084	0.729	0.532	6.071	0.730	0.532	6.068	0.732	0.535	6.050
2. P.64	0.682	0.465	7.649	0.682	0.464	7.659	0.680	0.460	7.682	0.681	0.461	7.677
3. P.21	0.695	0.484	3.975	0.696	0.484	3.973	0.697	0.485	3.969	0.699	0.488	3.958
4. P.47	0.672	0.451	10.473	0.674	0.455	10.443	0.674	0.454	10.444	0.670	0.449	10.494
5. P.20	0.673	0.452	12.568	0.673	0.453	12.564	0.672	0.452	12.577	0.671	0.450	12.597
6. P.71	0.718	0.515	13.258	0.721	0.519	13.200	0.730	0.533	13.016	0.715	0.511	13.310
7. P.4A	0.632	0.399	15.030	0.631	0.398	15.051	0.630	0.397	15.064	0.630	0.397	15.061
8. P.14	0.726	0.528	25.291	0.725	0.525	25.361	0.725	0.525	25.353	0.725	0.526	25.348
9. P.67	0.774	0.599	23.453	0.780	0.608	23.194	0.775	0.600	23.419	0.774	0.600	23.426
10. P.1	0.692	0.479	42.050	0.693	0.480	42.039	0.693	0.480	42.018	0.693	0.480	42.039
11. W.17	0.746	0.556	6.132	0.747	0.558	6.117	0.747	0.559	6.116	0.749	0.561	6.100
12. W.20	0.716	0.512	6.726	0.718	0.515	6.708	0.726	0.527	6.626	0.720	0.518	6.688
13. W.16A	0.770	0.593	11.810	0.773	0.597	11.742	0.775	0.601	11.686	0.771	0.594	11.788
14. W.3A	0.702	0.492	46.988	0.704	0.495	46.837	0.702	0.493	46.933	0.700	0.490	47.086
15. Y.30	0.605	0.366	2.603	0.603	0.363	2.609	0.601	0.361	2.612	0.601	0.361	2.612
16. Y.34	0.769	0.591	5.036	0.771	0.594	5.017	0.769	0.591	5.033	0.768	0.589	5.046
17. Y.24	0.633	0.401	9.692	0.639	0.408	9.632	0.641	0.410	9.617	0.643	0.413	9.592
18. Y.26	0.606	0.367	10.555	0.609	0.371	10.520	0.612	0.375	10.486	0.617	0.380	10.440
19. Y.31	0.749	0.562	23.928	0.751	0.564	23.862	0.752	0.565	23.825	0.754	0.569	23.726
20. Y.20	0.813	0.661	50.083	0.814	0.663	49.923	0.816	0.667	49.664	0.819	0.670	49.401
21. Y.1C	0.804	0.647	66.173	0.806	0.649	65.983	0.807	0.650	65.843	0.807	0.651	65.760
22. N.66	0.735	0.541	3.138	0.739	0.545	3.122	0.742	0.551	3.105	0.746	0.556	3.086
23. N.49	0.662	0.438	14.998	0.662	0.438	14.994	0.662	0.439	14.986	0.663	0.440	14.974
24. N.62	0.691	0.477	6.859	0.693	0.481	6.838	0.700	0.490	6.774	0.697	0.486	6.802
25. N.59	0.712	0.507	8.548	0.714	0.510	8.525	0.713	0.509	8.529	0.719	0.517	8.462
26. N.65	0.609	0.371	23.646	0.609	0.371	23.643	0.610	0.373	23.606	0.621	0.386	23.353
27. N.63	0.705	0.498	7.465	0.705	0.498	7.464	0.706	0.498	7.462	0.707	0.500	7.447
28. N.55	0.777	0.603	18.367	0.779	0.607	18.291	0.780	0.609	18.237	0.780	0.609	18.236
29. N.36	0.761	0.579	24.212	0.764	0.584	24.059	0.765	0.585	24.039	0.766	0.586	23.999
30. N.24	0.802	0.643	28.892	0.798	0.637	29.173	0.798	0.637	29.173	0.798	0.637	29.173
31. N.42	0.788	0.620	54.271	0.790	0.624	54.000	0.792	0.627	53.786	0.793	0.628	53.697
32. N.64	0.884	0.781	64.640	0.884	0.781	64.559	0.884	0.781	64.588	0.884	0.782	64.471
33. N.40	0.744	0.554	61.481	0.745	0.556	61.372	0.746	0.556	61.324	0.746	0.557	61.275
34. N.1	0.860	0.739	79.835	0.860	0.740	79.732	0.860	0.739	79.811	0.861	0.741	79.527
35. N.22	0.713	0.508	74.550	0.714	0.510	74.399	0.714	0.510	74.409	0.713	0.509	74.453
36. N.13A	0.849	0.721	190.311	0.850	0.722	190.136	0.849	0.721	190.557	0.849	0.720	190.673

Appendix Table C4 (Continued)

Discharge Station	API critical range model for runoff estimation											
	50% of $API_{critical}$			60% of $API_{critical}$			70% of $API_{critical}$			80% of $API_{critical}$		
	r	NSE	RMSE	r	NSE	RMSE	r	NSE	RMSE	r	NSE	RMSE
1. P.24A	0.733	0.536	6.045	0.734	0.539	6.025	0.736	0.542	6.005	0.725	0.526	6.107
2. P.64	0.674	0.454	7.728	0.668	0.444	7.799	0.668	0.444	7.799	0.668	0.444	7.799
3. P.21	0.696	0.484	3.975	0.696	0.484	3.972	0.696	0.485	3.971	0.693	0.480	3.988
4. P.47	0.671	0.450	10.487	0.673	0.452	10.465	0.676	0.457	10.418	0.675	0.455	10.436
5. P.20	0.672	0.451	12.583	0.671	0.450	12.589	0.673	0.453	12.564	0.669	0.447	12.624
6. P.71	0.707	0.500	13.461	0.707	0.500	13.461	0.707	0.500	13.461	0.707	0.500	13.461
7. P.4A	0.631	0.398	15.043	0.636	0.404	14.969	0.633	0.401	15.017	0.627	0.393	15.110
8. P.14	0.726	0.526	25.326	0.726	0.527	25.313	0.724	0.524	25.382	0.724	0.524	25.382
9. P.67	0.773	0.598	23.480	0.771	0.594	23.590	0.771	0.594	23.590	0.771	0.594	23.590
10. P.1	0.691	0.478	42.124	0.691	0.477	42.130	0.690	0.476	42.190	0.690	0.476	42.166
11. W.17	0.747	0.558	6.118	0.744	0.554	6.151	0.743	0.552	6.158	0.743	0.552	6.158
12. W.20	0.715	0.511	6.732	0.715	0.511	6.732	0.715	0.511	6.732	0.715	0.511	6.732
13. W.16A	0.773	0.597	11.750	0.783	0.613	11.504	0.775	0.601	11.693	0.769	0.591	11.831
14. W.3A	0.700	0.489	47.118	0.700	0.489	47.118	0.700	0.489	47.118	0.700	0.489	47.118
15. Y.30	0.601	0.361	2.612	0.601	0.361	2.612	0.601	0.361	2.612	0.601	0.361	2.612
16. Y.34	0.775	0.601	4.975	0.776	0.602	4.965	0.773	0.598	4.992	0.768	0.589	5.045
17. Y.24	0.642	0.412	9.598	0.643	0.414	9.588	0.659	0.435	9.416	0.631	0.398	9.712
18. Y.26	0.624	0.390	10.362	0.626	0.392	10.342	0.606	0.367	10.553	0.600	0.360	10.610
19. Y.31	0.752	0.566	23.809	0.749	0.562	23.930	0.749	0.562	23.930	0.749	0.562	23.930
20. Y.20	0.814	0.662	50.009	0.812	0.659	50.248	0.812	0.659	50.248	0.812	0.659	50.248
21. Y.1C	0.805	0.648	66.080	0.804	0.646	66.293	0.804	0.646	66.293	0.804	0.646	66.293
22. N.66	0.753	0.567	3.048	0.738	0.544	3.127	0.735	0.541	3.139	0.733	0.537	3.149
23. N.49	0.663	0.439	14.976	0.664	0.441	14.951	0.665	0.443	14.932	0.664	0.440	14.963
24. N.62	0.691	0.478	6.856	0.692	0.479	6.848	0.693	0.480	6.838	0.691	0.478	6.857
25. N.59	0.721	0.520	8.434	0.712	0.507	8.551	0.711	0.505	8.561	0.713	0.509	8.531
26. N.65	0.628	0.395	23.189	0.619	0.384	23.396	0.609	0.371	23.641	0.606	0.367	23.706
27. N.63	0.710	0.504	7.417	0.709	0.502	7.429	0.705	0.497	7.467	0.705	0.497	7.467
28. N.55	0.776	0.602	18.384	0.776	0.602	18.396	0.776	0.602	18.389	0.776	0.602	18.389
29. N.36	0.765	0.586	24.014	0.764	0.584	24.073	0.763	0.583	24.106	0.763	0.583	24.097
30. N.24	0.798	0.637	29.173	0.798	0.637	29.173	0.798	0.637	29.173	0.798	0.637	29.173
31. N.42	0.794	0.630	53.542	0.795	0.632	53.443	0.794	0.631	53.487	0.801	0.642	52.720
32. N.64	0.884	0.782	64.527	0.886	0.786	63.909	0.885	0.783	64.301	0.883	0.780	64.690
33. N.40	0.747	0.559	61.159	0.745	0.555	61.394	0.745	0.554	61.460	0.745	0.554	61.450
34. N.1	0.859	0.738	79.904	0.860	0.740	79.608	0.861	0.741	79.548	0.859	0.737	80.110
35. N.22	0.713	0.508	74.505	0.713	0.508	74.543	0.713	0.509	74.463	0.713	0.508	74.500
36. N.13A	0.848	0.720	190.911	0.847	0.718	191.413	0.848	0.719	191.071	0.848	0.719	191.213

Appendix Table C4 (Continued)

Discharge Station	<i>API</i> critical range model for runoff estimation					
	90% of $API_{critical}$			100% of $API_{critical}$		
	r	NSE	RMSE	r	NSE	RMSE
1. P.24A	0.725	0.526	6.107	0.725	0.526	6.107
2. P.64	0.668	0.444	7.799	0.668	0.444	7.799
3. P.21	0.693	0.480	3.988	0.693	0.480	3.988
4. P.47	0.678	0.460	10.388	0.669	0.448	10.506
5. P.20	0.669	0.447	12.624	0.669	0.447	12.624
6. P.71	0.707	0.500	13.461	0.707	0.500	13.461
7. P.4A	0.627	0.393	15.110	0.627	0.393	15.110
8. P.14	0.724	0.524	25.382	0.724	0.524	25.382
9. P.67	0.771	0.594	23.590	0.770	0.593	23.630
10. P.1	0.690	0.476	42.166	0.690	0.476	42.166
11. W.17	0.743	0.552	6.158	0.743	0.552	6.158
12. W.20	0.715	0.511	6.732	0.715	0.511	6.732
13. W.16A	0.769	0.591	11.831	0.769	0.591	11.831
14. W.3A	0.700	0.489	47.118	0.700	0.489	47.118
15. Y.30	0.601	0.361	2.612	0.601	0.361	2.612
16. Y.34	0.768	0.589	5.047	0.767	0.588	5.051
17. Y.24	0.631	0.398	9.712	0.631	0.398	9.712
18. Y.26	0.600	0.360	10.610	0.600	0.360	10.610
19. Y.31	0.749	0.562	23.930	0.747	0.558	24.034
20. Y.20	0.812	0.659	50.248	0.812	0.659	50.247
21. Y.1C	0.804	0.646	66.293	0.804	0.646	66.293
22. N.66	0.733	0.538	3.149	0.732	0.536	3.155
23. N.49	0.664	0.440	14.964	0.661	0.437	15.011
24. N.62	0.690	0.476	6.865	0.690	0.476	6.866
25. N.59	0.709	0.502	8.590	0.707	0.500	8.609
26. N.65	0.605	0.366	23.739	0.604	0.365	23.753
27. N.63	0.705	0.497	7.467	0.705	0.497	7.467
28. N.55	0.775	0.600	18.443	0.772	0.597	18.518
29. N.36	0.766	0.587	23.976	0.756	0.571	24.424
30. N.24	0.798	0.637	29.173	0.798	0.637	29.173
31. N.42	0.805	0.649	52.208	0.785	0.617	54.519
32. N.64	0.883	0.779	64.865	0.883	0.779	64.865
33. N.40	0.745	0.554	61.458	0.744	0.553	61.530
34. N.1	0.859	0.738	79.999	0.859	0.738	80.030
35. N.22	0.712	0.506	74.646	0.711	0.505	74.748
36. N.13A	0.847	0.717	191.698	0.847	0.717	191.698

Appendix Table C5 Statistical measures of the similarity between simulated and observed hydrographs using critical API range model 5.

Discharge Station	API critical range model for runoff estimation											
	10% of $API_{critical}$			20% of $API_{critical}$			30% of $API_{critical}$			40% of $API_{critical}$		
	r	NSE	RMSE	r	NSE	RMSE	r	NSE	RMSE	r	NSE	RMSE
1. P.24A	0.730	0.534	6.061	0.731	0.534	6.056	0.734	0.538	6.030	0.741	0.549	5.960
2. P.64	0.688	0.473	7.591	0.687	0.472	7.599	0.689	0.475	7.580	0.692	0.479	7.550
3. P.21	0.692	0.479	3.993	0.694	0.481	3.985	0.694	0.482	3.982	0.693	0.481	3.987
4. P.47	0.681	0.464	10.353	0.690	0.476	10.238	0.690	0.476	10.231	0.691	0.478	10.221
5. P.20	0.673	0.453	12.557	0.673	0.454	12.554	0.673	0.454	12.554	0.675	0.456	12.530
6. P.71	0.714	0.510	13.324	0.709	0.503	13.419	0.729	0.531	13.039	0.706	0.498	13.486
7. P.4A	0.631	0.398	15.046	0.631	0.398	15.049	0.631	0.399	15.040	0.632	0.399	15.035
8. P.14	0.725	0.526	25.346	0.725	0.525	25.356	0.725	0.526	25.334	0.724	0.525	25.375
9. P.67	0.773	0.598	23.487	0.778	0.606	23.251	0.776	0.602	23.348	0.776	0.603	23.343
10. P.1	0.691	0.478	42.124	0.692	0.479	42.081	0.693	0.480	42.042	0.692	0.479	42.061
11. W.17	0.746	0.556	6.130	0.747	0.558	6.119	0.748	0.559	6.114	0.749	0.561	6.096
12. W.20	0.715	0.512	6.731	0.717	0.515	6.710	0.725	0.525	6.635	0.725	0.525	6.637
13. W.16A	0.764	0.584	11.935	0.771	0.594	11.790	0.777	0.603	11.658	0.771	0.594	11.791
14. W.3A	0.699	0.488	47.158	0.699	0.488	47.174	0.700	0.490	47.075	0.697	0.485	47.305
15. Y.30	0.607	0.369	2.597	0.603	0.363	2.608	0.602	0.363	2.609	0.602	0.363	2.609
16. Y.34	0.775	0.600	4.979	0.775	0.601	4.970	0.775	0.601	4.972	0.780	0.609	4.921
17. Y.24	0.640	0.410	9.616	0.645	0.416	9.569	0.650	0.422	9.521	0.653	0.427	9.481
18. Y.26	0.603	0.364	10.579	0.605	0.366	10.561	0.610	0.370	10.529	0.612	0.371	10.523
19. Y.31	0.748	0.559	23.991	0.751	0.564	23.871	0.751	0.564	23.868	0.753	0.567	23.794
20. Y.20	0.813	0.660	50.132	0.814	0.663	49.964	0.816	0.666	49.701	0.818	0.669	49.485
21. Y.1C	0.806	0.650	65.915	0.807	0.651	65.745	0.806	0.649	65.940	0.805	0.648	66.117
22. N.66	0.734	0.539	3.146	0.735	0.540	3.141	0.736	0.542	3.133	0.748	0.559	3.074
23. N.49	0.658	0.433	15.069	0.657	0.432	15.075	0.660	0.435	15.031	0.659	0.434	15.044
24. N.62	0.690	0.476	6.865	0.690	0.476	6.869	0.690	0.476	6.871	0.692	0.479	6.849
25. N.59	0.711	0.505	8.561	0.711	0.505	8.562	0.711	0.506	8.558	0.718	0.516	8.470
26. N.65	0.608	0.370	23.659	0.606	0.368	23.702	0.606	0.367	23.712	0.609	0.371	23.630
27. N.63	0.706	0.499	7.454	0.707	0.499	7.451	0.706	0.499	7.457	0.720	0.518	7.309
28. N.55	0.775	0.601	18.410	0.776	0.602	18.387	0.774	0.599	18.471	0.777	0.604	18.348
29. N.36	0.764	0.583	24.093	0.765	0.585	24.035	0.765	0.585	24.027	0.765	0.586	24.017
30. N.24	0.802	0.643	28.915	0.801	0.641	28.988	0.801	0.641	28.988	0.801	0.642	28.972
31. N.42	0.794	0.630	53.546	0.796	0.634	53.259	0.802	0.642	52.664	0.807	0.652	51.977
32. N.64	0.884	0.782	64.495	0.885	0.782	64.400	0.884	0.782	64.507	0.883	0.780	64.708
33. N.40	0.744	0.554	61.512	0.744	0.553	61.526	0.743	0.552	61.651	0.743	0.551	61.654
34. N.1	0.859	0.738	79.909	0.860	0.740	79.712	0.860	0.740	79.692	0.861	0.741	79.534
35. N.22	0.712	0.506	74.655	0.711	0.505	74.723	0.711	0.505	74.743	0.710	0.505	74.788
36. N.13A	0.849	0.720	190.613	0.850	0.722	190.263	0.849	0.721	190.440	0.848	0.719	191.164

Appendix Table C5 (Continued)

Discharge Station	<i>API</i> critical range model for runoff estimation											
	50% of <i>API_{critical}</i>			60% of <i>API_{critical}</i>			70% of <i>API_{critical}</i>			80% of <i>API_{critical}</i>		
	r	NSE	RMSE	r	NSE	RMSE	r	NSE	RMSE	r	NSE	RMSE
1. P.24A	0.738	0.544	5.992	0.738	0.545	5.988	0.737	0.544	5.995	0.730	0.533	6.062
2. P.64	0.690	0.476	7.568	0.677	0.459	7.695	0.677	0.459	7.695	0.677	0.459	7.695
3. P.21	0.693	0.481	3.987	0.694	0.482	3.983	0.694	0.482	3.982	0.691	0.478	3.999
4. P.47	0.691	0.478	10.219	0.694	0.481	10.186	0.692	0.479	10.207	0.683	0.467	10.323
5. P.20	0.676	0.457	12.515	0.674	0.455	12.542	0.674	0.454	12.550	0.672	0.452	12.575
6. P.71	0.698	0.488	13.629	0.698	0.488	13.629	0.698	0.488	13.629	0.698	0.488	13.629
7. P.4A	0.633	0.400	15.020	0.637	0.406	14.954	0.634	0.402	14.996	0.631	0.398	15.043
8. P.14	0.724	0.525	25.374	0.724	0.525	25.368	0.723	0.522	25.433	0.723	0.522	25.433
9. P.67	0.776	0.603	23.335	0.772	0.596	23.550	0.772	0.596	23.550	0.772	0.596	23.550
10. P.1	0.690	0.477	42.156	0.690	0.477	42.163	0.689	0.475	42.237	0.689	0.475	42.237
11. W.17	0.751	0.564	6.080	0.750	0.562	6.089	0.745	0.555	6.138	0.745	0.555	6.138
12. W.20	0.712	0.508	6.759	0.712	0.508	6.759	0.712	0.508	6.759	0.712	0.508	6.759
13. W.16A	0.769	0.592	11.823	0.780	0.608	11.588	0.770	0.591	11.840	0.765	0.584	11.932
14. W.3A	0.696	0.485	47.317	0.698	0.484	47.362	0.697	0.484	47.347	0.697	0.484	47.346
15. Y.30	0.602	0.363	2.609	0.602	0.363	2.609	0.602	0.363	2.609	0.602	0.363	2.609
16. Y.34	0.781	0.611	4.912	0.776	0.602	4.966	0.776	0.603	4.961	0.774	0.599	4.982
17. Y.24	0.650	0.422	9.517	0.653	0.424	9.503	0.650	0.421	9.530	0.640	0.410	9.620
18. Y.26	0.616	0.374	10.492	0.620	0.379	10.454	0.608	0.365	10.569	0.604	0.361	10.606
19. Y.31	0.749	0.560	23.967	0.747	0.557	24.044	0.747	0.557	24.044	0.747	0.557	24.044
20. Y.20	0.815	0.664	49.829	0.811	0.658	50.289	0.811	0.658	50.289	0.811	0.658	50.289
21. Y.1C	0.803	0.643	66.531	0.803	0.643	66.555	0.803	0.643	66.555	0.803	0.643	66.555
22. N.66	0.755	0.570	3.037	0.748	0.559	3.074	0.745	0.555	3.088	0.738	0.544	3.126
23. N.49	0.659	0.434	15.047	0.664	0.442	14.948	0.663	0.439	14.976	0.661	0.437	15.009
24. N.62	0.691	0.478	6.856	0.692	0.479	6.850	0.693	0.480	6.838	0.691	0.478	6.857
25. N.59	0.720	0.519	8.446	0.713	0.508	8.536	0.711	0.506	8.555	0.712	0.507	8.546
26. N.65	0.609	0.370	23.650	0.609	0.370	23.652	0.606	0.367	23.710	0.600	0.360	23.852
27. N.63	0.719	0.517	7.322	0.713	0.509	7.379	0.711	0.505	7.409	0.711	0.506	7.405
28. N.55	0.773	0.598	18.482	0.773	0.598	18.484	0.774	0.598	18.479	0.773	0.597	18.507
29. N.36	0.765	0.586	24.011	0.766	0.587	23.987	0.765	0.586	24.015	0.765	0.585	24.037
30. N.24	0.801	0.642	28.972	0.801	0.641	28.988	0.801	0.641	28.988	0.801	0.641	28.988
31. N.42	0.808	0.653	51.902	0.811	0.658	51.512	0.812	0.659	51.425	0.808	0.653	51.909
32. N.64	0.883	0.779	64.924	0.885	0.783	64.368	0.882	0.778	65.068	0.882	0.777	65.172
33. N.40	0.746	0.556	61.321	0.746	0.556	61.332	0.746	0.556	61.312	0.746	0.556	61.331
34. N.1	0.859	0.738	80.001	0.858	0.737	80.168	0.858	0.736	80.318	0.858	0.735	80.371
35. N.22	0.710	0.504	74.797	0.712	0.507	74.607	0.713	0.508	74.549	0.712	0.507	74.612
36. N.13A	0.846	0.716	192.205	0.842	0.709	194.500	0.842	0.709	194.572	0.841	0.707	195.275

Appendix Table C5 (Continued)

Discharge Station	<i>API</i> critical range model for runoff estimation					
	90% of $API_{critical}$			100% of $API_{critical}$		
	r	NSE	RMSE	r	NSE	RMSE
1. P.24A	0.730	0.533	6.062	0.730	0.533	6.062
2. P.64	0.677	0.459	7.695	0.677	0.459	7.695
3. P.21	0.691	0.478	3.999	0.691	0.478	3.999
4. P.47	0.682	0.465	10.344	0.675	0.456	10.433
5. P.20	0.672	0.452	12.577	0.672	0.452	12.575
6. P.71	0.698	0.488	13.629	0.698	0.488	13.629
7. P.4A	0.631	0.398	15.043	0.631	0.398	15.043
8. P.14	0.723	0.522	25.433	0.723	0.522	25.433
9. P.67	0.772	0.596	23.550	0.772	0.596	23.550
10. P.1	0.689	0.475	42.237	0.689	0.475	42.237
11. W.17	0.745	0.555	6.138	0.745	0.555	6.138
12. W.20	0.712	0.508	6.759	0.712	0.508	6.759
13. W.16A	0.765	0.584	11.932	0.762	0.578	12.017
14. W.3A	0.697	0.484	47.345	0.697	0.484	47.345
15. Y.30	0.602	0.363	2.609	0.602	0.363	2.609
16. Y.34	0.774	0.599	4.982	0.774	0.599	4.982
17. Y.24	0.640	0.410	9.620	0.640	0.410	9.620
18. Y.26	0.604	0.361	10.606	0.604	0.360	10.607
19. Y.31	0.747	0.557	24.044	0.747	0.557	24.044
20. Y.20	0.811	0.658	50.289	0.811	0.658	50.289
21. Y.1C	0.803	0.643	66.555	0.803	0.643	66.555
22. N.66	0.737	0.543	3.132	0.733	0.537	3.150
23. N.49	0.659	0.435	15.042	0.657	0.430	15.099
24. N.62	0.690	0.476	6.871	0.689	0.475	6.875
25. N.59	0.715	0.511	8.516	0.711	0.506	8.559
26. N.65	0.601	0.362	23.815	0.601	0.361	23.828
27. N.63	0.711	0.506	7.405	0.711	0.506	7.405
28. N.55	0.771	0.594	18.583	0.769	0.591	18.649
29. N.36	0.767	0.588	23.958	0.762	0.581	24.164
30. N.24	0.801	0.641	28.988	0.801	0.641	28.988
31. N.42	0.809	0.655	51.720	0.793	0.629	53.619
32. N.64	0.881	0.776	65.290	0.881	0.776	65.290
33. N.40	0.745	0.555	61.442	0.743	0.552	61.618
34. N.1	0.857	0.734	80.538	0.856	0.733	80.710
35. N.22	0.710	0.504	74.831	0.708	0.501	75.030
36. N.13A	0.841	0.707	195.275	0.841	0.707	195.129

Appendix Table C6 Statistical measures of the similarity between simulated and observed hydrographs using critical API range model 6.

Discharge Station	API critical range model for runoff estimation											
	10% of $API_{critical}$			20% of $API_{critical}$			30% of $API_{critical}$			40% of $API_{critical}$		
	r	NSE	RMSE	r	NSE	RMSE	r	NSE	RMSE	r	NSE	RMSE
1. P.24A	0.659	0.435	6.672	0.680	0.457	6.537	0.683	0.456	6.546	0.655	0.409	6.824
2. P.64	0.631	0.397	8.123	0.660	0.431	7.887	0.668	0.440	7.828	0.662	0.429	7.900
3. P.21	0.664	0.441	4.137	0.655	0.418	4.219	0.651	0.401	4.283	0.642	0.382	4.351
4. P.47	0.634	0.400	10.953	0.652	0.425	10.722	0.660	0.433	10.646	0.664	0.437	10.613
5. P.20	0.612	0.374	13.437	0.632	0.397	13.192	0.628	0.374	13.438	0.601	0.329	13.916
6. P.71	0.684	0.468	13.892	0.685	0.460	13.990	0.684	0.438	14.269	0.684	0.436	14.302
7. P.4A	0.589	0.347	15.672	0.598	0.357	15.556	0.598	0.343	15.725	0.589	0.326	15.923
8. P.14	0.706	0.498	26.071	0.677	0.450	27.285	0.680	0.418	28.083	0.678	0.406	28.353
9. P.67	0.730	0.533	25.314	0.751	0.553	24.756	0.729	0.511	25.903	0.708	0.467	27.030
10. P.1	0.650	0.422	44.311	0.647	0.399	45.172	0.645	0.386	45.666	0.631	0.361	46.595
11. W.17	0.659	0.433	6.928	0.697	0.479	6.645	0.696	0.469	6.705	0.679	0.435	6.917
12. W.20	0.663	0.437	7.224	0.692	0.474	6.983	0.709	0.493	6.856	0.664	0.422	7.320
13. W.16A	0.691	0.473	13.427	0.722	0.519	12.829	0.731	0.528	12.717	0.704	0.481	13.332
14. W.3A	0.662	0.437	49.420	0.672	0.446	49.017	0.668	0.438	49.398	0.656	0.419	50.227
15. Y.30	0.568	0.314	2.707	0.560	0.297	2.740	0.554	0.288	2.759	0.554	0.288	2.759
16. Y.34	0.712	0.437	5.904	0.710	0.501	5.558	0.735	0.537	5.353	0.733	0.528	5.408
17. Y.24	0.547	0.287	10.574	0.552	0.290	10.553	0.580	0.333	10.223	0.587	0.340	10.171
18. Y.26	0.577	0.332	10.841	0.588	0.345	10.738	0.595	0.351	10.683	0.587	0.339	10.780
19. Y.31	0.698	0.486	25.906	0.718	0.511	25.283	0.725	0.518	25.087	0.714	0.500	25.546
20. Y.20	0.732	0.534	58.740	0.764	0.579	55.785	0.765	0.577	55.936	0.752	0.549	57.740
21. Y.1C	0.739	0.543	75.249	0.762	0.576	72.515	0.760	0.568	73.234	0.741	0.532	76.220
22. N.66	0.653	0.419	3.531	0.695	0.483	3.330	0.716	0.511	3.238	0.730	0.530	3.175
23. N.49	0.631	0.397	15.529	0.654	0.426	15.159	0.654	0.425	15.166	0.650	0.417	15.271
24. N.62	0.667	0.443	7.078	0.669	0.446	7.063	0.668	0.441	7.092	0.666	0.437	7.121
25. N.59	0.651	0.423	9.250	0.683	0.465	8.900	0.687	0.470	8.859	0.698	0.484	8.742
26. N.65	0.596	0.356	23.926	0.602	0.361	23.822	0.598	0.350	24.034	0.604	0.351	24.015
27. N.63	0.661	0.436	7.912	0.688	0.470	7.668	0.695	0.476	7.622	0.687	0.461	7.735
28. N.55	0.738	0.544	19.699	0.748	0.554	19.475	0.744	0.544	19.683	0.738	0.530	19.996
29. N.36	0.703	0.493	26.564	0.715	0.505	26.244	0.718	0.507	26.207	0.726	0.515	25.983
30. N.24	0.771	0.588	31.074	0.725	0.512	33.794	0.725	0.512	33.811	0.725	0.512	33.811
31. N.42	0.737	0.544	59.485	0.754	0.563	58.196	0.757	0.561	58.365	0.758	0.558	58.563
32. N.64	0.832	0.690	76.887	0.843	0.710	74.312	0.846	0.709	74.482	0.856	0.716	73.625
33. N.40	0.694	0.481	66.326	0.708	0.497	65.269	0.712	0.501	65.032	0.708	0.492	65.586
34. N.1	0.793	0.624	95.750	0.814	0.662	90.875	0.820	0.667	90.164	0.822	0.662	90.833
35. N.22	0.673	0.451	78.696	0.681	0.460	78.044	0.682	0.458	78.212	0.675	0.446	79.096
36. N.13A	0.796	0.631	218.952	0.817	0.665	208.639	0.817	0.655	211.886	0.812	0.637	217.152

Appendix Table C6 (Continued)

Discharge Station	<i>API</i> critical range model for runoff estimation											
	50% of <i>API_{critical}</i>			60% of <i>API_{critical}</i>			70% of <i>API_{critical}</i>			80% of <i>API_{critical}</i>		
	r	NSE	RMSE	r	NSE	RMSE	r	NSE	RMSE	r	NSE	RMSE
1. P.24A	0.666	0.420	6.760	0.670	0.420	6.759	0.666	0.408	6.827	0.645	0.377	7.004
2. P.64	0.641	0.396	8.127	0.615	0.362	8.356	0.615	0.362	8.356	0.615	0.362	8.356
3. P.21	0.644	0.383	4.344	0.644	0.379	4.359	0.643	0.379	4.361	0.642	0.377	4.367
4. P.47	0.646	0.410	10.864	0.628	0.384	11.099	0.640	0.394	11.006	0.632	0.380	11.136
5. P.20	0.591	0.304	14.169	0.585	0.292	14.292	0.586	0.287	14.341	0.569	0.264	14.571
6. P.71	0.678	0.428	14.406	0.678	0.428	14.406	0.678	0.428	14.406	0.678	0.428	14.406
7. P.4A	0.577	0.306	16.152	0.587	0.317	16.032	0.575	0.300	16.221	0.561	0.283	16.428
8. P.14	0.673	0.399	28.541	0.671	0.390	28.736	0.670	0.390	28.749	0.670	0.390	28.749
9. P.67	0.693	0.435	27.829	0.693	0.433	27.872	0.693	0.433	27.872	0.693	0.433	27.872
10. P.1	0.622	0.346	47.133	0.620	0.342	47.257	0.620	0.342	47.264	0.620	0.342	47.266
11. W.17	0.659	0.402	7.115	0.644	0.377	7.267	0.638	0.368	7.315	0.638	0.368	7.315
12. W.20	0.661	0.417	7.352	0.661	0.417	7.352	0.661	0.417	7.352	0.661	0.417	7.352
13. W.16A	0.705	0.476	13.390	0.713	0.485	13.279	0.716	0.489	13.224	0.691	0.450	13.724
14. W.3A	0.651	0.411	50.576	0.650	0.410	50.605	0.650	0.410	50.605	0.650	0.410	50.605
15. Y.30	0.554	0.288	2.759	0.554	0.288	2.759	0.554	0.288	2.759	0.554	0.288	2.759
16. Y.34	0.761	0.526	5.418	0.765	0.533	5.378	0.741	0.492	5.611	0.712	0.437	5.904
17. Y.24	0.597	0.350	10.092	0.580	0.329	10.256	0.623	0.380	9.859	0.547	0.287	10.574
18. Y.26	0.588	0.339	10.784	0.584	0.333	10.831	0.581	0.331	10.847	0.579	0.328	10.876
19. Y.31	0.695	0.468	26.371	0.685	0.454	26.712	0.685	0.454	26.712	0.685	0.454	26.712
20. Y.20	0.726	0.506	60.445	0.718	0.494	61.213	0.718	0.494	61.213	0.718	0.494	61.213
21. Y.1C	0.729	0.509	78.030	0.727	0.508	78.153	0.727	0.508	78.153	0.727	0.508	78.153
22. N.66	0.733	0.533	3.166	0.694	0.471	3.366	0.674	0.437	3.475	0.682	0.444	3.452
23. N.49	0.644	0.407	15.398	0.637	0.395	15.555	0.633	0.387	15.666	0.632	0.386	15.675
24. N.62	0.658	0.425	7.191	0.654	0.419	7.229	0.654	0.418	7.241	0.648	0.409	7.296
25. N.59	0.698	0.483	8.753	0.677	0.449	9.039	0.668	0.435	9.150	0.670	0.435	9.152
26. N.65	0.614	0.358	23.887	0.591	0.327	24.457	0.593	0.329	24.412	0.593	0.329	24.411
27. N.63	0.694	0.468	7.683	0.690	0.461	7.734	0.668	0.425	7.983	0.663	0.418	8.031
28. N.55	0.733	0.522	20.164	0.731	0.514	20.324	0.730	0.512	20.370	0.729	0.510	20.405
29. N.36	0.725	0.513	26.034	0.709	0.489	26.663	0.710	0.489	26.659	0.710	0.490	26.657
30. N.24	0.725	0.512	33.811	0.725	0.512	33.811	0.725	0.512	33.811	0.725	0.512	33.811
31. N.42	0.753	0.543	59.562	0.755	0.547	59.258	0.738	0.518	61.124	0.749	0.533	60.197
32. N.64	0.857	0.715	73.733	0.863	0.723	72.658	0.858	0.712	74.132	0.837	0.671	79.184
33. N.40	0.701	0.482	66.272	0.689	0.464	67.429	0.686	0.456	67.870	0.681	0.451	68.214
34. N.1	0.820	0.653	92.068	0.821	0.651	92.252	0.817	0.638	93.994	0.801	0.607	97.914
35. N.22	0.670	0.438	79.676	0.663	0.427	80.443	0.661	0.424	80.662	0.660	0.422	80.799
36. N.13A	0.811	0.634	218.171	0.807	0.625	220.922	0.805	0.619	222.483	0.796	0.602	227.341

Appendix Table C6 (Continued)

Discharge Station	<i>API</i> critical range model for runoff estimation					
	90% of $API_{critical}$			100% of $API_{critical}$		
	r	NSE	RMSE	r	NSE	RMSE
1. P.24A	0.645	0.377	7.004	0.645	0.377	7.004
2. P.64	0.615	0.362	8.356	0.615	0.362	8.356
3. P.21	0.642	0.377	4.367	0.642	0.377	4.367
4. P.47	0.656	0.407	10.889	0.611	0.341	11.478
5. P.20	0.569	0.264	14.571	0.569	0.264	14.571
6. P.71	0.678	0.428	14.406	0.678	0.428	14.406
7. P.4A	0.561	0.283	16.428	0.561	0.283	16.428
8. P.14	0.670	0.390	28.749	0.670	0.390	28.749
9. P.67	0.693	0.433	27.872	0.693	0.433	27.872
10. P.1	0.620	0.342	47.266	0.620	0.342	47.266
11. W.17	0.638	0.368	7.315	0.638	0.368	7.315
12. W.20	0.661	0.417	7.352	0.661	0.417	7.352
13. W.16A	0.691	0.450	13.724	0.691	0.450	13.724
14. W.3A	0.650	0.410	50.605	0.650	0.410	50.605
15. Y.30	0.554	0.288	2.759	0.554	0.288	2.759
16. Y.34	0.712	0.437	5.904	0.712	0.437	5.904
17. Y.24	0.547	0.287	10.574	0.547	0.287	10.574
18. Y.26	0.579	0.328	10.876	0.579	0.328	10.876
19. Y.31	0.685	0.454	26.712	0.685	0.454	26.712
20. Y.20	0.718	0.494	61.213	0.718	0.494	61.213
21. Y.1C	0.727	0.508	78.153	0.728	0.508	78.153
22. N.66	0.676	0.435	3.480	0.651	0.396	3.600
23. N.49	0.632	0.385	15.692	0.631	0.384	15.694
24. N.62	0.648	0.408	7.300	0.646	0.404	7.324
25. N.59	0.651	0.408	9.365	0.636	0.386	9.539
26. N.65	0.590	0.326	24.468	0.590	0.326	24.469
27. N.63	0.663	0.418	8.031	0.663	0.418	8.031
28. N.55	0.729	0.510	20.414	0.729	0.510	20.417
29. N.36	0.709	0.487	26.736	0.686	0.454	27.574
30. N.24	0.725	0.512	33.811	0.725	0.512	33.811
31. N.42	0.765	0.555	58.720	0.723	0.491	62.844
32. N.64	0.833	0.664	80.062	0.833	0.664	80.062
33. N.40	0.680	0.449	68.344	0.680	0.448	68.392
34. N.1	0.795	0.596	99.247	0.795	0.596	99.252
35. N.22	0.660	0.422	80.799	0.660	0.422	80.799
36. N.13A	0.796	0.602	227.433	0.796	0.602	227.433

Appendix Table C7 Parameters of 112 small watersheds.

No.	Small Watersheds Code	Watersheds Parameter			
		A (sq.km)	L (km)	L _c (km)	S _{avg}
1.	C_1	1,545.83	112.84	32.77	0.00073
2.	C_2	3,401.69	103.40	40.05	0.00078
3.	N_1	2,228.40	143.76	51.94	0.00270
4.	N_2	790.12	73.69	41.79	0.00204
5.	N_3	1,536.76	128.43	54.49	0.01357
6.	N_4	600.56	66.58	31.94	0.00463
7.	N_5	591.43	55.04	23.50	0.00414
8.	N_6	781.25	77.22	48.74	0.00374
9.	N_7	3,195.67	184.21	47.69	0.00104
10.	N_8	2,206.21	173.50	99.32	0.00267
11.	N_9	1,046.72	72.22	37.39	0.00266
12.	N_11	2,429.65	163.40	89.02	0.00204
13.	N_12	1,095.06	109.50	43.60	0.00023
14.	N_13	339.67	87.91	14.45	0.00065
15.	N_14	1,727.56	148.67	77.68	0.00139
16.	N_15	688.24	78.02	38.98	0.00111
17.	N_16	5,583.44	232.46	151.40	0.00154
18.	N_17	219.89	51.84	28.37	0.00035
19.	N_18	158.46	45.01	25.85	0.00002
20.	N_19	259.45	62.13	29.55	0.00002
21.	N_20	2,615.91	229.89	47.97	0.00208
22.	N_21	271.77	62.84	28.54	0.00000
23.	N_22	1,226.22	70.21	38.07	0.00118
24.	N_23	205.20	55.22	30.01	0.00007
25.	N_24	2,208.96	102.60	52.02	0.00099
26.	N_25	1,426.18	124.82	55.33	0.00078
27.	N_26	2,142.74	149.30	72.87	0.00030
28.	N_27	988.53	112.26	35.62	0.00248
29.	P_1	1,912.74	141.58	69.26	0.00212
30.	P_2	1,286.47	98.94	41.05	0.00295
31.	P_3	1,961.74	152.14	70.67	0.00427
32.	P_4	1,530.67	133.46	63.95	0.00058
33.	P_5	53.44	26.18	11.62	0.00758
34.	P_6	562.05	58.59	32.30	0.00667
35.	P_7	2,894.30	108.59	28.17	0.00188
36.	P_8	1,745.75	123.60	60.63	0.00492
37.	P_9	2,100.52	155.09	80.14	0.00149
38.	P_10	620.93	50.82	15.95	0.01843
39.	P_11	3,194.35	172.72	69.61	0.00006
40.	P_12	1,971.02	97.34	47.47	0.00434
41.	P_13	1,935.41	114.92	64.96	0.00358
42.	P_14	522.07	56.33	25.52	0.00404
43.	P_15	3,179.69	242.68	128.10	0.00210
44.	P_16	845.40	70.39	40.45	0.00108
45.	P_17	166.08	32.36	26.59	0.00554

Appendix Table C7 (Continued)

No.	Small Watersheds Code	Watersheds Parameter			
		A (sq.km)	L (km)	L _c (km)	S _{avg}
46.	P_18	527.90	63.72	37.24	0.00489
47.	P_19	654.36	77.77	40.79	0.00445
48.	P_20	274.51	43.29	20.13	0.00168
49.	P_21	959.53	95.72	50.95	0.00162
50.	P_22	367.57	50.31	21.37	0.00056
51.	P_23	383.54	46.72	20.55	0.00707
52.	P_24	759.00	83.03	46.88	0.00417
53.	P_25	293.50	42.38	19.69	0.00064
54.	P_26	1,222.97	117.09	54.14	0.00329
55.	P_27	211.17	66.13	33.35	0.00024
56.	P_28	549.15	56.53	30.07	0.00146
57.	P_29	1,351.47	104.53	49.02	0.00125
58.	P_30	532.15	82.85	39.18	0.00077
59.	P_31	237.67	38.00	18.82	0.00039
60.	P_32	133.25	46.87	27.55	0.00096
61.	W_1	1,645.68	158.82	81.86	0.00190
62.	W_2	736.11	62.44	36.29	0.00296
63.	W_3	967.36	88.63	43.97	0.00250
64.	W_4	403.91	44.86	17.94	0.00637
65.	W_5	455.09	76.79	30.67	0.00265
66.	W_6	1,758.75	116.39	66.20	0.00141
67.	W_7	736.48	56.18	24.30	0.00396
68.	W_8	863.30	79.02	43.15	0.00226
69.	W_9	282.53	24.53	14.23	0.00853
70.	W_10	232.81	21.73	23.38	0.00357
71.	W_11	281.77	21.14	18.27	0.00422
72.	W_12	230.08	34.35	15.55	0.00676
73.	W_13	149.13	23.88	21.25	0.00575
74.	W_14	182.87	22.14	13.39	0.00196
75.	W_15	362.83	48.61	30.29	0.00286
76.	W_16	340.06	49.85	23.57	0.00549
77.	W_17	308.38	53.37	34.66	0.00147
78.	W_18	256.61	34.91	27.81	0.00567
79.	W_19	378.76	65.98	26.70	0.00419
80.	W_20	215.53	39.56	22.30	0.00169
81.	W_21	22.36	34.27	20.13	0.00024
82.	Y_1	2,119.68	163.83	75.39	0.00150
83.	Y_2	873.55	63.10	32.35	0.00365
84.	Y_3	658.84	57.14	24.36	0.00528
85.	Y_4	1,760.07	105.97	39.70	0.00334
86.	Y_5	214.68	24.24	8.76	0.00481
87.	Y_6	374.67	57.60	38.32	0.00410
88.	Y_7	332.06	40.49	17.46	0.00147
89.	Y_8	246.06	33.67	21.37	0.00524
90.	Y_9	1,032.13	80.09	47.14	0.00231

Appendix Table C7 (Continued)

No.	Small Watersheds Code	Watersheds Parameter			
		A (sq.km)	L (km)	L _c (km)	S _{avg}
91.	Y_10	149.72	29.51	13.79	0.00364
92.	Y_11	532.40	30.71	30.70	0.00653
93.	Y_12	246.04	37.51	32.68	0.00273
94.	Y_13	710.99	57.12	22.97	0.00313
95.	Y_14	439.67	36.17	31.55	0.00226
96.	Y_15	531.06	72.42	15.85	0.00106
97.	Y_16	214.37	59.59	24.82	0.00120
98.	Y_17	880.08	77.81	40.15	0.00211
99.	Y_18	832.84	90.61	72.15	0.00095
100.	Y_19	796.77	45.87	49.40	0.00135
101.	Y_20	768.35	76.32	39.95	0.00312
102.	Y_21	2,312.65	145.32	58.47	0.00155
103.	Y_22	491.33	87.39	51.53	0.00026
104.	Y_23	1,055.89	86.03	53.41	0.00167
105.	Y_24	1,572.14	92.05	52.42	0.00040
106.	Y_25	905.78	123.58	63.56	0.00008
107.	Y_26	545.44	80.60	40.47	0.00026
108.	Y_27	1,323.37	83.15	47.23	0.00023
109.	Y_28	656.33	80.29	57.12	0.00005
110.	Y_29	191.71	115.09	63.12	0.00016
111.	Y_30	655.33	130.46	59.96	0.00019
112.	Y_31	169.97	42.90	22.01	0.00023

CURRICULUM VITAE

NAME : Mr. Chaiyapong Thepprasit

BIRTH DATE : April 08, 1975

BIRTH PLACE : Nong Khai, Thailand

EDUCATION	: YEAR	INSTITUTE	DEGREE/DIPLOMA
	1997	Kasetsart University	B.Eng (Water Resources Engineering)
	2003	Kasetsart University	M.Eng (Water Resources Engineering)

SCHOLARSHIP/AWARDS : Thailand Research Fund
Office of the Higher Education Commission